Università Politecnica delle Marche
Dottorato di Ricerca in Ingegneria dell'Informazione
Curriculum "Ingegneria Informatica, Gestionale e dell'Automazione"

Model Predictive Control aimed at energy efficiency improvement in process industries

Ph.D. Dissertation of:
Crescenzo Pepe

Advisor:
Prof. Silvia M. Zanoli

Curriculum Supervisor:
Prof. Claudia Diamantini

XV edition - new series

Università Politecnica delle Marche
Dottorato di Ricerca in Ingegneria dell'Informazione
Curriculum "Ingegneria Informatica, Gestionale e dell'Automazione"

Model Predictive Control aimed at energy efficiency improvement in process industries

Ph.D. Dissertation of:
Crescenzo Pepe

Advisor:
Prof. Silvia M. Zanoli

Curriculum Supervisor:
Prof. Claudia Diamantini

XV edition - new series

Università Politecnica delle Marche
Dottorato di Ricerca in Ingegneria dell'Informazione
Facoltà di Ingegneria
Via Brecce Bianche – 60131 Ancona (AN), Italy

to Marsia, for her ability in the compensation of my time delays

a Marsia, per la sua capacità nel compensare i miei ritardi

Acknowledgments

The Ph.D. research (start: November 2013; end: October 2016) has been funded by an "Eureka Project" sponsored by:

- Università Politecnica delle Marche (Dipartimento di Ingegneria dell'Informazione (D.I.I.), Laboratory for Interconnected Systems Supervision and Automation (L.I.S.A.));
- i.Process (Italian Plant Realtime Optimization & Control for Energy Saving Services) S.r.l.;
- Regione Marche.

I will always be grateful to myself for seeking and trying the Ph.D. experience. I will always be grateful to Prof. Silvia M. Zanoli of D.I.I. L.I.S.A. and to Ing. Luca Barboni of i.Process S.r.l. for their fundamental support during these three beautiful years. I hope I have awarded their patience and trust with my research activity.
I will always be grateful to i.Process S.r.l. staff and in particular to Francesco Cocchioni, Matteo Rocchi, Giacomo Astolfi, David Barchiesi, and Lorenzo Orlietti for their cooperation in my research studies.
I need to thank my family for the constant love, help, and support.
This dissertation is dedicated to Marsia, that is my girlfriend and my future wife.

Ancona, November 2016

Crescenzo Pepe

Abstract

The research activity has been focused on the study of Advanced Process Control (APC) techniques aimed at applications oriented to energy efficiency achievement in process industries. Studies about theoretical and practical aspects of APC have been conducted, focusing on Model Predictive Control (MPC) techniques. An APC framework based on a two-layer linear MPC architecture has been developed. Innovative contributions have consisted in the coherent and consistent formulation of the two MPC modules within the two-layer scheme, together with improvements on the cooperation policy between them. Additional contributions about input-output time delays handling have been provided. Specific methodologies about parameters and constraints changes handling have been obtained and infeasibility prevention has been achieved. Additional innovative contributions in the controller formulation concerned the online introduction of process variables status values and the online inhibition of selected control inputs with respect to defined outputs. The basic APC framework has been customized for its installation on real industrial processes, in particular steel industry billets reheating furnaces and cement industry clinker rotary kilns.

In steel industry, the innovative contributions concerned the formulation of virtual sensors, the usage of Linear Parameter-Varying models within MPC modules, and the development of stoichiometric ratios control methods and of methodologies for online adaptation of the time horizons. In cement industry, process variables constraints correction methodologies through sporadic feedback have been introduced.

The APC software tool has been installed on different European steel and cement industries obtaining energy efficiency certificates, together with improvements on process control. The developed steel industry control method has been awarded with an Italian patent; the first steel industry project has been awarded with an energy efficiency award.

Keywords: Advanced Process Control, Model Predictive Control, constraints softening, time delay, energy efficiency, environmental impact decreasing, billets reheating furnace, cement rotary kiln.

Sommario

L'attività di ricerca ha riguardato lo studio di tecniche di controllo avanzato orientate al risparmio energetico nelle industrie di processo. Sono stati approfonditi aspetti teorici e pratici del controllo avanzato, focalizzando l'attenzione su tecniche di controllo predittivo. È stato sviluppato un pacchetto di controllo avanzato basato su un'architettura di controllo predittivo lineare a due livelli. Contributi innovativi hanno riguardato lo sviluppo di una formulazione coerente e consistente dei due livelli, insieme a miglioramenti della loro politica di cooperazione. Ulteriori contributi nella formulazione hanno riguardato la gestione dei ritardi ingresso-uscita. Sono state introdotte metodologie per i cambiamenti di parametri e vincoli e per la prevenzione di situazioni di infeasibility. Sono state introdotte la formulazione online di uno stato per le variabili di processo e l'inibizione di ingressi di controllo selezionati.
Il pacchetto di controllo avanzato è stato customizzato per essere installato su processi industriali, in particolare forni di riscaldo di billette nell'industria dell'acciaio e forni rotativi per la produzione del clinker nell'industria del cemento.
Nell'industria dell'acciaio l'innovazione ha riguardato la formulazione di sensori virtuali, l'utilizzo di modelli lineari con parametri variabili nei moduli di controllo predittivo e lo sviluppo di metodologie di controllo dei rapporti stechiometrici e di adattamento online degli orizzonti temporali. Nell'industria del cemento sono state introdotte metodologie di correzione dei vincoli delle variabili di processo tramite feedback intermittente.
Il pacchetto di controllo avanzato è stato installato in varie acciaierie e cementifici ottenendo titoli di efficienza energetica e migliorie nel controllo di processo. Il pacchetto relativo all'industria dell'acciaio ha ottenuto un brevetto italiano; il primo progetto sviluppato in tale ambito è stato premiato con un premio sull'efficienza energetica.

Contents

List of Figures

List of Tables

Chapter 1

Introduction

> The essence of mathematics is not to make simple things complicated, but to make complicated things simple.
>
> S. Gudder

Process industries, in recent decades, registered an increasing need for innovations in the production chain, as well as an increased need for a high level of automation. These requirements have been motivated by the need to guarantee an optimal trade-off between production targets meeting, product quality specifications fulfillment, and energy efficiency achievement, complying with increasingly stringent environmental standards. Plant managers and engineers are focusing their attention on solutions able to increase profitability while maintaining good quality standards in the long term. The translation of these ideas in practical specifications results in the research of the most advantageous trade-off between opposing objectives, e.g. throughput and yields increasing, costs reduction, and product quality improvement. Minimum payback time solutions are preferred so as to maximize the return on investment: new control and management strategies should be evaluated as alternative to hardware investments. In this context, the installation of Advanced Process Control (APC) systems often provides the best solution, minimizing the payback time compared to the replacement of a whole hardware unit. Adopting APC based solutions, payback time is in the order of weeks, or months, in opposition to the years required by a relevant replace of an hardware unit [1].
APC strategies have the key objective of stabilize the processes operations, pointing toward the overcoming of the limitations of the classical local controllers. In this way, the processes can more safely operate closer to their operating constraints, thus obtaining energy efficiency improvements [2].
Energy efficiency and energy conservation are gaining importance as key components in many national and international strategies to mitigate the impact of climate change, to improve security of energy supply, and to increase competi-

tiveness. Energy represents a fundamental aspect in the modern technological development, but at the same time its use affects the quality of the environment. For this reason, *Green Economy* energy policies are needed that could guarantee a rational energy usage, with consumption and energy needs reduction. In the last years, energy efficiency certificates (Italian acronym TEE, also called "white certificates") have been introduced, in order to promote applications that respect environmental and energy standards. These certificates allow obtaining government incentives, based on energy consumption evaluation with respect to defined projects baselines [3].
APC projects require economic assessments, in order to really quantify the economic benefits resulting from plants implementation. Business cases can be created, introducing direct relationships between the process control systems and the economic benefits [1].
The most important phase of an APC system design is represented by the selection of the control method. Techniques based on constraint control and split-range control are frequently used, but in the present work a Model Predictive Control (MPC) approach has been chosen for its strong capability to deal with constrained multivariable processes [4]. Exploiting a multivariable chemical, physical and economic modellization of the considered processes, the adoption of an MPC approach facilitates the reaching of the goal of stabilizing the processes operations, pointing toward the overcoming of the limitations of the classical local controllers, e.g. PID (Proportional Integral Derivative) controllers manually run by plant operators.

1.1 Research Activity and Objectives

The Ph.D. research activity reported in the present dissertation has been funded by a project sponsored by a cooperation between Università Politecnica delle Marche (Dipartimento di Ingegneria dell'Informazione (D.I.I.), Laboratory for Interconnected Systems Supervision and Automation (L.I.S.A.)), the regione Marche, and i.Process (Italian Plant Realtime Optimization & Control for Energy Saving Services) S.r.l., an Italian company that works on the development of control automation solutions for process industries. In November 2013, when the Ph.D. research started, this company had the need to develop APC systems aimed at energy efficiency achievement and improvement in different process industries, i.e. steel industries and cement industries. An initial research objective was defined: the development of a proprietary APC framework, able to profitably manage multivariable constrained processes. The choice of not depend on commercial industrial products was motivated by the need to perform algorithms *customization* whenever the process at study re-

quired it.
In the first part of the research activity, in order to address the initial research objective, a study of APC techniques aimed at applications oriented to energy efficiency achievement in process industries has been conducted. In particular, the attention has been focused on MPC techniques, given their strong effectiveness and reliability in the solution of constrained multivariable control problems. Studies about different aspects of MPC have been performed. A *two-layer* linear MPC scheme based on a state space approach has been formulated, based on two cascaded optimization problems. Theoretical and practical aspects related to the *two-layer* scheme have been analyzed and addressed. In order to guarantee the effectiveness of the developed MPC formulation versus typical industrial processes features, a proper handling of input-output time delays has been introduced in the MPC formulation. Different theoretical issues tied to time delays handling have been studied and addressed.
In order to improve this initial release of the APC framework, further issues strictly related to industrial applications have been studied and solved. In particular, the option to online specify the subset of process variables to be taken into account in the controller structure has been introduced by a tailored formulation, based on a proper status definition for each process variable. Furthermore, methodologies for the online inhibition of selected control inputs with respect to defined outputs have been developed.
After the first part of the research activity where the outlined APC framework has been formulated and developed, detailed studies on the real processes that had to be considered have been conducted. The real processes at issue were billets reheating furnaces in steel industries and rotary kilns for the clinker production phase in cement industries. From the conducted analysis, the need to differently *customize* the basic APC framework was ascertained.
In steel industry, some specific requirements have been encountered and addressed, concerning the need of providing virtual sensors, the cascading of different model types, and *ad hoc* control solutions for particular variables to be controlled.
In cement industry, the need to exploit sporadic feedback information has been studied and addressed. Furthermore, tailored control policies related to a proper handling of input-output time delays have been introduced.

1.2 Main Research Contributions

In the research context mentioned in the previous section, the following innovative research contributions have been provided:

i. cooperation policy improvements in a *two-layer* linear MPC scheme;
ii. an alternative approach aimed at the inhibition of the control action of

selected inputs on defined outputs;

iii. a direct connection between the alternative approach (*ii*) and the process variables status values definition;

iv. a control method for steel industries billets reheating furnaces that, as it will be explained, has been awarded with an Italian patent and, in one of the different real applications, it has been also awarded with an energy efficiency award;

v. a control method for stoichiometric ratios within a *two-layer* MPC scheme;

vi. a constraints *softening* decoupling strategy oriented to input-output time delays handling, which has been applied in cement industries APC;

vii. the exploitation of the constraints *softening* decoupling strategy (*vi*) as a solution of a particular single-layer linear MPC problem;

viii. a methodology for MPC constraints correction based on sporadic feedback information in cement industries APC.

1.3 Dissertation Organization

In Chapter 1, an overview of the Ph.D. research activity context has been described, highlighting the main steps pursued and the main and the most significant research contributions.
In Chapter 2, the main concepts related to the MPC strategy are provided, presenting the basic idea and a brief industrial MPC history. Furthermore, a literature review related to the analyzed MPC aspects is given. In particular, feasibility and constraints management concepts are introduced, together with an overview of the existing solutions related to the MPC location in industrial control hierarchy. At this regard, general concepts and solutions related to the *two-layer* MPC architecture are provided. Finally, the general problem of input-output time delays handling is presented.
Chapter 3 describes the developed APC framework, based on a *two-layer* linear MPC scheme. The two MPC modules are detailed, together with the formulations of their optimization problems. At this regard, the improvements on the cooperation policy between the two layers are accurately described. Furthermore, the decoupling strategy that constitutes an alternative approach aimed at the inhibition of the control action of selected inputs on defined outputs is described. Subsequently, a status value is introduced for each process variable involved in the control problem setup. A direct connection between the decoupling strategy and the process variables status definition is also provided. Finally, some remarks on constraints handling, reference trajectories management, and tuning within the proposed basic APC framework are given.
Chapters 4-5 are focused on the detailed description of the analyzed process industries.

Chapter 4 refers to steel industry and in particular to the billets reheating furnace sub-process. The related control problems and specifications are accurately explained and a literature review of the existing control solutions is provided. Then, the proposed control method and, more in general, the *customized* billets reheating furnaces APC system is detailed. Also tuning and furnaces management details are provided. Finally, two real case studies are described and a further *customization* of the basic APC framework is proposed, related to a stoichiometric ratios control method.
Chapter 5 refers to cement industry and in particular to the clinker production phase sub-process. The related control problems and specifications are accurately explained and a brief literature review of the existing control solutions is provided. Then, the developed control method and, more in general, the *customized* clinker production phase APC system is detailed. At this regard, the introduced constraints softening decoupling strategy is described. Furthermore, a brief digression on its usage also within a particular single-layer linear MPC problem is given. Finally, within the *customized* clinker production phase APC system, the proposed methodology aimed at exploiting sporadic feedback information is described and two real case studies are proposed.
Simulation and real results related to the considered steel industry and cement industry case studies are reported in Chapters 6-7. Finally, conclusions and future work are summarized in Chapter 8.

Chapter 2

Model Predictive Control Strategy

Model Predictive Control (MPC) represents the most prevalent Advanced Process Control (APC) incarnation, mainly due to its strong capability to deal with constrained multivariable processes.
The term MPC refers to a set of control techniques which make explicit use of a model of the considered process to formulate an optimization problem, based on the minimization of an objective function. In this way, the control signal to be applied to the plant at each control instant is obtained.
MPC represents the most widely used APC technique in process industry, due to various reasons:

- its capability to deal with multivariable control problems;
- its capability to handle constraints on process variables;
- its capability to allow a trade-off between theory and practice;
- the related control concepts are very intuitive;
- its capability to control processes characterized by very simple or complex dynamics, including time-delay systems, nonminimum phase and unstable ones;
- measured disturbances can be naturally compensated through feedforward.

These MPC advantages are among the motivations that explain its strong impact on control technology development in the process industries with respect to other significant control techniques, e.g. Linear Quadratic Gaussian (LQG) control [5], [6].
The MPC formulation is based on a prior knowledge of the process model and it is independent of it, but the obtained control benefits are strictly related to the plant-model mismatch. The need of an accurate model of the process to be controlled is, in fact, one of the major drawbacks of the MPC approach [7]. Another problem was traditionally represented by the amount of computation for the control law achievement, but with the computing power available today, this is not anymore a crucial problem for most MPC applications in process industry.
From a practical point of view, MPC strategy, modifying the statistical prop-

erties of the main process variables, allows approaching processes operating constraints (compared to standalone controllers), leading to major profitability and short payback times [8], [9].

2.1 MPC basic idea

As previously stated, MPC uses a mathematical model of the considered process in order to capture the dynamic relationships between the input-output variables. Among all input trajectories capable to maintain process variables within the (possibly) assigned constraints, the one that provides the best performances in term of minimization of a cost function is computed.
As typical in industrial APC applications, three basic groups of process variables are defined. Manipulated Variables (MVs), Disturbance Variables (DVs), and Controlled Variables (CVs). MVs group represents the measured input variables that can be used by the controller, while DVs group is constituted by the measured input variables that cannot be moved by the controller (they can be only used in a feedforward way). Finally the CVs group represents the (output) process variables that have to be controlled. MVs are included in a $u \in \mathbb{R}^{l_u \times 1}$ vector, DVs are represented by a $d \in \mathbb{R}^{l_d \times 1}$ vector and CVs are included in a $y \in \mathbb{R}^{m_y \times 1}$ vector.

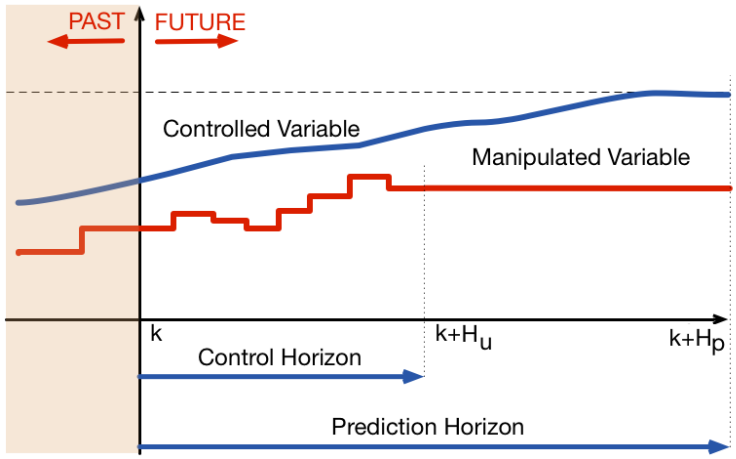

Figure 2.1: MPC basic idea.

MPC family is characterized by a basic idea, named as *receding horizon* idea, shown in Fig. 2.1. Considering a discrete time process model, the *receding horizon* idea can be expressed as follows [8], [9]:

- CVs, together with MVs and DVs, are predicted on a time horizon, called *prediction horizon* (H_p). The CVs predictions $\hat{y}(k+i|k)$ $(i=1\dots H_p)$[1] exploit past information (e.g. the actual CVs value $y(k)$ if available) and depend on future MVs values $\hat{u}(k+i|k)$ $(i=0\dots H_p-1)$ and DVs values $\hat{d}(k+i|k)$ $(i=0\dots H_p-1)$. The future MVs values have to be calculated and sent to the plant;
- based on the process variables predictions, an optimization problem (possibly constrained) is formulated and solved, taking into account CVs and MVs tracking errors with respect to defined reference trajectories and/or MVs future changes magnitude with respect to the actual MVs value $u(k-1)$. Some assumptions about the structure of the MVs future values can be included, e.g. defining a *control horizon* (H_u, $1 \leq H_u \leq H_p$) that represents the number of possibly nonzero MVs future changes (typically the possibly nonzero MVs future changes are assumed on the first H_u prediction instants);
- among the computed MVs future values, only the first value $\hat{u}(k|k) = u(k)$ is applied to the process, discarding the other future control signals. At the next sampling instant $k+1$ the *prediction horizon* is moved one step ahead and the entire procedure is repeated, calculating the MVs value $\hat{u}(k+1|k+1) = u(k+1)$ (which theoretically can be different from $\hat{u}(k+1|k)$ given the updated process information).

With regard to the definition of the control horizon H_u, it represents the number of possibly nonzero MVs future changes (moves), i.e. the MVs are assumed to possibly change H_u times over the prediction horizon H_p. A typical design assumes that the possibly nonzero MVs future changes are made on the first H_u prediction instants. Denoting with M_j $(j=1\dots H_u;\ 0\leq M_j \leq H_p-1)$ the prediction instants related to the assumed MVs moves $\Delta\hat{u}(k+M_j|k)$ $(j=1\dots H_u)$, the typical design choice assumes that $M_j = j-1$ $(j=1\dots H_u)$ and that $\Delta\hat{u}(k+j-1|k)$ $(j=1\dots H_u)$ are the possibly nonzero MVs future moves. Clearly, for any design must be $M_1 = 0$, i.e. the first MVs move must be always assumed at the first prediction instant; furthermore $2 \leq M_h \leq H_p - 1$ and $M_{h-1} < M_h$ $(h=2\dots H_u)$.
More advanced design choices assume that the MVs remain constant over *blocks* of sampling intervals, i.e. the M_j prediction instants are not all consecutive. This feature has been named as *blocking* [10]. A general example of *blocking*

[1] This notation indicates the prediction at instant $k+i$ calculated with the information up to instant k.

can be expressed as:

$$\begin{aligned}
&\hat{u}(k+M_1|k) = \cdots = \hat{u}(k+M_2-1|k) = u(k-1) + \Delta\hat{u}(k+M_1|k) \\
&\hat{u}(k+M_2|k) = \cdots = \hat{u}(k+M_3-1|k) = \hat{u}(k+M_1|k) + \Delta\hat{u}(k+M_2|k) = \\
&\qquad = u(k-1) + \Delta\hat{u}(k+M_1|k) + \Delta\hat{u}(k+M_2|k) \\
&\qquad\qquad \vdots
\end{aligned} \tag{2.1}$$

$$\begin{aligned}
\hat{u}(k+M_{H_u-1}|k) &= \cdots = \hat{u}(k+M_{H_u}-1|k) = \hat{u}(k+M_{H_u-2}|k) + \Delta\hat{u}(k+M_{H_u-1}|k) = \\
&= u(k-1) + \Delta\hat{u}(k+M_1|k) + \ldots + \Delta\hat{u}(k+M_{H_u-1}|k)
\end{aligned}$$

$$\begin{aligned}
\hat{u}(k+M_{H_u}|k) &= \cdots = \hat{u}(k+H_p-1|k) = \hat{u}(k+M_{H_u-1}|k) + \Delta\hat{u}(k+M_{H_u}|k) = \\
&= u(k-1) + \Delta\hat{u}(k+M_1|k) + \ldots + \Delta\hat{u}(k+M_{H_u}|k)
\end{aligned}$$

In MPC literature, different blocking strategies have been proposed [11], [12], [13].
The MPC problems can be characterized by the optimization of various types of criteria, such as linear or quadratic ones. A typical and widely used cost function to be minimized is:

$$\begin{aligned}
V(k) = &\sum_{i=H_w}^{H_p} \|\hat{y}(k+i|k) - r(k+i|k)\|^2_{Q(i)} + \sum_{i=0}^{H_u-1} \|\Delta\hat{u}(k+i|k)\|^2_{R(i)} + \\
&+ \sum_{i=0}^{H_p-1} \|\hat{u}(k+i|k) - u_r(k+i|k)\|^2_{S(i)}
\end{aligned} \tag{2.2}$$

where $||\cdot||$ is the Euclidean norm. $u_r(k+i|k)$ and $r(k+i|k)$ represent the MVs and CVs reference trajectories value at ith prediction instant, respectively; the related tracking errors are weighted by positive (semi-)definite matrices $S(i) \in \mathbb{R}^{l_u \times l_u}$ and $Q(i) \in \mathbb{R}^{m_y \times m_y}$. $R(i) \in \mathbb{R}^{l_u \times l_u}$ are positive (semi-)definite matrices that weight the magnitude of MVs future moves. $R(i)$, due to their action on the penalization of the MVs future moves, are sometimes called *move suppression factors*. H_w is a *window* parameter ($1 \leq H_w \leq H_p$), useful for example for time delays handling on the CVs-MVs channels [8].

Typical constraints on MVs and CVs can be expressed as follows:

$$\begin{aligned} &i)\ lb_{du}(i) \leq \Delta\hat{u}(k+i|k) \leq ub_{du}(i), \quad i = 0 \dots H_u - 1 \\ &ii)\ lb_u(i) \leq \hat{u}(k+i|k) \leq ub_u(i), \quad i = 0 \dots H_u - 1 \\ &iii)\ lb_y(i) \leq \hat{y}(k+i|k) \leq ub_y(i), \quad i = H_w \dots H_p \end{aligned} \tag{2.3}$$

where the magnitude of MVs future moves is constrained by $lb_{du}(i)$ and $ub_{du}(i)$ and the magnitude of MVs future values is constrained by $lb_u(i)$ and $ub_u(i)$. Constraints (2.3) *i)* - *ii)* typically refer to actuators limitations. In particular, $lb_{du}(i)$ and $ub_{du}(i)$ represent possible actuator slew rates, while $lb_u(i)$ and $ub_u(i)$ represent possible actuator ranges. Finally, (2.3) *iii)* constrains the magnitude of CVs future values by $lb_y(i)$ and $ub_y(i)$.
Assuming a linear model for the considered process, the optimization problem characterized by the minimization of the cost function (2.2) subject to the constraints expressed in (2.3) can be recast as a Quadratic Programming (QP) problem. For example, formulating all terms as function of the MVs future moves $\Delta\hat{u}(k+i|k)$, the cost function (2.2) is quadratic and the constraints (2.3) are linear. With a suitable definition of $S(i)$, $Q(i)$, and $R(i)$ matrices, a positive definite Hessian of the QP problem can be obtained. In this way, the QP problem to be solved is convex and, if no constraints are considered, an explicit solution can be obtained; otherwise, an iterative optimization method has to be used, e.g. active-set or interior point methods [14], [9].
The control and prediction horizons H_u and H_p, the parameter H_w, the weight matrices $S(i)$, $Q(i)$, and $R(i)$, and the reference trajectories $u_r(k+i|k)$ and $r(k+i|k)$ have a strong impact on the controller performances. They represent *tuning parameters*. In some cases, some of these parameters, e.g. the weight matrices, may be associated with the economic objectives of the control system.

2.2 Industrial MPC brief history

MPC techniques have been simultaneously introduced by several industrial researchers in the late seventies. Researchers of the French company *Adersa* proposed predictive control as *Model Predictive Heuristic Control* (later known as *Model Algorithmic Control*, *MAC*), emphasizing a control methodology able to handle control problems that were difficult to solve with conventional PID control [15]. Other researchers proposed an MPC approach calling it *Dynamic Matrix Control* (*DMC*) [16]. *DMC* became the most well known of the commercial MPC products. All these products shared the crucial feature of predictive control: the utilization of a plant internal model in order to compute the control signal through (constrained) optimization strategies, based on the *receding*

horizon idea. All these pioneer MPC techniques exploit impulse response or step response models; this feature, together with the simplicity of the algorithm, made MPC very popular, particularly in chemical process industries.
Early academic results on predictive control can be found in [17], [18], [19], [20]. Other research trends arose around adaptive control ideas, leading to other MPC algorithms: *Predictor-Based Self Tuning Control* [21] and *Extended Horizon Adaptive Control* (*EHAC*) [22], together with *Extended Prediction Self Adaptive Control* (*EPSAC*) [23], *Generalized Predictive Control* (*GPC*) [24], [25], and *Predictive Functional Control* (*PFC*) [26].
A pioneer work for MPC state space formulation was [27]. The introduction of state space formulation in MPC represented a very important phase, mainly due to the ability of this model representation to generalize more complex cases such as multivariable processes, nonlinear processes and systems with stochastic disturbances and noise in the measured variables [9].
Today there are many companies that have proprietary MPC software tools [28], [29], [30]. Among the most popular tools, there are the AspenTech *DMC-Plus* (*Dynamic Matrix Control Plus*) and the Honeywell *RMPCT* (*Robust MPC Technology*) [31]. The main differences between the industrial MPC tools are tied to the exploited model (e.g. linear/nonlinear, step response/state space), to the criterion to be minimized, to the choice of the prediction horizon (finite or infinite), to the constraints, and to the feedback introduction in the controller formulation [30].

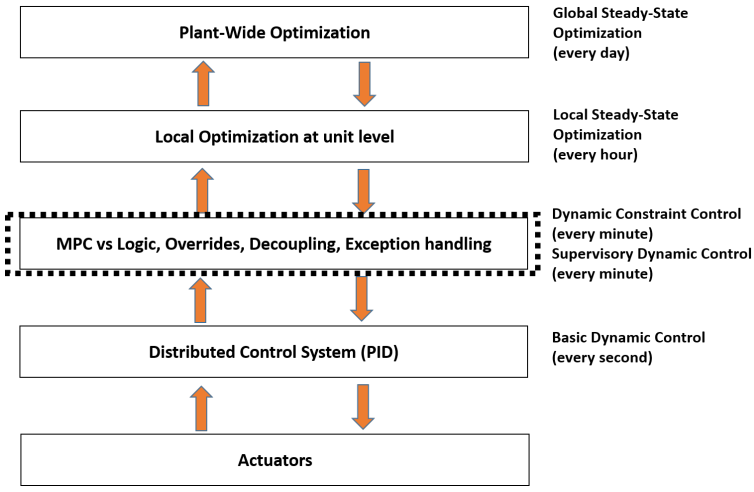

Figure 2.2: MPC in the control hierarchy for multivariable process control systems.

Fig. 2.2 shows the position of MPC within process industries control hierarchy. Hierarchical (or multilayer) approach is widely used in process industry [32], [33], [34]. The top level includes the determination of set-points, usually through steady-state optimization. This type of optimization can be executed on more levels: plant-wide optimization may be performed once a day, but unit level optimization may be performed every hour. At the bottom level there are standalone local controllers that are typically represented by PI or PID controllers (e.g. for pressures, flows or temperatures control), while at the lowest level there are the control loops related to single actuators (e.g. valve positioning). The middle level represents the traditional location of MPC within the control hierarchy of process industries [35], [36]. It, mainly thanks to its ability and flexibility in the handling of constrained multivariable systems, has replaced a complex layer that included logic, overrides, decoupling networks, and exception handling [37]. The replaced complex layer consisted of a set of *ad hoc* solutions to individual problems and a global view of plant behaviour was not provided. So, MPC, due to its integrated view, provides strongly better performances [8], [30].

2.3 Addressed MPC problems

In this section, a literature review on the MPC technique focused on some of the problems that have been addressed in the author research activity is reported. Feasibility, constraints management, and *two-layer* (*two-stage*) MPC formulation are analyzed. Then, references to the input-output time delays handling problem are provided.

2.3.1 Feasibility and constraints management

As stated in Section 2.1, MPC formulation is typically based on a constrained optimization problem. Usually, in process industries, there are constraints on the process variables that have to be met. For example, the MVs constraints reported in (2.3) usually correspond to physical MVs constraints. Considering the cost function (2.2) subject to the constraints (2.3) and assuming a linear process model, a critical situation is that the related QP problem may result infeasible [8], [38]. Infeasibility causes can be related to unexpected large disturbances or to plant-model mismatch. Within the considered QP problem, all constraints have been formulated as *hard* constraints, i.e. they can not be violated. In the infeasibility case, the sequence of MVs future values $\hat{u}(k+i|k)$ is not obtained: this situation is unacceptable for an APC system that must provide input signals to the plant at each control instant. For this reason, in the design phase of an MPC strategy, it is a key aspect to prevent infeasibility

or to have an alternative method of computing the MVs values. At this regard, different solutions have been formulated [8]:

- *ad hoc* policies;
- avoid *hard* constraints on the CVs;
- actively manage the constraints definition at each control instant k;
- actively manage the horizons H_p and H_u at each control instant k;
- use non-standard solution algorithms.

Examples of *ad hoc* policies are the exploitation of the same control signal as in the previous step or the usage of the control signal $\hat{u}(k|k-1)$ computed and discarded at the previous step. An automatic strategy to prevent infeasibility is to *soften* (*relax*) the constraints: the constraints are not considered as *hard* and their violation is admitted only if it is really necessary. At this regard, substantial distinctions have to be made between MVs and CVs constraints. Usually MVs constraints really are *hard* constraints, because for example actuators have limited ranges of action and limited slew rates. Once these have been approached they can not be crossed: MVs constraints are usually not softened. A simple idea of CVs constraints softening is to add new variables, named as *slack variables*, which are computed as nonzero values only if the related constraints are violated [8]. These slack variables are introduced as decision variables in the MPC problem; an example of modification of (2.3) is:

$$\begin{aligned}
&lb_{du}(i) \leq \Delta\hat{u}(k+i|k) \leq ub_{du}(i), \quad i = 0 \dots H_u - 1 \\
&lb_u(i) \leq \hat{u}(k+i|k) \leq ub_u(i), \quad i = 0 \dots H_u - 1 \\
&lb_y(i) - \varepsilon_i(k) \leq \hat{y}(k+i|k) \leq ub_y(i) + \varepsilon_i(k), \quad i = H_w \dots H_p \\
&\varepsilon_i(k) \geq 0, \quad i = H_w \dots H_p
\end{aligned} \tag{2.4}$$

where $\varepsilon_i(k)$ are nonnegative slack variables vectors. In this example, CVs lower and upper constraints at a generic prediction instant share the same slack variable. Since the violation of the original constraints should be discouraged, the $\varepsilon_i(k)$ vectors are introduced in the cost function. For example, the cost function (2.2) could be modified as follows:

$$\begin{aligned}
V(k) = &\sum_{i=H_w}^{H_p} \|\hat{y}(k+i|k) - r(k+i|k)\|^2_{Q(i)} + \sum_{i=0}^{H_u-1} \|\Delta\hat{u}(k+i|k)\|^2_{R(i)} + \\
&+ \sum_{i=0}^{H_p-1} \|\hat{u}(k+i|k) - u_r(k+i|k)\|^2_{S(i)} + \sum_{i=H_w}^{H_p} \|\varepsilon_i(k)\|^2_{\rho(i)}
\end{aligned} \tag{2.5}$$

In this case, a quadratic penalty for constraints violations has been introduced through $\rho(i)$ positive (semi-)definite matrices [39]. As $\rho(i) \to 0$, the optimization problem tends to a problem with no CVs constraints, while as $\rho(i) \to \infty$

CVs constraints become *hard* constraints.
Other penalties have been introduced for slack variables in the MPC cost functions, i.e. $1-$norm penalty or $\infty-$norm penalty [8]. More sophisticated strategies of "constraints management" try to *soften* (*relax*) the least-important constraints in order to regain feasibility [40]. In [10] an approach based on the exploitation of a single slack variable is proposed, using suitable coefficients to differently scale constraints *softening*. These coefficients have been named as *Equal Concern for the Relaxation* (*ECR*) coefficients.

2.3.2 Two-layer MPC

In APC industrial applications, economic specifications are of major importance. These specifications can be suitably translated into control objectives [41]. Considering the MPC position in the control hierarchy of Fig. 2.2, at each control instant (e.g. every minute) its dynamic optimization must provide optimal MVs values to the lower level; in order to compute the best input paths, suitable reference set-points are needed for MVs and CVs (see for example $u_r(k+i|k)$ and $r(k+i|k)$ in the cost function (2.2)). Typically, a real-time optimizer, hourly or daily, computes the economic target values for MVs and CVs, based on a suitable nonlinear steady-state model of the plant. Real-time operations optimization (RTO) is performed at the upper layers with respect to the MPC layer in Fig. 2.2 [42], [43], [44]. RTO takes into account planning and scheduling specifications, such as the production objectives and their timing; the optimization problem formulated and solved at the RTO layer is often incoherent from MPC layer point of view, because it supplies targets that may be unreachable. The main reason of this unreachability lies in the fact that the models exploited in MPC and RTO layers are not consistent. In fact, while RTO layer may be based on a complex steady-state (nonlinear) process model, usually MPC layer is based on a simplified dynamic (linear) process model. Another crucial aspect is the different sample time that characterizes the RTO and the MPC layers. The RTO steady-state nonlinear economic optimization is performed with a major sample time with respect to the MPC optimization; this discrepancy can be bypassed if the disturbances that affect the considered process have slow dynamics with respect to the process dynamics. On the other hand, when the disturbances dynamics are comparable to the process dynamics, the described sampling time discrepancy can strongly affect the performances. In [45] the consequences of the changes in the market of chemical processing industries and its consequences for process operation are discussed within the MPC-RTO integration. The MPC-RTO inconsistency has been addressed in [46], where a steady-state targets calculation module is considered within the MPC module, at the upper layer with respect to the basic

dynamic optimization. The introduced steady-state optimization module tries to cover the gap between RTO and MPC different models. The introduction of a steady-state targets calculation module with the same time scale of the basic dynamic controller at the upper layer of an MPC module corresponds to the inclusion of a steady-state controller at the upper layer with respect to the basic dynamic controller. This MPC structure is denoted as *two-stage* (*two-layer*) MPC [47]. The steady-state targets calculation module solves a suitable optimization problem, based on the information provided by the RTO module and the basic MPC module; in this way, it computes the MVs and CVs steady-state targets for the basic dynamic MPC module. Different solutions have been proposed in this context, based on different cost functions (e.g. linear or quadratic) and, in general, on different formulations of the two optimization problems. In [47], the steady-state optimization module, represented by a LP problem, forwards steady-state targets to a *DMC* controller. In [48] a LP approach based on linear inequality constraints on combinations of the process inputs and outputs is proposed. In [49] a LP approach is incorporated into the *Shell Multivariable Optimising Controller* (*SMOC*) [50] and a solution that avoids offsets on CVs due to unreachable economic objectives is proposed. A steady-state target optimization that determines the steady-state state and input targets for a constrained, linear, state space regulator is formulated in [51]. Linear, linear-quadratic, and piecewise-linear formulations of the steady-state target optimization module are analysed in [52], [53]. An analysis of the properties and of the limitations of the *two-stage* approach are reported in [54], [55].

The introduction of the steady-state target optimization module inside the MPC layer is shown in Fig. 2.3.

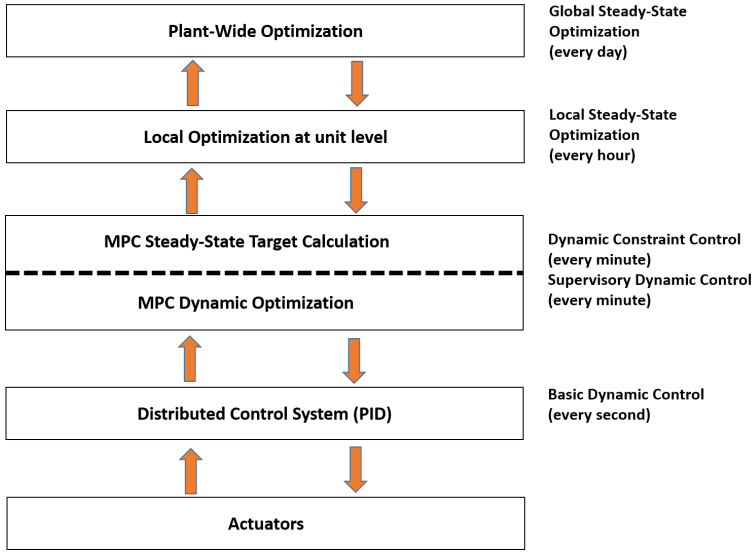

Figure 2.3: Two-layer MPC in the control hierarchy for multivariable process control systems.

2.3.3 Time delays handling

Time delays (also denoted as dead times) on the input-output channels represent a typical feature of process industries. They are mainly due to the time needed to transport energy, mass, or information, but they can also be due to cascaded dynamic systems. For processes with time delays on the input-output channels, the control actions performed on MVs will be active on the CVs after the related time delays. Dead-time control problems have attracted the studies of researchers and engineers. For example, *dead-time compensator* (*DTC*) controller, which includes CVs predictions, has been developed for dealing with time delays. The ability to deal with dead-time processes represented a key MPC feature on its wide application in process industries [56]. In [56] the introduction of time delays in the MPC formulation is proposed, adopting the *GPC* and the *DMC* formulations. In particular, the SISO and MIMO cases are discussed. In the MIMO case, the single dead-time case and the multiple dead-time case are formulated. The single dead-time case refers to situations where the same time delay characterizes all input-output channels; in the multiple dead-time case, different time delays can characterize the different input-output channels. Furthermore, a distinction between the management of MVs-CVs and DVs-CVs dead times is provided. In [57], the differences between implicit and explicit dead-time compensation within the linear state space MPC framework are addressed: the drawbacks tied to the use of an augmented state space rep-

resentation for implicit dead-time compensation are discussed and an explicit dead-time compensation technique is presented. This technique, modelling the dead times directly into the control inputs part of the state space formulation as reported in [58], [59], allows to efficiently compensate single and multiple dead times on the MVs-CVs channels. In [60], an MPC approach for linear systems with time delays on the MVs-CVs channels that takes into account constraints on the MVs is proposed. In [61] a state space model based on the analytical step response model is extended to the case of integrating time systems with time delays. This model is then exploited within an MPC strategy that takes into account targets (possibly unreachable) on some inputs and/or outputs and zone control for the remaining outputs. A practical MPC approach for solar collector plants is proposed in [62], through the formulation of a quadratic program similarly to a linear MPC. In [63] a solution to the problem of MPC of time delay processes with both integrating and stable modes is formulated, leading to zone control and input target tracking.

Chapter 3

Developed APC framework

The present research activity has been co-sponsored by a company that works on the development of control automation solutions. The first part of the research activity has been devoted to the development of an APC framework able to control and optimize constrained multivariable processes. In particular, the interest was the development of a proprietary environment for advanced control solutions and, as first application, it was required to optimize the production of a billets reheating process within an Italian steel plant (see Chapter 4). From the analysis of the steel process at issue and from the study of the literature, a linear MPC approach was chosen. Fig. 3.1 reports the architecture of the APC system. The APC framework has been based on a *two-layer* linear MPC strategy: it is considered to be placed at the middle level of the control hierarchy reported in Fig. 2.3.

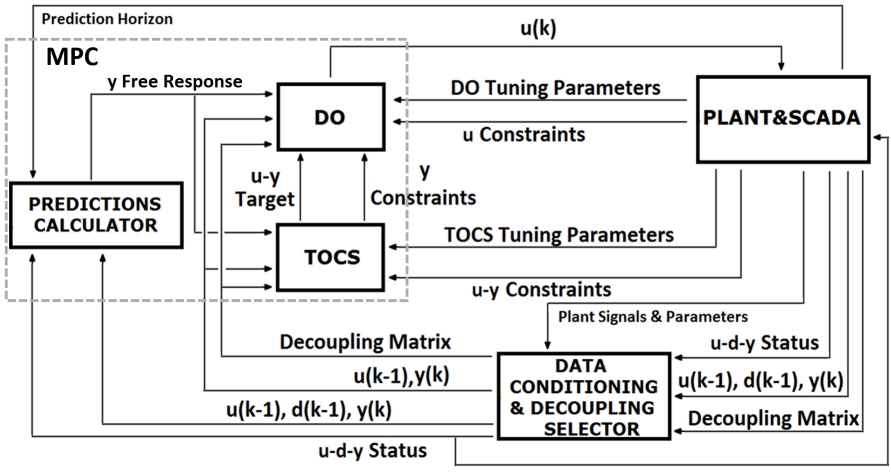

Figure 3.1: Basic architecture of the designed APC system.

At each control instant k, a Supervisory Control and Data Acquisition (*SCADA*) system [64] supplies new measurements ($u(k-1)$, $d(k-1)$, $y(k)$) of the process variables: the Manipulated Variables (MVs) set is denoted with an $u \in \mathbb{R}^{l_u \times 1}$ vector, while the measured input disturbances (Disturbance Variables, DVs) are grouped in a $d \in \mathbb{R}^{l_d \times 1}$ vector. The Controlled Variables (CVs) set (the CVs are assumed all measured) is indicated with a $y \in \mathbb{R}^{m_y \times 1}$ vector. *Data Conditioning & Decoupling Selector* (*DC & DS*) block checks for bad conditions or local control loops faults, possibly conditioning field data. This block determines the process variables subset that has to be included in the MPC formulation at each control instant and, in addition, it defines the MVs to be exploited for the control requirements of each single CV (see Section 3.2). All this information is supplied to the *two-layer* linear *MPC* block. This block includes a *Predictions Calculator* module and it is based on the solution of two subsequent optimization problems (see Section 3.1). At the upper layer, a steady-state module, named as *Targets Optimizing and Constraints Softening* (*TOCS*) module solves the first optimization problem; *TOCS* module results are forwarded to the lower layer, constituted by a basic MPC *Dynamic Optimizer* (*DO*) module. This module, solving the second optimization problem, computes the MVs value $u(k)$ to be applied to the plant at the current control instant. *TOCS* and *DO* modules exploit the same basic linear model of the process to be controlled and the overall MPC computation is based on the *receding horizon* concept (see Section 2.1).

3.1 MPC block

The developed *MPC* block has been based on a *two-layer* scheme, in order to optimally control and optimize both the transient and steady states of the considered process.
The entire MPC formulation within the basic APC framework has been based on a discrete time state space linear time invariant model of the process to be controlled. This model is achieved from a realization procedure subsequent to a zero-order hold discretization of an identified continuous time linear time invariant model with a suitable sampling time T_s (that corresponds to the controller sample time). Asymptotically stable processes are assumed. Considering a process with $(l_u + l_d)$ measured inputs, that is l_u MVs and l_d DVs, and m_y output variables (CVs), the identified model is characterized by a $(m_y \times (l_u + l_d))$ transfer matrix; all transfer functions are assumed to be strictly proper. In the discretization procedure, all these features are assumed to be preserved. If the input-output channels are characterized by the absence of time delays, the considered discrete time state space linear time invariant model of the process

is:

$$x(k+1) = Ax(k) + B_u u(k) + B_d d(k) + w(k)$$
$$y(k) = C_y x(k) + v(k)$$

where $x(k) \in \mathbb{R}^{n\times 1}$ is the state vector, while $w(k) \in \mathbb{R}^{n\times 1}$ is the state unmeasured disturbances vector and $v(k) \in \mathbb{R}^{m_y\times 1}$ is the output unmeasured disturbances vector. The CVs are assumed all measured but generally the state $x(k)$ is not; in order to compute the CVs predictions over the prediction horizon H_p, at each control instant k an estimation of the state is needed. For this reason, a state estimator has to be designed. Assume the selection of any L such that $(A - ALC)$ is strictly Hurwitz: the MPC scheme based on the designed estimator (that supplies $\hat{x}(k|k)$) does not compensate for plant-model mismatch and persistent disturbances. In fact, the disturbances to be rejected should be suitably taken into account, in order to obtain an offset-free control [65], [66], [67], [68]. For this purpose, an integrating disturbances vector $m(k) \in \mathbb{R}^{n_m\times 1}$ is added to the state space model [69], [70]:

$$\begin{bmatrix} x(k+1) \\ m(k+1) \end{bmatrix} = \begin{bmatrix} A & B_m \\ 0_{n_m\times n} & I_{n_m\times n_m} \end{bmatrix} \begin{bmatrix} x(k) \\ m(k) \end{bmatrix} + \begin{bmatrix} B_u \\ 0_{n_m\times l_u} \end{bmatrix} u(k) + \begin{bmatrix} B_d \\ 0_{n_m\times l_d} \end{bmatrix} d(k) + \begin{bmatrix} w(k) \\ w_m(k) \end{bmatrix} \tag{3.1}$$
$$y(k) = \begin{bmatrix} C_y & C_m \end{bmatrix} \begin{bmatrix} x(k) \\ m(k) \end{bmatrix} + v(k)$$

where $w_m(k) \in \mathbb{R}^{n_m\times 1}$ represents an unmeasured disturbances vector that acts on the added term. A general design choice is $n_m = m_y$; thus, assuming that the defined (B_m, C_m) guarantees the observability of the augmented system (3.1), a $L = [L_x \quad L_m]^T$ such that

$$\left(\begin{bmatrix} A & B_m \\ 0_{m_y\times n} & I_{m_y\times m_y} \end{bmatrix} - \begin{bmatrix} A & B_m \\ 0_{m_y\times n} & I_{m_y\times m_y} \end{bmatrix} \begin{bmatrix} L_x \\ L_m \end{bmatrix} \begin{bmatrix} C_y & C_m \end{bmatrix} \right) \tag{3.2}$$

is strictly Hurwitz can be achieved. $I_{a\times a}$ represents a $(a \times a)$ identity matrix while $0_{a\times b}$ represents a $(a \times b)$ matrix with elements all equal to zero. The equation of the augmented estimator is:

$$\begin{bmatrix} \hat{x}(k|k) \\ \hat{m}(k|k) \end{bmatrix} = \begin{bmatrix} \hat{x}(k|k-1) \\ \hat{m}(k|k-1) \end{bmatrix} + \begin{bmatrix} L_x \\ L_m \end{bmatrix} \left(y(k) - \begin{bmatrix} C_y & C_m \end{bmatrix} \begin{bmatrix} \hat{x}(k|k-1) \\ \hat{m}(k|k-1) \end{bmatrix} \right) \tag{3.3}$$

A typical industrial design for asymptotically stable systems (A strictly Hurwitz) is:

$$n_m = m_y, \qquad B_m = 0_{n\times m_y}, \qquad C_m = I_{m_y\times m_y}, \qquad L_x = 0_{n\times m_y}, \qquad L_m = I_{m_y\times m_y} \tag{3.4}$$

This design assumes that any error $y(k) - C_y\hat{x}(k|k-1)$ is caused by a constant disturbance acting on the output. The filtered disturbance estimate is:

$$\hat{m}(k|k) = \hat{m}(k|k-1) + (y(k) - C_y\hat{x}(k|k-1) - \hat{m}(k|k-1)) = y(k) - C_y\hat{x}(k|k-1) \tag{3.5}$$

If $w(k)$, $w_m(k)$, and $v(k)$ are assumed as zero-mean white-noise disturbances, the designed estimator corresponds to a deadbeat Kalman Filter where:

$$Q_w = 0_{n\times n}, \qquad Q_{w_m} = I_{m_y\times m_y}, \qquad R_v \to 0_{m_y\times m_y} \tag{3.6}$$

where Q_w and Q_{w_m} represent the covariance matrices related to $w(k)$ and $w_m(k)$ in (3.1), while R_v represents the covariance matrix related to $v(k)$ in (3.1) [71].

In the previous considerations, time delays on the input-output channels have not been included. Especially in industrial applications, time delays represent a very common aspect that has to be taken into account. For this purpose, assume that the time delays matrices on the CVs-MVs and CVs-DVs channels (expressed in sampling instants) that characterize the obtained discretized model are indicated with $D_{yu} \in \mathbb{N}^{m_y\times l_u}$ and $D_{yd} \in \mathbb{N}^{m_y\times l_d}$. The number of different time delays in D_{yu} is indicated with nd_u while the number of different time delays in D_{yd} is indicated with nd_d. Furthermore, a vector $\alpha \in \mathbb{N}^{nd_u\times 1}$ is introduced that contains the CVs-MVs time delays sorted in ascending order without duplicates. Similarly, a vector $\beta \in \mathbb{N}^{nd_d\times 1}$ is introduced that contains the CVs-DVs time delays sorted in ascending order without duplicates.

Furthermore, assume that the obtained model considers deviations of the process variables from an operating point (u_0, d_0, y_0).

The considered discrete time state space linear time invariant model of the process, augmented with an integrating disturbance, is:

$$\begin{bmatrix} x(k+1) \\ m(k+1) \end{bmatrix} = \begin{bmatrix} A & 0_{n\times m_y} \\ 0_{m_y\times n} & I_{m_y\times m_y} \end{bmatrix} \begin{bmatrix} x(k) \\ m(k) \end{bmatrix} + \begin{bmatrix} B_u \\ 0_{m_y\times(nd_u\cdot l_u)} \end{bmatrix} u_{tot}(k) + \tag{3.7}$$
$$+ \begin{bmatrix} B_d \\ 0_{m_y\times(nd_d\cdot l_d)} \end{bmatrix} d_{tot}(k) + \begin{bmatrix} w(k) \\ w_m(k) \end{bmatrix}$$

$$y(k) = \begin{bmatrix} C_y & I_{m_y\times m_y} \end{bmatrix} \begin{bmatrix} x(k) \\ m(k) \end{bmatrix} + y_0 + v(k)$$

A different integrating disturbance acting on each CV is assumed ($n_m = m_y$). In (3.7), $A \in \mathbb{R}^{n\times n}$ (A is strictly Hurwitz), $B_u \in \mathbb{R}^{n\times(nd_u\cdot l_u)}$, $B_d \in \mathbb{R}^{n\times(nd_d\cdot l_d)}$, $C_y \in \mathbb{R}^{m_y\times n}$. Furthermore

$$u_{tot}(k) = \begin{bmatrix} u(k-\alpha_1) - u_0 \\ \vdots \\ u(k-\alpha_{nd_u}) - u_0 \end{bmatrix} \in \mathbb{R}^{(nd_u\cdot l_u)\times 1} \tag{3.8}$$

$$d_{tot}(k) = \begin{bmatrix} d(k-\beta_1) - d_0 \\ \vdots \\ d(k-\beta_{nd_d}) - d_0 \end{bmatrix} \in \mathbb{R}^{(nd_d\cdot l_d)\times 1} \tag{3.9}$$

where α_i and β_i represent the ith element of α and β.
The considered state space representation allows to explicitly compensate the dead times [57].
In the following, the steady-state gain matrices on the CVs-MVs and CVs-DVs channels will be indicated with $G_{yu} \in \mathbb{R}^{m_y\times l_u}$ and $G_{yd} \in \mathbb{R}^{m_y\times l_d}$.

3.1.1 Predictions Calculator module and DO module

In order to obtain, at each control instant k, an estimation of the state of (3.7), a state estimator has been introduced in the *Predictions Calculator* module of Fig. 3.1. The design parameters of the estimator have been set as in (3.4), thus obtaining the equations:

$$\begin{aligned} \hat{x}(k|k) &= \hat{x}(k|k-1) = A\hat{x}(k-1|k-1) + B_u u_{tot}(k-1) + B_d d_{tot}(k-1) \\ \hat{m}(k|k) &= y(k) - C_y\hat{x}(k|k-1) - y_0 \end{aligned} \tag{3.10}$$

where $\hat{x}(k-1|k-1)$ is the estimation of x at the control instant $k-1$ and $\hat{m}(k|k)$ is based on the information up to k.
As stated in Section 2.1, MPC strategy exploits the predictions of the process variables over a prediction horizon H_p. Based on (3.7) and on (3.10), the prediction model that has to be exploited in the proposed MPC formulation is:

$$\begin{aligned} \hat{x}(k+i|k) &= A\hat{x}(k+i-1|k) + B_u\hat{u}_{tot}(k+i-1|k) + B_d\hat{d}_{tot}(k+i-1|k) \\ \hat{m}(k+i|k) &= \hat{m}(k|k) = y(k) - C_y\hat{x}(k|k-1) - y_0 \quad (i = 1\dots H_p) \\ \hat{y}(k+i|k) &= C_y\hat{x}(k+i|k) + y_0 + \hat{m}(k+i|k) = C_y\hat{x}(k+i|k) + y_0 + \hat{m}(k|k) \end{aligned} \tag{3.11}$$

In (3.11), $\hat{u}_{tot}(k+i-1|k)$ and $\hat{d}_{tot}(k+i-1|k)$ notations are used because these terms may contain future MVs and DVs values (i.e. future MVs and DVs values with respect to the last values $u(k-1)$ and $d(k-1)$).

An important assumption that has been made regards the DVs predictions: at each control instant k, the future DVs behavior is assumed unknown, and $\hat{d}(k+i|k) = d(k-1)(i = 0 \dots H_p - 1)$, i.e. the future DVs behavior is considered constant at the last DVs value $d(k-1)$.
CVs and MVs predictions over H_p have been expressed as an explicit function of the information up to k and of the possibly nonzero MVs future moves (that will be computed by *DO* module) with respect to the actual MVs value $u(k-1)$ [8]. For this purpose, H_u (H_u is the control horizon, $1 \leq H_u \leq H_p$) MVs future moves have been defined and denoted by $\Delta\hat{u}(k + M_i|k)$ $(i = 1 \dots H_u)$, where $M_1 = 0$ and $2 \leq M_h \leq H_p - 1$ $(M_{h-1} < M_h,\ h = 2 \dots H_u)$. The MVs predictions over H_p can be expressed as:

$$\begin{aligned}
\hat{u}(k + M_1|k) &= \dots = \hat{u}(k + M_2 - 1|k) = u(k-1) + \Delta\hat{u}(k + M_1|k) \\
\hat{u}(k + M_2|k) &= \dots = \hat{u}(k + M_3 - 1|k) = \hat{u}(k + M_1|k) + \Delta\hat{u}(k + M_2|k) = \\
&= u(k-1) + \Delta\hat{u}(k + M_1|k) + \Delta\hat{u}(k + M_2|k) \\
&\vdots
\end{aligned} \tag{3.12}$$

$$\begin{aligned}
\hat{u}(k + M_{H_u-1}|k) &= \dots = \hat{u}(k + M_{H_u} - 1|k) = \hat{u}(k + M_{H_u-2}|k) + \Delta\hat{u}(k + M_{H_u-1}|k) = \\
&= u(k-1) + \Delta\hat{u}(k + M_1|k) + \dots + \Delta\hat{u}(k + M_{H_u-1}|k)
\end{aligned}$$

$$\begin{aligned}
\hat{u}(k + M_{H_u}|k) &= \dots = \hat{u}(k + H_p - 1|k) = \hat{u}(k + M_{H_u-1}|k) + \Delta\hat{u}(k + M_{H_u}|k) = \\
&= u(k-1) + \Delta\hat{u}(k + M_1|k) + \dots + \Delta\hat{u}(k + M_{H_u}|k)
\end{aligned}$$

A compact expression for MVs predictions over H_p is:

$$\begin{bmatrix} \hat{u}(k|k) \\ \hat{u}(k+1|k) \\ \vdots \\ \hat{u}(k + H_p - 1|k) \end{bmatrix} = span_{u-H_p} \cdot u(k-1) + mapping_{H_u-H_p} \cdot \Delta\mathcal{U}(k) \quad \in \mathbb{R}^{(l_u \cdot H_p) \times 1} \tag{3.13}$$

where

$$span_{u-H_p} = \begin{bmatrix} I_{l_u \times l_u} \\ I_{l_u \times l_u} \\ \vdots \\ I_{l_u \times l_u} \end{bmatrix} \in \mathbb{R}^{(l_u \cdot H_p) \times l_u} \tag{3.14}$$

$$\Delta\mathcal{U}(k) = \begin{bmatrix} \Delta\hat{u}(k+M_1|k) \\ \vdots \\ \Delta\hat{u}(k+M_{H_u}|k) \end{bmatrix} = \begin{bmatrix} \Delta\hat{u}(k|k) \\ \vdots \\ \Delta\hat{u}(k+M_{H_u}|k) \end{bmatrix} \in \mathbb{R}^{(l_u \cdot H_u)\times 1} \tag{3.15}$$

In (3.13), $mapping_{H_u-H_p} \in \mathbb{R}^{(l_u \cdot H_p)\times(l_u \cdot H_u)}$ is a suitable matrix that describes the prediction instants related to the possibly nonzero MVs future moves. Practically, the definition of a control horizon and of the related MVs movement instants corresponds to the enforcement of implicit constraints ($\Delta\hat{u}(k+s|k) = 0_{l_u\times 1}$, $(s \neq M_i)$) within the controller formulation.
Exploiting (3.11), the CVs predictions over H_p are:

$$\mathcal{Y}(k) = W_{C_y}\mathcal{X}(k) + \mathcal{Y}_0 \tag{3.16}$$

where

$$\mathcal{Y}(k) = \begin{bmatrix} \hat{y}(k+1|k) \\ \vdots \\ \hat{y}(k+H_p|k) \end{bmatrix} \in \mathbb{R}^{(m_y \cdot H_p)\times 1} \tag{3.17}$$

$$W_{C_y} = \begin{bmatrix} C_y & 0_{m_y\times n} & \cdots & 0_{m_y\times n} \\ 0_{m_y\times n} & C_y & \cdots & 0_{m_y\times n} \\ \vdots & \vdots & \ddots & \vdots \\ 0_{m_y\times n} & 0_{m_y\times n} & \cdots & C_y \end{bmatrix} \in \mathbb{R}^{(m_y \cdot H_p)\times(n \cdot H_p)} \tag{3.18}$$

$$\mathcal{X}(k) = \begin{bmatrix} \hat{x}(k+1|k) \\ \vdots \\ \hat{x}(k+H_p|k) \end{bmatrix} \in \mathbb{R}^{(n \cdot H_p)\times 1} \tag{3.19}$$

$$\mathcal{Y}_0 = (1_{H_p\times 1}) \otimes (y_0 + \hat{m}(k|k)) \quad \in \mathbb{R}^{(m_y \cdot H_p)\times 1} \tag{3.20}$$

In (3.20), $1_{a\times b}$ indicates a $(a \times b)$ matrix composed by elements all equal to 1 and $\otimes$ indicates the Kronecker product between matrices.
The term $\mathcal{X}(k)$ of (3.16) can be expressed as:

$$\mathcal{X}(k) = \begin{bmatrix} \hat{x}(k+1|k) \\ \hat{x}(k+2|k) \\ \vdots \\ \hat{x}(k+H_p|k) \end{bmatrix} = A_1\hat{x}(k|k) + A_2\mathcal{U}_{state}(k) + A_3 d_{past}(k) \tag{3.21}$$

where

$$A_1 = \begin{bmatrix} A \\ A^2 \\ \vdots \\ A^{H_p} \end{bmatrix} \in \mathbb{R}^{(n \cdot H_p) \times n} \tag{3.22}$$

$$A_2 = \begin{bmatrix} B_u & 0_{n \times (l_u \cdot nd_u)} & \cdots & 0_{n \times (l_u \cdot nd_u)} \\ AB_u & B_u & \cdots & 0_{n \times (l_u \cdot nd_u)} \\ \vdots & \vdots & \ddots & \vdots \\ A^{H_p-1}B_u & A^{H_p-2}B_u & \cdots & B_u \end{bmatrix} \in \mathbb{R}^{(n \cdot H_p) \times (nd_u \cdot l_u \cdot H_p)} \tag{3.23}$$

$$A_3 = \begin{bmatrix} B_d & 0_{n \times (l_d \cdot nd_d)} & \cdots & 0_{n \times (l_d \cdot nd_d)} \\ AB_d & B_d & \cdots & 0_{n \times (l_d \cdot nd_d)} \\ \vdots & \vdots & \ddots & \vdots \\ A^{H_p-1}B_d & A^{H_p-2}B_d & \cdots & B_d \end{bmatrix} \in \mathbb{R}^{(n \cdot H_p) \times (nd_d \cdot l_d \cdot H_p)} \tag{3.24}$$

$$\mathcal{U}_{state}(k) = \begin{bmatrix} \hat{u}_{tot}(k|k) \\ \hat{u}_{tot}(k+1|k) \\ \vdots \\ \hat{u}_{tot}(k+H_p-1|k) \end{bmatrix} \in \mathbb{R}^{(nd_u \cdot l_u \cdot H_p) \times 1} \tag{3.25}$$

$$d_{past}(k) = \begin{bmatrix} \hat{d}_{tot}(k|k) \\ \hat{d}_{tot}(k+1|k) \\ \vdots \\ \hat{d}_{tot}(k+H_p-1|k) \end{bmatrix} \in \mathbb{R}^{(nd_d \cdot l_d \cdot H_p) \times 1} \tag{3.26}$$

$$d_{past}(k) = \begin{bmatrix} \begin{bmatrix} \hat{d}(k-\beta_1) - d_0 \\ \hat{d}(k-\beta_2) - d_0 \\ \vdots \\ \hat{d}(k-\beta_{nd_d}) - d_0 \end{bmatrix} \\ \begin{bmatrix} \hat{d}(k-\beta_1+1) - d_0 \\ \hat{d}(k-\beta_2+1) - d_0 \\ \vdots \\ \hat{d}(k-\beta_{nd_d}+1) - d_0 \end{bmatrix} \\ \vdots \\ \begin{bmatrix} \hat{d}(k-\beta_1+H_p-1) - d_0 \\ \hat{d}(k-\beta_2+H_p-1) - d_0 \\ \vdots \\ \hat{d}(k-\beta_{nd_d}+H_p-1) - d_0 \end{bmatrix} \end{bmatrix} \tag{3.27}$$

The term $d_{past}(k)$ in (3.26) contains past and future DVs values. Considering (3.9), $d_{past}(k)$ can be expressed as in (3.27). In (3.27), in the generic component $\hat{d}(k-\beta_j+i)$ ($j=1\dots nd_d$, $i=0\dots H_p-1$) the past DVs values are introduced if $-\beta_j+i<-1$, $d(k-1)$ otherwise. At each control instant k, $d_{past}(k)$ represents a known term.
The term $\mathcal{U}_{state}(k)$ must be explicited with respect to the past MVs values and to the possibly nonzero MVs future moves $\Delta\hat{u}(k+M_i|k)$ ($i=1\dots H_u$). Considering (3.8), $\mathcal{U}_{state}(k)$ can be expressed as:

$$\mathcal{U}_{state}(k) = \begin{bmatrix} \begin{bmatrix} \hat{u}(k-\alpha_1) - u_0 \\ \hat{u}(k-\alpha_2) - u_0 \\ \vdots \\ \hat{u}(k-\alpha_{nd_u}) - u_0 \end{bmatrix} \\ \begin{bmatrix} \hat{u}(k-\alpha_1+1) - u_0 \\ \hat{u}(k-\alpha_2+1) - u_0 \\ \vdots \\ \hat{u}(k-\alpha_{nd_u}+1) - u_0 \end{bmatrix} \\ \vdots \\ \begin{bmatrix} \hat{u}(k-\alpha_1+H_p-1) - u_0 \\ \hat{u}(k-\alpha_2+H_p-1) - u_0 \\ \vdots \\ \hat{u}(k-\alpha_{nd_u}+H_p-1) - u_0 \end{bmatrix} \end{bmatrix} \tag{3.28}$$

A $u_{past}(k) \in \mathbb{R}^{(nd_u \cdot l_u \cdot H_p)\times 1}$ vector can be obtained from (3.28): in the generic component related to the $(k-\alpha_j+i)$th prediction instant ($j=1\dots nd_u$, $i=0\dots H_p-1$) the past MVs values are introduced if $-\alpha_j+i<-1$, $u(k-1)$ otherwise. At each control instant k, $u_{past}(k)$ represents a known term. Based

on $u_{past}(k)$ and taking into account (3.15), $\mathcal{U}_{state}(k)$ expression is:

$$\mathcal{U}_{state}(k) = u_{past}(k) + mapping_{\Delta u-u}\Delta\mathcal{U}(k) \tag{3.29}$$

where $mapping_{\Delta u-u} \in \mathbb{R}^{(nd_u \cdot l_u \cdot H_p)\times(l_u \cdot H_u)}$ is a submatrix of $mapping_{H_u-H_p}$ of (3.13).
Taking into account (3.21), (3.27), and (3.29), (3.16) becomes:

$$\begin{aligned}\mathcal{Y}(k) &= W_{C_y}\mathcal{X}(k) + \mathcal{Y}_0 = W_{C_y}A_1\hat{x}(k|k) + W_{C_y}A_2\mathcal{U}_{state}(k) + \\ &+ W_{C_y}A_3 d_{past}(k) + \mathcal{Y}_0 = W_{C_y}A_1\hat{x}(k|k) + W_{C_y}A_2 u_{past}(k) + \\ &+ W_{C_y}A_2 mapping_{\Delta u-u}\Delta\mathcal{U}(k) + W_{C_y}A_3 d_{past}(k) + \mathcal{Y}_0 = \\ &= \Psi\hat{x}(k|k) + \Upsilon u_{past}(k) + \Xi d_{past}(k) + \Theta\Delta\mathcal{U}(k) + \mathcal{Y}_0\end{aligned} \tag{3.30}$$

where

$$\Psi = W_{C_y}A_1 \quad \in \mathbb{R}^{(m_y \cdot H_p)\times n} \tag{3.31}$$

$$\Upsilon = W_{C_y}A_2 \quad \in \mathbb{R}^{(m_y \cdot H_p)\times(nd_u \cdot l_u \cdot H_p)} \tag{3.32}$$

$$\Xi = W_{C_y}A_3 \quad \in \mathbb{R}^{(m_y \cdot H_p)\times(nd_d \cdot l_d \cdot H_p)} \tag{3.33}$$

$$\Theta = W_{C_y}A_2 mapping_{\Delta u-u} \quad \in \mathbb{R}^{(m_y \cdot H_p)\times(l_u \cdot H_u)} \tag{3.34}$$

At each control instant k, based on the known terms of (3.30), a more compact expression for CVs predictions over H_p is:

$$\mathcal{Y}(k) = \Psi\hat{x}(k|k) + \Upsilon u_{past}(k) + \Xi d_{past}(k) + \Theta\Delta\mathcal{U}(k) + \mathcal{Y}_0 = \tag{3.35}$$

$$= \mathcal{Y}(k)|_{\Delta\mathcal{U}(k)=0} + \Theta\Delta\mathcal{U}(k) \tag{3.36}$$

where

$$\mathcal{Y}(k)|_{\Delta\mathcal{U}(k)=0} = \Psi\hat{x}(k|k) + \Upsilon u_{past}(k) + \Xi d_{past}(k) + \mathcal{Y}_0 \quad \in \mathbb{R}^{(m_y \cdot H_p)\times 1} \tag{3.37}$$

$\mathcal{Y}(k)|_{\Delta\mathcal{U}(k)=0}$ represents the CVs *free response* over H_p, namely the response that would be obtained if the MVs future values remain at the last value $u(k-1)$ [8]. CVs *free response* over H_p contains all available information up to k instant, included the DVs effect. In the proposed architecture shown in Fig. 3.1, the CVs *free response* is computed by *Predictions Calculator* module.
From (3.37), denoting with $\hat{y}(k+i|k)|_{\Delta\mathcal{U}(k)=0}$ the CVs *free response* at the ith prediction instant ($i = 1 \dots H_p$), the expression of CVs prediction at the ith

prediction instant is:

$$\begin{aligned} \hat{y}(k+i|k) &= \hat{y}(k+i|k)|_{\Delta\mathcal{U}(k)=0} + \Delta\hat{y}(k+i|k) \\ \Delta\hat{y}(k+i|k) &= \Theta_{(((i-1)\cdot m_y+1:i\cdot m_y),:)}\Delta\mathcal{U}(k) \end{aligned} \tag{3.38}$$

where $\Theta_{((r:s),:)} \in \mathbb{R}^{m_y \times (l_u \cdot H_u)}$ is composed by the m_y Θ rows from the rth to the sth.
With regard to the H_p choice, a crucial assumption is made: H_p is set long enough (finite value) to capture the steady-state effects of all future MVs moves. It is computed taking into account all time constants and time delays related to CVs-MVs and CVs-DVs continuous time transfer functions, evaluating them with respect to the adopted sampling time T_s. The adopted H_p definition represents the first consistency relationship between the *TOCS* and *DO* modules formulations of the MPC scheme proposed in the research activity reported in this dissertation.
Considering the steady-state assumption on the choice of the prediction horizon H_p, the following relationship holds:

$$G_{yu} \simeq \Theta_{(((H_p-1)\cdot m_y+1:H_p\cdot m_y),((i-1)\cdot l_u+1:i\cdot l_u))} \quad i = 1 \dots H_u \tag{3.39}$$

where G_{yu} is the steady-state gain matrix on the CVs-MVs channels and $\Theta_{((r:s),(p:q))} \in \mathbb{R}^{m_y \times (l_u \cdot H_u)}$ is composed by the Θ rows from the rth to the sth and by the Θ columns from the pth to the qth.
Θ matrix contains also crucial information about the CVs-MVs time delays. Considering the $D_{yu} \in \mathbb{N}^{m_y \times l_u}$ matrix of the CVs-MVs time delays, for the generic jth CV a parameter H_{w_j} is defined. H_{w_j} indicates the first prediction instant on which the first MVs future move (contained in $\Delta\hat{u}(k|k)$ vector) related to at least one MV tied to the jth CV ($j = 1 \dots m_y$), will be active:

$$H_{w_j} = \min(D_{yu_{(j,mask_j)}}) + 1 \tag{3.40}$$

where $mask_j$ is a vector that indicates the D_{yu} columns related to the MVs that are tied to the jth CV. $D_{yu_{(j,mask_j)}}$ is composed by the jth D_{yu} row and by the D_{yu} columns defined by $mask_j$. min indicates the minimum operation on vectors. The H_{w_j} parameter can also be determined from Θ matrix: considering the H_p Θ rows related to the jth CV and taking into account only the l_u Θ columns related to $\Delta\hat{u}(k|k)$ (i.e. the first l_u Θ columns), H_{w_j} is equal to the index of the first row where there is at least a nonzero entry. In the general case, where no additional assumptions or modifications are made, for each jth CV, its H_{w_j} parameter is a fixed parameter.
Based on the previous considerations and on the information provided by the other modules/blocks of the general APC architecture (Fig. 3.1), at each control instant k, the lower layer of the proposed MPC scheme, constituted by a

Dynamic Optimizer (*DO*) module, computes the MVs future moves $\Delta\hat{u}(k+M_i|k)$ $(i=1\dots H_u)$ $(M_1=0)$. *DO* module formulation has been based on a Quadratic Programming (QP) problem. The following quadratic cost function has to be minimized, subject to linear constraints:

$$\min_{\Delta U(k),\varepsilon_{yDO}(k)} V_{DO}(k) = \min_{\Delta U(k),\varepsilon_{yDO}(k)} (\sum_{j=1}^{m_y}\sum_{i=H_{w_j}}^{H_p} (Q_{(j,j)}(i)\cdot(\hat{y}_j(k+i|k)-r_j(k+i|k))^2)+$$
$$+\sum_{i=1}^{H_u}\|\Delta\hat{u}(k+M_i|k)\|^2_{R(i)}+\sum_{i=1}^{H_u}\|\hat{u}(k+M_i|k)-u_r(k+M_i|k)\|^2_{S(i)}+\|\varepsilon_{yDO}(k)\|^2_{\rho_{yDO}}) \tag{3.41}$$

subject to

$$\begin{aligned}
&lb_{duDO}(i)\le\Delta\hat{u}(k+M_i|k)\le ub_{duDO}(i),\quad i=1\dots H_u\\
&lb_{uDO}(i)\le\hat{u}(k+M_i|k)\le ub_{uDO}(i),\quad i=1\dots H_u\\
&lb_{yDO_j}(i)-\gamma_{lbyDO_j}(i)\cdot\varepsilon_{yDO}(k)\le\hat{y}_j(k+i|k)\le ub_{yDO_j}(i)+\gamma_{ubyDO_j}(i)\cdot\varepsilon_{yDO}(k),\\
&\quad j=1\dots m_y,\ i=H_{w_j}\dots H_p\\
&\varepsilon_{yDO}(k)\ge 0_{n_{\varepsilon yDO}\times 1}
\end{aligned} \tag{3.42}$$

where $||\cdot||$ is the Euclidean norm. $u_r(k+M_i|k)$ and $r(k+i|k)$ represent the MVs and CVs reference trajectories value at the ith prediction instant, respectively; the related tracking errors are weighted by positive semi-definite diagonal matrices $S(i)\in\mathbb{R}^{l_u\times l_u}$ and $Q(i)\in\mathbb{R}^{m_y\times m_y}$. $Q(i)$ matrices are obtained through diagonal composition of $Q_{(j,j)}(i)$ $(j=1\dots m_y)$ nonnegative scalars. MVs and CVs reference trajectories are obtained through a suitable processing (see Section 3.3) of the MVs and CVs reachable steady-state targets computed by *TOCS* module (see Subsection 3.1.2) and can change at different control instants (Fig. 3.1, *u-y Target*). $R(i)\in\mathbb{R}^{l_u\times l_u}$ are positive definite diagonal matrices that weight the magnitude of MVs future moves.
In (3.42), the magnitude of MVs future moves is constrained by $lb_{duDO}(i)$ (lower constraint) and $ub_{duDO}(i)$ (upper constraint) and the magnitude of MVs future values is constrained by $lb_{uDO}(i)$ (lower constraint) and $ub_{uDO}(i)$ (upper constraint). In the proposed formulation, $lb_{duDO}(i)$ terms are characterized by nonpositive values while $ub_{duDO}(i)$ are characterized by nonnegative values. MVs constraints are considered as *hard* constraints: they can never be violated and their feasibility has been suitably imposed (see Section 3.3). All MVs terms in (3.41)-(3.42) have been considered, without loss of generality, only on the H_u prediction instants related to the possibly nonzero MVs future moves, represented by M_i. In general, MVs constraints are considered always present and can change at different control instants. At each control instant k, *SCADA* system provides MVs moves and MVs magnitudes constraints over the control horizon H_u (Fig. 3.1, *u Constraints*). These constraints, that are possi-

bly preprocessed by *DO* module (e.g. introducing a ramp change for feasibility achievement, see Section 3.3) in the same way they are possibly preprocessed by *TOCS* module (see Subsection 3.1.2), are $lb_{duDO}(i)$, $ub_{duDO}(i)$, $lb_{uDO}(i)$, and $ub_{uDO}(i)$.
In (3.42), the magnitude of the jth CV future value at the ith prediction instant is constrained by $lb_{yDO_j}(i)$ (lower constraint) and $ub_{yDO_j}(i)$ (upper constraint). Given the above definition of the related H_{w_j} parameter (see (3.40)), each jth CV can be controlled (with reference trajectories and/or with constraints) only from the H_{w_j}th prediction instant. All *DO* CVs constraints, if present, can change at different control instants and they are forwarded by *TOCS* module (Fig. 3.1, *y Constraints*) as it will be explained in Subsection 3.1.2. In order to prevent infeasibility situations, CVs constraints can be assumed as *soft* constraints. In fact, in the running of an industrial plant, there may be cases where changes on the operating conditions and/or constraints modifications performed by plant operators could be such that no solution within the given set of operating constraints exists. Consequently, the controller could not find an output solution and no control action on the system would be performed. In the conduction of a real plant, this situation is not advisable so that, in order to find a solution of the control problem, the violation of some CVs constraints is admitted. In this way, a feasible solution is found that possibly *relaxes* one or more of the original set CVs constraints. Their *softening* is admitted in critical situations through the introduction of additional decision variables, represented by a nonnegative slack variables vector $\varepsilon_{yDO}(k) \in \mathbb{R}_0^{+n_{\varepsilon yDO}\times 1}$. In general, the minimum slack variables number is 1 (all CVs constraints *relaxations* are grouped), while the maximum one is $2\sum_{j=1}^{m_y}(H_p - H_{w_j} + 1)$. When $n_{\varepsilon yDO} = 2\sum_{j=1}^{m_y}(H_p - H_{w_j} + 1)$, each CVs *soft* constraint is equipped with an own slack variable. The slack variables vector has been introduced in the constraints (3.42) related to the generic jth CV at the ith prediction instant through nonnegative weights, contained in $\gamma_{lbyDO_j}(i) \in \mathbb{R}_0^{+1\times n_{\varepsilon yDO}}$ and $\gamma_{ubyDO_j}(i) \in \mathbb{R}_0^{+1\times n_{\varepsilon yDO}}$. $\gamma_{lbyDO_j}(i)$ and $\gamma_{ubyDO_j}(i)$ are vectors that could be characterized by at most an only nonzero positive element (on the correspondent position of the related slack variable in $\varepsilon_{yDO}(k)$). The slack variables vector has been introduced in the quadratic cost function (3.41) through a positive definite diagonal matrix $\rho_{yDO} \in \mathbb{R}^{n_{\varepsilon yDO}\times n_{\varepsilon yDO}}$. A joint setting of $\gamma_{lbyDO_j}(i)$, $\gamma_{ubyDO_j}(i)$, and ρ_{yDO} terms allows to suitably rank the importance of constraints *relaxations*, giving a priority order on CVs constraints.
H_p (clearly H_p is the same with respect to the parameter that is forwarded to *TOCS* and *Predictions Calculator* modules), H_u, M_i ($i = 1 \dots H_u$), $S(i)$, $Q(i)$, $R(i)$, $\gamma_{lbyDO_j}(i)$, $\gamma_{ubyDO_j}(i)$, ρ_{yDO}, $n_{\varepsilon yDO}$, and the grouping policies of CVs constraints *relaxations* are among *DO Tuning Parameters* of Fig. 3.1. They can be changed at different control instants.
At each control instant k, *DO* module solves the QP problem (3.41)-(3.42), computing $\Delta\hat{u}(k + M_i|k)$ ($i = 1 \dots H_u$) and $\varepsilon_{yDO}(k)$. Among computed MVs future values (3.13), only the first value $u(k) = \hat{u}(k|k) = u(k-1) + \Delta\hat{u}(k|k)$ is applied to the plant.

The problem (3.41)-(3.42) has been suitably parametrized as a function of the adopted decision variables vector, composed by $\Delta\hat{u}(k+M_i|k)$ $(i=1\dots H_u)$ and $\varepsilon_{yDO}(k)$.
The vector representing the MVs future values at the predictions instants related to the possibly nonzero MVs future moves, denoted by $\mathcal{U}_{H_u}(k) \in \mathbb{R}^{(l_u\cdot H_u)\times 1}$, can be expressed as:

$$\mathcal{U}_{H_u}(k) = \begin{bmatrix} \hat{u}(k+M_1|k) \\ \vdots \\ \hat{u}(k+M_{H_u}|k) \end{bmatrix} = \begin{bmatrix} \hat{u}(k|k) \\ \vdots \\ \hat{u}(k+M_{H_u}|k) \end{bmatrix} = span_{u-H_u}\cdot u(k-1) + mapping_{H_u-H_u}\cdot\Delta\mathcal{U}(k) \tag{3.43}$$

$$span_{u-H_u} = \begin{bmatrix} I_{l_u\times l_u} \\ I_{l_u\times l_u} \\ \vdots \\ I_{l_u\times l_u} \end{bmatrix} \in \mathbb{R}^{(l_u\cdot H_u)\times l_u} \tag{3.44}$$

where $mapping_{H_u-H_u} \in \mathbb{R}^{(l_u\cdot H_u)\times(l_u\cdot H_u)}$ is a submatrix of $mapping_{H_u-H_p}$ of (3.13).
For the expression of the problem (3.41)-(3.42) as a function of the selected decision variables, it is assumed $H_{w_j} = 1$ $(j = 1\dots m_y)$. Then, the adopted weights zeroing and constraints cut off policies will be described.
The cost function (3.41) can be formulated as:

$$V_{DO}(k) = \|\mathcal{Y}(k) - \mathcal{T}(k)\|^2_{\mathcal{Q}} + \|\Delta\mathcal{U}(k)\|^2_{\mathcal{R}} + \|\mathcal{U}_{H_u}(k) - \mathcal{U}_r(k)\|^2_{\mathcal{S}} + \|\varepsilon_{yDO}(k)\|^2_{\rho_{yDO}} \tag{3.45}$$

where $\mathcal{Y}(k)$, $\mathcal{U}_{H_u}(k)$, and $\Delta\mathcal{U}(k)$ are in (3.35), (3.43), (3.15) and

$$\mathcal{T}(k) = \begin{bmatrix} r(k+1|k) \\ \vdots \\ r(k+H_p|k) \end{bmatrix} \in \mathbb{R}^{(m_y\cdot H_p)\times 1} \tag{3.46}$$

$$\mathcal{U}_r(k) = \begin{bmatrix} u_r(k+M_1|k) \\ \vdots \\ u_r(k+M_{H_u}|k) \end{bmatrix} = \begin{bmatrix} u_r(k|k) \\ \vdots \\ u_r(k+M_{H_u}|k) \end{bmatrix} \in \mathbb{R}^{(l_u\cdot H_u)\times 1} \tag{3.47}$$

$$\mathcal{Q} = \begin{bmatrix} Q(1) & 0_{m_y\times m_y} & \cdots & 0_{m_y\times m_y} \\ 0_{m_y\times m_y} & Q(2) & \cdots & 0_{m_y\times m_y} \\ \vdots & \vdots & \ddots & \vdots \\ 0_{m_y\times m_y} & 0_{m_y\times m_y} & \cdots & Q(H_p) \end{bmatrix} \in \mathbb{R}^{(m_y\cdot H_p)\times(m_y\cdot H_p)} \tag{3.48}$$

$$\mathcal{R} = \begin{bmatrix} R(1) & 0_{l_u \times l_u} & \cdots & 0_{l_u \times l_u} \\ 0_{l_u \times l_u} & R(2) & \cdots & 0_{l_u \times l_u} \\ \vdots & \vdots & \ddots & \vdots \\ 0_{l_u \times l_u} & 0_{l_u \times l_u} & \cdots & R(H_u) \end{bmatrix} \in \mathbb{R}^{(l_u \cdot H_u) \times (l_u \cdot H_u)} \tag{3.49}$$

$$\mathcal{S} = \begin{bmatrix} S(1) & 0_{l_u \times l_u} & \cdots & 0_{l_u \times l_u} \\ 0_{l_u \times l_u} & S(2) & \cdots & 0_{l_u \times l_u} \\ \vdots & \vdots & \ddots & \vdots \\ 0_{l_u \times l_u} & 0_{l_u \times l_u} & \cdots & S(H_u) \end{bmatrix} \in \mathbb{R}^{(l_u \cdot H_u) \times (l_u \cdot H_u)} \tag{3.50}$$

Taking into account (3.46) and (3.37), the following term is defined [8]:

$$\mathcal{E}_y(k) = \mathcal{T}(k) - \mathcal{Y}(k)|_{\Delta\mathcal{U}(k)=0} \quad \in \mathbb{R}^{(m_y \cdot H_p) \times 1} \tag{3.51}$$

$\mathcal{E}_y(k)$ represents the future CVs tracking error if no MVs future moves are assumed. By analogy, taking into account (3.47), (3.44), the following term has been introduced in the proposed formulation:

$$\mathcal{E}_u(k) = \mathcal{U}_r(k) - span_{u-H_u} \cdot u(k-1) \quad \in \mathbb{R}^{(l_u \cdot H_u) \times 1} \tag{3.52}$$

$\mathcal{E}_u(k)$ represents the future MVs tracking error if no MVs future moves are assumed.
Exploiting (3.51) and (3.52), the expression (3.45) becomes:

$$\begin{aligned} &V_{DO}(k) = \|\mathcal{Y}(k) - \mathcal{T}(k)\|^2_{\mathcal{Q}} + \|\Delta\mathcal{U}(k)\|^2_{\mathcal{R}} + \|\mathcal{U}_{H_u}(k) - \mathcal{U}_r(k)\|^2_{\mathcal{S}} + \|\varepsilon_{yDO}(k)\|^2_{\rho_{yDO}} = \\ &= \|\Theta \cdot \Delta\mathcal{U}(k) - \mathcal{E}_y(k)\|^2_{\mathcal{Q}} + \|\Delta\mathcal{U}(k)\|^2_{\mathcal{R}} + \|mapping_{H_u-H_u} \cdot \Delta\mathcal{U}(k) - \mathcal{E}_u(k)\|^2_{\mathcal{S}} + \\ &+ \|\varepsilon_{yDO}(k)\|^2_{\rho_{yDO}} = (\Delta\mathcal{U}^T(k) \cdot \Theta^T - \mathcal{E}_y^T(k)) \cdot \mathcal{Q} \cdot (\Theta \cdot \Delta\mathcal{U}(k) - \mathcal{E}_y(k)) + \Delta\mathcal{U}^T(k) \cdot \mathcal{R} \cdot \Delta\mathcal{U}(k) + \\ &+ (\Delta\mathcal{U}^T(k) \cdot mapping^T_{H_u-H_u} - \mathcal{E}_u^T(k)) \cdot \mathcal{S} \cdot (mapping_{H_u-H_u} \cdot \Delta\mathcal{U}(k) - \mathcal{E}_u(k)) + \\ &+ \varepsilon_{yDO}(k)^T \cdot \rho_{yDO} \cdot \varepsilon_{yDO}(k) = \cdots = \\ &= \Delta\mathcal{U}^T(k) \cdot (\Theta^T \cdot \mathcal{Q} \cdot \Theta + \mathcal{R} + mapping^T_{H_u-H_u} \cdot \mathcal{S} \cdot mapping_{H_u-H_u}) \cdot \Delta\mathcal{U}(k) + \\ &+ (-2 \cdot \Theta^T \cdot \mathcal{Q} \cdot \mathcal{E}_y(k) - 2 \cdot mapping^T_{H_u-H_u} \cdot \mathcal{S} \cdot \mathcal{E}_u(k))^T \cdot \Delta\mathcal{U}(k) + \\ &+ \varepsilon_{yDO}(k)^T \cdot \rho_{yDO} \cdot \varepsilon_{yDO}(k) + const(k) \end{aligned} \tag{3.53}$$

where $const(k)$ represents a scalar that is known at each control instant k; it does not depend on the selected decision variables. $const(k)$ is given by:

$$const(k) = \mathcal{E}_y^T(k) \cdot \mathcal{Q} \cdot \mathcal{E}_y(k) + \mathcal{E}_u^T(k) \cdot \mathcal{S} \cdot \mathcal{E}_u(k) \tag{3.54}$$

The *DO* cost function (3.53) can be recast as the following QP standard cost function with respect to the selected decision variables [8]:

$$\min_{\theta} \frac{1}{2} \cdot \theta^T \cdot H \cdot \theta + f^T \cdot \theta \tag{3.55}$$

where

$$\theta = \begin{bmatrix} \Delta\mathcal{U}(k) \\ \varepsilon(k) \end{bmatrix} \tag{3.56}$$

$$H = 2 \cdot \begin{bmatrix} H_1 & 0_{(l_u \cdot H_u) \times n_{\varepsilon yDO}} \\ 0_{n_{\varepsilon yDO} \times (l_u \cdot H_u)} & \rho_{yDO} \end{bmatrix} \tag{3.57}$$

$$f = \begin{bmatrix} f_1 \\ 0_{n_{\varepsilon yDO} \times 1} \end{bmatrix} \tag{3.58}$$

where

$$\begin{aligned} H_1 &= \Theta^T \cdot \mathcal{Q} \cdot \Theta + \mathcal{R} + mapping_{H_u - H_u}^T \cdot \mathcal{S} \cdot mapping_{H_u - H_u} \quad \in \mathbb{R}^{(l_u \cdot H_u) \times (l_u \cdot H_u)} \\ f_1 &= -2 \cdot \Theta^T \cdot \mathcal{Q} \cdot \mathcal{E}_y(k) - 2 \cdot mapping_{H_u - H_u}^T \cdot \mathcal{S} \cdot \mathcal{E}_u(k) \quad \in \mathbb{R}^{(l_u \cdot H_u) \times 1} \end{aligned} \tag{3.59}$$

In order to obtain a general constrained standard QP form, also *DO* constraints (3.42), here reported,

$$\begin{aligned} &lb_{duDO}(i) \leq \Delta\hat{u}(k + M_i|k) \leq ub_{duDO}(i), \quad i = 1 \dots H_u \\ &lb_{uDO}(i) \leq \hat{u}(k + M_i|k) \leq ub_{uDO}(i), \quad i = 1 \dots H_u \\ &lb_{yDO_j}(i) - \gamma_{lbyDO_j}(i) \cdot \varepsilon_{yDO}(k) \leq \hat{y}_j(k + i|k) \leq ub_{yDO_j}(i) + \gamma_{ubyDO_j}(i) \cdot \varepsilon_{yDO}(k), \\ &\quad j = 1 \dots m_y, \; i = H_{w_j} \dots H_p \\ &\varepsilon_{yDO}(k) \geq 0_{n_{\varepsilon yDO} \times 1} \end{aligned}$$

are expressed as a function of the selected decision variables [8]. Remember the general assumption $H_{w_j} = 1$ ($j = 1 \dots m_y$).
The constraints related to $\Delta\hat{u}(k + M_i|k)$ variables can be expressed as

$$L \cdot [\Delta\hat{u}(k + M_1|k), \dots, \Delta\hat{u}(k + M_{H_u}|k)), \varepsilon_{yDO}(k), 1]^T \leq 0_{(2 \cdot l_u \cdot H_u) \times 1} \tag{3.60}$$

where

$$L = \begin{bmatrix} -I_{(l_u \cdot H_u)\times(l_u \cdot H_u)} & 0_{(l_u \cdot H_u)\times n_{\varepsilon yDO}} & lb_{duDO} \\ I_{(l_u \cdot H_u)\times(l_u \cdot H_u)} & 0_{(l_u \cdot H_u)\times n_{\varepsilon yDO}} & -ub_{duDO} \end{bmatrix} \in \mathbb{R}^{(2 \cdot l_u \cdot H_u)\times(l_u \cdot H_u + n_{\varepsilon yDO}+1)}$$

$$lb_{duDO} = \begin{bmatrix} lb_{duDO}(1) \\ lb_{duDO}(2) \\ \vdots \\ lb_{duDO}(H_u) \end{bmatrix} \in \mathbb{R}^{(l_u \cdot H_u)\times 1} \quad ub_{duDO} = \begin{bmatrix} ub_{duDO}(1) \\ ub_{duDO}(2) \\ \vdots \\ ub_{duDO}(H_u) \end{bmatrix} \in \mathbb{R}^{(l_u \cdot H_u)\times 1} \tag{3.61}$$

The following relationship holds:

$$L \cdot \begin{bmatrix} \Delta\mathcal{U}(k) \\ \varepsilon_{yDO}(k) \\ 1 \end{bmatrix} \leq 0_{(2 \cdot l_u \cdot H_u)\times 1} \tag{3.62}$$

L can be expressed as $L = [L_1 \;\; L_2 \;\; l_1]$, where $L_1 \in \mathbb{R}^{(2 \cdot l_u \cdot H_u)\times(l_u \cdot H_u)}$, $L_2 \in \mathbb{R}^{(2 \cdot l_u \cdot H_u)\times n_{\varepsilon yDO}}$, and $l_1 \in \mathbb{R}^{(2 \cdot l_u \cdot H_u)\times 1}$. L_1 and L_2 can be merged in a $W_u = [L_1 \;\; L_2] \in \mathbb{R}^{(2 \cdot l_u \cdot H_u)\times(l_u \cdot H_u + n_{\varepsilon yDO})}$. Furthermore we pose $w_u = -l_1 \in \mathbb{R}^{(2 \cdot l_u \cdot H_u)\times 1}$. Thus

$$L \cdot \begin{bmatrix} \theta \\ 1 \end{bmatrix} = \begin{bmatrix} W_u & -w_u \end{bmatrix} \cdot \begin{bmatrix} \theta \\ 1 \end{bmatrix} = W_u \cdot \theta - w_u \leq 0_{(2 \cdot l_u \cdot H_u)\times 1} \tag{3.63}$$

So the constraints related to $\Delta\hat{u}(k + M_i|k)$ variables can be expressed as

$$W_u \cdot \theta \leq w_u \tag{3.64}$$

The constraints related to $\hat{u}(k + M_i|k)$ variables can be expressed as

$$M \cdot \left[\hat{u}(k + M_1|k), \ldots, \hat{u}(k + M_{H_u}|k)), \varepsilon_{yDO}(k), 1\right]^T \leq 0_{(2 \cdot l_u \cdot H_u)\times 1} \tag{3.65}$$

where

$$M = \begin{bmatrix} -I_{(l_u \cdot H_u)\times(l_u \cdot H_u)} & 0_{(l_u \cdot H_u)\times n_{\varepsilon yDO}} & lb_{uDO} \\ I_{(l_u \cdot H_u)\times(l_u \cdot H_u)} & 0_{(l_u \cdot H_u)\times n_{\varepsilon yDO}} & -ub_{uDO} \end{bmatrix} \in \mathbb{R}^{(2 \cdot l_u \cdot H_u)\times(l_u \cdot H_u + n_{\varepsilon yDO}+1)}$$

$$lb_{uDO} = \begin{bmatrix} lb_{uDO}(1) \\ lb_{uDO}(2) \\ \vdots \\ lb_{uDO}(H_u) \end{bmatrix} \in \mathbb{R}^{(l_u \cdot H_u)\times 1} \quad ub_{uDO} = \begin{bmatrix} ub_{uDO}(1) \\ ub_{uDO}(2) \\ \vdots \\ ub_{uDO}(H_u) \end{bmatrix} \in \mathbb{R}^{(l_u \cdot H_u)\times 1} \tag{3.66}$$

The following relationship holds:

$$M\cdot\begin{bmatrix}\mathcal{U}_{H_u}(k)\\ \varepsilon_{yDO}(k)\\ 1\end{bmatrix}=M\cdot\begin{bmatrix}span_{u-H_u}\cdot u(k-1)+mapping_{H_u-H_u}\cdot\Delta\mathcal{U}(k)\\ \varepsilon_{yDO}(k)\\ 1\end{bmatrix}\leq 0_{(2\cdot l_u\cdot H_u)\times 1} \tag{3.67}$$

where $\mathcal{U}_{H_u}(k)$, $span_{u-H_u}$, and $mapping_{H_u-H_u}$ are given by (3.43), (3.44). M can be expressed as $M=[M_1 \;\; M_2 \;\; m_1]$, where $M_1\in\mathbb{R}^{(2\cdot l_u\cdot H_u)\times(l_u\cdot H_u)}$, $M_2\in\mathbb{R}^{(2\cdot l_u\cdot H_u)\times n_{\varepsilon yDO}}$, and $m_1\in\mathbb{R}^{(2\cdot l_u\cdot H_u)\times 1}$. Therefore

$$M_1\cdot span_{u-H_u}\cdot u(k-1)+M_1\cdot mapping_{H_u-H_u}\cdot\Delta\mathcal{U}(k)+M_2\cdot\varepsilon_{yDO}(k)+m_1\leq 0_{(2\cdot l_u\cdot H_u)\times 1}$$

$$M_1\cdot mapping_{H_u-H_u}\cdot\Delta\mathcal{U}(k)+M_2\cdot\varepsilon_{yDO}(k)\leq -M_1\cdot span_{u-H_u}\cdot u(k-1)-m_1$$

Finally

$$P_u\cdot\theta\leq p_u \tag{3.68}$$

where

$$P_u=\begin{bmatrix}M_1\cdot mapping_{H_u-H_u} & M_2\end{bmatrix}\in\mathbb{R}^{(2\cdot l_u\cdot H_u)\times(l_u\cdot H_u+n_{\varepsilon yDO})} \tag{3.69}$$

$$p_u=-M_1\cdot span_{u-H_u}\cdot u(k-1)-m_1 \quad\in\mathbb{R}^{(2\cdot l_u\cdot H_u)\times 1} \tag{3.70}$$

The constraints related to $\hat{y}(k+i|k)$ variables can be expressed as

$$N\cdot[\hat{y}(k+1|k),\ldots,\hat{y}(k+H_p|k)),\varepsilon_{yDO}(k),1]^T\leq 0_{(2\cdot m_y\cdot H_p)\times 1} \tag{3.71}$$

where

$$N = \begin{bmatrix} -I_{(m_y \cdot H_p)\times(m_y \cdot H_p)} & -\gamma_{lbyDO} & lb_{yDO} \\ I_{(m_y \cdot H_p)\times(m_y \cdot H_p)} & -\gamma_{ubyDO} & -ub_{yDO} \end{bmatrix} \in \mathbb{R}^{(2 \cdot m_y \cdot H_p)\times(l_u \cdot H_u + n_{\varepsilon yDO}+1)}$$

$$\gamma_{lbyDO} = \begin{bmatrix} \gamma_{lbyDO_1}(1) \\ \gamma_{lbyDO_2}(1) \\ \vdots \\ \gamma_{lbyDO_{m_y}}(1) \\ \gamma_{lbyDO_1}(2) \\ \gamma_{lbyDO_2}(2) \\ \vdots \\ \gamma_{lbyDO_{m_y}}(2) \\ \vdots \\ \vdots \\ \gamma_{lbyDO_1}(H_p) \\ \gamma_{lbyDO_2}(H_p) \\ \vdots \\ \gamma_{lbyDO_{m_y}}(H_p) \end{bmatrix} \quad \gamma_{ubyDO} = \begin{bmatrix} \gamma_{ubyDO_1}(1) \\ \gamma_{ubyDO_2}(1) \\ \vdots \\ \gamma_{ubyDO_{m_y}}(1) \\ \gamma_{ubyDO_1}(2) \\ \gamma_{ubyDO_2}(2) \\ \vdots \\ \gamma_{ubyDO_{m_y}}(2) \\ \vdots \\ \vdots \\ \gamma_{ubyDO_1}(H_p) \\ \gamma_{ubyDO_2}(H_p) \\ \vdots \\ \gamma_{ubyDO_{m_y}}(H_p) \end{bmatrix} \in \mathbb{R}^{(m_y \cdot H_p)\times n_{\varepsilon yDO}} \tag{3.72}$$

$$lb_{yDO} = \begin{bmatrix} lb_{yDO_1}(1) \\ lb_{yDO_2}(1) \\ \vdots \\ lb_{yDO_{m_y}}(1) \\ lb_{yDO_1}(2) \\ lb_{yDO_2}(2) \\ \vdots \\ lb_{yDO_{m_y}}(2) \\ \vdots \\ \vdots \\ lb_{yDO_1}(H_p) \\ lb_{yDO_2}(H_p) \\ \vdots \\ lb_{yDO_{m_y}}(H_p) \end{bmatrix} \in \mathbb{R}^{(m_y \cdot H_p)\times 1} \quad ub_{yDO} = \begin{bmatrix} ub_{yDO_1}(1) \\ ub_{yDO_2}(1) \\ \vdots \\ ub_{yDO_{m_y}}(1) \\ ub_{yDO_1}(2) \\ ub_{yDO_2}(2) \\ \vdots \\ ub_{yDO_{m_y}}(2) \\ \vdots \\ \vdots \\ ub_{yDO_1}(H_p) \\ ub_{yDO_2}(H_p) \\ \vdots \\ ub_{yDO_{m_y}}(H_p) \end{bmatrix} \in \mathbb{R}^{(m_y \cdot H_p)\times 1} \tag{3.73}$$

The following relationship holds:

$$N \cdot \begin{bmatrix} \mathcal{Y}(k) \\ \varepsilon_{yDO}(k) \\ 1 \end{bmatrix} = N \cdot \begin{bmatrix} \mathcal{Y}(k)|_{\Delta\mathcal{U}(k)=0} + \Theta\Delta\mathcal{U}(k) \\ \varepsilon_{yDO}(k) \\ 1 \end{bmatrix} \leq 0_{(2\cdot m_y \cdot H_p)\times 1} \tag{3.74}$$

where $\mathcal{Y}(k)$, $\mathcal{Y}(k)|_{\Delta\mathcal{U}(k)=0}$, and Θ are given by (3.35), (3.37), (3.34). N can be expressed as $N = [N_1 \;\; N_2 \;\; n_1]$, where $N_1 \in \mathbb{R}^{(2\cdot m_y \cdot H_p)\times(m_y \cdot H_p)}$, $N_2 \in \mathbb{R}^{(2\cdot m_y \cdot H_p)\times n_{\varepsilon yDO}}$, and $n_1 \in \mathbb{R}^{(2\cdot m_y \cdot H_p)\times 1}$. Therefore

$$N_1 \; \mathcal{Y}(k)|_{\Delta\mathcal{U}(k)=0} + N_1\Theta\Delta\mathcal{U}(k) + N_2\varepsilon_{yDO}(k) + n_1 \leq 0_{(2\cdot m_y \cdot H_p)\times 1}$$

$$N_1\Theta\Delta\mathcal{U}(k) + N_2\varepsilon_{yDO}(k) \leq -N_1 \; \mathcal{Y}(k)|_{\Delta\mathcal{U}(k)=0} - n_1$$

Finally

$$P_y \cdot \theta \leq p_y \tag{3.75}$$

where

$$P_y = \begin{bmatrix} N_1\Theta & N_2 \end{bmatrix} \in \mathbb{R}^{(2\cdot m_y \cdot H_p)\times(l_u \cdot H_u + n_{\varepsilon yDO})} \tag{3.76}$$

$$p_y = -N_1 \; \mathcal{Z}(k)|_{\Delta\mathcal{U}(k)=0} - n_1 \quad \in \mathbb{R}^{(2\cdot m_y \cdot H_p)\times 1} \tag{3.77}$$

The constraints related to $\varepsilon_{yDO}(k)$ vector can be expressed as

$$-\varepsilon_{yDO}(k) \leq 0_{n_{\varepsilon yDO}\times 1} \tag{3.78}$$

The following relationship holds:

$$O \cdot \begin{bmatrix} \Delta\mathcal{U}(k) \\ \varepsilon_{yDO}(k) \\ 1 \end{bmatrix} \leq 0_{n_{\varepsilon yDO}\times 1} \tag{3.79}$$

where

$$O = \begin{bmatrix} 0_{n_{\varepsilon yDO}\times(l_u \cdot H_u)} & -I_{n_{\varepsilon yDO}\times n_{\varepsilon yDO}} & 0_{n_{\varepsilon yDO}\times 1} \end{bmatrix} \in \mathbb{R}^{n_{\varepsilon yDO}\times(l_u \cdot H_u + n_{\varepsilon yDO}+1)} \tag{3.80}$$

O can be expressed as $O = [O_1 \;\; O_2 \;\; o_1]$, where $O_1 \in \mathbb{R}^{n_{\varepsilon yDO}\times(l_u \cdot H_u)}$, $O_2 \in \mathbb{R}^{n_{\varepsilon yDO}\times n_{\varepsilon yDO}}$, and $o_1 \in \mathbb{R}^{n_{\varepsilon yDO}\times 1}$. Finally

$$P_\varepsilon\theta \leq p_\varepsilon \tag{3.81}$$

where

$$P_\varepsilon = \begin{bmatrix} O_1 & O_2 \end{bmatrix} \in \mathbb{R}^{n_{\varepsilon yDO} \times (l_u \cdot H_u + n_{\varepsilon yDO})} \tag{3.82}$$

$$p_\varepsilon = -o_1 \quad \in \mathbb{R}^{n_{\varepsilon yDO} \times 1} \tag{3.83}$$

Given the expressions (3.64), (3.68), (3.75), and (3.81), the general expression of *DO* constraints is:

$$\left.\begin{aligned} W_u\theta \leq w_u \\ P_u\theta \leq p_u \\ P_y\theta \leq p_y \\ P_\varepsilon\theta \leq p_\varepsilon \end{aligned}\right\} \Rightarrow \Omega\theta \leq \omega \tag{3.84}$$

where

$$\begin{aligned} \Omega &= \begin{bmatrix} W_u \\ P_u \\ P_y \\ P_\varepsilon \end{bmatrix} \in \mathbb{R}^{(4 \cdot l_u \cdot H_u + 2 \cdot m_y \cdot H_p + n_{\varepsilon yDO}) \times (l_u \cdot H_u + n_{\varepsilon yDO})} \\ \omega &= \begin{bmatrix} w_u \\ p_u \\ p_y \\ p_\varepsilon \end{bmatrix} \in \mathbb{R}^{(4 \cdot l_u \cdot H_u + 2 \cdot m_y \cdot H_p + n_{\varepsilon yDO}) \times 1} \end{aligned} \tag{3.85}$$

Exploiting (3.55) and (3.84), the *DO* QP problem is solved using standard techniques, i.e. active-set or interior point algorithms [8].
In order to give the general *DO* QP formulation, the $H_{w_j} = 1$ $(j = 1 \dots m_y)$ assumption has been made. Really, for the generic jth CV, taking into account its H_{w_j} parameter that represents the first controllable prediction instant, all jth CV constraints related to the prediction instants $i < H_{w_j} (i \geq 1)$ are cut off by *DO* module. Similarly, all $Q_{(j,j)}(i)$ related to the prediction instants $i < H_{w_j} (i \geq 1)$ are zeroed by *DO* module. Note that, in *DO* cost function (3.41), even if $Q_{(j,j)}(i)$ related to the prediction instants $i < H_{w_j} (i \geq 1)$ are not zeroed, the QP problem decision variables optimal values do not change.
Furthermore, within *DO Tuning Parameters* of Fig. 3.1, in order to perform the desired CVs control methodology (with reference trajectories and/or with constraints), suitable weights zeroing and constraints cut off terms have been included.
Further weights zeroing and constraints cut off policies will be detailed in Section 3.2.

3.1.2 TOCS module

In the *DO* problem formulation described in the previous subsection, two terms, $r(k+i|k)$ and $u_r(k+M_i|k)$, representing the CVs and MVs reference trajecto-

ries, have been introduced (see (3.41)). In an industrial context, these terms are crucial parameters that strongly affect the plant performances; a proper setting of these terms can guarantee the reaching of a profitable economic/chemical operating point for the process. These reference signals may be manually set by operators based on their experience and skills. In order to overcome the limitations of plant operators' mental models, an optimization approach for the computation of the end terms of $r(k+i|k)$ and $u_r(k+M_i|k)$, i.e. $r(k+H_p|k)$ and $u_r(k+M_{H_u}|k)$, has been introduced. A *two-layer* MPC scheme has been adopted. As previously stated, the steady-state condition is supposed to be approached at the end of the prediction horizon H_p. The upper layer performs an online steady-state targets optimization, while the lower layer (i.e. *DO* module) performs an online quadratic, linear constrained, dynamic optimization as described in Subsection 3.1.1. At the upper layer of the proposed MPC scheme, a module has been developed, that provides correct and coherent *DO* module steady-state targets ($r(k+H_p|k)$ and $u_r(k+M_{H_u}|k)$). As additional design feature, this module, named *Targets Optimizing and Constraints Softening* (*TOCS*), computes correct and coherent steady-state constraints to be forwarded to the *DO* module.
As stated in Subsection 3.1.1, the steady-state assumption of the H_p definition represents the first consistency relationship between the *TOCS* and *DO* modules. In addition, the *TOCS* and *DO* modules (together with the overall APC scheme) run with the same sampling time and exploit the same basic linear process model (see (3.39)). So, to improve the consistency features between *DO* optimization problem and *TOCS* one, the proposed *TOCS* mathematical formulation considers CVs *free response* and $u(k-1)$ as starting points. In particular, because of the assumed relationship between the steady-state condition and the prediction horizon H_p, *TOCS* module has been based on the following expressions:

$$\hat{y}_{TOCS}(k) = \hat{y}(k+H_p|k)|_{\Delta\mathcal{U}(k)=0} + \Delta\hat{y}_{TOCS}(k) \tag{3.86}$$

$$\Delta\hat{y}_{TOCS}(k) = G_{yu}\Delta\hat{u}_{TOCS}(k) \tag{3.87}$$

$$\hat{u}_{TOCS}(k) = u(k-1) + \Delta\hat{u}_{TOCS}(k) \tag{3.88}$$

$\Delta\hat{y}_{TOCS}(k)$ and $\Delta\hat{u}_{TOCS}(k)$ represent the CVs and MVs steady-state change. $\hat{y}(k+H_p|k)|_{\Delta\mathcal{U}(k)=0}$ is the CVs *free response* at the end of the prediction horizon H_p and $\hat{y}_{TOCS}(k)$ and $\hat{u}_{TOCS}(k)$ are the CVs and MVs steady-state targets (values), respectively. Exploiting the CVs *free response*, DVs influence on the future process behavior is taken into account and an anticipative action can be obtained (see (3.35)). Based on (3.86), (3.88) and considering *DO* steady-state constraints, the following inequality constraints of *TOCS* optimization problem

can be derived:

$$
\begin{aligned}
&lb_{duTOCS} \leq \Delta\hat{u}_{TOCS}(k) \leq ub_{duTOCS} \\
&lb_{uTOCS} \leq \hat{u}_{TOCS}(k) \leq ub_{uTOCS} \\
&lb_{yTOCS} - \gamma_{lbyTOCS} \cdot \varepsilon_{lbyTOCS}(k) \leq \hat{y}_{TOCS}(k) \leq ub_{yTOCS} + \gamma_{ubyTOCS} \cdot \varepsilon_{ubyTOCS}(k) \\
&\varepsilon_{lbyTOCS}(k) \geq 0_{m_y \times 1} \\
&\varepsilon_{ubyTOCS}(k) \geq 0_{m_y \times 1}
\end{aligned}
\tag{3.89}
$$

In (3.89), the magnitude of MVs steady-state move is constrained by lb_{duTOCS} (lower constraint) and ub_{duTOCS} (upper constraint) and the magnitude of MVs steady-state value is constrained by lb_{uTOCS}(lower constraint) and ub_{uTOCS} (upper constraint). In the proposed formulation, coherently with *DO* one, lb_{duTOCS} terms are characterized by nonpositive values while ub_{duTOCS} are characterized by nonnegative values. Coherently with *DO* formulation, *TOCS* MVs constraints are considered as *hard* constraints: they can never be violated and their feasibility has been suitably imposed (see Section 3.3). In general, MVs constraints are considered always present and can change at different control instants.
In (3.89), the magnitude of CVs steady-state value is constrained by lb_{yTOCS} (lower constraint) and ub_{yTOCS} (upper constraint). In the proposed *TOCS* module formulation, CVs constraints are always present. All *TOCS* CVs constraints can change at different control instants. In order to prevent infeasibility situations, accordingly with *DO* formulation, *TOCS* CVs constraints can be assumed as *soft* constraints. Their *softening* is admitted in critical situations through the introduction of nonnegative slack variables, $\varepsilon_{lbyTOCS}(k)$ and $\varepsilon_{ubyTOCS}(k) \in \mathbb{R}_0^{+m_y \times 1}$. Differently from *DO* CVs constraints formulation (see (3.42)), *TOCS* CVs constraints *relaxations* are always structurally independent: each CV is equipped with two slack variables, also making always structurally independent the *TOCS relaxation* of its lower and upper constraints. The slack variables vectors have been introduced in the CVs constraints (3.89) through nonnegative weights, contained in $\gamma_{lbyTOCS}$, $\gamma_{ubyTOCS} \in \mathbb{R}_0^{+m_y \times m_y}$. $\gamma_{lbyTOCS}$ and $\gamma_{ubyTOCS}$ are matrices that are characterized by at most a single nonzero positive element for each row (on the correspondent position of the related slack variable in $\varepsilon_{lbyTOCS}(k)$ and $\varepsilon_{ubyTOCS}(k)$).
At each control instant k, *SCADA* system provides MVs move and MVs magnitude constraints over the control horizon H_u (Fig. 3.1, *u-y Constraints*). These constraints, that are possibly preprocessed by *TOCS* module (e.g. introducing a ramp change for feasibility achievement, see Section 3.3) in the same way they are possibly preprocessed by *DO* module, are $lb_{duDO}(i)$, $ub_{duDO}(i)$, $lb_{uDO}(i)$, and $ub_{uDO}(i)$; they represent the *DO* MVs constraints in (3.42). In order to guarantee a consistency between *TOCS* and *DO* MVs constraints, the following

relationships have been introduced:

$$\begin{aligned} lb_{duTOCS} &= \sum_{i=1}^{H_u} lb_{duDO}(i) \\ ub_{duTOCS} &= \sum_{i=1}^{H_u} ub_{duDO}(i) \\ lb_{uTOCS} &= lb_{uDO}(H_u) \\ ub_{uTOCS} &= ub_{uDO}(H_u) \end{aligned} \tag{3.90}$$

At each control instant k, *SCADA* system provides CVs constraints over the prediction horizon H_p (Fig. 3.1, *u-y Constraints*). These constraints, that are possibly preprocessed by *TOCS* module (e.g. introducing a ramp change, see Section 3.3), are indicated with $lb_{yop}(i)$ and $ub_{yop}(i)$ $(i = 1 \dots H_p)$. The last *TOCS-DO* consistency relationship in (3.89) is represented by the following equalities:

$$\begin{aligned} lb_{yTOCS} &= lb_{yop}(H_p) \\ ub_{yTOCS} &= ub_{yop}(H_p) \end{aligned} \tag{3.91}$$

where $lb_{yop}(H_p)$ and $ub_{yop}(H_p)$ represent the lower and upper constraints at the end of the prediction horizon H_p provided by *SCADA* system. In particular, they would represent the *DO* steady-state constraints if the *TOCS* module had not been included in the MPC scheme.
In order to formulate the *TOCS* optimization problem, the following linear cost function has been introduced:

$$V_{TOCS}(k) = c_u^T \cdot \Delta\hat{u}_{TOCS}(k) + c_y^T \cdot \Delta\hat{y}_{TOCS}(k) + \rho_{lbyTOCS}^T \cdot \varepsilon_{lbyTOCS}(k) + \rho_{ubyTOCS}^T \cdot \varepsilon_{ubyTOCS}(k) \tag{3.92}$$

The Linear Programming (LP) problem that characterizes the *TOCS* module is:

$$\begin{aligned} &\min_{\Delta\hat{u}_{TOCS}(k), \varepsilon_{lbyTOCS}(k), \varepsilon_{ubyTOCS}(k)} V_{TOCS}(k) = \\ &= \min_{\Delta\hat{u}_{TOCS}(k), \varepsilon_{lbyTOCS}(k), \varepsilon_{ubyTOCS}(k)} (c_u^T \cdot \Delta\hat{u}_{TOCS}(k) + c_y^T \cdot \Delta\hat{y}_{TOCS}(k) + \\ &+ \rho_{lbyTOCS}^T \cdot \varepsilon_{lbyTOCS}(k) + \rho_{ubyTOCS}^T \cdot \varepsilon_{ubyTOCS}(k)) \end{aligned} \tag{3.93}$$

subject to (3.89).
The introduced *TOCS* cost function allows to prioritize minimization and/or maximization directions for MVs and CVs, through the cost vectors $c_u \in \mathbb{R}^{l_u \times 1}$ and $c_y \in \mathbb{R}^{m_y \times 1}$ that weight the MVs and CVs steady-state move. The slack variables vectors $\varepsilon_{lbyTOCS}(k)$ and $\varepsilon_{ubyTOCS}(k)$ have been weighted in the linear cost function (3.93) through positive vectors $\rho_{lbyTOCS}$ and $\rho_{ubyTOCS} \in$

$\mathbb{R}^{+m_y \times 1}$. A joint setting of $\gamma_{lbyTOCS}$, $\gamma_{ubyTOCS}$, $\rho_{lbyTOCS}$, and $\rho_{ubyTOCS}$ terms allows to suitably rank the importance of constraints *relaxations*, giving a priority order on CVs constraints.
H_p, H_u (clearly H_p and H_u are the same with respect to those that are forwarded to *DO* and *Predictions Calculator* modules), c_u, c_y, $\gamma_{lbyTOCS}$, $\gamma_{ubyTOCS}$, $\rho_{lbyTOCS}$, and $\rho_{ubyTOCS}$ are among *TOCS Tuning Parameters* of Fig. 3.1. They can be changed at different control instants.
The constrained problem (3.93)-(3.89) has been suitably parametrized as a function of the adopted decision variables vector, composed by $\Delta\hat{u}_{TOCS}(k)$, $\varepsilon_{lbyTOCS}(k)$, and $\varepsilon_{ubyTOCS}(k)$.
The *TOCS* cost function can be recast as the following LP standard cost function with respect to the selected decision variables [8]:

$$\min_{\theta_{TOCS}} V_{TOCS}(k) = \min_{\theta_{TOCS}} f_{TOCS}^T \cdot \theta_{TOCS} \tag{3.94}$$

where

$$\theta_{TOCS} = \begin{bmatrix} \Delta\hat{u}_{TOCS}(k) \\ \varepsilon_{lbyTOCS}(k) \\ \varepsilon_{ubyTOCS}(k) \end{bmatrix} \quad \in \mathbb{R}^{(l_u+2\cdot m_y)\times 1} \tag{3.95}$$

$$f_{TOCS} = \begin{bmatrix} c_u^T + c_y^T G_{yu} & \rho_{lbyTOCS} & \rho_{ubyTOCS} \end{bmatrix}^T \quad \in \mathbb{R}^{(l_u+2\cdot m_y)\times 1} \tag{3.96}$$

In order to obtain a general constrained standard LP form, also *TOCS* constraints (3.89), here reported,

$lb_{duTOCS} \leq \Delta\hat{u}_{TOCS}(k) \leq ub_{duTOCS}$
$lb_{uTOCS} \leq \hat{u}_{TOCS}(k) \leq ub_{uTOCS}$
$lb_{yTOCS} - \gamma_{lbyTOCS} \cdot \varepsilon_{lbyTOCS}(k) \leq \hat{y}_{TOCS}(k) \leq ub_{yTOCS} + \gamma_{ubyTOCS} \cdot \varepsilon_{ubyTOCS}(k)$
$\varepsilon_{lbyTOCS}(k) \geq 0_{m_y \times 1}$
$\varepsilon_{ubyTOCS}(k) \geq 0_{m_y \times 1}$

have been expressed as a function of the selected decision variables.
At this regard, for the proposed *TOCS* formulation, additional matrices have been introduced, as detailed in the following.
The constraints related to $\Delta\hat{u}_{TOCS}(k)$ variable can be expressed as

$$W_{u_{TOCS}} \theta_{TOCS} \leq w_{u_{TOCS}} \tag{3.97}$$

where

$$W_{u_{TOCS}} = \begin{bmatrix} -I_{l_u \times l_u} & 0_{l_u \times (2\cdot m_y)} \\ I_{l_u \times l_u} & 0_{l_u \times (2\cdot m_y)} \end{bmatrix} \in \mathbb{R}^{(2\cdot l_u)\times(l_u+2\cdot m_y)} \tag{3.98}$$

$$w_{u_{TOCS}} = \begin{bmatrix} -lb_{duTOCS} \\ ub_{duTOCS} \end{bmatrix} \in \mathbb{R}^{(2 \cdot l_u) \times 1} \tag{3.99}$$

The constraints related to $\hat{u}_{TOCS}(k)$ variable can be expressed as

$$P_{u_{TOCS}} \theta_{TOCS} \leq p_{u_{TOCS}} \tag{3.100}$$

where

$$P_{u_{TOCS}} = \begin{bmatrix} -I_{l_u \times l_u} & 0_{l_u \times (2 \cdot m_y)} \\ I_{l_u \times l_u} & 0_{l_u \times (2 \cdot m_y)} \end{bmatrix} \in \mathbb{R}^{(2 \cdot l_u) \times (l_u + 2 \cdot m_y)} \tag{3.101}$$

$$p_{u_{TOCS}} = \begin{bmatrix} u(k-1) - lb_{duTOCS} \\ -u(k-1) + ub_{duTOCS} \end{bmatrix} \in \mathbb{R}^{(2 \cdot l_u) \times 1} \tag{3.102}$$

The constraints related to $\hat{y}_{TOCS}(k)$ variable can be expressed as

$$P_{y_{TOCS}} \cdot \theta_{TOCS} \leq p_{y_{TOCS}} \tag{3.103}$$

where

$$P_{y_{TOCS}} = \begin{bmatrix} -G_{yu} & -diag(\gamma_{lbyTOCS}) & 0_{m_y \times m_y} \\ G_{yu} & 0_{m_y \times m_y} & -diag(\gamma_{ubyTOCS}) \end{bmatrix} \in \mathbb{R}^{(2 \cdot m_y) \times (l_u + 2 \cdot m_y)} \tag{3.104}$$

$$p_{y_{TOCS}} = \begin{bmatrix} \hat{y}(k + H_p|k)|_{\Delta \mathcal{U}(k)=0} - lb_{yTOCS} \\ -\hat{y}(k + H_p|k)|_{\Delta \mathcal{U}(k)=0} + ub_{yTOCS} \end{bmatrix} \in \mathbb{R}^{(2 \cdot m_y) \times 1} \tag{3.105}$$

where $diag(a) \in \mathbb{R}^{p \times p}$ represents a diagonal matrix with the elements of $a \in \mathbb{R}^{p \times 1}$ on the main diagonal.
The constraints related to $\varepsilon_{lbyTOCS}(k)$ and $\varepsilon_{ubyTOCS}(k)$ variables can be expressed as

$$P_{\varepsilon_{TOCS}} \cdot \theta_{TOCS} \leq p_{\varepsilon_{TOCS}} \tag{3.106}$$

where

$$P_{\varepsilon_{TOCS}} = \begin{bmatrix} 0_{m_y \times l_u} & -I_{m_y \times m_y} & 0_{m_y \times m_y} \\ 0_{m_y \times l_u} & 0_{m_y \times m_y} & -I_{m_y \times m_y} \end{bmatrix} \in \mathbb{R}^{(2 \cdot m_y) \times (l_u + 2 \cdot m_y)} \tag{3.107}$$

$$p_{\varepsilon_{TOCS}} = \begin{bmatrix} 0_{m_y \times 1} \\ 0_{m_y \times 1} \end{bmatrix} \in \mathbb{R}^{(2 \cdot m_y) \times 1} \tag{3.108}$$

Given the expressions (3.97), (3.100), (3.103), and (3.106), the general expression of *TOCS* constraints is:

$$\left.\begin{array}{l} W_{u_{TOCS}}\theta_{TOCS} \leq w_{u_{TOCS}} \\ P_{u_{TOCS}}\theta_{TOCS} \leq p_{u_{TOCS}} \\ P_{y_{TOCS}}\theta_{TOCS} \leq p_{y_{TOCS}} \\ P_{\varepsilon_{TOCS}}\theta_{TOCS} \leq p_{\varepsilon_{TOCS}} \end{array}\right\} \Rightarrow \Omega_{TOCS}\theta_{TOCS} \leq \omega_{TOCS} \tag{3.109}$$

where

$$\begin{aligned} \Omega_{TOCS} &= \begin{bmatrix} W_{u_{TOCS}} \\ P_{u_{TOCS}} \\ P_{y_{TOCS}} \\ P_{\varepsilon_{TOCS}} \end{bmatrix} \in \mathbb{R}^{(4\cdot l_u + 4\cdot m_y)\times(l_u + 2\cdot m_y)} \\ \omega_{TOCS} &= \begin{bmatrix} w_u \\ p_u \\ p_y \\ p_\varepsilon \end{bmatrix} \in \mathbb{R}^{(4\cdot l_u + 4\cdot m_y)\times 1} \end{aligned} \tag{3.110}$$

Exploiting (3.94) and (3.109), the *TOCS* LP problem is solved using standard techniques, e.g. simplex or interior point algorithms [8].
Weights zeroing and constraints cut off policies in the *TOCS* LP problem will be detailed in Section 3.2.
TOCS module, at each control instant k, solving its LP problem, optimally computes $\Delta\hat{u}_{TOCS}(k)$, $\varepsilon_{lbyTOCS}(k)$, and $\varepsilon_{ubyTOCS}(k)$ vectors. Based on (3.86) and (3.88), the CVs and MVs steady-state targets are obtained. They are forwarded to *DO* (Fig. 3.1, *u-y Target*) and represent the end points of *DO* CVs and MVs reference trajectories in (3.41):

$$\begin{aligned} r(k + H_p|k) &= \hat{y}_{TOCS}(k) \\ u_r(k + M_{H_u}|k) &= \hat{u}_{TOCS}(k) \end{aligned} \tag{3.111}$$

The relationships of (3.111) represent the first *TOCS-DO* cooperation policy. Due to the steady-state optimization performed by *TOCS* module and due to the imposed consistency constraints between *TOCS* and *DO* formulations, the computed $r(k + H_p|k)$ and $u_r(k + M_{H_u}|k)$ steady-state values are reachable targets, i.e. *DO* module, through a suitable tuning and management of its QP problem, can effectively lead the process to this operating point. If in *DO* module formulation there are no CVs constraints, i.e. the CVs are controlled through tracking of the computed reference trajectories (see Section 3.3), the defined first *TOCS-DO* cooperation policy represents the only expedient needed to guarantee the reachability of the *TOCS*-computed steady-state targets. On the other hand, if in *DO* module formulation some CVs constraints are included, these constraints must be coherent with the *TOCS*-computed CVs

steady-state targets and steady-state constraints. In fact, during the driving of a process, in some abnormal situations, e.g. caused by improper operators' maneuvers and settings or by process critical conditions, the CVs constraints over the prediction horizon H_p (Fig. 3.1, *u-y Constraints*) provided by *SCADA* system and possibly preprocessed by *TOCS* module (e.g. introducing a ramp change, see Section 3.3) may result not coherent with the chemical, physical, or safety principles of the plant to be controlled. Given these considerations, a protection against these unexpected events must be introduced: ignoring this potential problem can result in driving the process towards dangerous and/or inefficient transient states. From *DO* module formulation point of view, this fact leads to CVs constraints that are not coherent with the desired steady-state configuration and the resulting incorrect conflicting objectives may affect the promptness and the correctness of the overall control action. So, to guarantee a correct *DO* optimization problem statement in all conditions, its steady-state targets and constraints need to be properly set. The first cooperation mode guarantees, as already pointed out, the reachability of the *TOCS*-computed *DO* steady-state targets. In order to ensure correct *DO* CVs constraints, an additional *TOCS-DO* cooperation policy has been introduced. *TOCS* module, at each control instant k, solving its LP problem, besides $\Delta\hat{u}_{TOCS}(k)$, computes also $\varepsilon_{lbyTOCS}(k)$ and $\varepsilon_{ubyTOCS}(k)$ vectors. Based on these values, *TOCS* module possibly modifies the CVs constraints over the prediction horizon H_p (Fig. 3.1, *u-y Constraints*) provided by *SCADA* system and possibly preprocessed by *TOCS* module (e.g. introducing a ramp change, see Section 3.3) itself before solving its LP problem ($lb_{yop}(i)$ and $ub_{yop}(i)$ ($i=1\dots H_p$)). The modified CVs constraints become the *DO* CVs constraints (Fig. 3.1, *y Constraints*) that will be (possibly) used in its QP problem (3.41)-(3.42).
In the proposed formulation, these CVs constraints are computed by *TOCS* module through the following expressions:

$$\begin{aligned} lb_{yDO_j}(i) &= \min(lb_{yop_j}(i), lb_{yTOCS_j} - \gamma_{lbyTOCS_j} \cdot \varepsilon_{lbyTOCS}(k)) \\ ub_{yDO_j}(i) &= \max(ub_{yop_j}(i), ub_{yTOCS_j} + \gamma_{ubyTOCS_j} \cdot \varepsilon_{ubyTOCS}(k)) \\ j &= 1 \dots m_y,\ i = H_{w_j} \dots H_p \end{aligned} \tag{3.112}$$

where min and max represent the minimum and maximum operation between scalars. $lb_{yop_j}(i)$ and $ub_{yop_j}(i)$ refer to the jth CV at the ith prediction instant; lb_{yTOCS_j} and ub_{yTOCS_j} are the jth CV constraints used in *TOCS* LP problem, while $\gamma_{lbyTOCS_j}$ and $\gamma_{ubyTOCS_j}$ represent the jth row of $\gamma_{lbyTOCS}$ and $\gamma_{ubyTOCS}$.
Therefore, the just detailed second *TOCS-DO* cooperation policy consists of a possible CVs constraints *pre-softening* (*pre-relaxation*). Note that, through this additional feature, *DO* CVs *relaxations* caused by the steady-state *DO* CVs

constraints will be zero.
The overall *TOCS-DO* cooperation, together with the introduced consistency relationships, ensures a correct management of targets and constraints in all conditions.
According to the author knowledge, the proposed cooperation improvement in a *two-layer* MPC scheme represents a contribution of the research activity reported in the present dissertation [72], [73].

3.2 Data Conditioning & Decoupling Selector block

Data Conditioning & Decoupling Selector (*DC & DS*) block represents an auxiliary supervision block that strictly cooperates with the proposed *two-layer* MPC scheme in Fig. 3.1. *DC & DS* block exploits updated plant measurements (Fig. 3.1, $u(k-1)$, $d(k-1)$, $y(k)$) and local control loops information (Fig. 3.1, *Plant Signals & Parameters*). Together with this information, a status value for each process variable is defined, that allows to specify the variables to be included in the MPC control problem at the current control instant. In fact, in the development of the controller formulation, it was necessary to take into account a particular feature of the daily running of industrial control processes. In the conduction of these processes it is not unusual that operators decide to "exclude" from the automatic controller setup one or more variables in order, for example, to manually operate on it/them; possibly, this/these variable/s will be returned to the automatic controller setup after a time period. The introduction of the status information in the formulation allows simplifying the handling of this feature within a single problem formulation. In addition, *DC & DS* block performs suitable processing and checking algorithms on field data and possibly, if abnormal situations are detected, *SCADA* status information is processed and the final status value for each variable is suitably set. Status definition and handling will be detailed in Subsection 3.2.2.
Furthermore, *DC & DS* block implements a decoupling strategy that, suitably forwarded to the MPC scheme, enables a selection on which MVs have to be exploited for controlling each single CV. In particular, as it will be detailed, an alternative equivalent approach with respect to common industrial practices has been introduced and a direct connection between the decoupling strategy and the status definition has been defined [74].

3.2.1 Decoupling Strategy

Typically, the control of a generic CV can be performed through the MVs tied to that CV: this information is contained in the G_{yu} CVs-MVs steady-state gain matrix. In the general case, for the generic ith CV, all MVs tied to it can

act for the satisfaction of its specifications. In order to give additional degrees of freedom, a suitable decoupling strategy that is not dependent on the tuning parameters has been introduced: this strategy enables a selection on which MVs to exploit for controlling each single CV; in this way, an inhibition of the action of given MVs on such CVs is obtained.
In the present research work, two different approaches to the MVs action inhibition problem are proposed and discussed. The first approach modifies the setup of the initial control problem, following a typical industrial practice. In this case, as it will be clarified in the sequel, the original CVs-MVs and CVs-DVs transfer matrices are modified and a new control problem is formulated. In the research activity reported in the present dissertation an alternative equivalent decoupling methodology has been successively proposed that, not requiring the modification of the original setup of the control problem, allows a more intuitive and straight approach, especially in the cases where the considered specifications may be required to be online changed.
Consider a control problem consisting of l_u MVs, l_d DVs, and m_y CVs. A binary matrix B_{yu} defined by the following logical computation is introduced:

$$B_{yu} = op_{\neq}(G_{yu}, 0_{m_y \times l_u}) \tag{3.113}$$

The generic (i, j) element of B_{yu} matrix is equal to 1 if there is a nonzero relationship between the jth MV and the ith CV, otherwise it is equal to 0. The $op_{\neq}(\cdot, \cdot)$ indicates the matrix element-wise inequality logical operation.
An *ad hoc* mathematical formulation developed for the implementation of the first approach is now described. Let denote by p the number of MVs to be *inhibited* for the control of at least one CV. p can be easily determined from the B_{yu} matrix (each MV can be counted maximum once). The generic jth MV can be *inhibited* if in the jth column of B_{yu} matrix there is at least a row i (related to ith CV) for which both the following conditions hold:

- the generic (i, j) element of B_{yu} is nonzero;
- the control specifications require the inhibition of the jth MV control actions for the ith CV.

After the determination of the p value, together with the information on all pairs CV-MV to inhibit, the initial CVs-MVs transfer matrix is modified by zeroing each (i, j) element to inhibit. Then, the p selected MVs are duplicated as DVs, thus resulting in a new $(m_y \times (l_d + p))$ CVs-DVs transfer matrix and the removed MV-CVs transfer functions are restored in each of the added p columns. In this way, the original CVs-MVs and CVs-DVs transfer matrices are modified and a new control problem is obtained.
An illustrative example is proposed. We assume that in the initial control problem $l_u = 2$ (MVs), $l_d = 1$ (DVs), and $m_y = 3$ (CVs); the CVs-MVs and

CVs-DVs mapping matrices reported in Tables 3.1-3.2 are assumed (a nonzero relationship has been indicated by a cross).

Table 3.1: Initial CVs-MVs setup of Decoupling Strategy illustrative example.

Variable	MV_1	MV_2
CV_1		X
CV_2	X	X
CV_3	X	X

Table 3.2: Initial CVs-DVs setup of Decoupling Strategy illustrative example.

Variable	DV_1
CV_1	X
CV_2	X
CV_3	X

Assume that the control specifications require the inhibition of MV_2 for the control of CV_1. In this case, starting from initial (3×2) CVs-MVs and (3×1) CVs-DVs transfer matrices, the B_{yu} matrix is:

$$B_{yu} = \begin{bmatrix} 0 & 1 \\ 1 & 1 \\ 1 & 1 \end{bmatrix}$$

From B_{yu} matrix, we have $p = 1$; from the described procedure, the CVs-MVs and CVs-DVs mapping matrices reported in Tables 3.1-3.2 are modified as in Tables 3.3-3.4. The new setup of the control problem gives rise to a modified (3×2) CVs-MVs transfer matrix and to a new (3×2) CVs-DVs transfer matrix. From an MPC formulation point of view, this decoupling approach aims to exploit, at a generic control instant k, all MVs past information up to k in the

Table 3.3: Modified CVs-MVs setup of Decoupling Strategy illustrative example.

Variable	MV_1	MV_2
CV_1		
CV_2	X	X
CV_3	X	X

Table 3.4: Modified CVs-DVs setup of Decoupling Strategy illustrative example.

Variable	DV_1	$DV_2(MV_2)$
CV_1	X	**X**
CV_2	X	
CV_3	X	

free response computation over H_p (3.37) of a generic CV. Therefore, the MVs that are *inhibited* for a generic CV only affect its *free response* computation over H_p; so the MVs that are *inhibited* for a generic CV are considered as fictitious DVs. With regard to the "forced" (i.e. those that depend on the MVs future moves) components of the CV predictions, only the future moves related to the MVs that are *not inhibited* for the control of the considered CV are taken into account.

The second decoupling approach does not modify the original setup of the control problem, but it aims to fully exploit the information and the structure of matrix Θ in (3.38) and of matrix G_{yu} in (3.86). These matrices properly introduce the *DO* MVs future moves, $\Delta\hat{u}(k + M_i|k)$ $(i = 1 \dots H_u)$, and the *TOCS* MVs steady-state move, $\Delta\hat{u}_{TOCS}(k)$, in the "forced" (i.e. those that depend on the MVs future moves) components of CVs predictions related to *DO* and *TOCS* formulations.

The definition of a *Decoupling Matrix* $D_E \in \mathbb{R}^{m_y \times l_u}$ is performed; an (i, j) element of the D_E matrix is set to 0 if both the following conditions hold:

- the generic (i, j) element of B_{yu} is nonzero;
- the control specifications require the inhibition of the jth MV control actions for the ith CV.

The generic (i, j) element is equal to 1, otherwise.

SCADA system, at each control instant k, forwards the described *Decoupling Matrix* D_E to *DC & DS* block (Fig. 3.1, right side of *Data Conditioning & Decoupling Selector* block, *Decoupling Matrix*). The initial *Decoupling Matrix* D_E can change at different control instants, according to the control specifications.

With respect to the example discussed in Tables 3.1-3.2, the introduced *Decoupling Matrix* D_E is reported in Table 3.5.

The proof of the equivalence between the common decoupling industrial practice and the introduced approach is based on the definition of the CVs *free response* over the prediction horizon H_p.

Assuming that all MVs and CVs have to be considered in the MPC problem at the generic control instant k, the D_E matrix can be straightly included in the

Table 3.5: Proposed *Decoupling Matrix* of Decoupling Strategy illustrative example.

Variable	MV_1	MV_2
CV_1	1	**0**
CV_2	1	1
CV_3	1	1

formulation of *DO* and *TOCS* modules.
With regard to *DO* formulation, (3.38) is modified as in the following:

$$\begin{aligned} \hat{y}(k+i|k) &= \hat{y}(k+i|k)|_{\Delta\mathcal{U}(k)=0} + \Delta\hat{y}(k+i|k) \\ \Delta\hat{y}(k+i|k) &= (\Theta_{(((i-1)\cdot m_y+1:i\cdot m_y),:)} \circ D_E^{ext})\Delta\mathcal{U}(k) \end{aligned} \tag{3.114}$$

where $\circ$ indicates the element-wise product between matrices and D_E^{ext} is given by:

$$D_E^{ext} = (1_{1\times H_u}) \otimes D_E \quad \in \mathbb{R}^{m_y\times(l_u\cdot H_u)} \tag{3.115}$$

In (3.115) $1_{a\times b}$ indicates a $(a \times b)$ matrix composed by elements all equal to 1 and $\otimes$ indicates the Kronecker product between matrices. Practically, the D_E matrix is introduced in (3.38) through a D_E^{ext} matrix that modifies the original Θ matrix.
Furthermore, for an overall correct introduction of the D_E matrix in the *DO* formulation, also the general definition of the H_{w_j} parameter reported in (3.40) must be revised. For the generic jth CV, the H_{w_j} indicated the first prediction instant on which the first MVs future move (contained in $\Delta\hat{u}(k|k)$ vector) related to at least one MV tied to the jth CV will be active. The modified definition is: for the generic jth CV, the H_{w_j} indicated the first prediction instant on which the first MVs future move (contained in $\Delta\hat{u}(k|k)$ vector) related to at least one MV tied to the jth CV and *not inhibited* for controlling the jth CV will be active.
The revised H_{w_j} parameter can be determined from the modified Θ matrix: considering the H_p Θ rows related to the jth CV and taking into account only the l_u Θ columns related to $\Delta\hat{u}(k|k)$ (i.e. the first l_u Θ columns), H_{w_j} is equal to the index of the first row where there is at least a nonzero entry. Furthermore, the revised H_{w_j} can also be determined through the following updated version of (3.40):

$$H_{w_j} = \min(D_{yu_{(j,mask_j)}}) + 1 \tag{3.116}$$

where in this case $mask_j$ is a vector that indicates the D_{yu} columns related to the MVs that are tied to the jth CV and that are *not inhibited* for controlling the jth CV.
Given the above considerations, for each jth CV, the relative H_{w_j} parameter can change at different control instants. Consequently, the weights zeroing and constraints cut off policies described in Subsection 3.1.1 are updated.
In order to include the D_E matrix in *TOCS* formulation, (3.86) is modified as in the following:

$$\hat{y}_{TOCS}(k) = \hat{y}(k + H_p|k)|_{\Delta\mathcal{U}(k)=0} + \Delta\hat{y}_{TOCS}(k) \tag{3.117}$$

$$\Delta\hat{y}_{TOCS}(k) = (G_{yu} \circ D_E)\Delta\hat{u}_{TOCS}(k) \tag{3.118}$$

where $\circ$ indicates the element-wise product between matrices. Practically, the D_E matrix modifies the original G_{yu} matrix in (3.86).
It can be concluded that the introduced second decoupling approach allows a more intuitive and straight handling of the related MVs inhibition specifications in the MPC formulation, especially in the cases where these specifications may be required to be online changed.
According to the author knowledge, the proposed alternative decoupling strategy, based on the online definition of a *Decoupling Matrix* D_E represents a contribution of the research activity reported in the present dissertation [75].

3.2.2 Process variables status definition

An APC system must be able to manage, in the best manner, process variables in all process conditions. For example, the exclusion of some process variables could be necessary based on *ad hoc* plant needs (e.g. direct operators intervention), on the detection of bad situations (e.g. hardware devices failures), or of local control loops faults [28], [30], [76], [77]. As introduced at the beginning of the present section, in the designed APC framework, for each process variable involved in the initial MPC setup, a status value has been introduced. Status values are different for CVs, MVs, and DVs and can change at different control instants [78].

CV status

At each control instant k, CVs updated plant measurements are provided by *SCADA* system to *DC & DS* block (Fig. 3.1, right side of *DC & DS* block, $y(k)$). *DC & DS* block possibly modifies $y(k)$ value (e.g. performing a filtering action), obtaining the $y(k)$ value that will be exploited in the MPC scheme for feedback inclusion (Fig. 3.1, left side of *DC & DS* block, $y(k)$). Filtering parameters have been included in *Plant Signals & Parameters* of Fig. 3.1.

For each CV, two possible status values have been assumed: "1" and "0". A status value equal to "1" indicates that the MPC scheme must have in control that variable, i.e. the CV is *active*. Conversely, a CV status value equal to "0" indicates that the CV is *inactive*: at the current control instant the MPC scheme has not in control that CV, i.e. MVs must not act to satisfy its specifications.
At each control instant k, *SCADA* system provides an initial status value for each CV (Fig. 3.1, right side of *DC & DS* block, *u-d-y Status*). The initial status value takes into account plant driving specifications and needs, together with particular CVs plant conditions. Particular CVs plant conditions may refer, for example, to the substitution of its sensor device. The initial CVs status is included in a $Status_{ySCADA} \in \mathbb{R}^{m_y \times 1}$ vector; its values are "0" for the CVs that have been set as *inactive* ("1", otherwise). As additional task , *DC & DS* block performs bad detection on the $y(k)$ value: the meeting of the CVs validity bounds is verified, together with the compliance of the rate of change bounds (spikes) and of the freezing percentage associated to each CV. Bad detection results are grouped in a $Status_{yBAD} \in \mathbb{R}^{m_y \times 1}$ vector. When positive results for a generic CV are notified by the bad detection procedure, its status value in $Status_{yBAD}$ vector is set to "0" ("1" otherwise). The final CVs status value (Fig. 3.1, left side of *DC & DS* block, *u-d-y Status*) is defined by an element-wise logical "AND" between $Status_{ySCADA}$ vector, $Status_{yBAD}$ vector, and an additional vector that takes into account the relationship between the MVs status value and the CVs status value (see 3.2.2).

MV status

At each control instant k, MVs updated plant measurements are provided by *SCADA* system to *DC & DS* block (Fig. 3.1, right side of *DC & DS* block, $u(k-1)$). Given the industrial application purposes of the designed APC framework, MVs typically provide set-points to local control loops based on standalone controllers (e.g. PI or PID). The related variables that constitute the outputs of the local control loops are reported in $u_{pv}(k-1) \in \mathbb{R}^{l_u \times 1}$ (the same measurement units and the same physical meaning are assumed between u and u_{pv}). $u_{pv}(k-1)$ is contained in *Plant Signals & Parameters* term of Fig. 3.1. *DC & DS* block possibly modifies $u_{pv}(k-1)$ value (e.g. performing a filtering action). Filtering parameters have been included in *Plant Signals & Parameters* of Fig. 3.1. Among MVs, the variables that not support a local control loop are always characterized by the equality between the set-point and the output.
For each MV, three possible status values have been assumed: "1", "0", and "-1". A status value equal to "1" indicates that at the current control instant that MV is *active*, i.e. it is used for control purposes by *MPC* block, and its

final $u(k-1)$ value (Fig. 3.1, left side of *DC & DS* block) has to be exploited for CVs *free response* (see (3.37)) computation. Status values "0" and "−1" indicate that at the current control instant that MV has not to be used in *MPC* block, i.e. the *DO*-computed MVs future moves and the *TOCS*-computed MVs steady-state move must be zero. Practically, an MV with status value "0" or "−1" is considered in *MPC* block as a DV. Moreover, for a generic MV, status value "0" indicates that its final value in $u(k-1)$ vector (Fig. 3.1, left side of *DC & DS* block) must not be used for CVs *free response* (see (3.37)) computation, differently from "1" and "−1" status values.
At each control instant k, *SCADA* system provides an initial status value for each MV (Fig. 3.1, right side of *DC & DS* block, *u-d-y Status*). The initial status value takes into account plant driving specifications and needs, together with particular MVs plant conditions. Particular MVs plant conditions may refer, for example, to the substitution of an actuator. The initial MVs status is included in a $Status_{uSCADA} \in \mathbb{R}^{l_u \times 1}$ vector; its values are "0" or "−1" for the MVs that have been set as *inactive* ("1" otherwise). For example, when an actuator is faulted, "0" is set; on the other hand, whenever an operator decides to take in control an MV, a value of "−1" is set as MV initial status. Moreover, when, for an MV that provides a set-point to a local control loop, the related values in $u(k-1)$ and in $u_{pv}(k-1)$ differ by more than a defined threshold, a value of "−1" is set. In this *deviation* case (deviation between elements in $u(k-1)$ and $u_{pv}(k-1)$ related to a generic MV), *DC & DS* block replaces the field value in $u(k-1)$ with the related element of $u_{pv}(k-1)$. This information is provided to *DC & DS* block by *SCADA* system that includes *deviation* flags in *Plant Signals & Parameters* term of Fig. 3.1.
DC & DS block, analyzing the final $u_{pv}(k-1)$ value, applies bad detection procedures: the meeting of the MVs validity bounds is verified, together with the compliance of the rate of change bounds (spikes) and of the freezing percentage associated with each MV. Bad detection results are grouped in a $Status_{uBAD} \in \mathbb{R}^{l_u \times 1}$ vector. When positive results for a generic MV are notified by bad detection, its status value in $Status_{uBAD}$ vector is set to "0" ("1" otherwise). The final MVs status value (Fig. 3.1, left side of *DC & DS* block, *u-d-y Status*) is defined by a truth table, taking into account $Status_{uSCADA}$ vector, $Status_{uBAD}$ vector, and an additional vector that takes into account the relationship between the CVs status value and the MVs status value (see 3.2.2).

DV status

At each control instant k, DVs updated plant measurements are provided by *SCADA* system to *DC & DS* block (Fig. 3.1, right side of *DC & DS* block, $d(k-1)$). As previously mentioned for MVs, also DVs, in industrial applica-

tions, typically provide set-points to local control loops based on standalone controllers. The related variables that constitute the outputs of the local control loops are reported in $d_{pv}(k-1) \in \mathbb{R}^{l_d \times 1}$ (the same measurement units and the same physical meaning are assumed between d and d_{pv}). $d_{pv}(k-1)$ is contained in *Plant Signals & Parameters* term of Fig. 3.1. *DC & DS* block possibly modifies $d_{pv}(k-1)$ value (e.g. performing a filtering action). Filtering parameters have been included in *Plant Signals & Parameters* of Fig. 3.1. Among DVs, the variables that not support a local control loop are always characterized by the equality between the set-point and the output.
For each DV, two possible status values have been assumed: "1" (*active*) or "0" (*inactive*). For a generic DV, its final $d(k-1)$ value (Fig. 3.1, left side of *DC & DS* block) has to be exploited for CVs *free response* (see (3.37)) computation only when its status value is "1".
At each control instant k, *SCADA* system provides an initial status value for each DV (Fig. 3.1, right side of *DC & DS* block, *u-d-y Status*). The initial status value takes into account particular DVs plant conditions. Particular DVs plant conditions may refer, for example, to the substitution of an actuator. The initial DVs status is included in a $Status_{dSCADA} \in \mathbb{R}^{l_d \times 1}$ vector; its value is "0" for the DVs that have been set as *inactive* ("1" otherwise). For example, when an actuator is faulted, a "0" value is set. Furthermore, when, for a DV that provides a set-point to a local control loop, the related values in $d(k-1)$ and in $d_{pv}(k-1)$ differ by more than a defined threshold, "1" is set. In this *deviation* case (deviation between elements in $d(k-1)$ and $d_{pv}(k-1)$ related to a generic DV), *DC & DS* block replaces the field value in $d(k-1)$ with the related element of $d_{pv}(k-1)$. This information is provided to *DC & DS* block by *SCADA* system that includes *deviation* flags in *Plant Signals & Parameters* term of Fig. 3.1.
DC & DS block, based on the final $d_{pv}(k-1)$ value, performs bad detection: the meeting of the DVs validity bounds is verified, together with the compliance of the rate of change bounds (spikes) and of the freezing percentage associated with each DV. Bad detection results are grouped in a $Status_{dBAD} \in \mathbb{R}^{l_d \times 1}$ vector. When positive results for a generic DV are notified by bad detection, its status value in $Status_{dBAD}$ vector is set to "0" ("1" otherwise). The final DVs status value (Fig. 3.1, left side of *DC & DS*, *u-d-y Status*) is defined by an element-wise logical "AND" between $Status_{DVSCADA}$ vector and $Status_{dBAD}$ vector.

Mutual effects between MVs and CVs status values

As additional feature of the developed methodology for the setting of the status of MVs and CVs, mutual effects between their status values have been considered. This feature is a design choice that aims to take into account also

CVs-MVs relationships and MVs inhibition specifications.
In particular, an MV cannot be *active* if there is not at least one *active* CV tied to that MV and on which that MV can act (see Subsection 3.2.1). Denoting with $Status_{u-y} \in \mathbb{R}^{l_u \times 1}$ the vector related to the influence of CVs status on MVs status, its elements can be equal to "-1" or "1". Practically, CVs status can influence only the *active* inclusion of MVs in the MPC problem, but cannot determine their exclusion from CVs *free response* (see (3.37)) computation. The truth table for the definition of the final MVs status vector, denoted by $Status_u \in \mathbb{R}^{l_u \times 1}$, can be summarized for the generic jth MV as follows:

- if, among the jth elements of $Status_{uSCADA}$, $Status_{uBAD}$ and $Status_{u-y}$ vectors, there is at least a "0" value, the jth element of $Status_u$ will be "0";
- if, among the jth elements of $Status_{uSCADA}$, $Status_{uBAD}$ and $Status_{u-y}$ vectors, there are no "0" values and there is at least a "-1" value, the jth element of $Status_u$ will be "-1";
- if all jth elements of $Status_{uSCADA}$, $Status_{uBAD}$ and $Status_{u-y}$ vectors are "1", the jth element of $Status_u$ will be "1".

A CV cannot be *active* if there is not at least one *active* MV tied to that CV and that can act for its control specifications fulfillment (see Subsection 3.2.1). Denoting with $Status_{y-u} \in \mathbb{R}^{m_y \times 1}$ the vector related to the influence of MVs status on CVs status, its elements can be equal to "0" or "1". MVs status can influence the *active* inclusion of CVs in the MPC problem. The final CVs status value, denoted by $Status_y \in \mathbb{R}^{m_y \times 1}$, is defined by the following element-wise logical "AND":

$$Status_y = Status_{ySCADA} \wedge Status_{yBAD} \wedge Status_{y-u} \tag{3.119}$$

where $\wedge$ represents the element-wise logical "AND".
The final MVs, CVs and DVs status vectors are provided by *DC & DS* block to *Predictions Calculator* module and to *SCADA* block (Fig. 3.1, left side of *DC & DS* block, *u-d-y Status*). The final MVs, CVs and DVs status vectors affect the CVs *free response* computation over H_p. In particular, for MVs and DVs with final status value equal to "0", the related element in the final $u(k-1)$ and $d(k-1)$ vectors are set equal to the correspondent element in u_0 and d_0 vectors, respectively. In this way, the current value of the inputs with final status value equal to "0" does not influence the CVs *free response* computation over H_p. Furthermore, when the status value of an MV or of a DV switches from "0" to "1" or "-1", the option to change the related element in u_0 or d_0 has been included in the control framework.
The final MVs and CVs status information is provided by *DC & DS* block to *TOCS* and *DO* modules introducing it in the *Decoupling Matrix* D_E described

in Subsection 3.2.1. In order to exploit the decoupling approach also for MVs and CVs status introduction, an extension of this strategy has been proposed. In fact, D_E matrix, as it has been defined in Subsection 3.2.1, does not depend on the status information of process variables. At each control instant, the *DC & DS* block can modify the initial D_E matrix supplied by *SCADA*, introducing information contained in $Status_u$ and in $Status_y$ terms. The generic (i, j) element of initial D_E matrix is zeroed by *DC & DS* block if at least one of the two conditions holds:

- the jth MV is *inactive*;
- the ith CV is *inactive*.

The final updated D_E matrix is provided to *TOCS* and *DO* modules (Fig. 3.1, left side of *DC & DS*, *Decoupling Matrix*).
The introduced extended decoupling strategy ensures a unified approach to the problem of the selection of the MVs to be exploited for the control specifications of each single CV in all process conditions.
According to the author knowledge, the proposed unified approach to the problem of the selection of the MVs to be exploited for the control specifications of each single CV in all process conditions, based on the online definition and processing of a *Decoupling Matrix* D_E, represents a contribution of the research activity reported in the present dissertation [79].

Impact on DO and TOCS formulation

The final updated D_E matrix provided to the *MPC* block by the described cooperative action of *SCADA* block and *DC & DS* block impacts on the mathematical formulation of *TOCS* and *DO* modules. Based on the final process variables status values, the control problem can change at different control instants. As a consequence, the structure of the optimization problem of *TOCS* and *DO* modules, together with the related degrees of freedom, can change dynamically.
Similarly to what described in Subsection 3.2.1, in order to include the final updated D_E matrix in *TOCS* formulation, (3.86) is modified as in the following:

$$\hat{y}_{TOCS}(k) = \hat{y}(k + H_p|k)|_{\Delta\mathcal{U}(k)=0} + \Delta\hat{y}_{TOCS}(k) \tag{3.120}$$

$$\Delta\hat{y}_{TOCS}(k) = (G_{yu} \circ D_E)\Delta\hat{u}_{TOCS}(k) \tag{3.121}$$

where $\circ$ indicates the element-wise product between matrices. Practically, the D_E matrix modifies the original G_{yu} matrix in (3.86). In order to include D_E matrix information in the other crucial terms of *TOCS* LP problem (3.93)-

(3.89), the following vectors are defined:

$$p_u = op_{\neq}(\sum_{i=1}^{m_y} D^T_{E_{(i,:)}}, 0_{l_u \times 1})$$
$$p_y = op_{\neq}(\sum_{j=1}^{l_u} D_{E_{(:,j)}}, 0_{m_y \times 1}) \tag{3.122}$$

where $D_{E_{(i,:)}}$ and $D_{E_{(:,j)}}$ represent the ith row and the jth column of D_E matrix, respectively. The initial c_u and c_y terms in (3.92) are modified as follows:

$$c_u = c_u \circ p_u \tag{3.123}$$

Note that, in (3.92), $\rho_{lbyTOCS}$ and $\rho_{ubyTOCS}$ positive vectors are not affected by D_E matrix information.
Furthermore, considering p_u vector, when its generic jth element ($j = 1 \dots l_u$) is equal to zero, all the constraints related to the jth MV in (3.89) are cut off by *TOCS* module. Similarly, taking into account p_y vector, when its generic ith element ($i = 1 \dots m_y$) is equal to zero, all the constraints related to the ith CV in (3.89) are cut off by *TOCS* module.
Similarly to what described in Subsection 3.2.1, in order to include the final updated D_E matrix in *DO* formulation, (3.38) is modified as in the following:

$$\hat{y}(k+i|k) = \hat{y}(k+i|k)|_{\Delta\mathcal{U}(k)=0} + \Delta\hat{y}(k+i|k) \tag{3.124}$$
$$\Delta\hat{y}(k+i|k) = (\Theta_{(((i-1)\cdot m_y+1:i\cdot m_y),:)} \circ D^{ext}_E)\Delta\mathcal{U}(k)$$

where $\circ$ indicates the element-wise product between matrices and D^{ext}_E is given by:

$$D^{ext}_E = (1_{1\times H_u}) \otimes D_E \quad \in \mathbb{R}^{m_y \times (l_u \cdot H_u)} \tag{3.125}$$

In (3.115) $1_{a\times b}$ indicates a matrix composed by elements all equal to 1 and $\otimes$ indicates the Kronecker product between matrices. Practically, the D_E matrix is introduced in (3.38) through a D^{ext}_E matrix that modifies the original Θ matrix. In order to include D_E matrix information in the other crucial terms of *DO* QP problem (3.41)-(3.42), taking into account (3.122), the following diagonal matrices are defined:

$$T_u = diag(p_u)$$
$$T_y = diag(p_y) \tag{3.126}$$

where $diag(a) \in \mathbb{R}^{r\times r}$ represents a diagonal matrix with the elements of $a \in \mathbb{R}^{r\times 1}$ on the main diagonal. The initial $S(i)$ and $Q(i)$ terms in (3.41) are

modified as follows:

$$\begin{aligned} S(i) &= S(i) \circ T_u \\ Q(i) &= Q(i) \circ T_y \end{aligned} \tag{3.127}$$

Note that, in (3.41), $R(i)$ and ρ_{yDO} positive definite diagonal matrices are not affected by D_E matrix information: this feature allows obtaining an always "well-posed" *DO* QP problem.
Furthermore, considering p_u vector, when its generic jth element ($j = 1 \dots l_u$) is equal to zero, all the constraints related to the jth MV in (3.42) are cut off by *DO* module. Similarly, taking into account p_y vector, when its generic ith element ($i = 1 \dots m_y$) is equal to zero, all the constraints related to the ith CV in (3.42) are cut off by *DO* module.
Furthermore, for an overall correct introduction of the D_E matrix in the *DO* formulation, also the general definition of the H_{w_j} parameter reported in (3.40)-(3.116) must be revised. The final H_{w_j} definition is: for the generic jth *active* CV, the H_{w_j} indicated the first prediction instant on which the first MVs future move (contained in $\Delta\hat{u}(k|k)$ vector) related to at least one *active* MV tied to the jth *active* CV and *not inhibited* for controlling the jth *active* CV will be active.
The revised H_{w_j} parameter can be determined from the final Θ matrix: considering the H_p Θ rows related to the jth *active* CV and taking into account only the l_u Θ columns related to $\Delta\hat{u}(k|k)$ (i.e. the first l_u Θ columns), H_{w_j} is equal to the index of the first row where there is at least a nonzero entry. Furthermore, the revised H_{w_j} can be determined through the following updated final version of (3.40)-(3.116):

$$H_{w_j} = \min(D_{yu_{(j,mask_j)}}) + 1 \tag{3.128}$$

where in this final case, $mask_j$ is a vector that indicates the D_{yu} columns related to the *active* MVs that are tied to the jth *active* CV and that are *not inhibited* for controlling the jth *active* CV.
Given these considerations, for each jth *active* CV, its H_{w_j} parameter can change at different control instants. Consequently, the weights zeroing and constraints cut off policies described in Subsection 3.1.1 are updated.
Given the previous considerations, for each rth *inactive* CV, its H_{w_r} parameter is irrelevant.
The proposed approach ensures that, for *inactive* MVs, the related *DO*-computed future moves and the related *TOCS*-computed steady-state move are zero. Furthermore, for an *inactive* CV, all MVs tied to it are inhibited.

3.3 Constraints handling, reference trajectories management and tuning

The designed *two-layer* linear MPC scheme has been based on two cascaded optimizers characterized by a structure that can change dynamically. Suitable constraints handling and reference trajectories management policies, and in general a proper tuning are needed for the achievement of the desired control specifications.
In [80], a H_p tuning strategy for MIMO (Multiple-Input Multiple-Output) open-loop stable processes that are modelled with FOPDT (First Order Plus Dead-Time) models discretized with zero-order hold is proposed:

$$H_p = \max(\frac{5\tau_{i,j}}{T_s} + k_{i,j}), \quad i = 1 \dots m_y, \ j = 1 \dots (l_u + l_d) \tag{3.129}$$

where $k_{i,j} = \frac{\tau_{d_{i,j}}}{T_s} + 1$.
In (3.129), $\tau_{i,j}$ represents a time constant and $\tau_{d_{i,j}}$ represents a time delay, while T_s is the sampling time. Other H_p tuning methods take into account the reaching of defined percentages of the process steady-state or suitable combinations of the rise times [81], [82].
The control horizon H_u choice affects the aggressiveness or the conservativeness of the control action and strongly influences the computational load [83]. In [80], a H_u tuning strategy for MIMO open-loop stable processes is proposed that is consistent with (3.129):

$$H_u = \max(\frac{\tau_{i,j}}{T_s} + k_{i,j}), \quad i = 1 \dots m_y, \ j = 1 \dots (l_u + l_d) \tag{3.130}$$

where $k_{i,j} = \frac{\tau_{d_{i,j}}}{T_s} + 1$.
In [84], it is suggested to choose the control horizon "as large as possible within the computational limits" and then to detune for robustness achievement [83]. In many applications $M_i = i - 1$ ($i = 1 \dots H_u$), i.e. the future MVs moves (to be computed by *DO*) are assumed on the first H_u prediction instants [8].
In the proposed MPC scheme, with regard to the H_p choice, a steady-state assumption has been made in Subsection 3.1.1 that contributes to the achievement of consistency between the formulations of *TOCS* and *DO* modules. This assumption requires a joint setting of H_p, H_u and M_i ($i = 1 \dots H_u$) parameters. In general, a trade-off between computational complexity and load and performances optimization has to be reached.
TOCS module has been based on the LP problem (3.93)-(3.89). In this problem, constraints related to *active* CVs are always present. They contribute to the definition of a region where the considered process has to be controlled.

As mentioned in Subsection 3.1.2, the initial CVs constraints over H_p that are provided by *SCADA* can be preprocessed by *TOCS* module before solving its LP problem, obtaining $lb_{yop}(i)$ and $ub_{yop}(i)$ $(i = 1 \dots H_p)$. For example, when the status value of a CV switches from *inactive* to *active*, or when there is a constraints change for an *active* CV, if the CV last known value does not satisfy the imposed constraints, the option of a constraints ramp change is available (Fig. 3.1, *TOCS Tuning Parameters*). For the generic jth CV, the last known value has to be intended as the jth CV prediction at instant $(H_{w_j} - 1)$: this prediction is represented by the $y(k)$ jth element if $H_{w_j} = 1$, while it corresponds to the jth CVs *free response* at the $(H_{w_j} - 1)$th prediction instant if $(H_{w_j} > 1)$. An additional feature allows the choice of the point from which the ramp change must start: it may be the old constraint or the last known value. The introduction of a ramp change can lead to a more sluggish and less aggressive control action.
As described in Subsection 3.1.2, *TOCS* CVs constraints *relaxations* are always structurally independent: each CV is equipped with two slack variables, also making always structurally independent its lower and upper constraints *TOCS relaxation*. A joint setting of $\gamma_{lbyTOCS}$, $\gamma_{ubyTOCS}$, $\rho_{lbyTOCS}$ and $\rho_{ubyTOCS}$ terms allows to suitably rank the importance of constraints *relaxations*, giving a priority order between CVs constraints. In particular, conflicting control requirements between different CVs must be addressed in the desired way.
In *TOCS* module formulation, preferences on minimization and/or maximization directions for *active* MVs and CVs can be formulated through a proper tuning of c_u and c_y cost vectors in (3.92). Positive values correspond to minimization specifications. Clearly, in most cases, the cost vectors c_u and c_y must be tuned in order to guarantee the desired process optimization within the assigned constraints related to *active* MVs and CVs, i.e. the *TOCS* slack variables must assume nonzero values only if the related constraints must be really violated.
Both the proposed *TOCS* and *DO* modules formulations consider the constraints related to *active* MVs as *hard* constraints. MVs constraints are always present in the majority of industrial cases (physical constraints). Due to the assumed *hard* type, feasibility must be ensured in all conditions. As mentioned in Subsections 3.1.1-3.1.2, *TOCS* and *DO* modules can possibly preprocess, in the same way, constraints related to *active* MVs. The constraints related to the *DO* MVs future values and to the *TOCS* MVs steady-state value may be inconsistent with respect to the constraints related to the *DO* MVs future moves and to the *TOCS* MVs steady-state move. In fact, in *DO* constraints (3.42), at the generic M_ith $(i = 1 \dots H_u)$ prediction instant, the constraints $lb_{uDO}(i)$ and $ub_{uDO}(i)$ must be able to be met through the i $\Delta\hat{u}(k + M_r|k)$ $(r = 1 \dots i)$ available MVs future moves, which are constrained by $lb_{duDO}(r)$

and $ub_{duDO}(r)$ terms. In *TOCS* constraints (3.89), the constraints lb_{uTOCS} and ub_{uTOCS} must be able to be met through the $\Delta\hat{u}_{TOCS}(k)$ MVs steady-state move, which is constrained by lb_{duTOCS} and ub_{duTOCS} terms. When an MV switches from *inactive* to *active*, or when there is a constraints change for an *active* MV, if the MV last value (contained in $u(k-1)$) does not satisfy the defined *SCADA* constraints, a ramp change is imposed. The point from which the ramp change must start is the MV last value. The related constraints that are not satisfied are subjected to a ramp change characterized by a slope that depends on $lb_{duDO}(i)$ or $ub_{duDO}(i)$ terms and that exploits the definition of the control horizon H_u. In this way, correct $lb_{uDO}(i)$ and $ub_{uDO}(i)$ terms are obtained and infeasibility problems are prevented and avoided.
Given the industrial application purposes of the designed APC framework, another important consideration about MVs constraints is related to situations where the possible related control loops require an inhibition of the increase and/or of the decrease directions [76], [77]. When, for an MV tied to a local control loop, the inhibition of the increase (decrease) direction is required, the *SCADA* system provides initial upper (lower) constraints that are set equal to the current MV value (contained in the initial $u(k-1)$ vector).
With regard to the *DO* module, it has been based on the QP problem (3.41)-(3.42). In (3.41), the $u_r(k+M_i|k)$ terms can be set equal to $\hat{u}_{TOCS}(k)$, thus extending (3.111) to all MVs predictions over H_u. Then, through a suitable tuning of the diagonal terms of $S(i)$ matrices, the desired convergence speed of *active* MVs predictions toward the *TOCS*-computed optimal steady-state targets can be obtained. Theoretically, after solving *DO* and *TOCS* optimization problems, the following relationships must be obtained:

$$\begin{aligned} \sum_{i=1}^{H_u} \Delta\hat{u}(k+M_i|k) &= \Delta\hat{u}_{TOCS}(k) \\ \hat{u}(k+M_{H_u}|k) &= \hat{u}_{TOCS}(k) \end{aligned} \tag{3.131}$$

In the proposed *DO* formulation, a constraint set for the enforcement of (3.131) has not been introduced, in order to avoid the increasing of the related QP problem complexity. The relationships reported in (3.131) can be met through a suitable tuning of the diagonal elements of $S(H_u)$ matrix, thus providing nominal stability [28]. The relationships indicated in (3.131) are "well-posed" because of the introduced relationship between the prediction horizon H_p and the steady-state condition (see (3.39)).
In (3.41), $R(i)$ are positive definite diagonal matrices that weight the magnitude of MVs future moves. Together with ρ_{yDO} positive definite diagonal matrix, $R(i)$ are not affected by D_E matrix information: this feature allows obaining an always "well-posed" *DO* QP problem, characterized by a Hessian that is always positive definite (see Subsection 3.2.2). The diagonal elements of $R(i)$

matrices affect the aggressiveness or the conservativeness of the control action: a proper tuning may ensure that the controller is not too aggressive or too sluggish [83].
In the *DO* control problem (3.41)-(3.42), the desired paths for *active* CVs can be achieved with reference trajectories and/or with constraints. At each control instant k, the *active* CVs that have to track $r(k+i|k)$ over H_p require a proper definition of the related reference trajectories. The reference trajectories related to *active* CVs are obtained through a suitable processing of the CVs reachable steady-state targets computed by *TOCS* module. For example, for the generic jth *active* CV an exponential reference trajectory can be generated as follows [8]:

$$r_j(k+i|k) = (1 - e^{(-(i-H_{w_j}+1)\cdot T_s/T_{ref_j})})r_j(k+H_p|k) + e^{(-(i-H_{w_j}+1)\cdot T_s/T_{ref_j})}y_{s_j}(k)$$
$$i = 1 \dots H_p - H_{w_j} + 1 \tag{3.132}$$

where T_{ref_j} indicates the desired closed-loop continuous time time constant for the jth *active* CV and T_s is the sampling time. $r_j(k+H_p|k) = \hat{y}_{TOCS_j}(k)$ represents the steady-state target given by *TOCS* module related to the jth *active* CV (see (3.111)) and it is assumed to can be reached with T_{ref_j} definition. $y_{s_j}(k)$ represents the starting point of the reference trajectory $r_j(k+i|k)$. In the proposed controller formulation, the starting point is represented by the last known value of the jth *active* CV. The last known value has to be intended as the jth CV prediction at instant $(H_{w_j} - 1)$: this prediction is represented by the $y(k)$ jth element if $H_{w_j} = 1$, while it corresponds to the jth CV *free response* at the $(H_{w_j} - 1)$th prediction instant if $(H_{w_j} > 1)$. The reference trajectories can be used in order to smooth the convergence from the last known value to the steady-state target [24]. In [85] a performance ratio for the reference trajectory generation is proposed: it is represented by the ratio of the desired closed-loop settling time to the open-loop settling time.
In (3.41), the diagonal nonnegative elements of $Q(i)$ matrices allow to weight the importance of tracking errors (with respect to the assigned reference trajectories) minimization for *active* CVs; a suitable tuning can ensure the desired priority in the minimization of the CVs tracking errors.
In the *DO* control problem (3.41)-(3.42), the *active* CVs that are characterized by constraints over H_p (these constraints are supplied by *TOCS* module) require a joint tuning of $\gamma_{lbyDO_j}(i)$, $\gamma_{ubyDO_j}(i)$, ρ_{yDO}, $n_{\varepsilon yDO}$ and suitable grouping policies for constraints *relaxations*. Tuning of these terms must allow to suitably rank the importance of the minimization of the slack variables related to constraints *relaxations*, giving a priority order between CVs constraints. In particular, conflicting control requirements between different CVs must be addressed in the desired way. In general, the $n_{\varepsilon yDO}$ *DO* slack variables must be computed as nonzero values only if the related constraints must be really

violated; for this purpose, in the tuning of the *DO* constrained minimization problem, high importance have to be given to the slack variables. With regard to the grouping policies for *active* CVs that have to be kept within *TOCS*-computed constraints, the easiest case is $n_{\varepsilon yDO} = 1$: in this situation, all *soft* constraints share the same single slack variable and a priority order between different constraints *relaxations* can be only defined through $\gamma_{lbyDO_j}(i)$ and $\gamma_{ubyDO_j}(i)$ parameters; furthermore in this case ρ_{yDO} is a positive scalar and it is only exploited to weight the magnitude of the single slack variable in *DO* optimization problem. On the other hand, when each *soft* constraint is equipped with an own slack variable, there is a structural independence between different constraints. In this case, ρ_{yDO} is a matrix and a joint tuning of $\gamma_{lbyDO_j}(i)$, $\gamma_{ubyDO_j}(i)$, and ρ_{yDO} can give the desired priority order between different constraints *relaxations*. Finally, in the situations where there are some groups composed by two or more constraints that share the same slack variable, a joint tuning of $\gamma_{lbyDO_j}(i)$, $\gamma_{ubyDO_j}(i)$, and ρ_{yDO} allows to assign the desired priority order within and between the different groups. Clearly, $n_{\varepsilon yDO}$ affects the number of the decision variables of *DO* optimization problem; so, an optimal trade-off between computational load retaining and the achievement of the desired performances has to be guaranteed.

In general, when two or more constraints are grouped under the same slack variable, "induced" constraints *relaxations* may happen: if at least one constraint of a generic group requires to be *softened*, the slack variable magnitude is propagated to all the constraints of the same group, weighted by $\gamma_{lbyDO_j}(i)$ or $\gamma_{ubyDO_j}(i)$ terms [86]. The described "induced" constraints *relaxations* may affect the controller performances causing, for example, a less prompt response of the control action [87]. The proposed cooperation improvement between *TOCS* and *DO* modules (see Subsection 3.1.2) contributes to smooth the side effects tied to the "induced" constraints *relaxations*, even when there are nonzero (and possibly different) time delays on the CVs-MVs channels. However, the proposed cooperation improvement between *TOCS* and *DO* modules always guarantees that the *DO* steady-state constraints (i.e. the *DO* constraints $lb_{yDO}(H_p)$ and $ub_{yDO}(H_p)$) do not require any *relaxation*; thanks to the introduced *presoftening* feature, the CVs steady-state constraints configuration does not influence the *relaxation* of the previous constraints (i.e. the constraints related to the prediction instants before H_p).

Chapter 4

Steel Industry Billets Reheating Furnaces APC system

Nowadays, energy efficiency achievement constitutes one of the main challenges in iron and steel industry. A crucial aspect is represented by the optimization of reheating and rolling related processes [88]. These processes are characterized by complex phases, activated by thermodynamic and physical reactions. Several phases take place, resulting in high energy consumptions. Each reaction process can be enhanced improving the automation level [89]. At this regard, software or hardware solutions are available. In order to guarantee the most profitable balance between throughput and yields maximization, costs minimization, and product quality improvement, plant managers and engineers, whenever possible, opt for software control solutions, which ensure minimum payback time with an almost immediate return on investment. In this way, through the introduction of APC systems, full advantage from already existent processes devices is obtained without requiring hardware modifications.
In Chapter 3, an APC framework able to control and optimize constrained multivariable processes has been designed and formulated. The APC framework has been based on a *two-layer* linear MPC strategy that tightly cooperates with an additional functional block.
The basic APC framework has been then *customized* for its installation on five billets reheating furnaces located in steel industries of various European countries, in order to achieve energy efficiency and process control improvements. The formulated billets reheating furnaces control method has been introduced in a proprietary software tool and it has been awarded with an Italian patent [90]. A proprietary software tool has been developed, shrinking the economic burdens tied to the utilization of commercial and industrial products. In this way, it has been possible to perform algorithms *customization* whenever the process at study required it.

4.1 Billets Reheating Furnaces

The general production chain of the studied steel industries is schematically depicted in Fig. 4.1. Raw materials, e.g. waste steel products, are processed in the first phase (*Raw materials processing* phase), so as to obtain steel bars at an intermediate stage of manufacture. These bars are called *billets*. In the investigated processes, billets can be characterized by a rectangular or a quadratic section and by different lengths. The billets are then introduced in a reheating furnace, where a *Reheating* phase takes place. When they enter the furnace, billets can be characterized by very different temperatures. A typical inlet temperature range is 30 [$°C$] - 700 [$°C$]. The billets that are inside the furnace are moved toward the furnace exit and they are reheated according to specific temperature profiles, guaranteeing given outlet temperatures. At the furnace exit, billets temperature can vary, according to the specifications of the subsequent *Rolling* phase. A typical outlet temperature range is 1000 [$°C$] - 1100 [$°C$]. After their path along the furnace, the billets are moved toward the rolling mill stands: here they are subjected to a plastic deformation, suitably performed by stands cylinders (*Rolling* phase). These cylinders deform the reheated billets according to the finished products specifications. Examples of finished products are angle bars, iron rods, or tube rounds [89].

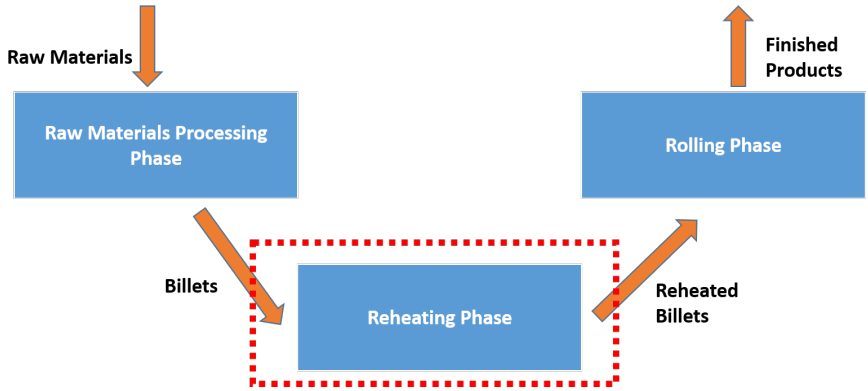

Figure 4.1: General steel industries workflow.

In steel industry, the crucial phase from an energy efficiency and product quality point of view is represented by the middle phase, i.e. the *Reheating* phase. As already described, this phase takes place in a reheating furnace. The importance of this phase is due to the high energy amount required: an optimal trade-off between conflicting requirements, i.e. environmental impact decreas-

ing, energy saving, and production and product quality increasing has to be ensured. The basic APC framework described in Chapter 3 has been suitably *customized* in order to control and optimize the *Reheating* phase of the considered steel industries.

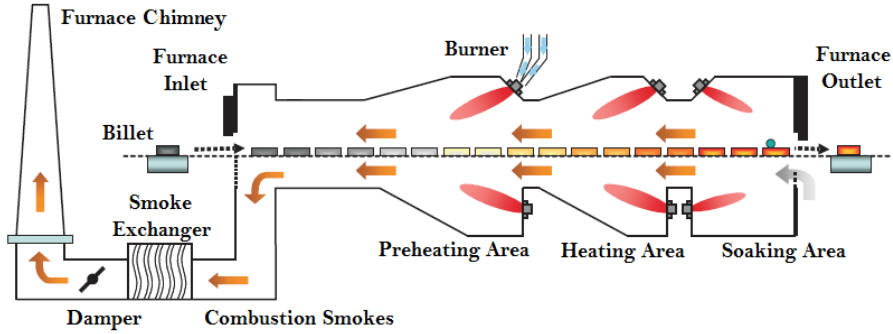

Figure 4.2: General representation of a reheating furnace.

The *Reheating* phase in a furnace is schematically represented in Fig. 4.2: the billets are introduced in the reheating furnace from the left side (Fig. 4.2, *Furnace Inlet*) and they are moved toward the outlet of the furnace. A furnace can contain up to a maximum number of billets that may dynamically change according to the billets dimension; generally, the billets transit on furnace places but, depending on the coupling with previous processing phases and on production requirements, there could be empty places within the furnace, where no billets are present. Different typologies of furnaces exist, characterized by different ways billets are moved toward the furnace outlet (Fig. 4.2, *Furnace Outlet*). Typically, furnaces are named according to billets movement characteristics. The studied steel industries are characterized by two different billets movement types: in the first billets are moved toward the outlet of the furnace by a revolving beam (*walking beam* reheating furnace) while in the second billets are moved toward the outlet of the furnace by pushers (*pusher type* reheating furnace) [91], [88]. Billets progress along the furnace is driven by a defined furnace production rate, that can vary according to the plant production planning and scheduling and to the subsequent *Rolling* phase requirements; for example, finished products changes or delays in the rolling mill may result in a temporary stop or slowdown of the billets movement along the furnace [89]. Within the furnace, air/fuel burners (located on the furnace top walls) trigger combustion reactions: in this way, thermal energy is transferred

to the billets during their permanence in the furnace by radiation, convection and conduction phenomena. In the considered case studies, natural gas is exploited as fuel.
Along their path along the furnace, billets are subjected to increasing temperatures. Based on local temperatures and according to the role played on the billets reheating process, three main areas are identified along the furnace; each area can be characterized by one or more zones. Starting from the furnace inlet, on the left side of Fig. 4.2, they are:

- *Preheating Area*: this furnace area can be characterized by the presence or by the absence of burners. This area, exploiting hot gases from downstream areas, performs a billets preheating process.
- *Heating Area*: in this furnace area the crucial phase of billets reheating process takes place. In this area, through the effect of burners combustion, billets are significantly heated up to their internal layers.
- *Soaking Area*: in this furnace area, through burners combustion, the billets complete their reheating process. In particular, the final part of the heating related to the billets surface layers takes place.

The combustion air supplied to each burner is preheated by a heat exchanger (also denoted as *smoke-exchanger*): it is located near the entrance of the *Preheating Area* and it exploits the hot combustion smokes to raise combustion air temperature (Fig. 4.2, *Smoke Exchanger* and *Combustion Smokes*). The combustion smokes are ejected through a chimney (Fig. 4.2, *Furnace Chimney*). Furthermore, the furnace pressure is controlled through a suitable handling of a damper that is located near the furnace chimney (Fig. 4.2, *Damper*).

4.1.1 Processes sensors equipment and control specifications

In the analyzed reheating furnaces, measurements of the temperature of each furnace zone (within each furnace area) and of the smoke-exchanger are acquired by thermocouples suitably positioned within the furnace. *Heating* and *Soaking* furnace areas are equipped with flowmeters for fuel (natural gas) and air flow rates measurement. Air and furnace pressures are measured by manometers positioned near the furnace chimney. The billets temperature at their entrance in the furnace is registered by an optical pyrometer. An additional pyrometer measures the temperature of the processed billets. This additional pyrometer is placed at the exit of the first stage of the rolling mill stands. Billets transition at the furnace inlet and outlet is detected by photocells. No temperature information for the billets that are in the furnace is available.
A control system designed for billets reheating furnaces must ensure correct triggering of the involved thermodynamic and physical reactions, in order to

guarantee a safe furnace conduction and the desired billets outlet temperature. The minimization of the fuel specific consumption, together with the furnace production rate maximization, clearly represents the crucial factor for energy efficiency achievement and improvement.
In addition to these requirements, there is also the need to meet stringent quality standards of the finished products and to comply with stringent environmental standards (CO_2 emissions reduction). So the most challenging management requirement in a reheating furnace is the research of an optimal equilibrium between reheated billets quality and the binomial constituted by energy saving and pollution impact decreasing, tied to fuel specific consumption minimization. In this context, energy saving can be interpreted as direct fuel saving and as indirect energy use reduction due to products quality improvements [89], [92].
Before the introduction of the developed *customized* APC system, the studied reheating furnaces were regulated by plant operators' manual conduction of local PID temperature controllers. These controllers were implemented on plant PLC (Programmable Logic Controller); each furnace zone (within each furnace area) was equipped with a PID temperature controller able to control the local combustion. Operators, based on the furnace conditions, on the production requirements, and on their experience and skills, manually set the zones temperature targets. Furthermore, before the introduction of the developed *customized* APC system, plant operators had no information about billets heating temperature profile exhibited inside the furnace.
After initial study and analysis phases, repeated and targeted meetings with plant managers, engineers, and operators were conducted in order to define targets and possible strategies for energy efficiency achievement and improvement. For this purpose, the following control specifications have been defined for the considered *customized* APC system [89], [93], [94]:

i. Compliance with the defined billets temperature constraints and/or targets at the furnace outlet, guaranteeing an uniform heating profile between the different internal and surface layers of the billets and based on the specifications for the subsequent plastic deformation in the *Rolling* phase. For this purpose, an optimized and safe management of the furnace zones temperature is needed so to ensure a smooth billets reheating process. The constraints and/or targets that define the desired billets temperature at the furnace outlet can vary between different billets and/or at different control instants depending on the required typology for the finished products.
ii. Compliance with quality requirements: reduced scale formation, reduced decarburization, reduced surface melting, and reduced geometrical distortion. In particular, the scale formation causes a loss of valuable materials

and affects the heat transfer behavior, so a reduction of the scale formation always results in an indirect energy demand decreasing. The scale is defined as an iron oxide layer: it is caused by the reactions between the furnace gases and the increasing billets surface temperature [95].

iii. Moving the furnace thermal barycenter toward the *Soaking Area*, thus limiting thermal energy dissipation in the combustion smokes. This requirement can be translated in assuring that the billets heating takes place as far as possible from the furnace inlet. For this purpose, a monotonic increase of the furnace zones temperature (from the furnace inlet to the furnace outlet) may be required.

iv. Stabilization and minimization of the excess of air that is used as comburent in the combustion process triggered by air/fuel burners; in this context, an ideal operating condition is represented by the meeting of the nominal stoichiometry between air and fuel flow rates. For this purpose, the compliance with nominal air/fuel stoichiometric ratios constraints is a fundamental requirement and an optimal balancing between air and fuel flow rates has to be ensured.

v. Compliance with total air flow rate and smoke-exchanger temperature limits, so as to preserve furnace safety.

vi. Control of defined process variables using only a defined set of control inputs. For example, the control of the temperature of each single furnace zone equipped with an own burners set must be performed using only the fuel flow rate related to its burners. Furthermore, the control of the temperature of each single furnace zone not equipped with an own burners set and of the temperature of the smoke-exchanger must be performed using only the fuel flow rates related to the burners of a defined set of furnace zones. Finally, the control of the total air flow rate must be performed using or only the air flow rate related to the burners of a defined set of furnace zones or only the fuel flow rate related to the burners of a defined set of furnace zones.

vii. Furnace management in all predictable conditions.

viii. Minimization of the fuel specific consumption, suitably handling the fuel flow rates and optimizing situations with constant and varying furnace production rate. In general, in the considered case studies, the furnace production rate cannot be moved by the APC system; it is externally defined according to the plant production planning and scheduling.

The simultaneous meeting of all the above requirements is not easily attainable by a manual conduction of the furnaces. In the previous conduction of the reheating furnaces, operators typically neglected the aspects more strictly tied to energy saving and environmental impact decreasing, being concentrated on assuring a suitable billets heating profile. So, with the previous furnace

management, billets were often reheated more than needed by the subsequent *Rolling* phase and energy efficiency aspects have been rarely considered. Furthermore, quality problems sometimes arose due to billets overheating. These considerations have motivated the development of a *customized* APC system and its installation on the reheating furnaces of the studied steel industries.

4.1.2 Literature Control Solutions

In the control literature different control solutions for reheating furnaces control and optimization are present; different ways to model and manage the process nonlinearities have been proposed. In [96], a computer control system for optimization of reheating furnaces has been developed that contains functions for fuel optimization, based on carpet diagrams and delay strategy multipliers. In [97], a nonlinear model-based controller for optimally tracking a prespecified slab temperature trajectory in a *walking beam* reheating furnace is proposed, based on a nonlinear temperature model related to the slabs that are within the furnace. A hybrid optimization set-point strategy for reheating furnaces temperatures is proposed in [98], based on steady-state zone temperature optimization and dynamic optimization performed by PID controllers. In [99], a dynamic model of the reheating furnace is derived using material and energy balances and a multivariable predictive controller design procedure is proposed. In [100], a feedback linearization method is applied to obtain a linear model of the reheating furnace and an MPC system is designed. In [101], an MPC system based on ARX (AutoRegressive eXogenous) models identified by data with a test slab equipped with thermocouples inside is proposed and simulated. In [102], the potential of nonlinear MPC techniques to improve the temperature control of the metal slabs in a hot mill reheat furnace is explored; in particular, a focus on energy consumption decreasing is presented. An integrated method of intelligent decoupling control based on a recurrent neural network for zones temperature estimation and a heat transfer model for billets temperature prediction is proposed in [103] for a *pusher type* reheating furnace. A Lyapunov-based MIMO state feedback controller is developed for slab temperatures in a continuous, fuel-fired reheating furnace in [104]. The controller modifies reference trajectories of furnace temperatures and is part of a cascade control scheme. In [105], a nonlinear MPC is designed for a continuous reheating furnace for steel slabs. Based on a first principles mathematical model, the controller defines local furnace temperatures so that the slabs reach their desired final temperatures.
As already mentioned, the basic APC framework described in Chapter 3 has been *customized* for energy efficiency and process control improvements on real billets reheating furnaces. The resulting reheating furnaces APC system has

been named as *E-FESTO*. In *E-FESTO* APC system, to overcome the absence of temperature sensors inside the furnace to measure billets temperature, a virtual sensor has been developed, based on a nonlinear model whose inputs are represented by linear combinations of the zones temperatures of the considered furnace. Besides, billets inlet temperature and position along the furnace are taken into account by the model. With respect to the cited literature control solutions for reheating furnaces, a Linear Parameter-Varying (LPV) model has been accordingly derived [106], [107]. Furthermore, the other furnace variables have been considered through linear time invariant predictors. The global process model has been used in a *two-layer* linear adaptive MPC scheme. The introduced reheating furnaces control method has been awarded with an Italian patent [90].

4.2 *E-FESTO* APC system

The schematic representation of *E-FESTO* APC system is shown in Fig. 4.3.

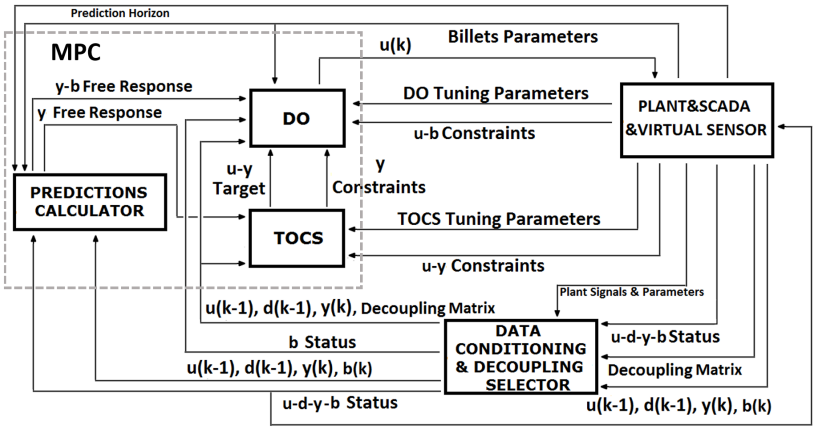

Figure 4.3: Schematic representation of *E-FESTO* APC system.

As already mentioned in the previous section, to overcome the absence of temperature sensors inside the furnace to measure billets temperature, a virtual sensor (Fig. 4.3, *Virtual Sensor*) has been developed. At this regard, it must pointed out that possible sensors placed on the billets cannot represent a feasible solution; furthermore, indirect measurements through additional pyrometers are corrupted by the internal furnace conditions. Therefore, the development of a virtual sensor has represented the best solution to overcome the

absence of temperature information for the billets inside the furnace. The developed virtual sensor has been based on a nonlinear first principles model whose inputs are represented by linear combinations of the zones temperatures of the considered furnace. Denoting with m_b the maximum number of billets that at the current control instant k can be contained in the considered furnace (this number may change at different control instants), the virtual sensor provides the estimation of the current temperature of at most m_b billets, also taking into account possible empty furnace places. The estimated billets current temperatures are grouped in a $b(k) \in \mathbb{R}^{m_b \times 1}$ vector (Fig. 4.3, $b(k)$) that is assumed to include all m_b terms. This choice has been done for notation convenience in the general case. The nonlinear first principles model takes into account heat phenomena and billets movements. For the development of the billets temperature first principles model, two modules have been designed: a *tracking* module and a *thermodynamic* module. The *tracking* module models the movement of each billet inside the furnace, providing the online configuration of the billets inside the furnace. This module takes into account all the furnace operations and features, such as the discharge of a billet, the furnace production rate, and sensors information (see Subsection 4.1.1). The *thermodynamic* module estimates the billets temperature inside the furnace taking into account *tracking* module information. The thermodynamic behavior of each billet has been modelled considering thermal diffusion equations of the different billet layers. The following continuous time conduction model has been considered [108]:

$$\dot{Q}_{cond} = -\lambda A \frac{dT}{dx} \qquad [W] \tag{4.1}$$

where A $[m^2]$ is the area related to the billet section that is normal to the heat transfer direction, λ $[W/(m \cdot k)]$ is the billet thermal conductivity, and $\frac{dT}{dx}$ $[K/m]$ is the temperature variation along the considered layer direction. The model (4.1) can be tailored with the needed number of billet layers. The convection and radiation phenomena have been modelled by the following standard equations [108]:

$$\dot{Q}_{conv} = hA(T_{bill} - T_{env}) \qquad [W] \tag{4.2}$$

$$\dot{Q}_{rad} = \epsilon \sigma A(T_{bill}^4 - T_{env}^4) \qquad [W] \tag{4.3}$$

where A $[m^2]$ is the area related to the exposed surface, h $[W/(m^2 \cdot k)]$ is the convection heat transfer coefficient, T_{bill} $[K]$ is the billet temperature, and T_{env} $[K]$ is the environment temperature of the fluid around the considered billet. σ is the Stefan-Boltzmann constant and ϵ is the emissivity coefficient [108].
The billets thermodynamic model acts as a virtual sensor for billets temper-

ature estimation and exploits a discretization (sampling time T_{s_b}) of the continuous time model based on the above differential equations. The inputs of the overall billets temperature nonlinear model are represented by linear combinations of the zones temperatures (all measured) of the considered furnace. The vector of the inputs of the overall billets temperature nonlinear model is indicated with $u_b \in \mathbb{R}^{l_{u_b} \times 1}$ vector. The exact value of the heat transfer coefficients that are used in the above equations is unknown; usually a physical range is known. These coefficients are online adapted by the *thermodynamic* module solving a constrained optimization problem, based on the minimization of the error between billets outlet measurements (optical pyrometer) and the related temperature estimations. The proposed adaptation procedure tries to repair to modellization uncertainties. In particular, for each billet that exits the furnace, a constrained optimization problem is solved: a nonlinear cost function minimizes the difference between the real outlet temperature and the estimated one. In this problem, the optical pyrometer measurements of the billets final temperature and all the temperature profile of the last billet that exited the furnace are exploited. In the considered case studies, the pyrometer that measures the temperature of the processed billets is placed at the exit of the first stage of the rolling mill stands. Because it is placed at the exit of the first stage of the rolling mill stands, a further term that models the billets temperature decrease in the path from the furnace outlet to the optical pyrometer has to be included. An optical pyrometer placed after the first stage of the rolling mill stands is more reliable with respect to an optical pyrometer that is placed at the furnace outlet. In fact, at the furnace outlet the scale on the billets surface has not been reduced yet and the scale may corrupt the pyrometer measurements. With the initial part of the *Rolling* phase, the scale on the billets surface is reduced, thus allowing measurements that are more reliable.
The virtual sensor runs with a sampling time T_{s_b} that is always smaller with respect to the sampling time T_s related to the *MPC* block and to the *DC & DS* block.
The computed updated coefficients are then applied for the temperature estimation of the billets that are still in the furnace and furthermore they are forwarded to *DO* and to *Predictions Calculator* modules within *Billets Parameters* term. Their usage in these modules will be described in the following of this section.

4.2.1 Development of a global furnace linear model

In order to *customize* the *two-layer* linear MPC strategy and the *DC & DS* block of the basic APC framework for the control and the optimization of bil-

lets reheating furnaces, the achievement of a proper linear process model is necessary. Through the analysis of the considered reheating furnaces, suitable process variables groups have been defined. In the Manipulated Variables (MVs) group, the fuel flow rate of each furnace zone equipped with an own burners set has been always considered. To complete the MVs group, based on the specific case studies, the air flow rate or the stoichiometric ratio of each furnace zone equipped with an own burners set has been considered. So, in certain case studies the MVs group is represented by fuel and air flow rates, while in the remaining plants it is composed by fuel flow rates and by the related stoichiometric ratios. In all case studies, the selected MVs act on local control loops regulated by PID controllers. In all case studies, in the Disturbance Variables (DVs) group, furnace and air pressures, together with furnace production rate, have been included. As in the basic APC framework, the MVs set is denoted by a $u \in \mathbb{R}^{l_u \times 1}$ vector, while the DVs set is denoted by a $d \in \mathbb{R}^{l_d \times 1}$ vector. Finally, two basic categories of Controlled Variables (CVs) have been defined: *zones* Controlled Variables (zCVs) and billets temperature (bCVs). zCVs group includes all furnace zones temperatures, temperature difference between adjacent furnace zones, smoke-exchanger temperature, total air flow rate, and the opening position (per cent) of the valves related to fuel flow rates. Furthermore, for the case studies that include air flow rates among MVs, also the opening position (per cent) of the valves related to air flow rates has been included in the zCVs group. zCVs have been grouped in a $y \in \mathbb{R}^{m_y \times 1}$ vector and, as it will be described, they correspond to the CVs that have been considered in the basic APC framework (see Chapter 3). MVs, DVs, and zCVs are all measured at each control instant. With regard to the bCVs group, the developed virtual sensor supplies an estimation of the temperature of the billets that are still in the furnace; as already stated, these variables have been included in a $b \in \mathbb{R}^{m_b \times 1}$ vector. At each control instant k, a measured or estimated value of all MVs, DVs, zCVs, and bCVs is supplied by the cooperative action of the *SCADA* system and of the developed virtual sensor.
A black-box identification phase has been executed in order to obtain zCVs-MVs/DVs models: accurate step test procedures have been performed acting on the selected input variables (MVs/DVs) and in all case studies linear time invariant asymptotically stable strictly proper models without delays on the inputs-outputs channels have been achieved [109], [110], [111]. Deviations of process variables from consistent operating points are considered for the formulation of these models. All practical and theoretical considerations that have been discussed in Chapter 3 with regard to MVs, DVs, and CVs are extended to MVs, DVs, and zCVs of the billets reheating furnaces *customized* APC framework. Furthermore, a new feature has been introduced within the *DC & DS* block: the definition of criticity relationships between the status values of dif-

ferent MVs. These relationships have been introduced in order to ensure that with the *inactivity* of the fuel flow rate of a furnace zone, the related air flow rate (MV) or the related stoichiometric ratio (MV) cannot be *active*. In this way, the controller cannot use the other MVs without the use of the primary MVs, that are represented by the fuel flow rates. The additional information that has to be exploited by *DC & DS* block for the criticity relationships between the status values of different MVs has been included in *Plant Signals & Parameters* term of Fig. 4.3.
In order to include bCVs in the setup of the *customized* APC system, a linearization of the billets temperature nonlinear first principles model (that is exploited by the virtual sensor) has been performed, obtaining the following Linear Parameter-Varying (LPV) model:

$$b(k+1) = A_b(p)b(k) + B_b(p)u_b(k) \tag{4.4}$$

where $b(k)$ represents the billets temperature estimation supplied by the virtual sensor at the current control instant k. On the generic jth position of $b(k)$ vector, there is the temperature estimation of the billet that at the current control instant k is located on the jth place of the furnace (the 1st place is assumed to be the closest place to the furnace inlet). This discrete time model, that will be included in the MPC formulation, is considered with the same sampling time T_s related to the *MPC* block and to the *DC & DS* block, that corresponds also to the sampling time that has been considered for the inclusion of the identified zCVs-MVs/DVs models in the controller formulation. In (4.4) $A_b(p) \in \mathbb{R}^{m_b \times m_b}$ and $B_b(p) \in \mathbb{R}^{m_b \times l_{u_b}}$ are matrices that depend on a $p \in \mathbb{R}^{n_p \times 1}$ vector of parameters that are obtained through combinations between the current values of the heat transfer coefficients updated by the virtual sensor and known billets parameters, e.g. the billets section, the billets mass, and the billets specific heat. Finally, $u_b(k)$, i.e. the inputs vector of (4.4), contains suitable linear combinations of the zones temperatures of the considered furnace.
In order to exploit the general model (4.4) in the controller formulation, a bCVs-MVs/DVs model must be achieved. Cascading the zCVs-MVs/DVs identified models (see (3.11)) and the LPV model, the following general prediction model is obtained:

$$\begin{aligned} \hat{b}(k+i|k) &= A_b(p)\hat{b}(k+i-1|k) + B_b(p)\hat{u}_b(k+i-1|k) \\ \hat{u}_b(k+i-1|k) &= M(k+i-1)\hat{y}(k+i-1|k) \end{aligned} \tag{4.5}$$

where $\hat{b}(k|k) = b(k)$ and $\hat{y}(k|k) = y(k)$. $M(k+i-1) \in \mathbb{R}^{l_{u_b} \times m_y}$ is a suitable mapping matrix that allows the inclusion of the desired linear combinations of

the zones temperatures (that are contained in zCVs y vector) on the $\hat{u}_b(k+i-1|k)$ rows. The M matrix can change at different prediction instants, because, according to the defined current furnace production rate (that is contained within $d \in \mathbb{R}^{l_d \times 1}$ vector), the billets can change their position along the furnace in the future instants. Usually, for the generic billet that at the current control instant k is located on the jth place of the furnace and that at the $(k+i-1)$th prediction instant will be located on the rth place ($r \geq j$) of the furnace, the related jth row of $M(k+i-1)$ matrix contains an only nonzero element (equal to 1) on the position that corresponds to the temperature of the furnace zone where the billet will be located at the $(k+i-1)$th prediction instant. As it will be described in Sections 4.3-4.4, there could be furnace zones that are transversally divided into two internal zones; in these cases for the billets that at the $(k+i-1)$th prediction instant transit within these furnace zones, the related rows of $M(k+i-1)$ matrix contain two nonzero elements (equal to 0.5) on the corresponding positions.
Exploiting (3.37) and (3.38), the following general expression for the predictions of the temperature of the generic billet that at the current control instant k is located on the jth place of the furnace is:

$$\begin{aligned} \hat{b}_j(k+i|k) &= \hat{b}_j(k+i|k)\Big|_{\Delta\mathcal{U}(k)=0} + \Delta\hat{b}_j(k+i|k) \\ \Delta\hat{b}_j(k+i|k) &= \Theta_{b_{j_{(i,:)}}} \Delta\mathcal{U}(k) \qquad j=1\dots m_b \quad i=1\dots e_j \\ e_j &= ceil(\frac{(T_{fm}\cdot(m_b+1-j))}{T_s}) \end{aligned} \tag{4.6}$$

where $\hat{b}_j(k+i|k)\Big|_{\Delta\mathcal{U}(k)=0}$ represents the *free response* of the jth billet temperature at the $(k+i)$th prediction instant, namely the response that would be obtained if the MVs future values remain at the last value $u(k-1)$ [8]. *Free response* contains all available information up to k instant, included the DVs effect. As already mentioned in Chapter 3, at each control instant k, the future DVs behavior is assumed unknown, so the future DVs behavior is considered constant at the last DVs value $d(k-1)$. In the DVs group there is the furnace production rate: its value at the current control instant is known, but the future values are assumed unknown. For this reason, at a generic control instant k, the same furnace production rate is assumed for all the considered future instants $(k+i)$. In the proposed architecture shown in Fig. 4.3, the bCVs *free response* is computed by *Predictions Calculator* module. For the generic billet that at the current control instant k is located on the jth place of the furnace, the temperature predictions that have to be considered are the temperature predictions related to the time window from $(k+1)$ to $(k+e_j)$. e_j represents the predicted future prediction instant related to the exit of the jth billet from

the furnace. T_{fm} is the current furnace movement time, defined as the time passed between the last two exited billets; in (4.6), T_{fm} is assumed to be indicated with the same measurement unit of the T_s sampling time. $ceil(x)$ rounds x to the nearest integer greater than or equal to x. At each control instant k, T_{fm} and the current furnace production rate are related by the following general expression:

$$T_{fm} = \frac{(3600[s] \cdot mass[t])}{(1[h] \cdot Prod[t/h])} \qquad [s] \tag{4.7}$$

where $mass$ indicates the mass of the last billet that exited the furnace (measured in *tons*, $[t]$) while $Prod$ indicates the current furnace production rate (measured in $[t/h]$) that is included in the final $d(k-1)$ vector. The general expression (4.7) can be subjected to small modifications in case of the presence in the furnace of billets with different lengths that exit in sequence.
Based on the previous considerations, each billet that at the current control instant is located inside the furnace is represented by an own "steady-state", represented by the related e_j instant. In (4.6), $\Theta_{b_{j_{(i,:)}}} \in \mathbb{R}^{1\times(l_u \cdot H_u)}$ represents the relationship between the "forced" component $\Delta\hat{b}_j(k+i|k)$ and the future MVs moves. Within $\Theta_{b_{j_{(i,:)}}}$ terms, because of the cascading of the zCVs-MVs/DVs identified models and of the LPV model, also information contained in the Θ matrix of (3.38) is included.

4.2.2 Billets status and APC modes

As described in Chapter 3, *Data Conditioning & Decoupling Selector* (*DC & DS*) block (Fig. 4.3) represents an auxiliary supervision block that, among its functions, defines the final status value for each process variable, which allows specifying the variables to be included in the MPC control problem at the current control instant. In the *E-FESTO* APC system, *DC & DS* block must also determine the final status value of each of the variables included in bCVs group.
At each control instant k, bCVs updated estimations are provided by the virtual sensor to *DC & DS* block (Fig. 4.3, right side of *DC & DS* block, $b(k)$). Together with $b(k)$ values, also an initial bCVs status value is provided to *DC & DS* block, thanks to a cooperative action of the *SCADA* system and of the developed virtual sensor. For each bCV, two status values have been introduced: "1" and "0". The status value "1" related to a generic bCV indicates that the MPC scheme must control that variable, i.e. the bCV is *active*. Conversely, the bCV status value equal to "0" indicates that the bCV is *inactive*: at the current control instant the MPC scheme has not in control that bCV, i.e. MVs must not act to satisfy its specifications.

The initial bCVs status value takes into account plant driving specifications and needs, together with particular bCVs plant conditions. Plant driving specifications and needs refer to the need of a temporary furnace stop (planned or unforeseen), where the furnace production rate approaches to 0 $[t/h]$ and the computation of e_j instants of (4.6) is not possible. Particular bCVs plant conditions refer to bad estimations of the virtual sensor, to empty furnace places, or to the substitution of a device that is needed for a correct virtual sensor action, i.e. the optical pyrometers. In the proposed APC system, bad estimations by the virtual sensor can be detected using different techniques, e.g. suitable temperature thresholds. The initial bCVs status is included in a $Status_{bSCADAVS} \in \mathbb{R}^{m_b \times 1}$ vector; it contains "0" values for the bCVs that have been set as *inactive* ("1" otherwise). For example, in the positions of $Status_{bSCADAVS}$ related to furnace empty places, "0" value is included. Furthermore, in case of a temporary furnace stop, bad estimations of the virtual sensor, or crucial devices substitution, all elements of $Status_{bSCADAVS}$ vector are equal to "0". *DC & DS* block, for each jth billet that is currently in the furnace and that is characterized by a "1" on the jth position of $Status_{bSCADAVS}$ vector, computes the related e_j parameter (see (4.6)). If for the jth billet this parameter results equal to 1, *DC & DS* block zeroes the related element in the initial $Status_{bSCADAVS}$ vector. This condition derives from the cascading of the zCVs-MVs/DVs identified models and of the LPV model. Practically, this situation means that the considered billet cannot be controlled, i.e. the related $\Theta_{b_{j_{(1,:)}}}$ in (4.6) is composed by elements all equal to zero. The final bCVs status value (Fig. 4.3, left side of *DC & DS* block, *u-d-y-b Status*) is defined by an element-wise logical "AND" between $Status_{bSCADAVS}$ vector and an additional vector that takes into account the definition of criticity relationships between the zCVs status value and the bCVs status value. Considering u_b vector, i.e. the inputs vector of (4.4) that contains suitable linear combinations of the zones temperatures of the considered furnace, and remembering that the zones temperatures of the furnace are included in the zCVs group, at least one of the zCVs that appear in u_b vector is considered as a critical input for the final bCVs status value. The number of critical inputs may vary between 1 and the total number of zCVs that appear in u_b vector. Practically, a bCV cannot be *active* if there is at least one critical *inactive* zCV (that appears in the u_b vector). Denoting with $Status_{b-y} \in \mathbb{R}^{m_b \times 1}$ the vector related to the influence of zCVs status on bCVs status, its elements can be equal to "0" or "1". The final bCVs status value, denoted by $Status_b \in \mathbb{R}^{m_b \times 1}$, is defined by the following element-wise logical "AND":

$$Status_b = Status_{bSCADAVS} \wedge Status_{b-y} \tag{4.8}$$

where $\wedge$ represents the element-wise logical "AND".
The final bCVs status vector is provided by *DC & DS* block to *Predictions Calculator* module, to *DO* module, and to *SCADA* block (Fig. 4.3, left side of *DC & DS* block, *u-d-y-b Status* and *b Status*). The additional information that has to be exploited by *DC & DS* block for bCVs status processing and final computation has been included in *Plant Signals & Parameters* term of Fig. 4.3.
Based on the final bCVs status vector, in order to always ensure the control specifications described in Subsection 4.1.1, two main control modes have been defined in *E-FESTO* APC system:

1. *adaptive* APC mode: use of both identified zCVs-MVs/DVs linear time invariant models and first principles billets temperature LPV model and exploitation of billets virtual sensor information within a *customized two-layer* linear adaptive MPC strategy for control specifications fulfilment;
2. *zones* APC mode: use of the only zCVs-MVs/DVs identified linear time invariant models within a *two-layer* linear MPC strategy for control specifications fulfilment.

Practically, the basic control mode is constituted by the *adaptive* APC mode (see Subsection 4.2.3); in this control mode at least a bCV is *active*. When all bCVs are *inactive*, *E-FESTO* APC system switches to *zones* APC mode (see Subsection 4.2.4) [112], [113].

4.2.3 The *adaptive* APC mode

As mentioned in Subsection 4.2.1, each billet that at the current control instant is located inside the furnace is represented by an own "steady-state", represented by the related e_j instant (see (4.6)). For this reason, the *customization* related to the introduction of the developed overall linear billets temperature model in the basic *two-layer* linear MPC strategy of Chapter 3 only interests the *Predictions Calculator* module and the *DO* module formulations. *TOCS* module formulation does not take into account the information provided by the developed overall linear billets temperature model, so *TOCS* module formulation remains the same of Subsection 3.1.2 and is based on the zCVs-MVs/DVs linear time invariant models. As it will be clarified in the following, suitable tuning procedures can guarantee the desired control performances.
The bCVs *free response* is computed by *Predictions Calculator* module, as it has been already described; for the generic billet that at the current control instant k is located on the jth place of the furnace, the temperature predictions that have to be considered are the temperature predictions related to the time window from $(k+1)$ to $(k+e_j)$, where e_j represents the predicted future prediction instant related to the exit of the jth billet from the furnace. In order to

consider all predictions of all the billets temperatures in the entire related time windows, the prediction horizon H_p within the *adaptive* APC mode is always set as the maximum value among e_j values related to *active* bCVs. For example, if the 1st bCV is *active*, the prediction horizon H_p is set as e_1, i.e. the sampling instants that the 1st billet in the furnace requires to traverse the entire furnace (the 1st place is assumed to be the closest place to the furnace inlet). So, the prediction horizon H_p within the *adaptive* APC mode changes whenever the furnace movement time (and the furnace production rate) changes: a direct relationship between H_p and the furnace movement time (and the furnace production rate) has been defined. For example, when the furnace movement time decreases (and the furnace production rate increases), H_p decreases. For the definition of the control horizon H_u within the *adaptive* APC mode, the following relationship has been introduced:

$$H_u = ceil(\frac{H_p}{r_{H_p - H_u}}) \tag{4.9}$$

where $r_{H_p - H_u}$ represents the desired ratio between H_p and H_u. $ceil(x)$ rounds x to the nearest integer greater than or equal to x. The prediction instants related to the MVs future moves M_i ($i = 1 \dots H_u$; $M_1 = 0$) are defined in order to ensure several MVs control moves in the first prediction instants and to ensure the required number of MVs control moves over the prediction horizon H_p. Clearly, also M_i ($i = 1 \dots H_u$; $M_1 = 0$) are online adapted, together with H_p and H_u.
So, within the *adaptive* APC mode, the horizons H_p and H_u, together with the M_i ($i = 1 \dots H_u$; $M_1 = 0$) terms, can change at different control instants due to the modification of the furnace movement time (and of the furnace production rate). This adaptation procedure of H_p, H_u and M_i ($i = 1 \dots H_u$; $M_1 = 0$) terms guarantees a sufficient H_p for the evaluation of the billets temperatures inside the furnace, together with a sufficient number of properly spaced MVs future moves for the *DO* optimization problem solution.
The described methodology for the definition of the H_p, H_u and M_i ($i = 1 \dots H_u$; $M_1 = 0$) terms must always guarantee that H_p is set long enough (finite value) to capture the steady-state effects of all future MVs moves, with regard to the zCVs-MVs/DVs linear time invariant models. In this way, the first consistency relationship between the *TOCS* and *DO* modules formulations with regard to the zCVs-MVs/DVs linear time invariant models is always guaranteed.
In order to handle particular and infrequent furnace conditions (e.g. large number of empty places), *ad hoc* variations of the described methodology have been defined.
Within the *adaptive* APC mode, the basic *DO* module formulation (3.41)-(3.42)

has been *customized* as follows:

$$\min_{\Delta U(k),\varepsilon_{yDO}(k),\varepsilon_{bDO}(k)} V_{DO}(k) = \min_{\Delta U(k),\varepsilon_{yDO}(k),\varepsilon_{bDO}(k)} (\sum_{j=1}^{m_y} \sum_{i=H_{w_j}}^{H_p} (Q_{(j,j)}(i) \cdot (\hat{y}_j(k+i|k)$$

$$- r_j(k+i|k))^2) + \sum_{i=1}^{H_u} \|\Delta\hat{u}(k+M_i|k)\|^2_{R(i)} + \sum_{i=1}^{H_u} \|\hat{u}(k+M_i|k) - u_r(k+M_i|k)\|^2_{S(i)} +$$

$$+ \|\varepsilon_{yDO}(k)\|^2_{\rho_{yDO}} + \sum_{j=1}^{m_b} \sum_{i=1}^{e_j} (Q_{b_{(j,j)}}(i) \cdot (\hat{b}_j(k+i|k) - r_{b_j}(k+i|k))^2) + \|\varepsilon_{bDO}(k)\|^2_{\rho_{bDO}}) \tag{4.10}$$

subject to

$$lb_{duDO}(i) \leq \Delta\hat{u}(k+M_i|k) \leq ub_{duDO}(i), \quad i = 1 \dots H_u$$

$$lb_{uDO}(i) \leq \hat{u}(k+M_i|k) \leq ub_{uDO}(i), \quad i = 1 \dots H_u \tag{4.11}$$

$$lb_{yDO_j}(i) - \gamma_{lbyDO_j}(i) \cdot \varepsilon_{yDO}(k) \leq \hat{y}_j(k+i|k) \leq ub_{yDO_j}(i) + \gamma_{ubyDO_j}(i) \cdot \varepsilon_{yDO}(k),$$

$$j = 1 \dots m_y, \; i = H_{w_j} \dots H_p$$

$$lb_{bDO_j}(i) - \gamma_{lbbDO_j}(i) \cdot \varepsilon_{bDO}(k) \leq \hat{b}_j(k+i|k) \leq ub_{bDO_j}(i) + \gamma_{ubbDO_j}(i) \cdot \varepsilon_{bDO}(k),$$

$$j = 1 \dots m_b, \; i = 1 \dots e_j$$

$$\varepsilon_{yDO}(k) \geq 0_{n_{\varepsilon yDO} \times 1}$$

$$\varepsilon_{bDO}(k) \geq 0_{n_{\varepsilon bDO} \times 1}$$

where $||\cdot||$ is the Euclidean norm.
In the *customized DO* module formulation within the *adaptive* APC mode, the additional terms with respect to the basic *DO* module formulation (3.41)-(3.42) are represented by the expressions related to the bCVs. $r_{b_j}(k+i|k)$ represents the reference trajectory value of the jth bCV at ith prediction instant; the related tracking error is weighted by a nonnegative scalar $Q_{b_{(j,j)}}(i)$. bCVs reference trajectories are supplied by the *SCADA* system within *Billets Parameters* term of Fig. 4.3 and can change at different control instants, based on the *Rolling* phase specifications.
In (4.10), the magnitude of the jth bCV future value at the ith prediction instant is constrained by $lb_{bDO_j}(i)$ (lower constraint) and $ub_{bDO_j}(i)$ (upper constraint). Each jth bCV can be controlled (with reference trajectories and/or with constraints) on the related time window. All *DO* bCVs constraints, if present, can change at different control instants (based on the *Rolling* phase specifications) and they are forwarded by *SCADA* system (Fig. 4.3, *u-b Constraints*). In order to prevent infeasibility situations, bCVs constraints can been assumed as *soft* constraints. In fact, in the running of an industrial plant, there may be cases where changes on the operating conditions and/or

constraints modifications performed by plant operators could be such that no solution within the given set of operating constraints exists. Consequently, the controller could not find an output solution and no control action on the system would be performed. In the conduction of a real plant, this situation is not advisable so that, in order to find a solution of the control problem, the violation of some bCVs constraints is admitted. In this way, a feasible solution is found that possibly *relaxes* one or more of the original set bCVs constraints. Their *softening* is admitted in critical situations through the introduction of additional decision variables, represented by a nonnegative slack variables vector $\varepsilon_{bDO}(k) \in \mathbb{R}_0^{+n_{\varepsilon bDO}\times 1}$. In general, the minimum slack variables number is 1 (all bCVs constraints *relaxations* are grouped), while the maximum one is $2\sum_{j=1}^{m_b} e_j$. When $n_{\varepsilon bDO} = 2\sum_{j=1}^{m_b} e_j$, each bCVs *soft* constraint is equipped with an own slack variable. The slack variables vector has been introduced in the constraints (4.11) related to the generic jth bCV at the ith prediction instant through nonnegative weights, contained in $\gamma_{lbbDO_j}(i) \in \mathbb{R}_0^{+1\times n_{\varepsilon bDO}}$ and $\gamma_{ubbDO_j}(i) \in \mathbb{R}_0^{+1\times n_{\varepsilon bDO}}$. $\gamma_{lbbDO_j}(i)$ and $\gamma_{ubbDO_j}(i)$ are vectors that could be characterized by at most an only nonzero positive element (on the correspondent position of the related slack variable in $\varepsilon_{bDO}(k)$). The slack variables vector has been introduced in the quadratic cost function (4.10) through a positive definite diagonal matrix $\rho_{bDO} \in \mathbb{R}^{n_{\varepsilon bDO}\times n_{\varepsilon bDO}}$. A joint setting of $\gamma_{lbbDO_j}(i)$, $\gamma_{ubbDO_j}(i)$ and ρ_{bDO} terms allows to suitably rank the importance of constraints *relaxations*, giving a priority order between bCVs constraints. Considering also $\gamma_{lbyDO_j}(i)$, $\gamma_{ubyDO_j}(i)$ and ρ_{yDO} terms related to zCVs, a global priority order between bCVs-zCVs constraints can be obtained.
$S(i)$, $Q(i)$, $R(i)$, $\gamma_{lbyDO_j}(i)$, $\gamma_{ubyDO_j}(i)$, ρ_{yDO}, $n_{\varepsilon yDO}$, $\gamma_{lbbDO_j}(i)$, $\gamma_{ubbDO_j}(i)$, ρ_{bDO}, the adaptation methodology of H_u and M_i, and the grouping policies of zCVs-bCVs constraints *relaxations* are among *Billets Parameters* of Fig. 4.3, together with all the other *DO* parameters related to zCVs that have been described in Chapter 3. They can be changed at different control instants.
Within *Billets Parameters* of Fig. 4.3, in order to perform the desired bCVs-zCVs control methodology (with reference trajectories and/or with constraints), suitable weights zeroing and constraints cut off terms have been included. Furthermore, the final bCVs status $Status_b$ vector information provided by *DC & DS* block must be included in the *DO* formulation. When the generic jth element ($j=1\dots m_b$) of the $Status_b$ vector is equal to zero, all the constraints related to the jth bCV in (4.11) are cut off by *DO* module. Moreover, when the generic jth element ($j=1\dots m_b$) of the $Status_b$ vector is equal to zero, all $Q_{b_{(j,j)}}(i)$ terms are zeroed by *DO* module.
The problem (4.10)-(4.11) has been suitably parametrized as a function of the adopted decision variables vector, composed by $\Delta\hat{u}(k+M_i|k)$ ($i=1\dots H_u$), $\varepsilon_{yDO}(k)$, and $\varepsilon_{bDO}(k)$. The parametrization methodology is similar to that de-

scribed in Chapter 3. At each control instant k where *E-FESTO* APC system exploits the *adaptive* APC mode, *DO* module, exploiting also the information provided by *TOCS* module solution, solves the QP problem (3.41)-(3.42), computing $\Delta\hat{u}(k+M_i|k)$ $(i=1\dots H_u)$, $\varepsilon_{yDO}(k)$, and $\varepsilon_{bDO}(k)$. Among computed MVs future values, only the first value $u(k)=\hat{u}(k|k)=u(k-1)+\Delta\hat{u}(k|k)$ is applied to the plant.

4.2.4 The *zones* APC mode

When all bCVs are *inactive*, *E-FESTO* APC system switches to *zones* APC mode; practically, this control mode corresponds exactly to the control mode described within the basic APC framework of Chapter 3. The only introduced feature is related to the criticity relationships between the status values of different MVs (see Subsection 4.2.1), that interest also the *adaptive* APC mode. Note that, in both *adaptive* and *zones* APC modes, *TOCS* module exploits the only zCVs-MVs/DVs identified linear time invariant models. The only differences between the two *TOCS* module formulations are represented by the different computation methodologies related to H_p and H_u. As described in Chapter 3, when both *DO* and *TOCS* modules exploit the same linear time invariant process model, H_p and H_u parameters are forwarded by *SCADA* system and they can be set as explained in Section 3.3.
In general, the parameters related to zCVs and MVs of the optimization problems solved by *DO* module in *adaptive* and *zones* APC modes can be different. However, the optimization problems solved by *DO* module in *adaptive* and *zones* APC modes are always different.

4.2.5 Tuning and furnace management details

In order to fulfil the specifications defined in Subsection 4.1.1, an accurate tuning procedure has to be performed for both the defined control modes.
In all the considered case studies, both *adaptive* and *zones* APC modes share some tuning features. They do not consider *DO* tracking objectives for zCVs. For this purpose, all $Q(i)$ matrices are always composed by elements all equal to zero. zCVs are always controlled through suitable *soft* constraints. Furthermore, among zCVs, the most important variables are the air flow rate and the smoke-exchanger temperature; the compliance with the assigned constraints guarantees furnace safety. Then there are the temperature difference between adjacent furnace zones and the furnace zones temperatures; finally, there is the valves opening position (per cent). Usually, the temperature difference between adjacent furnace zones is considered more important with respect to the zones temperatures, in order to ensure, when needed, a monotonic increase of the furnace zones temperature along the furnace (from the furnace inlet to the fur-

nace outlet). With regard to zCVs constrained control using only a defined set of control inputs, the decoupling strategy described in Section 3.2 is exploited, as will be described in Sections 4.3-4.4.
In the *adaptive* APC mode, bCVs can be controlled with reference trajectories and/or with constraints, based on the specifications of the *Rolling* phase. In all the considered case studies, the generic jth *active* bCV is always controlled only at the related e_jth prediction instant; practically, its target or its constraints are considered only at the related furnace exit prediction instant. bCVs specifications have been always considered less important than zCVs control requirements, in order to first ensure a safe furnace conduction.
Within the *TOCS* module formulation of both APC modes, the just mentioned priority order among zCVs has been imposed. Furthermore, in order to minimize the fuel specific consumption and the excess of air within the assigned MVs and zCVs constraints, the *TOCS* c_u weights related to air/fuel stoichiometric ratios (when present among the defined MVs) and to fuel flow rates have been set as positive. In particular, the minimization of the fuel flow rates related to the furnace zones closer to the furnace inlet is considered as more important with respect to the minimization of the fuel flow rates related to the last furnace zones. This tuning feature contributes to the achievement of a monotonic increase of the furnace zones temperature along the furnace. The *TOCS* c_u weights related to the air flow rates (when present among the defined MVs) have been always set to zero, together with the *TOCS* c_y weights.
In *TOCS* and *DO* modules within both APC modes, MVs constraints are always considered as *hard* constraints. In the case studies where stoichiometric ratios have been included among MVs, air/fuel stoichiometric ratios constraints are automatically considered. In the case studies where the MVs group includes air and fuel flow rates, the stoichiometric ratios constraints must be suitably included within *TOCS* and *DO* modules formulation within both APC modes (see Section 4.4).
With regard to the compliance with the defined billets temperature constraints and/or targets at the furnace outlet, these specifications are included in the *DO* formulation of the *adaptive* APC mode (see Subsection 4.2.3) and within this APC mode they are directly considered in the computation of the *DO* optimization problem solution. For this reason, within the *adaptive* APC mode, zCVs and MVs constraints are usually set very large, while assuring process safety. In this way, the information provided by the billets temperature virtual sensor and by the LPV model can be optimally exploited by *DO* module. As described in Subsection 4.2.3, *TOCS* module formulation does not take into account the information provided by the developed overall linear billets temperature model; for this reason, the steady-state targets supplied by *TOCS* module may be unreachable in the *adaptive* APC mode and the considerations

of Section 3.3 about tuning of the diagonal terms of $S(i)$ matrices must be revised within this APC mode. Complying with zCVs constraints, a profitable trade-off between MVs tracking and bCVs requirements (tracking and/or constraints tightening) has been ensured, weighting also MVs moves magnitude. In particular, *ad hoc* adaptive $S(i)$ tuning strategies have been defined, based on the adaptation procedure of H_p, H_u and M_i ($i = 1 \dots H_u$; $M_1 = 0$) terms. The basic idea lies in the introduced relationship between H_p and the furnace production rate: with the furnace production rate decrease, H_p increases and the billets remain longer inside the furnace; for this reason, with the furnace production rate decrease, the diagonal terms of $S(i)$ matrices must ensure a dominance of the specifications related to the fuel minimization with respect to the billets temperature specifications fulfilment.
Billets temperature specifications are not directly included in the *zones* APC mode. Thanks to the *adaptive* APC mode, suitable zCVs and MVs constraints tables have been defined for the *zones* APC mode. The defined tables (that are exploited by plant operators) take into account different furnace boundary conditions, e.g. the furnace production rate, the billets inlet temperature, and the required outlet temperature. Furthermore, in some cases, when *E-FESTO* APC system switches to *zones* APC mode, information provided by the future zCVs predictions within the previous *adaptive* APC mode control instants can be taken into account for an online definition of the future zCVs constraints. In this way, in both *adaptive* and *zones* APC modes, the compliance with outlet billets temperature specifications is ensured and the furnace thermal barycenter is moved toward the *Soaking Area*, thus limiting also billets overheating and scale formation.
Thanks to the two defined APC modes, all furnace conditions can be efficiently handled and optimized.
According to the author knowledge, the proposed billets reheating furnaces control method represents a contribution of the research activity reported in the present dissertation [114], [115]. The proposed billets reheating furnaces control method has been awarded with an Italian patent [90].

4.3 Case study: *pusher type* reheating furnace

In this section the description of one of the five billets reheating furnaces where the *E-FESTO* APC system has been installed is reported. It is a *pusher type* reheating furnace.
The *Reheating* phase of the *pusher type* reheating furnace at issue is schematically represented in Fig. 4.4.
The considered furnace can contain up to 136 billets ($m_b = 136$). The billets are characterized by a rectangular section ($0.2\ [m] \times 0.16\ [m]$), with a length

of 9 $[m]$. Billets mass is equal to about 2 $[t]$. The billets inlet temperature varies approximately on the range 20 $[°C]$ - 700 $[°C]$, while the outlet temperature can vary according to specifications related to the subsequent plastic deformation phase. For example, outlet temperature can range on 1030 $[°C]$ - 1080 $[°C]$. The inlet billets temperature is measured by an optical pyrometer that is located near the inlet of the furnace. The outlet billets temperature is measured by an optical pyrometer that is located at the exit of first stage of rolling mill stands.

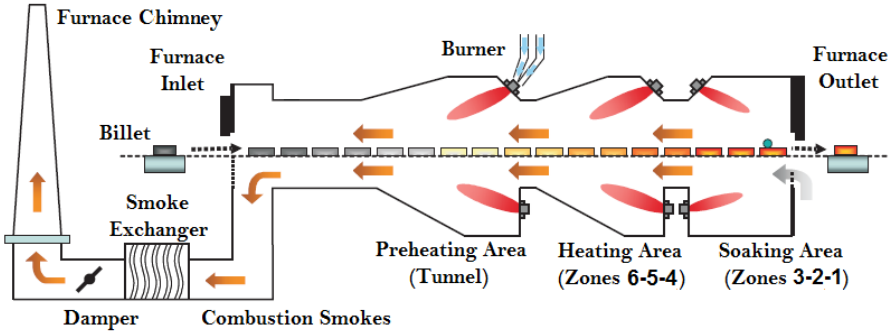

Figure 4.4: Representation of the *pusher type* reheating furnace.

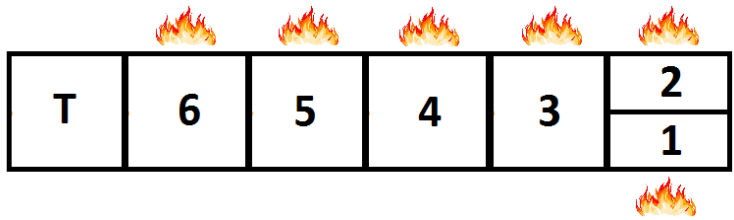

Figure 4.5: Detail of the *pusher type* reheating furnace zones disposition.

During transport through the furnace, billets are moved through different furnace zones with a maximum furnace production rate of about 120 $[t/h]$. Starting from the furnace inlet (Fig. 4.4, left side), the furnace zones are named *tunnel*, *zone 6*, *zone 5*, *zone 4*, *zone 3*, *zone 2*, and *zone 1*; the furnace temperatures reach up to 1250 $[°C]$. The seven furnace zones are grouped in the three main areas that have been described in Section 4.1: *Preheating Area*, *Heating*

Area, and *Soaking Area*. *Preheating Area* is the only furnace area characterized by the absence of burners. *Soaking Area* is characterized by a transversal disposition of its zones, i.e. *zone 2* and *zone 1*. This detail is reported in Fig. 4.5. Table 4.1 reports details on the furnace zones: their length, the (maximum) related number of billets contained and typical temperature ranges are shown.

Table 4.1: *Pusher type* reheating furnace zones features.

Furnace Zone	**Length**	**Billets Number**	**Temperature Range**
Tunnel	4.733 $[m]$	38	550 $[°C]$ - 950 $[°C]$
Zone 6	3.477 $[m]$	16	800 $[°C]$ - 1150 $[°C]$
Zone 5	6.4 $[m]$	32	800 $[°C]$ - 1150 $[°C]$
Zone 4	3.2 $[m]$	16	800 $[°C]$ - 1200 $[°C]$
Zone 3	4.546 $[m]$	22	1000 $[°C]$ - 1250 $[°C]$
Zones 2-1	3.2 $[m]$	12	1000 $[°C]$ - 1250 $[°C]$

Table 4.2: *Pusher type* reheating furnace MVs.

Variable Name	**Acronym [Units]**	**MVs Range**
Zone 6 Fuel Flow Rate	$Fuel_6$ $[Nm3/h]$	0 $[Nm3/h]$ - 800 $[Nm3/h]$
Zone 5 Fuel Flow Rate	$Fuel_5$ $[Nm3/h]$	0 $[Nm3/h]$ - 1600 $[Nm3/h]$
Zone 4 Fuel Flow Rate	$Fuel_4$ $[Nm3/h]$	0 $[Nm3/h]$ - 650 $[Nm3/h]$
Zone 3 Fuel Flow Rate	$Fuel_3$ $[Nm3/h]$	0 $[Nm3/h]$ - 650 $[Nm3/h]$
Zone 2 Fuel Flow Rate	$Fuel_2$ $[Nm3/h]$	0 $[Nm3/h]$ - 250 $[Nm3/h]$
Zone 1 Fuel Flow Rate	$Fuel_1$ $[Nm3/h]$	0 $[Nm3/h]$ - 250 $[Nm3/h]$
Zone 6 Stoich. Ratio	R_6 []	10.8 - 12
Zone 5 Stoich. Ratio	R_5 []	9.9 - 12
Zone 4 Stoich. Ratio	R_4 []	10.5 - 11.5
Zone 3 Stoich. Ratio	R_3 []	10 - 11.5
Zone 2 Stoich. Ratio	R_2 []	9.6 - 10.8
Zone 1 Stoich. Ratio	R_1 []	9.8 - 10.8

Table 4.3: *Pusher type* reheating furnace DVs.

Variable Name	**Acronym [Units]**	**DVs Range**
Furnace Production Rate	$Prod$ $[t/h]$	0 $[t/h]$ - 120 $[t/h]$
Furnace Pressure	$FurnPress$ $[mm/H2O]$	0.7 $[mm/H2O]$ - 1.2 $[mm/H2O]$
Air Pressure	$AirPress$ $[mbar]$	65 $[mbar]$ - 90 $[mbar]$

Table 4.4: *Pusher type* reheating furnace main zCVs.

Variable Name	**Acronym [Units]**
Tunnel Temperature	Tun $[°C]$
Zone 6 Temperature	$Temp_6$ $[°C]$
Zone 5 Temperature	$Temp_5$ $[°C]$
Zone 4 Temperature	$Temp_4$ $[°C]$
Zone 3 Temperature	$Temp_3$ $[°C]$
Zone 2 Temperature	$Temp_2$ $[°C]$
Zone 1 Temperature	$Temp_1$ $[°C]$
Smoke-Exchanger Temp.	$Temp_{SE}$ $[°C]$
Total Air Flow Rate	$TotAir$ $[Nm3/h]$
Tunnel - Zone 6 Temp. Diff.	$TDiff_{T6}$ $[°C]$
Zone 6 - Zone 5 Temp. Diff.	$TDiff_{65}$ $[°C]$
Zone 5 - Zone 4 Temp. Diff.	$TDiff_{54}$ $[°C]$
Zone 4 - Zone 3 Temp. Diff.	$TDiff_{43}$ $[°C]$
Zone 3 - Mean Zones 2-1 Temp. Diff.	$TDiff_{321}$ $[°C]$
Zone 1 - Zone 2 Temp. Diff.	$TDiff_{12}$ $[°C]$

From the analysis of the overall process, suitable variables have been selected. MVs group six fuel flow rates, together with the related stoichiometric ratios ($l_u = 12$, see Table 4.2). These variables act on local control loops regulated by PID controllers. Among DVs, furnace and air pressures, together with furnace production rate, have been included ($l_d = 3$, see Table 4.3). Furnace and air pressures act on local control loops regulated by PID controllers. Among zCVs furnace zones temperature (tunnel included), temperature difference between adjacent furnace zones, smoke-exchanger temperature and fuel valves opening position (per cent) have been included ($m_y = 21$). The main zCVs are listed in Table 4.4.

A black-box identification phase has been executed in order to obtain zCVs-MVs/DVs models: linear time invariant asymptotically stable first and second order strictly proper minimum phase models without delays on the inputs-outputs channels have been achieved. Deviations of process variables from consistent operating points are considered for the formulation of these models. Tables 4.5-4.6-4.7 symbolically represent the main zCVs-MVs and zCVs-DVs gain matrices, i.e. submatrices of $G_{yu} \in \mathbb{R}^{21\times12}$ and $G_{yd} \in \mathbb{R}^{21\times3}$: a nonzero mapping on a MV-zCV pair or on a DV-zCV pair has been indicated by the gain sign of the correspondent transfer function. The structure of Table 4.5 is in accordance with the physical behavior of the process where hot gases from downstream zones influence upstream zone temperatures, but not vice versa.

Table 4.5: *Pusher type* reheating furnace zCVs-MVs mapping matrix (I).

Acronym	$Fuel_6$	$Fuel_5$	$Fuel_4$	$Fuel_3$	$Fuel_2$	$Fuel_1$
Tun	+	+	+	+	+	+
$Temp_6$	+	+	+	+	+	+
$Temp_5$		+	+	+	+	+
$Temp_4$			+	+	+	+
$Temp_3$				+	+	+
$Temp_2$					+	+
$Temp_1$					+	+
$Temp_{SE}$	+	+	+	+	+	+
$TotAir$	+	+	+	+	+	+

Table 4.6: *Pusher type* reheating furnace zCVs-MVs mapping matrix (II).

Acronym	R_6	R_5	R_4	R_3	R_2	R_1
Tun						
$Temp_6$	−					
$Temp_5$		−				
$Temp_4$			−			
$Temp_3$				−		
$Temp_2$					−	−
$Temp_1$					−	−
$Temp_{SE}$						
$TotAir$	+	+	+	+	+	+

Table 4.7: *Pusher type* reheating furnace zCVs-DVs mapping matrix.

Acronym	$Prod$	$FurnPress$	$AirPress$
Tun	−	+	−
$Temp_6$	−	+	−
$Temp_5$	−	+	−
$Temp_4$	−	+	−
$Temp_3$	−	+	−
$Temp_2$	−	+	−
$Temp_1$	−	+	−
$Temp_{SE}$	−	+	−
$TotAir$			

Table 4.8: *Pusher type* reheating furnace initial *Decoupling Matrix* (I).

Acronym	$Fuel_6$	$Fuel_5$	$Fuel_4$	$Fuel_3$	$Fuel_2$	$Fuel_1$
Tun	1	1	0	0	0	0
$Temp_6$	1	0	0	0	0	0
$Temp_5$	1	1	0	0	0	0
$Temp_4$	1	1	1	0	0	0
$Temp_3$	1	1	1	1	0	0
$Temp_2$	1	1	1	1	1	0
$Temp_1$	1	1	1	1	0	1
$Temp_{SE}$	1	1	0	0	0	0
$TotAir$	1	1	0	0	0	0

Table 4.9: *Pusher type* reheating furnace initial *Decoupling Matrix* (II).

Acronym	R_6	R_5	R_4	R_3	R_2	R_1
Tun	1	1	1	1	1	1
$Temp_6$	1	1	1	1	1	1
$Temp_5$	1	1	1	1	1	1
$Temp_4$	1	1	1	1	1	1
$Temp_3$	1	1	1	1	1	1
$Temp_2$	1	1	1	1	1	0
$Temp_1$	1	1	1	1	0	1
$Temp_{SE}$	1	1	1	1	1	1
$TotAir$	0	0	0	0	0	0

The control specification *vi* listed in Subsection 4.1.1 requires that the constrained control of certain zCVs must be performed using only a defined set of control inputs. As described in Subsection 4.2.5, the decoupling strategy reported in Section 3.2 is exploited for this purpose. At this regard, in this specific case study, the following specifications related to the MVs to be exploited for the zCVs constrained control have been defined:

- the temperature of all furnace zones, except tunnel, must be controlled exploiting only the related fuel flow rate and the related stoichiometric ratio;
- the temperatures of the tunnel and of the smoke-exchanger, together with the total air flow rate must be controlled exploiting only zone 6 and zone 5 fuel flow rates.

For the compliance with these control specifications, the subpart of the initial

Decoupling Matrix D_E supplied by *SCADA* system to *DC & DS* block related to the interested zCVs has been shown in Tables 4.8-4.9 (the not reported rows are composed by elements all equal to 1).
With regard to the *DO* module zCVs constrained control, a single slack variable for each *active* zCV has been assigned within both *zones* and *adaptive* APC modes. This choice allows to assign the desired priority order (see Subsection 4.2.5) exploiting a joint setting of $\gamma_{lbyDO}(i)$, $\gamma_{ubyDO}(i)$ and ρ_{yDO} terms in the *DO* module optimization problem related to the *zones* and the *adaptive* APC modes.
With regard to the billets temperature nonlinear model exploited by the virtual sensor and to the derived LPV model, the u_b inputs vector is represented by the first five zone temperatures (tunnel-zone 3) and by the mean between zone 1 and zone 2 temperatures ($l_{u_b} = 6$). For this reason, the mean between zone 1 and zone 2 temperatures appears in Table 4.4 (Mean Zones 2-1, acronym $TempM_{21}$); in this way, a monotonic increase of the furnace zones temperature along the furnace (from the furnace inlet to the furnace outlet) that considers also the transversal disposition of zone 2 and zone 1 is achievable. The u_b vector is:

$$u_b = \begin{bmatrix} Tun \\ Temp_6 \\ Temp_5 \\ Temp_4 \\ Temp_3 \\ TempM_{21} \end{bmatrix} \in \mathbb{R}^{6\times 1} \tag{4.12}$$

In this case study all zCVs that appear in u_b vector are considered as critical inputs for the final bCVs status value (see Subsection 4.2.2). bCVs cannot be *active* if there is at least one *inactive* zCV that appears in u_b vector. Practically, the *adaptive* APC mode can be exploited only when all the seven zone temperatures (tunnel included) are *active*. Furthermore, in both *adaptive* and *zones* APC modes, for the generic jth furnace zone with an own burners set, the related stoichiometric ratio cannot be *active* when the related fuel flow rate is *inactive*.
With regard to the parameter $r_{H_p-H_u}$ (see (4.9)) within the *adaptive* APC mode, it has been set equal to 5. In this way a sufficient number of MVs future moves for the *DO* optimization problem solution has been provided, assuring also a feasible computational load.
With regard to the control of *active* bCVs within the *adaptive* APC mode, they are controlled with targets or constraints only at the related furnace exit prediction instant (see Subsection 4.2.5). A single slack variable for each *active* constrained bCV has been assigned within the *adaptive* APC mode. This choice allows to assign the desired priority order (see Subsection 4.2.5) exploit-

ing a joint setting of $\gamma_{lbbDO}(i)$, $\gamma_{ubbDO}(i)$ and ρ_{bDO} terms in the *DO* module optimization problem related to the *adaptive* APC mode.
With regard to the choice of the sampling times, T_{s_b}, i.e. the virtual sensor sampling time, it has been chosen always equal to 5 $[s]$; in this way, all furnace significant events can be taken into account. On the other hand, the *MPC* block and the *DC & DS* block run with a sampling time T_s equal to 1 $[min]$, in accordance to the obtained process model and to the computational load required by the overall control algorithm.
Within the *zones* APC mode, the prediction horizon H_p has been set equal to 60 ($[min]$), while the control horizon H_u has been set equal to 8 moves. The related M_i terms have been set as $M_i = i - 1$ $(i = 1 \dots 8)$, i.e. the 8 admitted MVs moves are assumed in the first eight prediction steps. The joint tuning of H_p, H_u and M_i parameters allows to capture the steady-state effects of all future MVs moves on the linear time invariant model considered within the *zones* APC mode. Furthermore, with this choice, the controller is equipped with a suitable number of decision variables for the solution of the involved optimization problems.
Simulation and field results related to the application of *E-FESTO* APC system on the described *pusher type* reheating furnace will be provided and discussed in Chapter 6.

4.4 Case study: *walking beam* reheating furnace

In this section the description of one of the five billets reheating furnaces where the *E-FESTO* APC system has been installed is reported. It is a *walking beam* reheating furnace.
The *Reheating* phase of the *walking beam* reheating furnace at issue is schematically represented in Fig. 4.6.
The considered furnace can contain up to 80 billets ($m_b = 80$). The billets are characterized by a rectangular (0.2 $[m]$ × 0.16 $[m]$) or a quadratic section (0.16 $[m]$ × 0.16 $[m]$ or 0.15 $[m]$ × 0.15 $[m]$). Billets length can be 4.5 $[m]$ or 9 $[m]$; billets mass can be equal to about 1 $[t]$ or 2 $[t]$, based on the related length. The billets inlet temperature varies approximately on the range 30 $[°C]$ - 700 $[°C]$, while the outlet temperature can vary according to specifications related to the subsequent plastic deformation phase. For example, outlet temperature can range on 1000 $[°C]$ - 1100 $[°C]$. The inlet billets temperature is measured by an optical pyrometer that is located near the inlet of the furnace. The outlet billets temperature is measured by an optical pyrometer that is located at the exit of first stage of rolling mill stands.

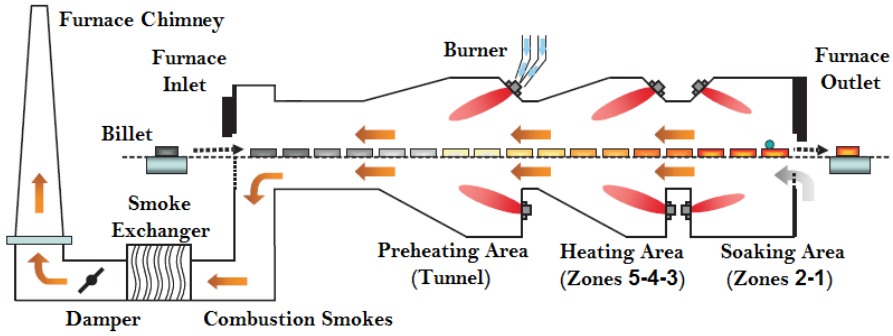

Figure 4.6: Representation of the *walking beam* reheating furnace.

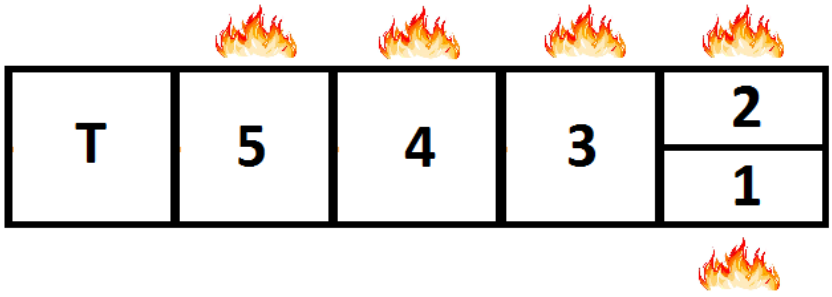

Figure 4.7: Detail of the *walking beam* reheating furnace zones disposition.

During transport through the furnace, billets are moved through different furnace zones with a maximum furnace production rate of about 120 $[t/h]$. Starting from the furnace inlet (Fig. 4.6, left side), the furnace zones are named *tunnel*, *zone 5*, *zone 4*, *zone 3*, *zone 2*, and *zone 1*; the furnace temperatures reach up to 1250 $[°C]$. The six furnace zones are grouped in the three main areas that have been described in Section 4.1: *Preheating Area*, *Heating Area*, and *Soaking Area*. *Preheating Area* is the only furnace area characterized by the absence of burners. *Soaking Area* is characterized by a transversal disposition of its zones, i.e. *zone 2* and *zone 1*. This detail is reported in Fig. 4.7. Table 4.10 reports details on the furnace zones: their length, the (maximum) related number of billets contained, the related number of air/fuel burners contained and typical temperature ranges are shown.

Table 4.10: *Walking beam* reheating furnace zones features.

Furnace Zone	**Length**	**Billets Number**	**Burners Number**	**Temperature Range**
Tunnel	7 $[m]$	30	0	500 $[°C]$ - 850 $[°C]$
Zone 5	4 $[m]$	10	12	750 $[°C]$ - 1150 $[°C]$
Zone 4	4 $[m]$	10	12	750 $[°C]$ - 1150 $[°C]$
Zone 3	4 $[m]$	10	12	750 $[°C]$ - 1150 $[°C]$
Zones 2-1	5 $[m]$	20	24	1100 $[°C]$ - 1250 $[°C]$

From the analysis of the overall process, suitable variables have been selected. MVs group five fuel flow rates, together with the related air flow rates ($l_u = 10$, see Table 4.11). These variables act on local control loops regulated by PID controllers. Among DVs, furnace and air pressures, together with furnace production rate, have been included ($l_d = 3$, see Table 4.12). Furnace and air pressures act on local control loops regulated by PID controllers. Among zCVs furnace zones temperature (tunnel included), temperature difference between adjacent furnace zones, smoke-exchanger temperature and fuel and air valves opening position (per cent) have been included ($m_y = 23$). The main zCVs are listed in Table 4.13.

Table 4.11: *Walking beam* reheating furnace MVs.

Variable Name	**Acronym [Units]**	**MVs Range**
Zone 5 Fuel Flow Rate	$Fuel_5$ $[Nm3/h]$	0 $[Nm3/h]$ - 500 $[Nm3/h]$
Zone 4 Fuel Flow Rate	$Fuel_4$ $[Nm3/h]$	0 $[Nm3/h]$ - 720 $[Nm3/h]$
Zone 3 Fuel Flow Rate	$Fuel_3$ $[Nm3/h]$	0 $[Nm3/h]$ - 750 $[Nm3/h]$
Zone 2 Fuel Flow Rate	$Fuel_2$ $[Nm3/h]$	0 $[Nm3/h]$ - 420 $[Nm3/h]$
Zone 1 Fuel Flow Rate	$Fuel_1$ $[Nm3/h]$	0 $[Nm3/h]$ - 420 $[Nm3/h]$
Zone 5 Air Flow Rate	Air_5 $[Nm3/h]$	0 $[Nm3/h]$ - 5900 $[Nm3/h]$
Zone 4 Air Flow Rate	Air_4 $[Nm3/h]$	0 $[Nm3/h]$ - 7900 $[Nm3/h]$
Zone 3 Air Flow Rate	Air_3 $[Nm3/h]$	0 $[Nm3/h]$ - 8000 $[Nm3/h]$
Zone 2 Air Flow Rate	Air_2 $[Nm3/h]$	0 $[Nm3/h]$ - 4900 $[Nm3/h]$
Zone 1 Air Flow Rate	Air_1 $[Nm3/h]$	0 $[Nm3/h]$ - 4900 $[Nm3/h]$

Table 4.12: *Walking beam* reheating furnace DVs.

Variable Name	**Acronym [Units]**	**DVs Range**
Furnace Production Rate	$Prod$ $[t/h]$	0 $[t/h]$ - 120 $[t/h]$
Furnace Pressure	$FurnPress$ $[mm/H2O]$	0.7 $[mm/H2O]$ - 1.2 $[mm/H2O]$
Air Pressure	$AirPress$ $[mbar]$	65 $[mbar]$ - 90 $[mbar]$

Table 4.13: *Walking beam* reheating furnace main zCVs.

Variable Name	**Acronym [Units]**
Tunnel Temperature	Tun $[°C]$
Zone 5 Temperature	$Temp_5$ $[°C]$
Zone 4 Temperature	$Temp_4$ $[°C]$
Zone 3 Temperature	$Temp_3$ $[°C]$
Zone 2 Temperature	$Temp_2$ $[°C]$
Zone 1 Temperature	$Temp_1$ $[°C]$
Smoke-Exchanger Temp.	$Temp_{SE}$ $[°C]$
Total Air Flow Rate	$TotAir$ $[Nm3/h]$
Tunnel - Zone 5 Temp. Diff.	$TDiff_{T5}$ $[°C]$
Zone 5 - Zone 4 Temp. Diff.	$TDiff_{54}$ $[°C]$
Zone 4 - Zone 3 Temp. Diff.	$TDiff_{43}$ $[°C]$
Zone 3 - Mean Zones 2-1 Temp. Diff.	$TDiff_{321}$ $[°C]$
Zone 1 - Zone 2 Temp. Diff.	$TDiff_{12}$ $[°C]$

A black-box identification phase has been executed in order to obtain zCVs-MVs/DVs models: linear time invariant asymptotically stable first and second order strictly proper minimum phase models without delays on the inputs-outputs channels have been achieved. Deviations of process variables from consistent operating points are considered for the formulation of these models. Tables 4.14-4.15-4.16 symbolically represent the main zCVs-MVs and zCVs-DVs gain matrices, i.e. submatrices of $G_{yu} \in \mathbb{R}^{23\times10}$ and $G_{yd} \in \mathbb{R}^{23\times3}$: a nonzero mapping on a MV-zCV pair or on a DV-zCV pair has been indicated by the gain sign of the correspondent transfer function. The structure of Table 4.14 is in accordance with the physical behavior of the process where hot gases from downstream zones influence upstream zone temperatures, but not vice versa.

Table 4.14: *Walking beam* reheating furnace zCVs-MVs mapping matrix (I).

Acronym	$Fuel_5$	$Fuel_4$	$Fuel_3$	$Fuel_2$	$Fuel_1$
Tun	+	+	+	+	+
$Temp_5$	+	+	+	+	+
$Temp_4$		+	+	+	+
$Temp_3$			+	+	+
$Temp_2$				+	+
$Temp_1$				+	+
$Temp_{SE}$	+	+	+	+	+
$TotAir$					

Table 4.15: *Walking beam* reheating furnace zCVs-MVs mapping matrix (II).

Acronym	Air_5	Air_4	Air_3	Air_2	Air_1
Tun					
$Temp_5$	−				
$Temp_4$		−			
$Temp_3$			−		
$Temp_2$				−	
$Temp_1$					−
$Temp_{SE}$					
$TotAir$	+	+	+	+	+

Table 4.16: *Walking beam* reheating furnace zCVs-DVs mapping matrix.

Acronym	$Prod$	$FurnPress$	$AirPress$
Tun	−	+	−
$Temp_5$	−	+	−
$Temp_4$	−	+	−
$Temp_3$	−	+	−
$Temp_2$	−	+	−
$Temp_1$	−	+	−
$Temp_{SE}$	−	+	−
$TotAir$			

Table 4.17: *Walking beam* reheating furnace initial *Decoupling Matrix* (I).

Acronym	$Fuel_5$	$Fuel_4$	$Fuel_3$	$Fuel_2$	$Fuel_1$
Tun	1	1	0	0	0
$Temp_5$	1	0	0	0	0
$Temp_4$	1	1	0	0	0
$Temp_3$	1	1	1	0	0
$Temp_2$	1	1	1	1	0
$Temp_1$	1	1	1	0	1
$Temp_{SE}$	1	1	0	0	0
$TotAir$	1	1	1	1	1

Table 4.18: *Walking beam* reheating furnace initial *Decoupling Matrix* (II).

Acronym	Air_5	Air_4	Air_3	Air_2	Air_1
Tun	1	1	1	1	1
$Temp_5$	0	1	1	1	1
$Temp_4$	1	0	1	1	1
$Temp_3$	1	1	0	1	1
$Temp_2$	1	1	1	0	1
$Temp_1$	1	1	1	1	0
$Temp_{SE}$	1	1	1	1	1
$TotAir$	1	1	0	0	0

The control specification *vi* listed in Subsection 4.1.1 requires that the constrained control of certain zCVs must be performed using only a defined set of control inputs. As described in Subsection 4.2.5, the decoupling strategy reported in Section 3.2 is exploited for this purpose. At this regard, in this specific case study, the following specifications related to the MVs to be exploited for the zCVs constrained control have been defined:

- the temperature of all the furnace zones, except tunnel, must be controlled exploiting only the related fuel flow rate;
- the temperatures of the tunnel and of the smoke-exchanger must be controlled exploiting only zone 5 and zone 4 fuel flow rates;
- the total air flow rate must be controlled exploiting only zone 5 and zone 4 fuel flow rates.

For the compliance with these control specifications, the subpart of the initial *Decoupling Matrix* D_E supplied by *SCADA* system to *DC & DS* block related to the interested zCVs has been shown in Tables 4.17-4.18 (the not reported

rows are composed by elements all equal to 1).
With regard to the *DO* module zCVs constrained control, a single slack variable for each *active* zCV has been assigned within both *zones* and *adaptive* APC modes. This choice allows to assign the desired priority order (see Subsection 4.2.5) exploiting a joint setting of $\gamma_{lbyDO}(i)$, $\gamma_{ubyDO}(i)$ and ρ_{yDO} terms in the *DO* module optimization problem related to the *zones* and the *adaptive* APC modes.
With regard to the billets temperature nonlinear model exploited by the virtual sensor and to the derived LPV model, the u_b inputs vector is represented by the first four zone temperatures (tunnel-zone 3) and by the mean between zone 1 and zone 2 temperatures ($l_{u_b} = 5$). For this reason, the mean between zone 1 and zone 2 temperatures appears in Table 4.13 (Mean Zones 2-1, acronym $TempM_{21}$); in this way, a monotonic increase of the furnace zones temperature along the furnace (from the furnace inlet to the furnace outlet) that considers also the transversal disposition of zone 2 and zone 1 is achievable. The u_b vector is:

$$u_b = \begin{bmatrix} Tun \\ Temp_5 \\ Temp_4 \\ Temp_3 \\ TempM_{21} \end{bmatrix} \in \mathbb{R}^{5\times 1} \tag{4.13}$$

In this case study all zCVs that appear in u_b vector are considered as critical inputs for the final bCVs status value (see Subsection 4.2.2). bCVs cannot be *active* if there is at least one *inactive* zCV that appears in u_b vector. Practically, the *adaptive* APC mode can be exploited only when all the six zone temperatures (tunnel included) are *active*.
With regard to the parameter $r_{H_p-H_u}$ (see (4.9)) within the *adaptive* APC mode, it has been set equal to 5. In this way a sufficient number of MVs future moves for the *DO* optimization problem solution has been provided, assuring also a feasible computational load.
With regard to the control of *active* bCVs within the *adaptive* APC mode, they are controlled with targets or constraints only at the related furnace exit prediction instant (see Subsection 4.2.5). A single slack variable for each *active* constrained bCV has been assigned within the *adaptive* APC mode. This choice allows to assign the desired priority order (see Subsection 4.2.5) exploiting a joint setting of $\gamma_{lbbDO}(i)$, $\gamma_{ubbDO}(i)$ and ρ_{bDO} terms in the *DO* module optimization problem related to the *adaptive* APC mode.
With regard to the choice of the sampling times, T_{s_b}, i.e. the virtual sensor sampling time, it has been chosen always equal to 5 $[s]$; in this way, all furnace significant events can be taken into account. On the other hand, the *MPC* block and the *DC & DS* block run with a sampling time T_s equal to 1 $[min]$,

in accordance to the obtained process model and to the computational load required by the overall control algorithm.

4.4.1 The introduction of *ad hoc* stoichiometric ratios constraints

As described in Subsection 4.2.5, in the case studies where stoichiometric ratios have been included among MVs (for example see Section 4.3), air/fuel stoichiometric ratios constraints are automatically considered. In the case studies where the MVs group includes air and fuel flow rates, the stoichiometric ratios constraints must be suitably included within *TOCS* and *DO* modules formulation within both APC modes.
In order to include in the setup of the designed APC system air/fuel stoichiometric ratios, they have been introduced in a fifth process variables group, denoted as *ratio* Controlled Variables (rCVs) group. rCVs have been included in a $z \in \mathbb{R}^{m_z \times 1}$ vector. In the considered case study, because of the presence of five furnace zones with an own burners set, $m_z = 5$. Table 4.19 reports the rCVs together with their typical constraints. The stoichiometric ratios lower constraints represent safety conditions: their excessive violation can lead to a furnace stop. The upper constraints, as already mentioned, avoid air excess in the burners combustion, contributing to the achievement of furnace energy efficiency.
The rCVs have been suitably included in the APC scheme, leading to a further *customized* APC system, represented in Fig. 4.8.
With respect to Fig. 4.3, the introduction of the rCVs can be noted. In particular, this introduction interests the *DC & DS* block and the *two-layer* linear MPC strategy.

Table 4.19: *Walking beam* reheating furnace rCVs.

Variable Name	**Acronym [Units]**	**rCVs Constraints**
Zone 5 Stoich. Ratio	R_5 []	10.8 - 12.3
Zone 4 Stoich. Ratio	R_4 []	10.5 - 12
Zone 3 Stoich. Ratio	R_3 []	10.5 - 12
Zone 2 Stoich. Ratio	R_2 []	9.8 - 11.3
Zone 1 Stoich. Ratio	R_1 []	9.8 - 11.3

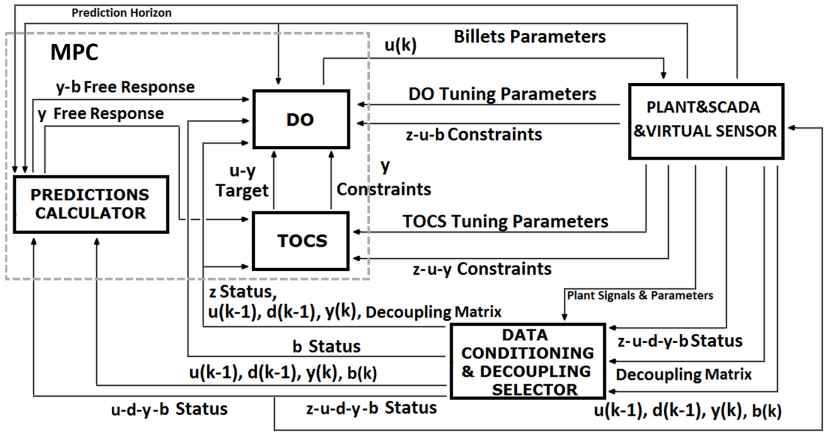

Figure 4.8: Schematic representation of *E-FESTO* APC system for the *walking beam* reheating furnace.

An initial rCVs status value is provided by *SCADA* system to *DC & DS* block. For each rCV, two status values have been introduced: "1" and "0". The status value "1" related to a generic rCV indicates that the MPC scheme must control that variable, i.e. the rCV is *active*. Conversely, the rCV status value equal to "0" indicates that the rCV is *inactive*: at the current control instant the MPC scheme has not in control that rCV, i.e. MVs must not act to satisfy its specifications.
The initial rCVs status value takes into account plant driving specifications and needs, i.e. the need of control of a furnace zone by a plant operator. The initial rCVs status is included in a $Status_{zSCADA} \in \mathbb{R}^{m_z \times 1}$ vector; it contains "0" values for the rCVs that have been set as *inactive* ("1" otherwise). The final rCVs status value $Status_z$ (Fig. 4.8, left side of *DC & DS* block, *z-u-d-y-b Status*) is defined by an element-wise logical "AND" between $Status_{zSCADA}$ vector and an additional vector that takes into account the definition of criticity relationships between the MVs status value and the rCVs status value. For the generic jth furnace zone with an own burners set, the related fuel flow rate cannot be *active* when the related stoichiometric ratio is *inactive* and vice versa. Furthermore, for the generic jth furnace zone with an own burners set, the related air flow rate cannot be *active* when the related fuel flow rate is *inactive*. The additional information that has to be exploited by *DC & DS* block for these logical operations has been included in *Plant Signals & Parameters* term of Fig. 4.8. The final rCVs status vector is provided by *DC & DS* block to *DO* and *TOCS* modules, and to *SCADA* block (Fig. 4.8, left side of *DC &*

DS block, *z-u-d-y-b Status* and *z Status*).
An *ad hoc* mathematical approach for stoichiometric ratios constrained control has been formulated, adding suitable linear constraints to *DO* and *TOCS* optimization problems of both *zones* and *adaptive* APC modes.
For what concern the *TOCS* module formulation, remember the steady-state MVs expression (3.88):

$$\hat{u}_{TOCS}(k) = u(k-1) + \Delta\hat{u}_{TOCS}(k) \tag{4.14}$$

Considering the MVs sorted as in Table 4.11, the exact generic steady-state jth ($j = 1 \dots m_z$, $m_z = 5$ in the considered case study) stoichiometric ratio is:

$$\hat{z}_{TOCS_j}(k) = \frac{\hat{u}_{TOCS_{j+m_z}}(k)}{\hat{u}_{TOCS_j}(k)} \tag{4.15}$$

where $\hat{u}_{TOCS_{j+m_z}}(k)$ and $\hat{u}_{TOCS_j}(k)$ represent the jth steady-state air and fuel flow rates. According to Table 4.11, air and fuel flow rates cannot assume negative values. Denoting the lower and upper *TOCS* constraints related to the jth stoichiometric ratio by lb_{zTOCS_j} and ub_{zTOCS_j}, we have:

$$lb_{zTOCS_j} \leq \hat{z}_{TOCS_j}(k) \leq ub_{zTOCS_j} \tag{4.16}$$

Exploiting expression (4.15), for nonzero steady-state values of $\hat{u}_{TOCS_j}(k)$ (jth fuel flow rate), (4.16) becomes:

$$\begin{aligned} lb_{zTOCS_j} \cdot \hat{u}_{TOCS_j}(k) - \hat{u}_{TOCS_{j+m_z}}(k) \leq 0 \\ -ub_{zTOCS_j} \cdot \hat{u}_{TOCS_j}(k) + \hat{u}_{TOCS_{j+m_z}}(k) \leq 0 \end{aligned} \tag{4.17}$$

Finally, exploiting expression (4.14), the total $2 \cdot m_z$ (10 in the considered case study) stoichiometric ratios constraints can be recast as linear constraints in the elements of $\Delta\hat{u}_{TOCS}(k)$ vector. These constraints can be straight introduced in the *TOCS* module formulation related to the *zones* and the *adaptive* APC modes. *TOCS* module stoichiometric ratios constraints are considered as *hard* constraints and their feasibility has been suitably imposed. This important assumption implies that the steady-state MVs target computed by *TOCS* module meets the assigned rCVs steady-state constraints.
For what concern the *DO* module formulation, the *DO* MVs expression has been reported in (3.12). Considering the MVs sorted as in Table 4.11, the exact generic jth ($j = 1 \dots m_z$, $m_z = 5$ in the considered case study) stoichiometric ratio at the M_ith ($i = 1 \dots H_u$) prediction instant is:

$$\hat{z}_j(k + M_i|k) = \frac{\hat{u}_{j+m_z}(k + M_i|k)}{\hat{u}_j(k + M_i|k)} \tag{4.18}$$

where $\hat{u}_{j+m_z}(k+M_i|k)$ and $\hat{u}_j(k+M_i|k)$ represent the jth air and fuel flow rates at the M_ith ($i=1\dots H_u$) prediction instant. According to Table 4.11, air and fuel flow rates cannot assume negative values. Denoting the lower and upper *DO* constraints related to the jth stoichiometric ratio at the M_ith ($i=1\dots H_u$) prediction instant by $lb_{zDO_j}(i)$ and $ub_{zDO_j}(i)$, we have:

$$\begin{aligned} &lb_{zDO_j}(i)-\gamma_{lbzDO_j}(i)\cdot\varepsilon_{zDO}(k)\le\hat{z}_j(k+M_i|k)\le ub_{zDO_j}(i)+\gamma_{ubzDO_j}(i)\cdot\varepsilon_{zDO}(k),\\ &\quad j=1\dots m_z,\ i=1\dots H_u \\ &\varepsilon_{zDO}(k)\ge 0_{n_{\varepsilon zDO}\times 1} \end{aligned} \tag{4.19}$$

The slack variables vector has been introduced in the constraints (4.19) related to the generic jth rCV at the ith prediction instant through nonnegative weights, contained in $\gamma_{lbzDO_j}(i)\in\mathbb{R}_0^{+1\times n_{\varepsilon zDO}}$ and $\gamma_{ubzDO_j}(i)\in\mathbb{R}_0^{+1\times n_{\varepsilon zDO}}$. $\gamma_{lbzDO_j}(i)$ and $\gamma_{ubzDO_j}(i)$ are vectors that could be characterized by at most an only nonzero positive element (on the correspondent position of the related slack variable in $\varepsilon_{zDO}(k)$). Exploiting (3.12) and (4.18), the jth stoichiometric ratio lower and upper constraints at the M_ith prediction instant can be recast as constraints in $\Delta\hat{u}(k+M_i|k)$ ($i=1\dots H_u$) and $\varepsilon_{zDO}(k)$ elements. So these constraints are introduced in the *DO* formulation of both *zones* and *adaptive* APC modes. For example, the basic *DO* formulation related to the *adaptive* APC mode reported in (4.10)-(4.11) becomes:

$$\begin{aligned} &\min_{\Delta U(k),\varepsilon_{yDO}(k),\varepsilon_{bDO}(k),\varepsilon_{zDO}(k)} V_{DO}(k)=\min_{\Delta U(k),\varepsilon_{yDO}(k),\varepsilon_{bDO}(k),\varepsilon_{zDO}(k)}\Big(\sum_{j=1}^{m_y}\sum_{i=H_{w_j}}^{H_p}(Q_{(j,j)}(i)\cdot\\ &\cdot(\hat{y}_j(k+i|k)-r_j(k+i|k))^2)+\sum_{i=1}^{H_u}\|\Delta\hat{u}(k+M_i|k)\|^2_{R(i)}+\sum_{i=1}^{H_u}\|\hat{u}(k+M_i|k)+\\ &-u_r(k+M_i|k)\|^2_{S(i)}+\|\varepsilon_{yDO}(k)\|^2_{\rho_{yDO}}+\sum_{j=1}^{m_b}\sum_{i=1}^{e_j}(Q_{b_{(j,j)}}(i)\cdot(\hat{b}_j(k+i|k)-r_{b_j}(k+i|k))^2)+\\ &+\|\varepsilon_{bDO}(k)\|^2_{\rho_{bDO}}+\|\varepsilon_{zDO}(k)\|^2_{\rho_{zDO}}\Big) \end{aligned} \tag{4.20}$$

subject to

$$
\begin{aligned}
&lb_{duDO}(i) \leq \Delta\hat{u}(k+M_i|k) \leq ub_{duDO}(i), \quad i=1\dots H_u \\
&lb_{uDO}(i) \leq \hat{u}(k+M_i|k) \leq ub_{uDO}(i), \quad i=1\dots H_u \\
&lb_{yDO_j}(i) - \gamma_{lbyDO_j}(i)\cdot\varepsilon_{yDO}(k) \leq \hat{y}_j(k+i|k) \leq ub_{yDO_j}(i) + \gamma_{ubyDO_j}(i)\cdot\varepsilon_{yDO}(k), \\
&\quad j=1\dots m_y,\ i=H_{w_j}\dots H_p \\
&lb_{bDO_j}(i) - \gamma_{lbbDO_j}(i)\cdot\varepsilon_{bDO}(k) \leq \hat{b}_j(k+i|k) \leq ub_{bDO_j}(i) + \gamma_{ubbDO_j}(i)\cdot\varepsilon_{bDO}(k), \\
&\quad j=1\dots m_b,\ i=1\dots e_j \\
&lb_{zDO_j}(i) - \gamma_{lbzDO_j}(i)\cdot\varepsilon_{zDO}(k) \leq \hat{z}_j(k+M_i|k) \leq ub_{zDO_j}(i) + \gamma_{ubzDO_j}(i)\cdot\varepsilon_{zDO}(k), \\
&\quad j=1\dots m_z,\ i=1\dots H_u \\
&\varepsilon_{yDO}(k) \geq 0_{n_{\varepsilon yDO}\times 1} \\
&\varepsilon_{bDO}(k) \geq 0_{n_{\varepsilon bDO}\times 1} \\
&\varepsilon_{zDO}(k) \geq 0_{n_{\varepsilon zDO}\times 1}
\end{aligned}
\tag{4.21}
$$

where $||\cdot||$ is the Euclidean norm.
$\varepsilon_{zDO}(k)$ has been introduced in the *DO* cost function through a positive definite diagonal matrix $\rho_{zDO} \in \mathbb{R}^{n_{\varepsilon zDO}\times n_{\varepsilon zDO}}$. In order to preserve the QP form of *DO* optimization problem, rCVs dynamic constraints have been considered as *soft* (in order to prevent infeasibility situations) but *quasi-hard* constraints, through a suitable tuning of $\gamma_{lbzDO_j}(i)$, $\gamma_{ubzDO_j}(i)$ and ρ_{zDO} terms [74]. In this way, the resulting nonlinearities that arise when the expression (4.19) is expressed as a function of $\Delta\hat{u}(k+M_i|k)$ $(i=1\dots H_u)$ and $\varepsilon_{zDO}(k)$ elements can be handled and ignored. In order to avoid "induced" constraints *relaxations* between different rCVs, in general a single slack variable for each rCV has been provided ($n_{\varepsilon zDO} = m_z$). Furthermore, within overall *DO soft* constraints priority order, the stoichiometric ratios constraints have to be considered the most important constraints (they are also more important with respect to smoke-exchanger and total air flow rate constraints). In the generic *DO* QP problem related to *zones* and *adaptive* APC modes, there are $2 \cdot m_z \cdot H_u$ total rCVs constraints.
In order to ensure a consistency between *TOCS* and *DO* rCVs constraints, the following relationships have been introduced:

$$
\begin{aligned}
lb_{zTOCS} &= lb_{zDO}(H_u) \\
ub_{zTOCS} &= ub_{zDO}(H_u)
\end{aligned}
\tag{4.22}
$$

The final rCVs status $Status_z$ vector information provided by *DC & DS* block must be included in the *DO* and *TOCS* modules formulation. When the generic jth element $(j=1\dots m_z)$ of the $Status_z$ vector is equal to zero (i.e. the jth

rCV is *inactive*), all *DO* and *TOCS* constraints related to the jth rCV are cut off by *DO* and *TOCS* modules. Furthermore, also for rCVs, the option of a constraints ramp change is available, similarly to the ramp changes described in Section 3.3.

In order to ensure that the *TOCS active* rCVs constraints are always feasible and "well-posed", an accurate analysis has been performed. First, considering (4.17) expressed as a function of $\Delta\hat{u}_{TOCS}(k)$ vector through (4.14), the evaluation of the situations where the last plant air flow rates and/or the last plant fuel flow rates (contained in $u(k-1)$) were zero has been performed. Second, considering (4.17) expressed as a function of $\Delta\hat{u}_{TOCS}(k)$ vector through (4.14), the evaluation of the situations where the *TOCS*-computed air flow rates and/or the *TOCS*-computed fuel flow rates (contained in $\hat{u}_{TOCS}(k)$) were zero has been performed. The results of the conducted analysis led to some considerations related to the bounds related to the MVs moves and to the definition of an empirical threshold vector $Thr_{rCV} \in \mathbb{R}^{m_z \times 1}$ that contains "critical" fuel flow rates values: when the generic jth fuel flow rate last value (contained in $u(k-1)$) is smaller than the jth element of the Thr_{rCV} vector, the upper bound ub_{zTOCS_j} related to the jth stoichiometric ratio is cut off by *TOCS* module (and by *DO* module in order to maintain the *TOCS-DO* consistency related to the rCVs constraints). Practically, the defined constraints for a generic stoichiometric ratio may cause some problems when the related fuel flow rate and/or the related air flow rate approaches to zero. In these situations, it could be necessary to violate a constraint: the less important stoichiometric ratios constraint is the upper constraint (as already described). When the related fuel flow rate and/or the related air flow rate approaches to zero, the upper constraint, i.e. the "energy efficiency" constraint, loses its importance with respect to situations characterized by higher air and fuel flow rates values. In the considered case study, all elements of Thr_{rCV} vector have been set to 90 $[Nm3/h]$.

According to the author knowledge, the proposed stoichiometric ratios control method represents a contribution of the research activity reported in the present dissertation [74].

Within the *zones* APC mode, the prediction horizon H_p has been set equal to 60 ($[min]$), while the control horizon H_u has been set equal to 8 moves. The related M_i terms have been set as $M_i = i - 1$ ($i = 1 \dots 8$), i.e. the 8 admitted MVs moves are assumed in the first eight prediction steps. The joint tuning of H_p, H_u and M_i parameters allows to capture the steady-state effects of all future MVs moves on the linear time invariant model considered within the *zones* APC mode. Furthermore, with this choice, the controller is equipped with a suitable number of decision variables for the solution of the involved optimization problems.

Simulation and field results related to the application of *E-FESTO* APC system on the described *walking beam* reheating furnace will be provided and discussed in Chapter 6.
The APC project related to the described *walking beam* case study has been the pioneer project of *E-FESTO* APC system. As it will be described in Chapter 6, it has been awarded with an important energy efficiency award.

Chapter 5

Cement Industry Clinker Production APC system

In today's world, cement is the substratum for civil engineering and its applications. In particular, cement forms a fundamental element of any housing or infrastructure development. In the last fifty years, the world cement production has grown in a constant manner, both in the developed and developing countries. Producing cement requires limestone and heat in significantly high quantities. Large quantities of limestone are ground and sent, in combination with other materials, like clay, to large rotary kilns. Very high temperatures cause chemical reactions that convert these combined materials into cement. The need to increase the cement quality, accompanied by higher energy efficiency requirements, has called, in the last decades, for innovations in the production chain and for the growth of automation level in the cement plants [116]. In order to fast and optimally react to frequent changing conditions while still meeting various and possibly conflicting objectives, APC solutions have to be applied. These innovative technologies are essential for leading to resource and energy efficiency and cost savings in the long term [117]. A key phase of cement producing process is the *clinker* production that is a highly energy consuming process characterized by high temperatures. The optimization of this phase can yield to significant benefits to the whole cement process. In the *clinker* production and in all cement manufacture in general, there are many conflicting control objectives, like production maximization, costs minimization, and efficiency maximization, maintaining at the same time quality specifications.
In Chapter 3 an APC framework able to control and optimize constrained multivariable processes has been designed and formulated. The APC framework has been based on a *two-layer* linear MPC strategy that tightly cooperates with an additional functional block.
The basic APC framework has been then *customized* for its installation on the *clinker* production phase of different European countries, in order to achieve energy efficiency and process control improvements. The proposed *clinker* pro-

duction phase control method has been introduced in a proprietary software tool. A proprietary software tool has been developed, in order to have the option of algorithms *customization* whenever the process at study required it. The developed cement industry software tool, in one of the different installations, has improved a control system inserted in the 2013 annual report on energy efficiency world best practices provided by International Energy Agency.

5.1 *Clinker* Production Phase

Cement is a hydraulic binder that has the form of a finely ground powder. Its hydraulic properties mainly derive from the formation, during the production stages, of calcium silicate hydrates. The general production chain of the studied dry cement industries is schematically depicted in Fig. 5.1.

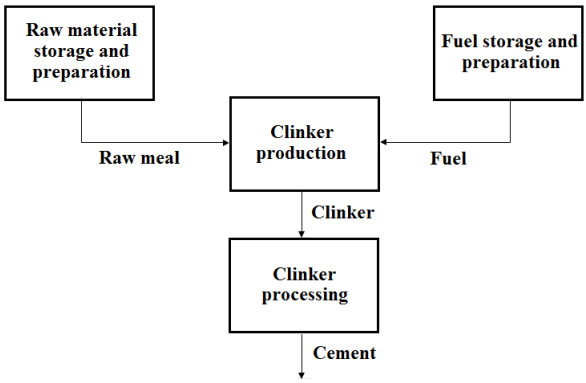

Figure 5.1: General cement industries workflow.

In a dry cement production chain, raw meal, derived from preprocessing of raw materials in a mill, interacts with fuel (coal) giving rise to the fundamental component of the cement, named *clinker*. Subsequently, *clinker* is grinded and combined with other components, such as calcium sulfate, pozzuolan, and limestone. In this way, various types of cement can be obtained. Exploited raw materials are lime, silica, alumina, iron and magnesium oxides [117]. The *clinker* production phase is the most important subpart of the cement production, in terms of energy saving and potential polluting emissions; this phase has great influence on the final quality and cost of the product. The basic APC framework described in Chapter 3 has been suitably *customized* in order to control and optimize the *clinker* production phase of the considered cement industries.

A generic representation of the *clinker* production phase is shown in Fig. 5.2 [118]. This process can be split in various steps, requiring a monotonically increasing temperature. Initially, raw meal feeds a suspension pre-heater (Fig. 5.2, left side), composed by a defined number of cyclones stages (five cyclones stages in Fig. 5.2). The cyclones stages are disposed one above the other, giving rise to a tower. Here raw meal is subject to a *preheating/drying* phase (typical temperatures range: 700 [$°C$] - 900 [$°C$]), while it is up in the air with exhaust gas from downstream zones, that is pulled by an induced draft (ID) fan. The suspension pre-heater increases the heat transfer rate, allowing a full and efficient heat exchange. Then the *calcination* phase starts: in each cyclone stage, there is a separation between raw meal and exhaust gas, and then their reunification before next cyclone stage. This cyclical process of blending, separation, and remixing is repeated until the material is discharged from the last cyclone stage to the rotary kiln. A rotary kiln is a steel cylinder, horizontally slightly sloped (about 2.5% - 4.5%), that rotates around its axis: its structure allows processed mixture to move along it. To withstand the high required temperature, the kiln is equipped with refractory materials. The furnace combustion is primarily supplied by an air/fuel (coal) burner placed at its end (Fig. 5.2, right side). In the rotary kiln, different areas can be distinguished, based on the different reactions that take place: *decarbonification* area (release of carbon dioxide and volatilization of alkali through calcination completion, typical temperatures range: 900 [$°C$] - 1000 [$°C$]), *transition* zone (creation of the first mineralogical compounds through solid phase reactions, typical temperatures range: 1000 [$°C$] - 1400 [$°C$]), *clinkering* zone (creation of chemical compounds having hydraulic properties, typical temperatures range: 1400 [$°C$] - 1500 [$°C$]). When the *clinker* leaves the kiln, it is characterized by a temperature of about 1200 [$°C$]; for this reason, the *clinker* is subjected to a *cooling* phase that is performed by a cooler, in order to obtain suitable *clinker* temperatures (about 100 [$°C$]) for the subsequent grinding phase. Furthermore, the cooler recovers the *clinker* excess heat and supplies it to the combustion air. The achieved hot air is referred as *secondary air* and it is supplied to the burner.
In some cases, there is a precalciner between the suspension pre-heater and the kiln. The additional precalciner burners trigger additional combustion reactions, which exploit additional hot air provided by the cooler through heat recovery. This hot air is named as *tertiary air* and its flow is regulated by a damper. The precalciner, when present, enhances the raw meal *calcination* phase, assuring that this phase is almost completed at the kiln inlet. In case of a high presence of volatile materials, it is needed a kiln gas by-pass, in order to ensure a continuous plant run.

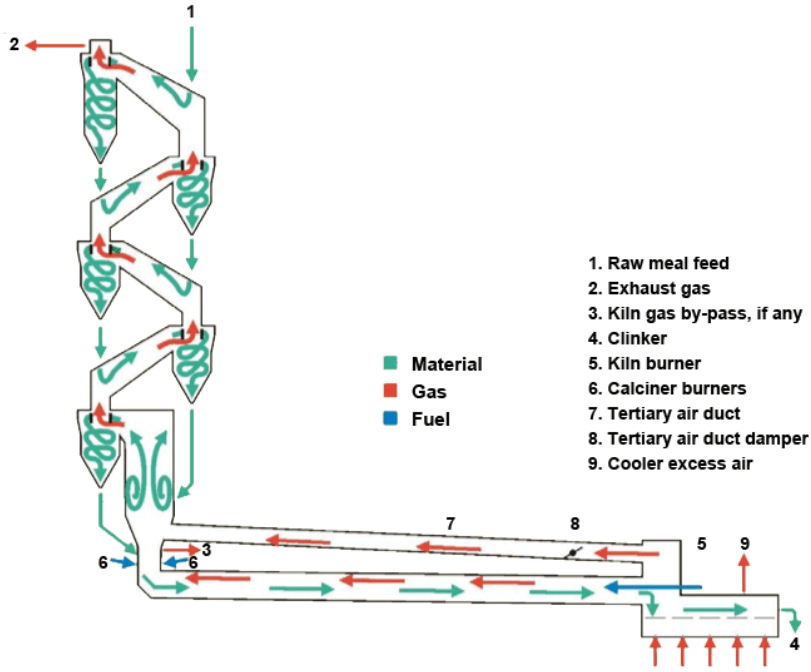

Figure 5.2: General representation of the *clinker* production phase.

5.1.1 Control specifications

An APC system in a *clinker* production unit of a cement plant must lead to productivity and efficiency increase, while assuring the desired quality of byproducts; in addition, pollution impact should be kept within given limits and fuel specific consumption should be minimized. For the attainment of such objectives, proper chemical and physical reactions have to be ensured, complying with environmental, thermodynamical and mechanical constraints. Large inertia, pure hysteresis, nonlinearity and strong coupling characteristics affect the considered process [119], [120], [121]. In a cement rotary kiln, the main thermodynamical constraints regard cyclones and furnace zones temperatures, together with oxygen concentration, while environmental ones refer to carbon dioxide, carbon monoxide and nitrogen oxides levels [87]. Mechanical constraints involve kiln torque. Furthermore, "quality constraints" are related to free lime analysis, performed on *clinker* samples, collected at the end of the cement rotary kiln [117]. All the mentioned crucial process variables to keep under control are measured through sensors and/or laboratory analysis. Fur-

ther details about the processes and the position of the sensors will be provided in Sections 5.3-5.4, where two of the addressed case studies are described.
Meeting the described constraints, APC searches for optimal operating points that minimize fuel specific consumption, thus monitoring energy saving and pollution impact aspects. The simultaneous meeting of all the above requirements is not easily attainable by a manual conduction of the *clinker* production phase. Before the introduction of the developed *customized* APC system, the *clinker* production phase of the studied cement industries was regulated by plant operators' manual conduction of local PID controllers. These controllers were implemented on plant PLC (Programmable Logic Controller). Operators, based on the furnace conditions, on the production requirements, and on their experience and skills, manually set the local temperatures targets. In the previous conduction of the cement rotary kilns related to the studied plants, operators typically neglected the aspects more strictly tied to energy saving and environmental impact decreasing, being concentrated on assuring suitable temperatures along the *clinker* production chain. Therefore, with the previous management, overburning conditions often happened. As it will be described in the following, overburning could lead to a lower quality of the finished products. These considerations have motivated the development of a *customized* APC system and its installation on the rotary kilns of the studied cement industries.

5.1.2 Literature Control Solutions

In the control literature different control solutions for the *clinker* production phase control and optimization are present; different ways to model and manage the process nonlinearities have been proposed. In [116], an MPC approach based on neural network models of the individual subprocesses is proposed; the efficiency of the adopted control solution has been proved through the effective reduction of the emissions and the improvement of *clinker* consistency. In [122], an adaptive MPC approach is proposed for controlling a white cement rotary kiln, exploiting a constrained generalized predictive controller. Simulation results prove the reliability of the proposed approach. In [121], an intelligent fuzzy predictive controller to solve the control difficulties of industry process with multi-variables is proposed. A generalized predictive control is adopted to realize the nonlinear multivariable system adaptive predictive control. The application on cement rotary kiln control is discussed in detail as a simulation example. In [123], a first principles model of a cement kiln is used to control and optimize the burning of *clinker* in the cement production process. A model predictive controller is used to stabilize a temperature profile along the rotary

kiln, guaranteeing good combustion conditions and maximizing production. As already mentioned, the basic APC framework described in Chapter 3 has been *customized* for energy efficiency and process control improvements on the *clinker* production phase of real cement industries. A black-box approach has been adopted for the identification phase, obtaining linear time invariant asymptotically stable strictly proper minimum phase models with delays on the inputs-outputs channels (in most cases FOPDT (First Order Plus Dead-Time) and SOPDT (Second Order Plus Dead-Time) models). An *ad hoc* constraints softening decoupling strategy oriented to time delays handling within the *two-layer* MPC strategy has been introduced. In order to efficiently handle time delays on the input-output channels, a *customization* of the *DO* formulation has been developed. The introduced control solution leads to a proper management, regardless of certain tuning parameters, of critical situations tied to possible different delays on a CV-MVs channel.

5.2 The developed *clinker* production phase APC system

The schematic representation of the *customized* APC framework for the *clinker* production phase is shown in Fig. 5.3.

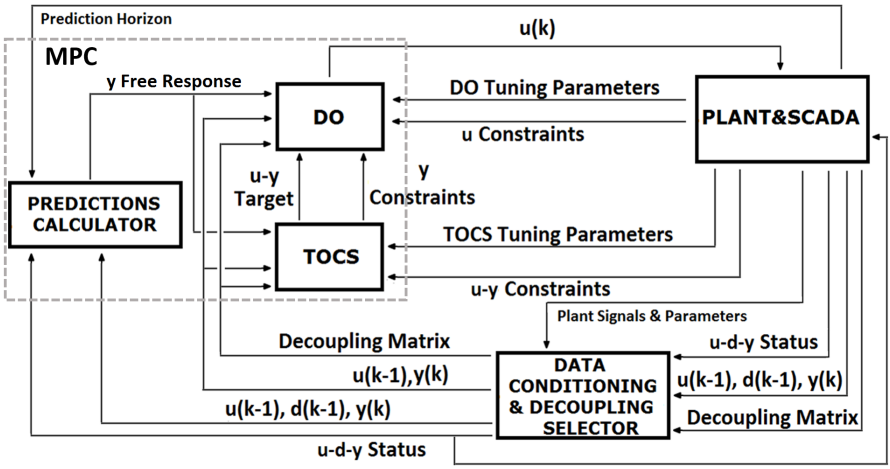

Figure 5.3: Schematic representation of *clinker* production phase APC system.

Because, as described in Subsection 5.1.2, linear time invariant asymptotically stable strictly proper minimum phase models with delays on the inputs-outputs channels are considered, the schematic representation is the same of Chapter 3. *DC & DS* block checks for bad conditions or local control loops faults, determining the process variables subset that has to be included in the MPC formulation at each control instant and defining the MVs to be exploited for the control requirements of each single CV. All this information is supplied to a *two-layer* linear *MPC* block, that includes a *Predictions Calculator* module. At the upper layer there is a steady-state module, named as *TOCS* module, while at the lower layer a *DO* module acts.
With regard to *DO* module formulation, in all the studied cement industries, a general tuning assumption has been made: according to the defined control specifications, *DO* tracking objectives for CVs are not considered; CVs are always controlled through suitable *soft* constraints. This design choice has been made in order to allow the controller to reach the optimal operating points without the need to exactly track CVs reference trajectories.
The *TOCS* module exploits a steady-state formulation (see Subsection 3.1.2): here time delays on the input-output channels are considered as vanished, so possible critical situations related to time delays handling in the transient state have to be solved by *DO* module. Remember that, at the generic control instant k, in the basic *MPC* block formulation reported in Chapter 3, the CVs *free response* over the prediction horizon H_p contained all available information up to k instant, included the overall DVs effect. So time delays information about CVs-DVs channels is all exploited and included in CVs *free response* computation, while time delays information about CVs-MVs channels is used both for CVs *free response* computation and for the related forced components (i.e. the components that depend on the future H_u MVs moves $\Delta\hat{u}(k+M_i|k)$ $(i=1\dots H_u)$ $(M_1=0)$). As already mentioned, an *ad hoc* constraints softening decoupling strategy oriented to time delays handling within the *two-layer* MPC strategy has been introduced. This strategy, that has been based on a suitable exploitation of the slack variables related to the CVs constraints, represents a theoretical *customization* with respect to the APC framework of Chapter 3 and it will be described in the following subsection (see Subsection 5.2.1).

5.2.1 Constraints softening decoupling strategy for time delays handling

According to the design choice related to the exclusion of *DO* tracking objectives for CVs, CVs are always controlled through suitable *soft* constraints. The general *DO* QP problem of Chapter 3 becomes:

$$\begin{aligned}\min_{\Delta U(k),\varepsilon_{yDO}(k)} V_{DO}(k) = \min_{\Delta U(k),\varepsilon_{yDO}(k)} (\sum_{i=1}^{H_u} \|\Delta\hat{u}(k+M_i|k)\|^2_{R(i)} + \\ + \sum_{i=1}^{H_u} \|\hat{u}(k+M_i|k) - u_r(k+M_i|k)\|^2_{S(i)} + \|\varepsilon_{yDO}(k)\|^2_{\rho_{yDO}})\end{aligned} \tag{5.1}$$

subject to

$$\begin{aligned}&lb_{duDO}(i) \leq \Delta\hat{u}(k+M_i|k) \leq ub_{duDO}(i), \quad i = 1 \dots H_u \\ &lb_{uDO}(i) \leq \hat{u}(k+M_i|k) \leq ub_{uDO}(i), \quad i = 1 \dots H_u \\ &lb_{yDO_j}(i) - \gamma_{lbyDO_j}(i) \cdot \varepsilon_{yDO}(k) \leq \hat{y}_j(k+i|k) \leq ub_{yDO_j}(i) + \gamma_{ubyDO_j}(i) \cdot \varepsilon_{yDO}(k), \\ &\quad j = 1 \dots m_y, \; i = H_{w_j} \dots H_p \\ &\varepsilon_{yDO}(k) \geq 0_{n_{\varepsilon yDO} \times 1}\end{aligned} \tag{5.2}$$

where $||\cdot||$ is the Euclidean norm.
Clearly, at each control instant k, both *TOCS* and *DO* formulations can be changed dynamically based on different events, e.g. the change of the status value of a process variable. According to the actual process condition and to the control specifications, at each control instant k, the parameter H_{w_j} is defined for each generic jth *active* CV, as described in Subsection 3.2.2:

$$H_{w_j} = \min(D_{yu_{(j,mask_j)}}) + 1 \tag{5.3}$$

where $mask_j$ is a vector that indicates the D_{yu} columns related to the *active* MVs that are tied to the jth *active* CV and that are *not inhibited* for controlling the jth *active* CV. $D_{yu} \in \mathbb{N}^{m_y \times l_u}$ represents the CVs-MVs time delays matrix. In general, on a single CV-MVs channel, there could be up to l_u different time delays. At each control instant k, for the generic jth *active* CV, a $f_j \in \mathbb{N}^{h_j \times 1}$ column vector can be constructed. This vector contains the elements of $D_{yu_{(j,mask_j)}}$, increased by one, sorted in ascending order, and without duplicates. f_j has the form:

$$f_j = \begin{bmatrix} f_{j_1} \\ \vdots \\ f_{j_{h_j}} \end{bmatrix} \tag{5.4}$$

Note that h_j might not be the same for each created f_j. Moreover, considering (5.3)-(5.4), the following expression holds:

$$f_{j_1} = H_{w_j} \tag{5.5}$$

In *DO* optimization problem (5.1)-(5.2), some problems related to constrained control of *active* CVs (especially in the transient state) in presence of different time delays on a CV-MVs channel may occur, caused by "induced" constraints *relaxations* (see Section 3.3): the promptness and the correctness of the overall control action could be strongly affected. These problems depend also on the tuning of the parameters $R(i)$, $S(i)$, $\gamma_{lbyDO_j}(i)$, $\gamma_{ubyDO_j}(i)$, ρ_{yDO} and $n_{\varepsilon yDO}$ in (5.1)-(5.2). Assume that the needed importance is given to the $n_{\varepsilon yDO}$ *DO* slack variables (taking into account also $R(i)$ terms), in order to desire that they are computed as nonzero values only if the related constraints must be really violated. In order to guarantee, regardless from the cited tuning parameters (except $n_{\varepsilon yDO}$), a proper handling of the constraints related to *active* CVs in all conditions, a particular structure has been assigned to the $\varepsilon_{yDO}(k)$ vector. First, *DO* constraints softening of the generic jth *active* CV has been set as not dependent by the softening of other *active* CVs. Second, the generic jth *active* CV has been equipped with h_j *DO* slack variables, shared by its lower and upper constraints. Based on these considerations, $\varepsilon_{yDO}(k)$ vector will have the following form (in these expressions all the CVs are considered as *active* for notation convenience):

$$\varepsilon_{yDO}(k) = \begin{bmatrix} \varepsilon_{yDO_1}(k) \\ \vdots \\ \varepsilon_{yDO_{m_y}}(k) \end{bmatrix} \qquad \varepsilon_{yDO_j}(k) = \begin{bmatrix} \varepsilon_{yDO_{j_1}}(k) \\ \vdots \\ \varepsilon_{yDO_{j_{h_j}}}(k) \end{bmatrix} \tag{5.6}$$

In the previous expressions, $\varepsilon_{yDO_j}(k) \in \mathbb{R}_0^{+h_j \times 1}$ represents the subset of $\varepsilon_{yDO_{j_q}}(k)$ $(q = 1 \dots h_j)$ h_j nonnegative slack variables for the jth CV. For the previous considerations, when all CVs are *active*, $\varepsilon_{yDO}(k) \in \mathbb{R}_0^{+(\sum_{j=1}^{m_y} h_j) \times 1}$ $(n_{\varepsilon yDO} = \sum_{j=1}^{m_y} h_j)$. f_j and h_j terms can change at different control instants, based on the actual form of $mask_j$; for this reason, the structure of the $\varepsilon_{yDO}(k)$ vector can change dynamically. The jth *active* CV is characterized by $2 \cdot (H_p - H_{w_j} + 1)$ constraints in (5.2): the introduction of the related slack variables is performed through $\gamma_{lbyDO_j}(i)$ and $\gamma_{ubyDO_j}(i)$ row vectors; these vectors are characterized by an only nonzero element. Considering all CVs as *active*, these vectors have the following structure:

$$\begin{bmatrix} 0_{1 \times (\sum_{n=1}^{j-1} h_n + c_{j_i} - 1)} & X & 0_{1 \times (\sum_{n=j}^{m_y} h_n - c_{j_i})} \end{bmatrix} \tag{5.7}$$

where

$$c_{j_i} = \max(t : t \in (1 \dots h_j) \wedge i \geq f_{j_t}) \tag{5.8}$$

In (5.7), the X symbol indicates the column of the nonzero value in $\gamma_{lbyDO_j}(i)$ and $\gamma_{ubyDO_j}(i)$ vectors. $0_{1\times 0}$ represents an empty vector. The introduction of the slack variables vector in the DO cost function takes place through the ρ_{yDO} positive definite diagonal matrix. Based on the previous considerations, this matrix assumes the following structure:

$$\begin{aligned} \rho_{yDO} &= blkdiag(\rho_{yDO_1}, \rho_{yDO_2}, \cdots, \rho_{yDO_{m_y}}) \in \mathbb{R}^{(\sum_{j=1}^{m_y} h_j)\times(\sum_{j=1}^{m_y} h_j)} \\ \rho_{yDO_j} &= blkdiag(\rho_{yDO_{j_1}}, \rho_{yDO_{j_2}}, \cdots, \rho_{yDO_{j_{h_j}}}) \in \mathbb{R}^{h_j \times h_j} \end{aligned} \tag{5.9}$$

where $blkdiag(a, b)$ represents the diagonal composition of the matrices a and b. ρ_{yDO_j} is a positive definite diagonal matrix while $\rho_{yDO_{j_r}}$ is a positive scalar. The proposed management of DO slack variables consists in a constraints softening decoupling strategy: it structurally decouples, for each jth *active* CV, the formulation of its constraints softening. For each jth *active* CV is introduced a number of slack variables equal to the number of different time delays of its relationships with the *active* MVs that are tied to the jth *active* CV and that are *not inhibited* for controlling the jth *active* CV.
An illustrative example is proposed. We assume that in the control problem $l_u = 2$ (MVs) and $m_y = 1$ (CVs); assume also that the unique CV is tied to both MVs and that both MVs can be used for its constrained control. Assume that the CV-MVs time delays are equal to 6 $[min]$ and 15 $[min]$ and that the adopted sampling time is equal to 1 $[min]$. Considering all process variables as *active* at the generic control instant k, we have $H_{w_1} = 7$ and $h_1 = 2$. Furthermore:

$$f_1 = \begin{bmatrix} f_{1_1} \\ f_{1_2} \end{bmatrix} = \begin{bmatrix} 7 \\ 16 \end{bmatrix} \qquad \varepsilon_{yDO}(k) = \begin{bmatrix} \varepsilon_{yDO_1}(k) \end{bmatrix} \qquad \varepsilon_{yDO_1}(k) = \begin{bmatrix} \varepsilon_{yDO_{1_1}}(k) \\ \varepsilon_{yDO_{1_2}}(k) \end{bmatrix} \tag{5.10}$$

Practically, for the DO constraints softening related to the considered CV, the task is split between $\varepsilon_{yDO_{1_1}}(k)$ and $\varepsilon_{yDO_{1_2}}(k)$ slack variables. Assuming a prediction horizon $H_p = 120$, $\varepsilon_{yDO_{1_1}}(k)$ is related to 7th-15th prediction instants, while $\varepsilon_{yDO_{1_2}}(k)$ is related to 16th-120th prediction instants. In this sense, a decoupling approach has been performed.
According to the author knowledge, the proposed constraints softening decoupling strategy represents a contribution of the research activity reported in the present dissertation [124].
The effectiveness of the proposed approach will be shown in Chapter 7.

5.2.2 A brief digression on a specific single-layer MPC problem

In the previous subsection, details on the introduction of a constraints softening decoupling strategy in the MPC lower layer formulation of the *customized* APC system have been reported. In this subsection, a brief digression on a specific single-layer MPC problem is reported.
Consider a single-layer MPC system, only composed by a *DO* module; assume that the *DO* module formulation is the following reduced version of (5.1)-(5.2):

$$\begin{aligned} &\min_{\Delta U(k),\varepsilon_{yDO}(k)} V_{DO}(k) = \min_{\Delta U(k),\varepsilon_{yDO}(k)} (\sum_{i=1}^{H_u} \|\Delta\hat{u}(k+M_i|k)\|^2_{R(i)} + \\ &+ \|\varepsilon_{yDO}(k)\|^2_{\rho_{yDO}}) \end{aligned} \tag{5.11}$$

subject to

$$\begin{aligned} &lb_{duDO}(i) \leq \Delta\hat{u}(k+M_i|k) \leq ub_{duDO}(i), \quad i = 1 \dots H_u \\ &lb_{uDO}(i) \leq \hat{u}(k+M_i|k) \leq ub_{uDO}(i), \quad i = 1 \dots H_u \\ &lb_{yDO_j}(i) - \gamma_{lbyDO_j}(i) \cdot \varepsilon_{yDO}(k) \leq \hat{y}_j(k+i|k) \leq ub_{yDO_j}(i) + \gamma_{ubyDO_j}(i) \cdot \varepsilon_{yDO}(k), \\ &\quad j = 1 \dots m_y, \; i = H_{w_j} \dots H_p \\ &\varepsilon_{yDO}(k) \geq 0_{n_{\varepsilon yDO} \times 1} \end{aligned} \tag{5.12}$$

where $||\cdot||$ is the Euclidean norm.
Suppose that the MVs have to be moved for CVs control requirements only when the CVs constraints are violated (all CVs constraints are assumed as *soft* constraints). Practically, the MVs must perform the smallest movements able to guarantee the CVs constraints meeting. Assume that the needed importance is given to the $n_{\varepsilon yDO}$ *DO* slack variables (taking into account also $R(i)$ terms), in order to desire that they are computed as nonzero values only if the related constraints must be really violated.
In the above control problem, some problems related to constrained control of *active* CVs in presence of different time delays on a CV-MVs channel may occur, caused by "induced" constraints *relaxations* (see Section 3.3): the promptness and the correctness of the overall control action could be strongly affected. These problems depend also on the tuning of the parameters $\gamma_{lbyDO_j}(i)$, $\gamma_{ubyDO_j}(i)$, ρ_{yDO}, and $n_{\varepsilon yDO}$. If each jth *active* CV is equipped with an own set of $(H_p - H_{w_j} + 1)$ slack variables, no problems occur. Especially for processes with many CVs and with a large prediction horizon, this solution may lead to an excessive computational load. An alternative solution may be the choice of a smaller number of slack variables for each CV (the extreme choice is to assign a single slack variable that is shared by all CVs) and a suitable

tuning of $\gamma_{lbyDO_j}(i)$ and $\gamma_{ubyDO_j}(i)$ terms. This choice could be reliable, but however there may be not covered situations where the promptness and the correctness of the control action can be strongly affected. Furthermore, *ad hoc* additional constraints cut off policies can be exploited, but however there may be not covered situations where the promptness and the correctness of the control action can be strongly affected. So, a structural solution, i.e. a solution that ensures a proper constraints handling independently by $\gamma_{lbyDO_j}(i)$ and $\gamma_{ubyDO_j}(i)$ tuning but that at the same time is characterized by a feasible computational load, can be required. The solution that requires the minimum number of slack variables for each CV is represented by the constraints softening decoupling strategy that has been introduced in the previous subsection. According to the author knowledge, the exploitation of the proposed constraints softening decoupling strategy as solution of the described control problem (5.11)-(5.12) represents a contribution of the research activity reported in the present dissertation.

5.3 Case study: dry cement industry *clinker* production phase without precalciner

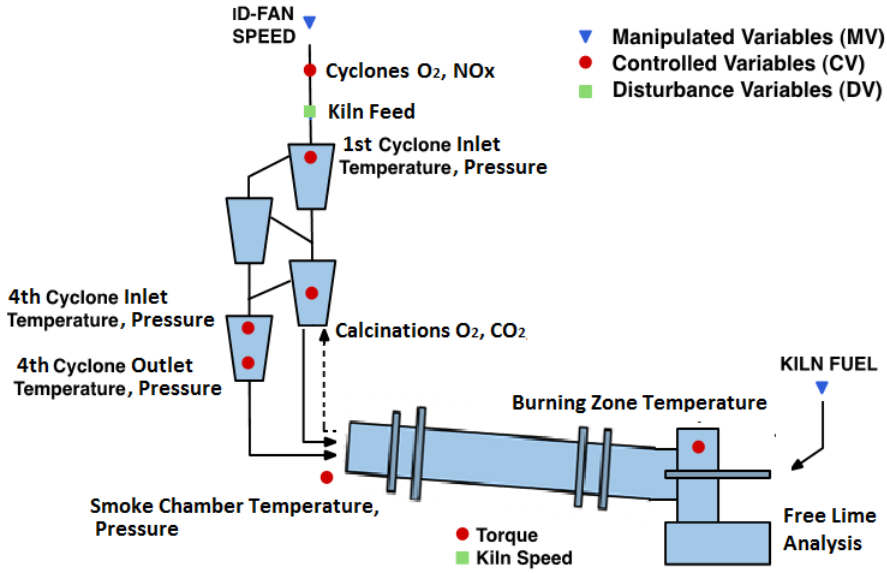

Figure 5.4: Representation of the *clinker* production phase without precalciner.

In this section, the description of the *clinker* production phase related to one of the different cement industries where the *customized* APC system has been installed is reported. In this case study, the precalciner is not present and the suspension pre-heater is composed by four cyclones stages.
The *clinker* production phase related to the cement industry at issue is schematically represented in Fig. 5.4.

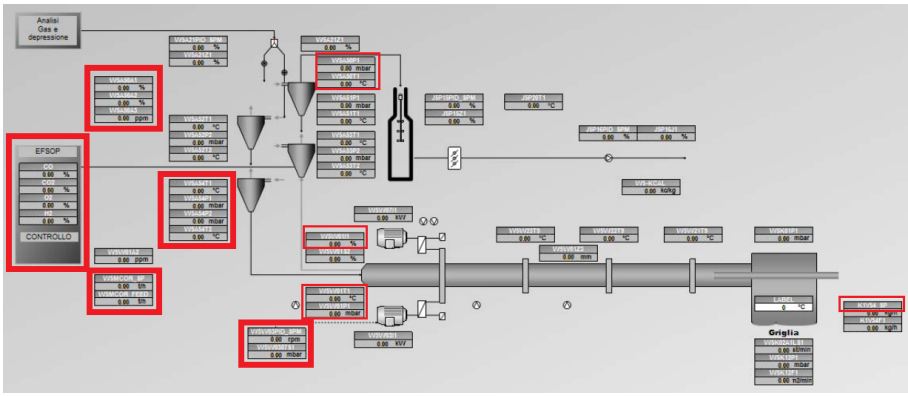

Figure 5.5: Plant representation of the *clinker* production phase without precalciner.

In order to satisfy the control specifications reported in Subsection 5.1.1, an accurate study of the chemical and physical phenomena involved in the considered cement rotary kiln has been conducted. In addition, with the support of plant operators' and engineers' interviews, a preliminary plant inspection has been accomplished in order to investigate about plant sensors/analyzers equipment, local control loops, and typical operations in the normal process driving. From this study, the fundamental process variables to be kept under control were identified as CVs: upstream (cyclones) oxygen and nitrogen oxides concentrations analysis, *calcination* area oxygen and carbon dioxide concentrations analysis, the inlet temperatures and pressures at the top (first cyclone) and at the bottom (fourth cyclone) of the pre-heater tower, the outlet temperatures and pressures at the bottom (fourth cyclone) of the pre-heater tower, the smoke chamber temperature and pressure, the kiln torque, and the burning zone temperature ($m_y = 14$). An important feature of the available set of analyzers lies in the presence of oxygen concentration analysis at the *calcination* area: this analyzer guarantees a greater feedback from the kiln combustion, compared to the classical cyclones oxygen analyzer, which is positioned upstream; in fact, given its upstream location, this analyzer may cause delayed responses and in-

accuracies on the combustion control. In case of bad measurements of oxygen concentration of the *calcination* area, the redundancy of the oxygen analyzers is exploited, temporarily controlling the kiln using only measurements from the cyclones oxygen data analyzer. As control inputs (MVs), ID fan speed and fuel flow rate (coal) have been selected ($l_u = 2$). In the plant configuration, fuel flow rate acts on a local control loop regulated by a PID controller. Furthermore, two DVs have been considered ($l_d = 2$): meal flow rate has been set as DV because of the management choice of keeping this variable under the direct control of operators. Kiln speed has been set as a second DV. In fact, this variable is exploited by operators to prevent arising of rings and preheater buildups. In the plant configuration, meal flow rate acts on a local control loop regulated by a PID controller. Tables 5.1-5.2-5.3-5.4 report the selected MVs, CVs, and DVs, together with some information, e.g. their typical range. In Fig. 5.4-5.5, sensors and actuators positions are depicted.

Table 5.1: *Clinker* production phase without precalciner MVs.

Variable Name	**TAG**	**Acronym [Units]**	**MVs Range**
ID Fan Speed	J5P16PID_SPM	*Fan Speed* [%]	30 [%] - 80 [%]
Coal	K1V54_SP	*Kiln Fuel* $[kg/h]$	6000 $[Kg/h]$ - 8000 $[kg/h]$

Table 5.2: *Clinker* production phase without precalciner CVs (I).

Variable Name	**TAG**	**Acronym [Units]**
Calcination Oxygen	EFSOP_O2	O_{2Ca} [%]
Calcination Carb. Diox.	EFSOP_CO2	CO_{2Ca} [%]
Cyclones Oxygen	W5A50A1	O_{2Cy} [%]
Cyclones Nitr. Oxid.	W5A50A3	NO_x $[ppm]$
1st Cycl. Inlet Temp.	W5A50T1	T_{1CyIn} $[°C]$
1st Cycl. Inlet Press.	W5A50P1	P_{1CyIn} $[mbar]$
4th Cycl. Inlet Press.	W5A54P1	P_{4CyIn} $[mbar]$
4th Cycl. Outlet Press.	W5A54P2	P_{4CyOut} $[mbar]$
4th Cycl. Inlet Temp.	W5A54T1	T_{4CyIn} $[°C]$
4th Cycl. Outlet Temp.	W5A54T2	T_{4CyOut} $[°C]$
Smoke Chamber Temp.	W5W01T1	T_{Sc} $[°C]$
Smoke Chamber Press.	W5W01P1	P_{Sc} $[mbar]$
Kiln Torque	W5W01I1	M_t [%]
Burning Zone Temp.	W5K01T2	T_{Bz} $[°C]$

Table 5.3: *Clinker* production phase without precalciner CVs (II).

Variable Name	**Sensor/ Analyzer**	**CVs Range**
Calcination Oxygen	Analyzer	1.5 [%] - 4 [%]
Calcination Carb. Diox.	Analyzer	10 [%] - 70 [%]
Cyclones Oxygen	Analyzer	1.5 [%] - 4 [%]
Cyclones Nitr. Oxid.	Analyzer	300 [ppm] - 1500 [ppm]
1st Cycl. Inlet Temp.	Sensor	150 [$°C$] - 400 [$°C$]
1st Cycl. Inlet Press.	Sensor	5 [$mbar$] - 50 [$mbar$]
4th Cycl. Inlet Press.	Sensor	5 [$mbar$] - 35 [$mbar$]
4th Cycl. Outlet Press.	Sensor	5 [$mbar$] - 35 [$mbar$]
4th Cycl. Inlet Temp.	Sensor	600 [$°C$] - 950 [$°C$]
4th Cycl. Outlet Temp.	Sensor	600 [$°C$] - 950 [$°C$]
Smoke Chamber Temp.	Sensor	700 [$°C$] - 1050 [$°C$]
Smoke Chamber Press.	Sensor	0 [$mbar$] - 7 [$mbar$]
Kiln Torque	Sensor	20 [%] - 80 [%]
Burning Zone Temp.	Sensor	800 [$°C$] - 1500 [$°C$]

Table 5.4: *Clinker* production phase without precalciner DVs.

Variable Name	**TAG**	**Acronym [Units]**	**DVs Range**
Meal Flow Rate	W5MCOR_FEED	*Meal* [t/h]	105 [t/h] - 125 [t/h]
Rotation Kiln Speed	W5W03PID_SPM	*Kiln Speed* [rpm]	1.5 [rpm] - 2.5 [rpm]

A black-box approach has been adopted for the identification phase, obtaining linear time invariant asymptotically stable strictly proper minimum phase models with delays on the inputs-outputs channels (FOPDT (First Order Plus Dead-Time) and SOPDT (Second Order Plus Dead-Time) models). Deviations of process variables from consistent operating points are considered for the formulation of these models. Tables 5.5-5.6 symbolically represent the CVs-MVs and CVs-DVs gain matrices, i.e. submatrices of $G_{yu} \in \mathbb{R}^{14\times2}$ and $G_{yd} \in \mathbb{R}^{14\times2}$: a nonzero mapping on a MV-CV pair or on a DV-CV pair has been indicated by the gain sign of the correspondent transfer function. Furthermore, the related time delays ([min]) have been reported in brackets. Note the presence of different time delays on certain single CV-MVs channels.

Table 5.5: *Clinker* production phase without precalciner CVs-MVs mapping matrix.

Acronym	*Fan Speed*	*Kiln Fuel*
O_{2Ca}	+ (0)	− (0)
CO_{2Ca}	− (0)	
O_{2Cy}	+ (0)	− (0)
NO_x	+ (15)	+ (6)
T_{1CyIn}	+ (0)	+ (0)
P_{1CyIn}	+ (0)	
P_{4CyIn}	+ (0)	
P_{4CyOut}	+ (0)	
T_{4CyIn}		+ (0)
T_{4CyOut}		+ (0)
T_{Sc}	+ (0)	+ (0)
P_{Sc}	+ (0)	
M_t		+ (0)
T_{Bz}	− (0)	+ (8)

Table 5.6: *Clinker* production phase without precalciner CVs-DVs mapping matrix.

Acronym	*Meal*	*Kiln Speed*
O_{2Ca}	− (3)	
CO_{2Ca}	+ (3)	
O_{2Cy}	− (3)	
NO_x	− (3)	
T_{1CyIn}	− (0)	
P_{1CyIn}	+ (0)	
P_{4CyIn}		
P_{4CyOut}		
T_{4CyIn}	− (0)	
T_{4CyOut}	− (0)	
T_{Sc}	− (0)	
P_{Sc}	+ (0)	
M_t		+ (0)
T_{Bz}		− (0)

Exploiting the obtained models, the *customized* APC system has to minimize fuel specific consumption, while meeting constraints related to *active* CVs. With regard to the constrained control of the considered CVs, the defined control specifications required that the constrained control of the burning zone temperature (14th CV) must be performed using only the fuel flow rate. The decoupling strategy related to the inhibition of the control action on defined MV-CV channels that has been described in Section 3.2 is exploited for this purpose. The initial *Decoupling Matrix* D_E supplied by *SCADA* system to *DC & DS* block is constituted by an only zero element, that corresponds to the $(14, 1)$ position, i.e. to the relationship between burning zone temperature and ID fan speed; ID fan speed must be inhibited for the control of the burning zone temperature.
With regard to the *DO* module CVs constrained control, the introduced constraints softening decoupling strategy (see Subsection 5.2.1) has been exploited for the adaptive definition of the slack variables number to assign to each single *active* CV. This choice allows to assign the desired priority order (see Section 3.3) exploiting a joint setting of $\gamma_{lbyDO}(i)$, $\gamma_{ubyDO}(i)$ and ρ_{yDO} terms in the *DO* module optimization problem.
Among CVs, the most important variables are the oxygen, the nitrogen oxides, and the carbon dioxide; in the middle, there are the different temperatures and pressures, while the less important variable is the kiln torque. Within *TOCS* and *DO* modules formulation, the just mentioned priority order among CVs has been imposed.
In *TOCS* module, in order to minimize the fuel specific consumption, the *TOCS* c_u weight related to fuel flow rate has been set as positive. The *TOCS* c_u weight related to ID fan speed has been always set to zero, together with the *TOCS* c_y weights.
With regard to the choice of the sampling time, the *MPC* block and the *DC & DS* block run with a sampling time T_s equal to 1 $[min]$, in accordance to the obtained process model and to the computational load required by the overall control algorithm. The prediction horizon H_p has been set equal to 120 ($[min]$), while the control horizon H_u has been set equal to 30 moves. The related M_i terms have been set as $M_i = i - 1$ $(i = 1 \dots 30)$, i.e. the 30 admitted MVs moves are assumed in the first thirty prediction steps. The joint tuning of H_p, H_u and M_i parameters allows to capture the steady-state effects of all future MVs moves on the linear time invariant model. Furthermore, with this choice, the controller is equipped with a suitable number of decision variables for the solution of the involved optimization problems.
In the considered cement plant, laboratory analysis on *clinker* samples, collected at the end of the cement rotary kiln, are carried out once a day. Free lime values ranging from 0.4 [%] to 1 [%] are considered acceptable. Outside

this range, critical situations for the *clinker* quality may occur, such as over-burning (when the free lime analysis is less than 0.4 [%]) or cooling (when the free lime analysis is greater than 1 [%]). This analysis has been exploited to suitably modify fuel flow rate constraints. Heuristic rules to be used for fuel flow rate constraints adjustments have been designed; they have been reported in Table 5.7. When a new free lime value is available, new fuel flow rate constraints adjustments are possibly considered as suggested from the defined lookup table (see Table 5.7).

Table 5.7: Heuristic rules for fuel flow rate constraints adjustements.

Lower Bound Change $[Kg/h]$	**Free Lime Analysis** [%]	**Upper Bound Change** $[Kg/h]$
-100	0.1	0
-100	0.2	0
-50	0.3	0
0	0.4	0
0	0.5	0
0	0.6	0
0	0.7	0
0	0.8	0
0	0.9	0
0	1	0
0	1.1	$+50$
0	1.2	$+100$
0	1.3	$+150$
0	1.4	$+200$
0	1.5	$+250$

The application of these constraints variations at each control instant k takes into account the actual last fuel flow rate value (contained in $u(k-1)$ term), as explained in Section 3.3. Consequently to the lower or upper bound fuel flow rate variation, some CVs constraints may need to be adjusted: *TOCS* module, when the new constraints setup becomes available, possibly *pre-relaxes* some of the CVs constraints, thus allowing to have a reachable *DO* steady-state configuration (see Chapter 3). If *pre-relaxations* are required by *TOCS* computation, plant operators are informed by a visual and acoustic alarm indicating the needed CVs constraints changes. Therefore, operators can modify the interested CVs operating bounds so to restore a correct constraints configuration. The described fuel constraints adjustements represent a practical *customization* with respect to the APC framework of Chapter 3.

According to the author knowledge, the introduced fuel flow rate constraints correction methodology through sporadic free lime feedback (laboratory analysis) in a *two-layer* MPC scheme represents a contribution of the research activity reported in the present dissertation [125].
Simulation and field results related to the application of the proposed APC system on the described *clinker* production phase without precalciner will be provided and discussed in Chapter 7.

5.4 Case study: dry cement industry *clinker* production phase with precalciner

In this section, the description of the *clinker* production phase related to one of the different cement industries where the *customized* APC system has been installed is reported. In this case study, the precalciner is present and the suspension pre-heater is composed by four cyclones stages.
The *clinker* production phase related to the cement industry at issue is schematically represented in Fig. 5.6. In order to satisfy the control specifications reported in Subsection 5.1.1, an accurate study of the chemical and physical phenomena involved in the considered cement rotary kiln has been conducted. In addition, with the support of plant operators' and engineers' interviews, a preliminary plant inspection has been accomplished in order to investigate about plant sensors/analyzers equipment, local control loops, and typical operations in the normal process driving. From this study, the fundamental process variables to be kept under control were identified as CVs: fan, cyclones and kiln oxygen, nitrogen oxides and carbon monoxide, cyclones temperatures and pressures, kiln motor power, and burning zone temperature ($m_y = 22$). As control inputs (MVs) ID fan speed, meal flow rate and kiln and precalciner fuel flow rates (coal) have been selected ($l_u = 4$). In the plant configuration, all MVs act on local control loops regulated by PID controllers. Furthermore, four DVs have been considered ($l_d = 4$): kiln speed, kiln and precalciner *tertiary air* flows, and radial air pressure (measured at the furnace outlet). In the plant configuration, kiln speed acts on a local control loop regulated by a PID controller. Tables 5.8-5.9-5.10-5.11 report the selected MVs, the main CVs, and the DVs, together with some information, e.g. their typical range. In Fig. 5.6, sensors and actuators positions are depicted. The not shown positions can be deduced by Fig. 5.2 and Fig. 5.4.
A black-box approach has been adopted for the identification phase, obtaining linear time invariant asymptotically stable strictly proper minimum phase models with delays on the inputs-outputs channels (FOPDT (First Order Plus Dead-Time) and SOPDT (Second Order Plus Dead-Time) models). Deviations

of process variables from consistent operating points are considered for the formulation of these models. Tables 5.12-5.13 symbolically represent the main CVs-MVs and CVs-DVs gain matrices, i.e. submatrices of $G_{yu} \in \mathbb{R}^{22\times4}$ and $G_{yd} \in \mathbb{R}^{22\times4}$: a nonzero mapping on a MV-CV pair or on a DV-CV pair has been indicated by the gain sign of the correspondent transfer function. Furthermore, the related time delays ($[min]$) have been reported in brackets. Note the many different time delays that are present on each single CV-MVs channel.

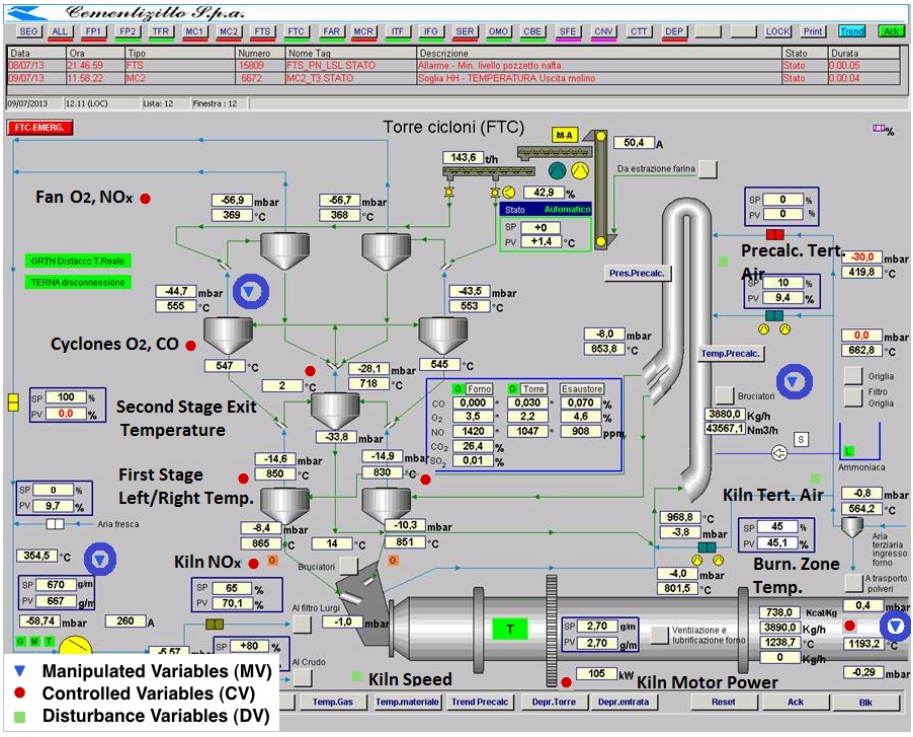

Figure 5.6: Representation of the *clinker* production phase with precalciner.

Table 5.8: *Clinker* production phase with precalciner MVs.

Variable Name	Acronym [Units]	MVs Range
Meal Flow Rate	$Total\ Meal\ [t/h]$	100 $[t/h]$ - 150 $[t/h]$
Kiln Coal	$Kiln\ Coal\ [kg/h]$	3000 $[Kg/h]$ - 4100 $[kg/h]$
Precalc. Coal	$Prec\ Coal\ [kg/h]$	3000 $[Kg/h]$ - 4100 $[kg/h]$
ID Fan Speed	$Fan\ Speed\ [kg/h]$	3000 $[Kg/h]$ - 4100 $[kg/h]$

Table 5.9: *Clinker* production phase with precalciner main CVs (I).

Variable Name	**Acronym [Units]**
Cyclones Oxygen	O_{2Cy} [%]
Fan Oxygen	O_{2fan} [%]
Kiln Nitr. Oxid.	NO_{xKiln} [ppm]
Fan Nitr. Oxid.	NO_{xFan} [ppm]
Cyclones Carbon Monoxide	CO_{Cy} [%]
First Stage Right Temp.	T_{1CyR} [$^{\circ}C$]
First Stage Left Temp.	T_{1CyL} [$^{\circ}C$]
Second Stage Exit Temp.	T_{2Cy} [$^{\circ}C$]
Kiln Power	Pow_{kiln} [kW]
Burning Zone Temp.	T_{Bz} [$^{\circ}C$]

Table 5.10: *Clinker* production phase with precalciner main CVs (II).

Variable Name	**Sensor/ Analyzer**	**CVs Range**
Cyclones Oxygen	Analyzer	1.5 [%] - 4 [%]
Fan Oxygen	Analyzer	2 [%] - 7 [%]
Kiln Nitr. Oxid.	Analyzer	1000 [ppm] - 1600 [ppm]
Fan Nitr. Oxid.	Analyzer	500 [ppm] - 1000 [ppm]
Cyclones Carbon Monoxide	Analyzer	0 [%] - 0.6 [%]
First Stage Right Temp.	Sensor	700 [$^{\circ}C$] - 900 [$^{\circ}C$]
First Stage Left Temp.	Sensor	700 [$^{\circ}C$] - 900 [$^{\circ}C$]
Second Stage Exit Temp.	Sensor	650 [$^{\circ}C$] - 850 [$^{\circ}C$]
Kiln Power	Sensor	50 [kW] - 150 [kW]
4th Cycl. Outlet Temp.	Sensor	600 [$^{\circ}C$] - 950 [$^{\circ}C$]
Burning Zone Temp.	Sensor	1000 [$^{\circ}C$] - 1600 [$^{\circ}C$]

Table 5.11: *Clinker* production phase with precalciner DVs.

Variable Name	**Acronym [Units]**	**DVs Range**
Rotation Kiln Speed	$Kiln\ Speed$ [rpm]	1 [rpm] - 2.5 [rpm]
Kiln Tert. Air	$Kiln\ TertAir$ [%]	10 [%] - 40 [%]
Prec. Tert. Air	$Prec\ TertAir$ [%]	10 [%] - 40 [%]
Radial Air Pressure	$Kiln\ Press$ [$mbar$]	100 [$mbar$] - 250 [$mbar$]

Table 5.12: *Clinker* production phase with precalciner CVs-MVs mapping matrix.

Acronym	*Total Meal*	*Kiln Coal*	*Prec Coal*	*Fan Speed*
O_{2Cy}	− (6)	− (5)	− (3)	− (0)
O_{2fan}	− (18)	− (0)	− (0)	+ (0)
NO_{xKiln}	− (20)	+ (16)		+ (0)
NO_{xFan}	− (12)	+ (24)		+ (0)
CO_{Cy}	+ (5)	+ (0)	+ (0)	− (0)
T_{1CyR}	− (3)	+ (0)	+ (5)	− (0)
T_{1CyL}	− (3)	+ (0)	+ (5)	− (0)
T_{2Cy}	− (3)	+ (6)	+ (5)	+ (0)
Pow_{kiln}	− (24)	+ (24)	+ (24)	+ (0)
T_{Bz}	− (20)	+ (15)		+ (6)

Table 5.13: *Clinker* production phase with precalciner CVs-DVs mapping matrix.

Acronym	*Kiln Speed*	*Kiln TertAir*	*Prec TertAir*	*Kiln Press*
O_{2Cy}				
O_{2fan}				
NO_{xKiln}			− (0)	+ (0)
NO_{xFan}			− (10)	+ (0)
CO_{Cy}				
T_{1CyR}			− (0)	
T_{1CyL}			− (0)	
T_{2Cy}				
Pow_{kiln}	− (12)			
T_{Bz}	− (6)		− (12)	

Exploiting the obtained models, the *customized* APC system has to find an optimal trade-off between fuels minimization and meal flow rate maximization, while meeting constraints related to *active* CVs. With regard to the constrained control of the considered CVs, the defined control specifications required that the constrained control of certain CVs must be performed using only a defined set of control inputs. The decoupling strategy described in Section 3.2 is exploited for this purpose. At this regard, in this specific case study, different specifications related to the MVs to be exploited for the CVs constrained con-

trol have been defined. In the following, the specifications related to the main CVs have been reported:

- meal flow rate has not to be used for fan and cyclones oxygen control and for carbon monoxide control;
- ID fan speed has not to be used for kiln nitrogen oxides control;
- meal flow rate and ID fan speed have not to be used for first stage left/right temperatures control;
- kiln fuel and ID fan speed have not to be used for second stage exit temperature control;
- precalciner fuel and ID fan speed have not to be used for kiln motor power control;
- ID fan speed has not to be used for burning zone temperature control.

For the compliance with these control specifications, the subpart of the initial *Decoupling Matrix* D_E supplied by *SCADA* system to *DC & DS* block related to the main CVs has been shown in Table 5.14.

Table 5.14: *Clinker* production phase with precalciner initial *Decoupling Matrix*.

Acronym	*Total Meal*	*Kiln Coal*	*Prec Coal*	*Fan Speed*
O_{2Cy}	0	1	1	1
O_{2fan}	0	1	1	1
NO_{xKiln}	1	1	1	0
NO_{xFan}	1	1	1	1
CO_{Cy}	0	1	1	1
T_{1CyR}	0	1	1	0
T_{1CyL}	0	1	1	0
T_{2Cy}	1	0	1	0
Pow_{kiln}	1	1	0	0
T_{Bz}	1	1	1	0

With regard to the *DO* module CVs constrained control, the introduced constraints softening decoupling strategy (see Subsection 5.2.1) has been exploited for the adaptive definition of the slack variables number to assign to each single *active* CV. This choice allows to assign the desired priority order (see Section 3.3) exploiting a joint setting of $\gamma_{lbyDO}(i)$, $\gamma_{ubyDO}(i)$ and ρ_{yDO} terms in the *DO* module optimization problem.
Among CVs, the most important variables are the oxygen, the nitrogen oxides, and the carbon monoxide; in the middle, there are the different temperatures and pressures, while the less important variable is the kiln motor power. Within

TOCS and *DO* modules formulation, the just mentioned priority order among CVs has been imposed.
In *TOCS* module, in order to ensure an optimal trade-off between fuels minimization and meal flow rate maximization, the *TOCS* c_u weight related to fuel flow rates has been set as positive, while the *TOCS* c_u weight related to meal flow rate has been set as negative. The desired trade-off has been ensured through a suitable balance among fuels and meal c_u weights. The *TOCS* c_u weight related to the ID fan speed has been always set to zero, together with the *TOCS* c_y weights.
With regard to the choice of the sampling time, the *MPC* block and the *DC & DS* block run with a sampling time T_s equal to 1 $[min]$, in accordance to the obtained process model and to the computational load required by the overall control algorithm. The prediction horizon H_p has been set equal to 150 ($[min]$), while the control horizon H_u has been set equal to 20 moves. The related M_i terms have been set as $M_i = i - 1$ $(i = 1 \dots 20)$, i.e. the 20 admitted MVs moves are assumed in the first twenty prediction steps. The joint tuning of H_p, H_u and M_i parameters allows to capture the steady-state effects of all future MVs moves on the linear time invariant model. Furthermore, with this choice, the controller is equipped with a suitable number of decision variables for the solution of the involved optimization problems.
In the considered cement plant, laboratory analysis on clinker samples, collected at the end of the cement rotary kiln, are carried out four times a day. Free lime values ranging from 0.8 [%] to 1.2 [%] are considered acceptable. Outside this range, critical situations for the *clinker* quality may occur, such as overburning (when the free lime analysis is less than 0.8 [%]) or cooling (when the free lime analysis is greater than 1.2 [%]). This analysis has been exploited to suitably modify fuel flow rate constraints. Heuristic rules similar to the rules reported in Section 5.3 have been defined.
Simulation and field results related to the application of the proposed APC system on the described *clinker* production phase with precalciner will be provided and discussed in Chapter 7.

Chapter 6

Steel Industry APC system Results

In this chapter, simulation and field results of the developed *E-FESTO* APC system for billets reheating furnaces control and optimization are reported. The effectiveness of the theoretical and practical considerations detailed in Chapter 4 is proved through the discussion of significant simulation and field examples related to the plants where the developed control system has been installed. In particular, different situations related to the *adaptive* and *zones* APC modes will be proposed. The shown results will refer to the two case studies detailed in Sections 4.3-4.4.

6.1 Case study results: *pusher type* reheating furnace

In this section, simulation and field results related to the *pusher type* reheating furnace described in Section 4.3 have been reported. Furthermore, energy efficiency evaluation and computation related to field applications are depicted.

6.1.1 Simulation results

To better understand the following simulation examples, remember that, in the considered case study, each *active* zCV has been equipped with an own slack variable in *DO* formulation (see Section 4.3). Furthermore, if not differently indicated, no plant-model mismatch on the zCVs-MVs/DVs model and no measurement noise are assumed; the identified zCVs-MVs/DVs model is exploited also as zCVs-MVs/DVs plant model in the proposed simulations.

Pusher type reheating furnace *zones* APC mode: first scenario

The effectiveness of the introduced decoupling strategy aimed at the inhibition of the control action of certain MVs on such CVs is shown through a simulation example. Tables 6.1-6.2 show the MVs and the zCVs that are assumed *active*, i.e. under the APC system handling. The other MVs and zCVs are assumed

inactive. Furthermore, the *inactive* MVs and all DVs are assumed constant, thus not influencing the controlled variables at issue. This choice is motivated only by the fact that, in this way, the performances of the proposed method can be more easily comprehended. Table 6.3 shows the steady-state gain signs of the considered zCVs-MVs transfer functions. Table 6.4 shows the subpart of the initial *Decoupling Matrix* D_E supplied by *SCADA* system to *DC & DS* block related to the zCVs that are considered in the simulation. *DC & DS* block and the other modules perform all the operations related to *inactive* process variables, as explained in Chapters 3-4. In particular, all (initial) D_E rows and columns related to *inactive* zCVs and MVs are zeroed by *DC & DS* block. This simulation example considers having only the furnace zones 6-5 fuel flow rates and temperatures under control of the proposed APC system. The control specifications require that each zone must be controlled using only the related fuel flow rate.
A typical operator's maneuver is simulated: because of the entry of cold billets in the furnace, a variation on both constraints of zone 6 temperature is performed. The effectiveness of the proposed decoupling strategy for the control specifications fulfillment is proved by comparing the system performances related to the *active* process variables, without and with its introduction.

Table 6.1: *Pusher type* reheating furnace *zones* APC mode simulation results, first scenario: considered set of MVs.

Variable Name	**Acronym [Units]**
Zone 6 Fuel Flow Rate	$Fuel_6$ $[Nm3/h]$
Zone 5 Fuel Flow Rate	$Fuel_5$ $[Nm3/h]$

Table 6.2: *Pusher type* reheating furnace *zones* APC mode simulation results, first scenario: considered set of zCVs.

Variable Name	**Acronym [Units]**
Zone 6 Temperature	$Temp_6$ $[°C]$
Zone 5 Temperature	$Temp_5$ $[°C]$

Table 6.3: *Pusher type* reheating furnace *zones* APC mode simulation results, first scenario: reduced zCVs-MVs mapping matrix.

Acronym	$Fuel_6$	$Fuel_5$
$Temp_6$	+	+
$Temp_5$		+

Table 6.4: *Pusher type* reheating furnace *zones* APC mode simulation results, first scenario: reduced initial *Decoupling Matrix*.

Acronym	$Fuel_6$	$Fuel_5$
$Temp_6$	1	0
$Temp_5$	1	1

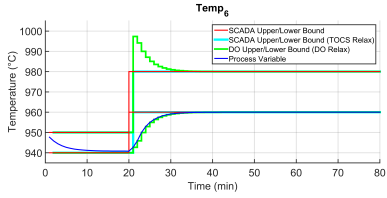

(a) $Temp_6$ with dec. strat.

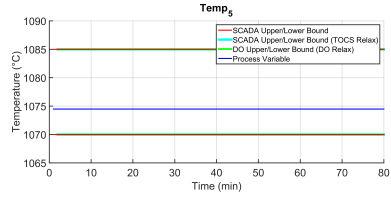

(b) $Temp_5$ with dec. strat.

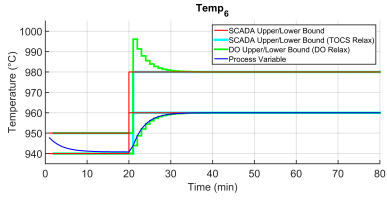

(c) $Temp_6$ without dec. strat.

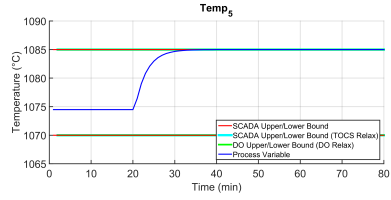

(d) $Temp_5$ without dec. strat.

Figure 6.1: *Pusher type* reheating furnace *zones* APC mode simulation results, first scenario: zCVs trends with and without the decoupling strategy.

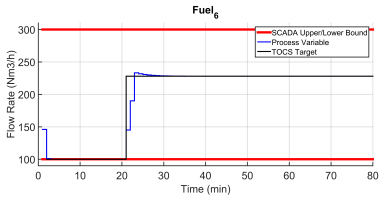

(a) $Fuel_6$ with dec. strat.

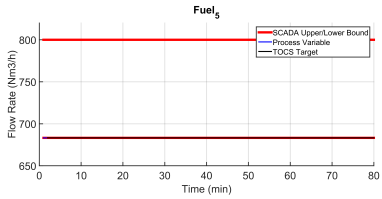

(b) $Fuel_5$ with dec. strat.

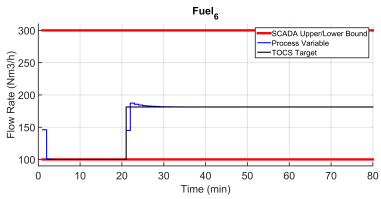

(c) $Fuel_6$ without dec. strat.

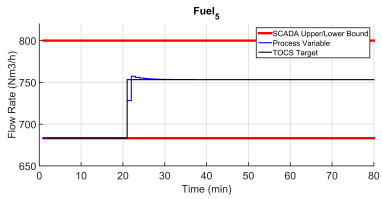

(d) $Fuel_5$ without dec. strat.

Figure 6.2: *Pusher type* reheating furnace *zones* APC mode simulation results, first scenario: MVs trends with and without the decoupling strategy.

In the presented simulation, a typical operating condition has been chosen as starting point: zone 6 fuel and zone 6 and zone 5 temperatures are inside their bounds, while zone 5 fuel lies on its lower limit. *DO* module, supported by *TOCS* module action, saves energy minimizing fuels flow rate. At time instant 20, as shown in Fig. 6.1, after the operator's move, the lower and upper constraints of zone 6 temperature are subjected to $+20$ $[°C]$ and $+30$ $[°C]$ change, respectively. Fig. 6.2 shows zone 5 and zone 6 fuel flow rates. In Fig. 6.1(c)-6.1(d) and in Fig. 6.2(c)-6.2(d) the control results without the decoupling strategy are reported, while Fig. 6.1(a)-6.1(b) and Fig. 6.2(a)-6.2(b) include the decoupling approach. In the first control solution, when the operator performs the constraints change, *TOCS* module, in order to fulfill the request, modifies both zone 6 and zone 5 fuel flow rates steady-state targets (black lines) and no steady-state relaxation is required (cyan, red and green lines in Fig. 6.1(c) overlap). Consequently, *DO* module moves both fuel flow rates (Fig. 6.2(c)-6.2(d), blue lines), driving the entire subsystem towards a new operating point. In this way, zone 6 temperature (Fig. 6.1(c), blue line), after a brief transient, which causes a *DO* relaxation (Fig. 6.1(c), green lines), approaches its new lower constraint. In the second control solution, thanks to the decoupling strategy, when the constraints change is performed, *TOCS* module moves only zone 6 fuel flow rate steady-state target, leaving unchanged zone 5 fuel flow rate one. No steady-state relaxation is required also in this second case. *DO* module, because of the inhibition of zone 5 fuel flow rate

action for zone 6 temperature control, acts on zone 6 fuel flow rate only, thus fulfilling the required management specification. Zone 6 temperature, after a transient (longer than in the first case but equally satisfactory), approaches its new lower constraint.

Pusher type **reheating furnace** ***adaptive*** **APC mode: first scenario**

In order to show the performances of the *adaptive* APC mode within the considered *pusher type* reheating furnace, an example simulating a plant operating condition is proposed. No plant-model mismatch on the zCVs-MVs/DVs model and no measurement noise are assumed; the identified zCVs-MVs/DVs model is exploited also as zCVs-MVs/DVs plant model. The developed billets temperature nonlinear model that is exploited by the virtual sensor is used also as plant model for simulating the relationships between billets temperature and the related input vector u_b. Remember that the input vector u_b is (see (4.12)):

$$u_b = \begin{bmatrix} Tun \\ Temp_6 \\ Temp_5 \\ Temp_4 \\ Temp_3 \\ TempM_{21} \end{bmatrix} \in \mathbb{R}^{6\times 1} \tag{6.1}$$

where $TempM_{21}$ represents the mean between zone 1 and zone 2 temperatures. Furthermore, remember that the pyrometer that measures the temperature of the processed billets is placed at the exit of the first stage of the rolling mill stands. Because it is placed at the exit of the first stage of the rolling mill stands, a further term that models the billets temperature decrease in the path from the furnace outlet to the optical pyrometer has been included. This term, which is used by the virtual sensor, has been included in the exploited overall plant model. The simulation time of the assumed overall plant model is set to 1 $[s]$.
As in the real case (see Section 4.3), the virtual sensor sampling time is set to 5 $[s]$, while the *MPC* block and the *DC & DS* block run with a sampling time of 1 $[min]$.
The proposed simulation assumes that, at the initial control instant at which the activation of the *adaptive* APC mode is requested, no empty places are in the furnace and the estimation performed by the virtual sensor gives positive results. Furthermore, the actual furnace movement time is equal to 120 $[s]$, which corresponds, for the case at issue, to a furnace production rate of about 70 $[t/h]$. These conditions lead to the *activation* of the *adaptive* APC mode related to the initial bCVs status value that is provided by *SCADA* system to

DC & DS block (see Subsection 4.2.2).
Tables 6.5-6.6 show the MVs and the zCVs that are assumed *active*, i.e. under the APC system handling. Without loss of generality, the other MVs and zCVs are assumed *inactive*. Furthermore, the *inactive* MVs and all DVs are assumed constant, thus not influencing the zCVs at issue. This choice is motivated only by the fact that, in this way, the performances of the proposed method can be more easily comprehended. The steady-state gain signs of the considered zCVs-MVs transfer functions can be observed in Tables 4.5-4.6, while the subpart of the initial *Decoupling Matrix* D_E supplied by *SCADA* system to *DC & DS* block related to the interested zCVs can be observed in Tables 4.8-4.9. *DC & DS* block and the other modules perform all the operations related to *inactive* process variables, as explained in Chapters 3-4. In particular, all (initial) D_E rows and columns related to *inactive* zCVs and MVs are zeroed by *DC & DS* block.

Table 6.5: *Pusher type* reheating furnace *adaptive* APC mode simulation results, first scenario: considered set of MVs.

Variable Name	**Acronym [Units]**
Zone 6 Fuel Flow Rate	$Fuel_6$ $[Nm3/h]$
Zone 5 Fuel Flow Rate	$Fuel_5$ $[Nm3/h]$
Zone 4 Fuel Flow Rate	$Fuel_4$ $[Nm3/h]$
Zone 3 Fuel Flow Rate	$Fuel_3$ $[Nm3/h]$
Zone 2 Fuel Flow Rate	$Fuel_2$ $[Nm3/h]$
Zone 1 Fuel Flow Rate	$Fuel_1$ $[Nm3/h]$

Practically, all fuel flow rates and the related zones temperatures are *active*, together with the differences between the elements of the u_b vector. The constraints related to the zones temperatures and to the fuel flow rates can be observed in Tables 4.1-4.2. The differences between the elements of the u_b vector (that represent the second part of the zCVs in Table 6.6) are only upper constrained by 0 $[°C]$.
Given the previous considerations about the variables status values and assuming them constant over the entire simulation, all the temperatures related to the billets that are and that will be in the furnace are considered as *active* bCVs. So the *adaptive* APC mode can be activated.
The 136 billets that are already present within the furnace are characterized by different temperatures (in the range 30 $[°C]$-1140 $[°C]$) and the billets that will enter the furnace will be assumed characterized by a constant furnace inlet temperature (about 170 $[°C]$). The actual furnace movement time (120 $[s]$)

is considered constant in the proposed simulation. Furthermore, it is assumed that the *Rolling* phase specifications require that the billets reach the first stage of the rolling mill stands with a temperature in the range 1020 [$°C$]-1040 [$°C$]. This specification, thanks to the online virtual sensor action, is online converted in a temperature range at the furnace outlet (constant at 1040 [$°C$]-1060 [$°C$] for the case at issue).

Table 6.6: *Pusher type* reheating furnace *adaptive* APC mode simulation results, first scenario: considered set of zCVs.

Variable Name	**Acronym [Units]**
Tunnel Temperature	Tun [$°C$]
Zone 6 Temperature	$Temp_6$ [$°C$]
Zone 5 Temperature	$Temp_5$ [$°C$]
Zone 4 Temperature	$Temp_4$ [$°C$]
Zone 3 Temperature	$Temp_3$ [$°C$]
Zone 2 Temperature	$Temp_2$ [$°C$]
Zone 1 Temperature	$Temp_1$ [$°C$]
Tunnel - Zone 6 Temp. Diff.	$TDiff_{T6}$ [$°C$]
Zone 6 - Zone 5 Temp. Diff.	$TDiff_{65}$ [$°C$]
Zone 5 - Zone 4 Temp. Diff.	$TDiff_{54}$ [$°C$]
Zone 4 - Zone 3 Temp. Diff.	$TDiff_{43}$ [$°C$]
Zone 3 - Mean Zones 2-1 Temp. Diff.	$TDiff_{321}$ [$°C$]

Remember that, in the considered case study, each *active* zCV and each *active* constrained bCV has been equipped with an own slack variable in *DO* formulation (see Section 4.3). Furthermore, as described in Subsection 4.2.3, the *TOCS* module formulation does not take into account the information provided by the developed billets temperature overall linear model; for this reason, the steady-state targets supplied by *TOCS* module may be unreachable in the *adaptive* APC mode and a profitable trade-off between MVs tracking and bCVs constraints satisfaction must be ensured (see Subsection 4.2.5).
As starting point of the proposed simulation, all the considered process variables are within the assigned constraints. The *TOCS-DO* cooperative action, together with the information provided by the billets temperature virtual sensor and by the LPV model within *DO* module, leads the process to a more profitable operating point. In particular, considering the actual furnace movement time, a prediction horizon H_p of 272 [min] is computed that is needed for the exit of the billet located in the 1st place (the 1st place is assumed to be the closest place to the furnace inlet) from the furnace. As can be observed

from Fig. 6.3, the exited billets that reach the first stage of the rolling mill stands are characterized by decreasing temperatures, obtained through a coordinated control action of the fuel flow rates of the different furnace zones (Fig. 6.5). The fuel flow rates control action is forwarded on the billets temperatures through the elements of the u_b vector (Fig. 6.4).

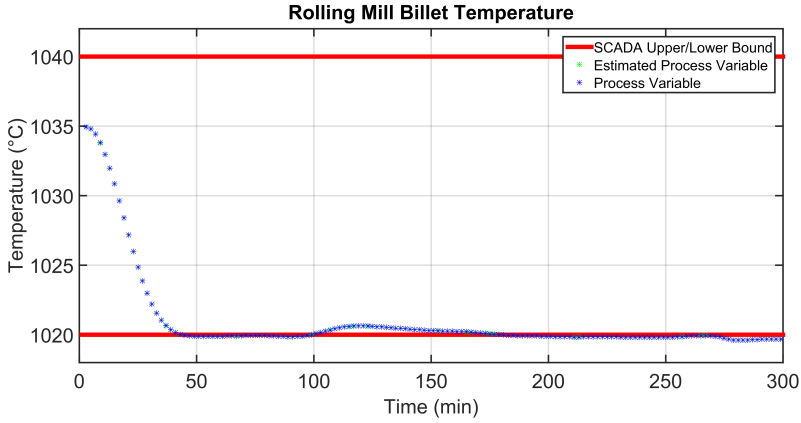

Figure 6.3: *Pusher type* reheating furnace *adaptive* APC mode simulation results, first scenario: bCVs trends.

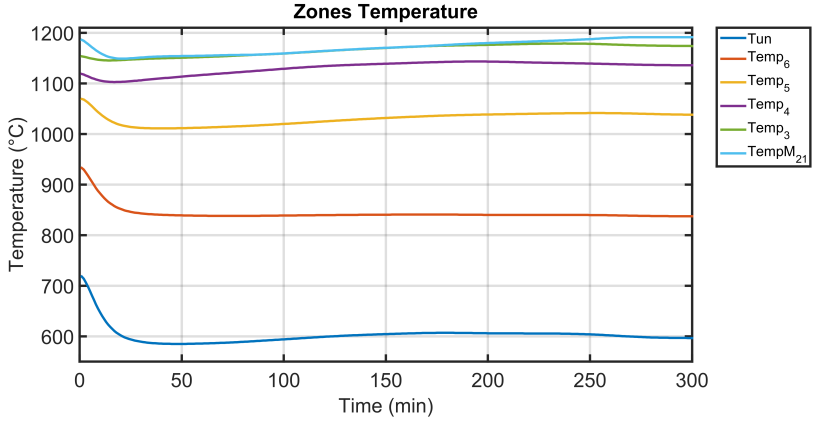

Figure 6.4: *Pusher type* reheating furnace *adaptive* APC mode simulation results, first scenario: u_b temperatures trends.

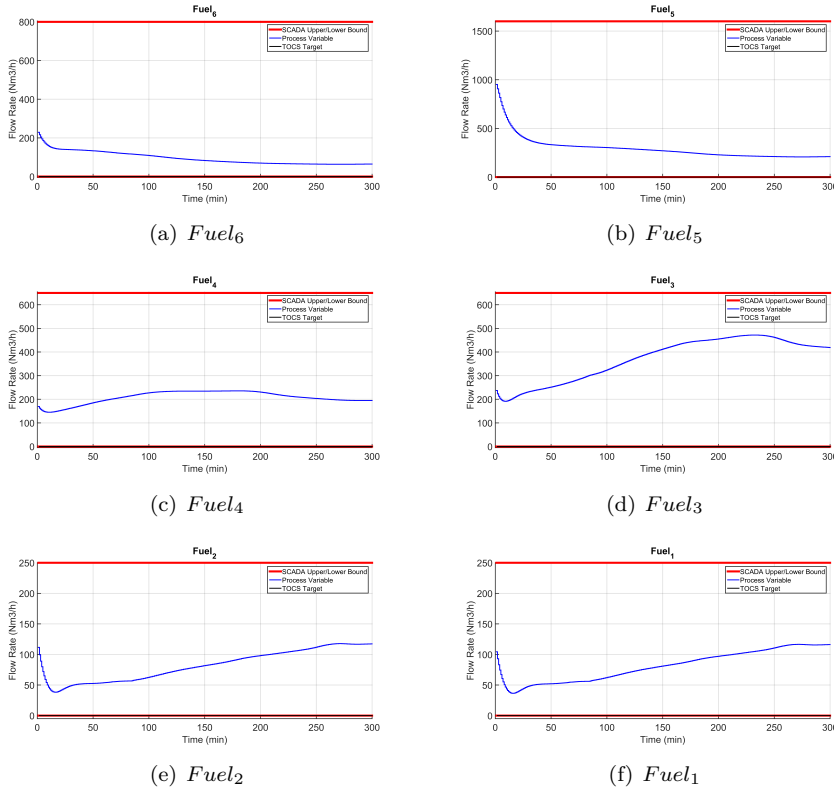

(a) $Fuel_6$ (b) $Fuel_5$

(c) $Fuel_4$ (d) $Fuel_3$

(e) $Fuel_2$ (f) $Fuel_1$

Figure 6.5: *Pusher type* reheating furnace *adaptive* APC mode simulation results, first scenario: MVs trends.

Pusher type **reheating furnace** ***adaptive*** **APC mode: second scenario**

In order to better clarify the performances of the *adaptive* APC mode within the considered *pusher type* reheating furnace, an additional example simulating a plant operating condition is proposed. All the example assumptions are the same with respect to the simulation example proposed in 6.1.1. The only changes are the following: it is assumed that the *Rolling* phase specifications require that the billets reach the first stage of the rolling mill stands with a temperature in the range 1030 [$°C$]-1040 [$°C$]. Then, after the first 100 simulation instants, the specification changes: a constraints change on the required billets temperature is simulated; the new desired operating range is 1040 [$°C$]-1050 [$°C$].

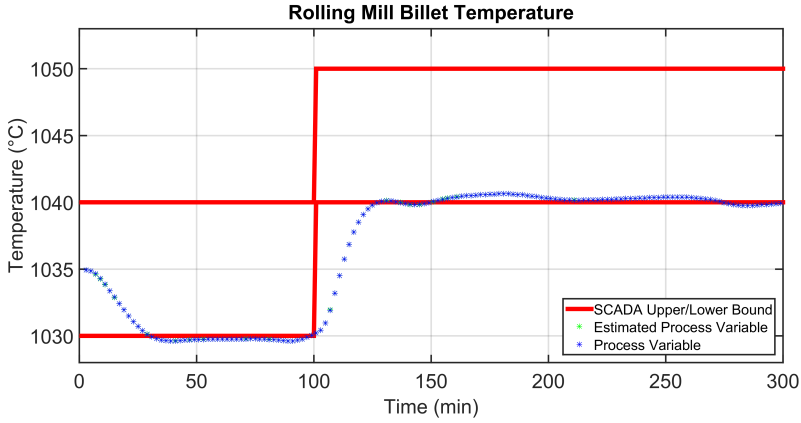

Figure 6.6: *Pusher type* reheating furnace *adaptive* APC mode simulation results, second scenario: bCVs trends.

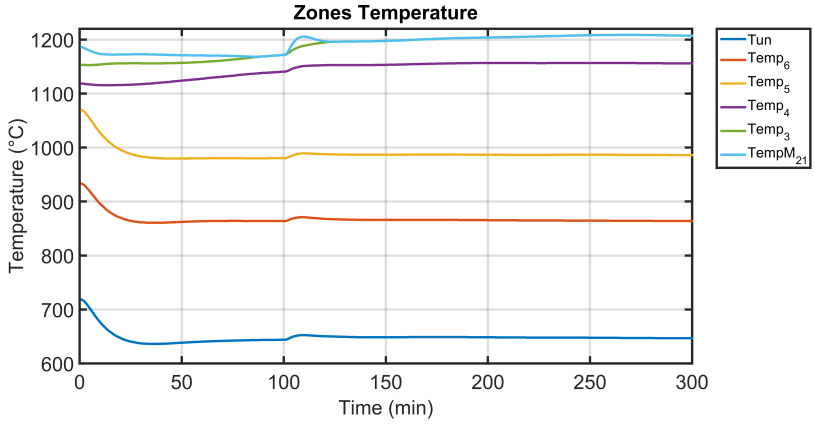

Figure 6.7: *Pusher type* reheating furnace *adaptive* APC mode simulation results, second scenario: u_b temperatures trends.

As starting point of the proposed simulation, all the considered process variables are within the assigned constraints. The *TOCS-DO* cooperative action, together with the information provided by the billets temperature virtual sensor and by the LPV model within *DO* module, leads the process to a more profitable operating point. In particular, considering the actual furnace movement time, a prediction horizon H_p of 272 $[min]$ is computed that is needed for the exit of the billet located in the 1st place (the 1st place is assumed to

be the closest place to the furnace inlet) from the furnace. As can be observed from Fig. 6.6, the exited billets that reach the first stage of the rolling mill stands are characterized by decreasing temperatures, obtained through a coordinated control action of the fuel flow rates of the different furnace zones (Fig. 6.8). The fuel flow rates control action is forwarded on the billets temperatures through the elements of the u_b vector (Fig. 6.7).
As can be noted, when the billets temperature constraints change, the fuel flow rates related to the last furnace zones ensure a quick response, while the fuel flow rates of the first furnace zones try to track their ideal *TOCS* target (Fig. 6.8). When the billets temperature constraints change, the *TOCS-DO* cooperative action, together with the information provided by the billets temperature virtual sensor and by the LPV model within *DO* module, leads the process to the desired operating point, satisfying the operator's request (Fig. 6.6).

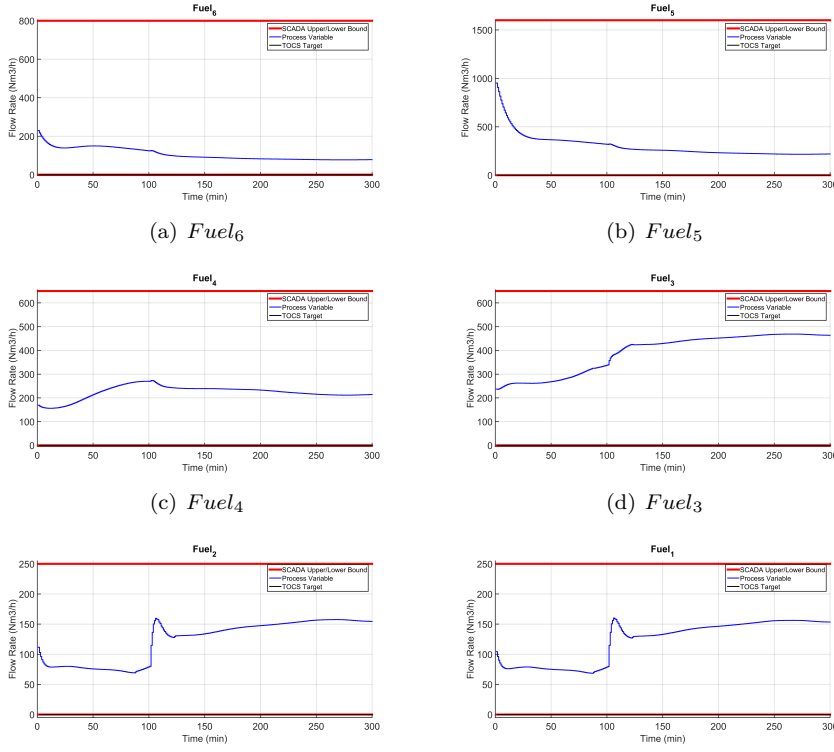

(a) $Fuel_6$ (b) $Fuel_5$

(c) $Fuel_4$ (d) $Fuel_3$

(e) $Fuel_2$ (f) $Fuel_1$

Figure 6.8: *Pusher type* reheating furnace *adaptive* APC mode simulation results, second scenario: MVs trends.

6.1.2 Field results

The study and design phases of the project for the development of the APC system began in January 2015 and ended in May 2015. In early June 2015, the system has been installed on the considered Italian steel industry for the optimization of the *Reheating* phase, substituting operators' manual driving of local PID controllers.
In Fig. 6.9-6.10-6.11-6.12-6.13-6.14, a real plant condition under the control of the developed *E-FESTO* APC system is shown. A five hours period is taken into account and the *adaptive* APC mode performances are shown.

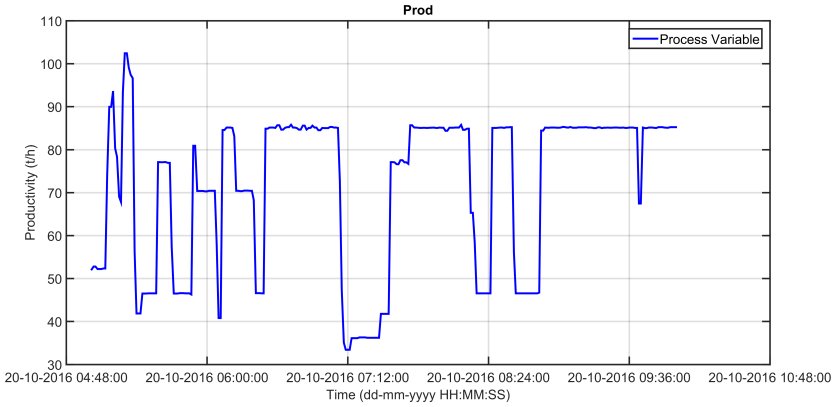

Figure 6.9: *Pusher type* reheating furnace *adaptive* APC mode field results: furnace production rate trends.

The initial plant conditions assume that the *adaptive* APC mode has been already activated; furthermore, the estimation performed by the virtual sensor (Fig. 6.11, green stars) gives positive results. The actual furnace production rate (Fig. 6.9) is equal to about 50 $[t/h]$. These conditions allow the *adaptive* APC mode to remain activated (initial bCVs status value, see Subsection 4.2.2). All 12 MVs are *active* (Fig. 6.13-6.14), all main zCVs (see Table 4.4) and all DVs (see Table 4.3) are *active*. The constraints related to the MVs can be observed in Fig. 6.13-6.14, while the constraints related to the *active* zCVs can be observed in Table 4.1. The temperature differences between the elements of the u_b vector (that represent the second part of the zCVs in Table 4.4) are only upper constrained by 0 $[°C]$. The constraints and trends related to the smoke-exchanger temperature and total air flow rate have not been reported, because they do not influence the considered real scenario.

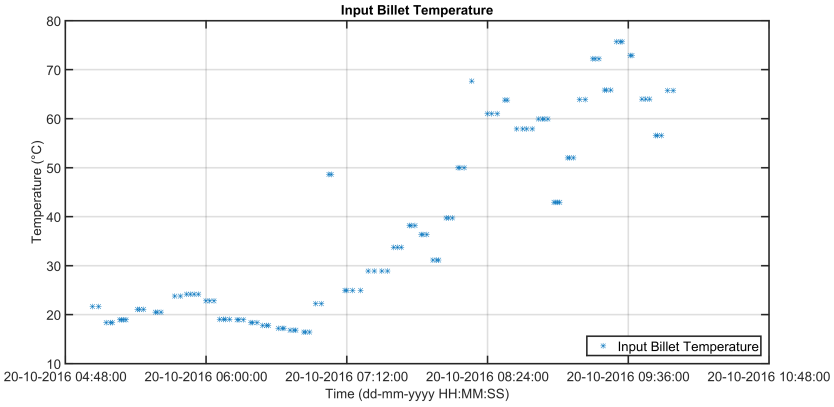

Figure 6.10: *Pusher type* reheating furnace *adaptive* APC mode field results: billets furnace inlet temperatures trends.

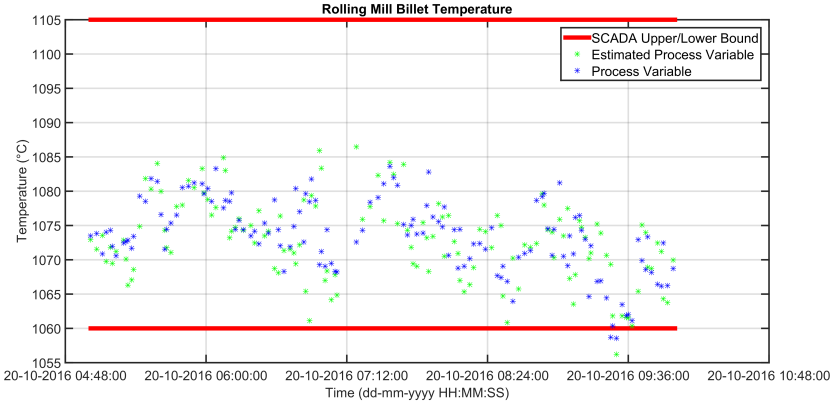

Figure 6.11: *Pusher type* reheating furnace *adaptive* APC mode field results: bCVs trends.

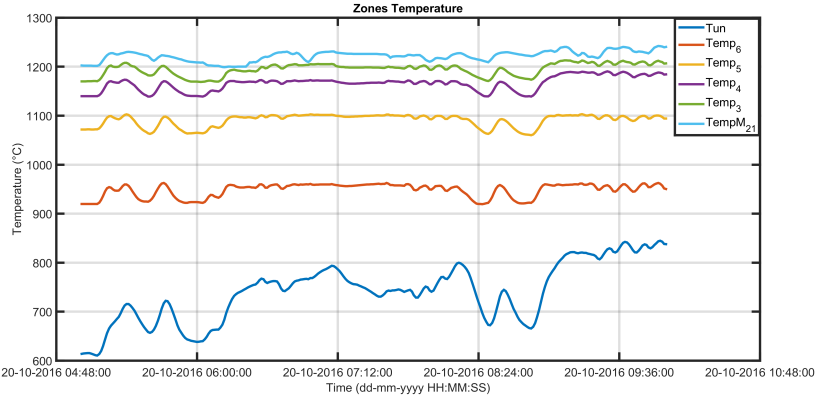

Figure 6.12: *Pusher type* reheating furnace *adaptive* APC mode field results: u_b temperatures trends.

Given the previous considerations about the variables status values, all the temperatures related to the billets that are in the furnace are considered as *active* bCVs. So the *adaptive* APC mode remains activated.
The 136 billets that are already present within the furnace are characterized by different temperatures (in the range 30 [$°C$]-1100 [$°C$]) and the billets that will enter the furnace in the future will be characterized by different inlet temperatures (in the range 15 [$°C$]-80 [$°C$], see Fig. 6.10). The furnace production rate varies in the range 30 [t/h]-105 [t/h] (see Fig. 6.9), while the furnace pressure and the air pressure are characterized by average values of about 0.75 [$mm/H2O$] and 84 [$mbar$], respectively. Furthermore, it is assumed that the *Rolling* phase specifications require that the billets reach the first stage of the rolling mill stands with a temperature in the range 1060 [$°C$]-1105 [$°C$]. This specification, thanks to the online virtual sensor action, is online converted in a temperature range at the furnace outlet that varies based on the process conditions (e.g. 1090 [$°C$]-1135 [$°C$]).

As starting point of the proposed plant condition, all the considered process variables are within the assigned constraints. The *TOCS-DO* cooperative action, together with the information provided by the billets temperature virtual sensor and by the LPV model within *DO* module, allows to maintain the process at a profitable operating configuration, despite the not constant furnace production rate and billets inlet temperatures. The exited billets that reach the first stage of the rolling mill stands are characterized by decreasing temperatures (Fig. 6.11), obtained through a coordinated control action of the MVs. The MVs control action is forwarded on the billets temperatures through the elements of the u_b vector (Fig. 6.12).

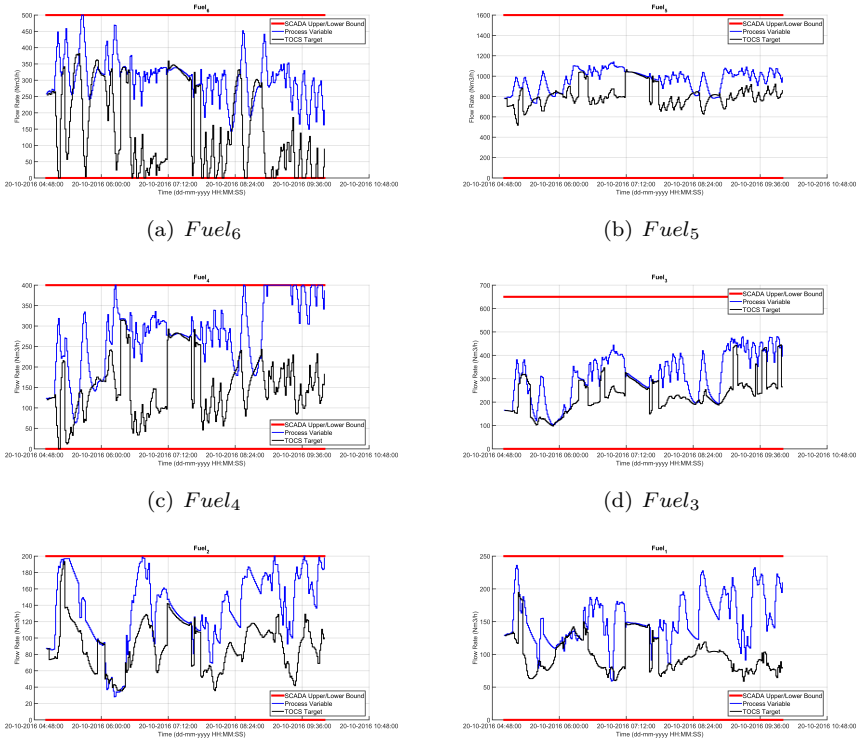

(a) $Fuel_6$ (b) $Fuel_5$

(c) $Fuel_4$ (d) $Fuel_3$

(e) $Fuel_2$ (f) $Fuel_1$

Figure 6.13: *Pusher type* reheating furnace *adaptive* APC mode field results: MVs trends (I).

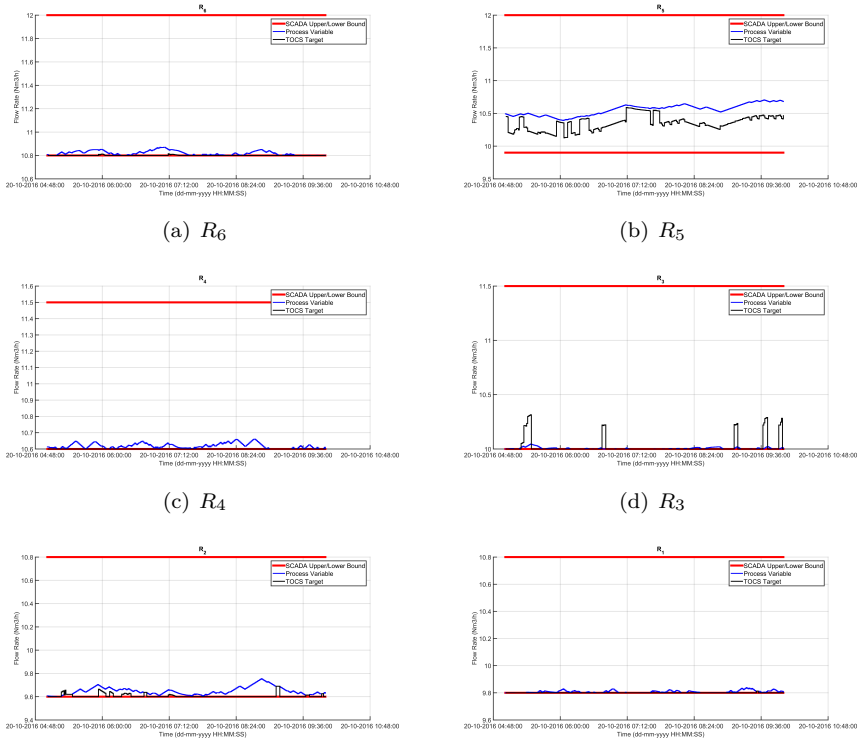

(a) R_6 (b) R_5

(c) R_4 (d) R_3

(e) R_2 (f) R_1

Figure 6.14: *Pusher type* reheating furnace *adaptive* APC mode field results: MVs trends (II).

The developed APC system has been implemented on a SCADA/HMI (Human-Machine Interface) platform that provides an user-friendly GUI (Graphical User Interface). Plant operators can easily handle the APC system: during the commissioning phase, training courses to plant operators have been provided [126]. For this purpose, a training framework has been created, thus allowing plant operators to become proficient in the utilization of the APC system. The implemented GUI is composed by different pages that enable plant operators to precisely observe and monitor the plant behavior under *E-FESTO* APC system control. Fig. 6.15-6.16 show subparts of the pages related to the process variables monitoring and management. Note the option to switch off or switch on a defined process variable; these settings compose the initial status value provided by *SCADA* system to *DC & DS* block. Note also the boxes where constraints related to the process variables can be introduced.

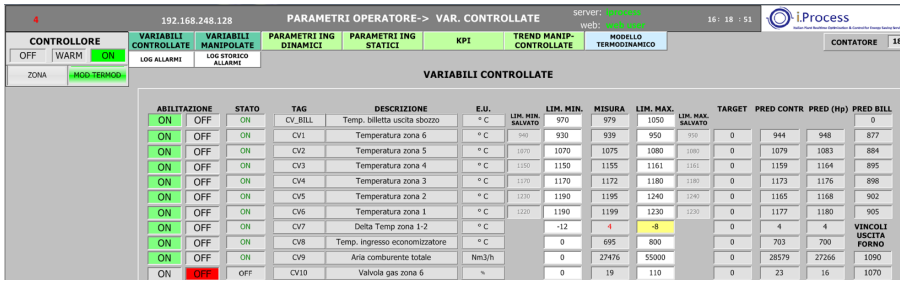

Figure 6.15: *Pusher type* reheating furnace GUI: CVs.

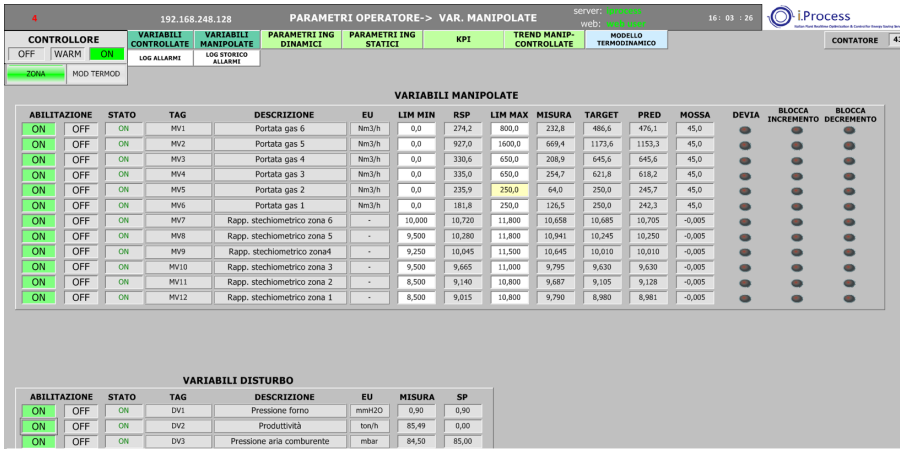

Figure 6.16: *Pusher type* reheating furnace GUI: MVs-DVs.

Before the introduction of the developed APC system, plant operators had no information about billets heating profile exhibited inside the furnace. Real performances of the virtual sensor have been shown in Fig. 6.11. Analyzing a year and a half process data, a Root Mean Square Error of Prediction (RMSEP) less than 10 $[°C]$ has been observed (about 1 [%] of the optical pyrometers measurement range). Thanks to the developed virtual sensor and to the implemented GUI, the billets estimated temperature has been provided (Fig. 6.17, blue line). In the synoptic, the billets have been represented with rectangles. Selecting a generic billet, its specific heating profile is available. Fig. 6.18 shows the actual heating profile (blue line) of the billet located at the 43th furnace place (furnace zone 6). In the synoptic, green rectangles represent billets

that have reached the minimum desired exit temperature. A minimum average number of green billets inside the furnace leads to energy saving.

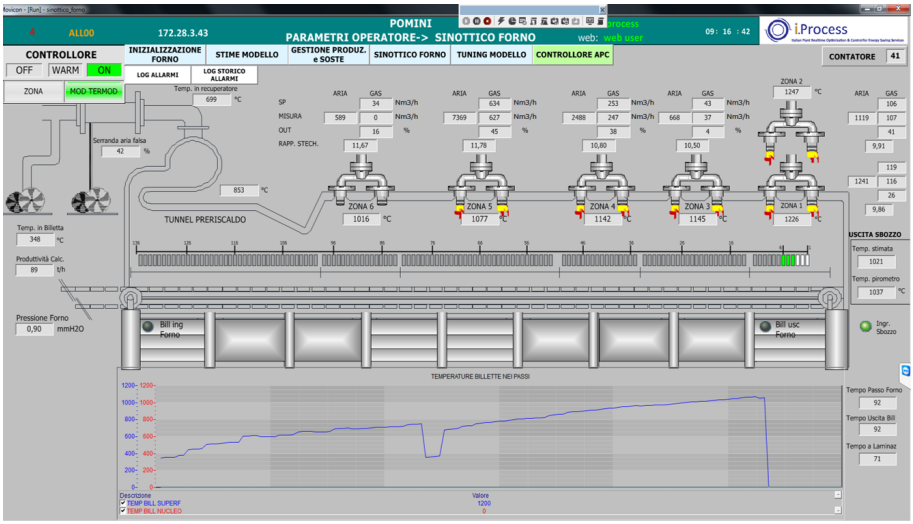

Figure 6.17: *Pusher type* reheating furnace GUI: furnace heating profile.

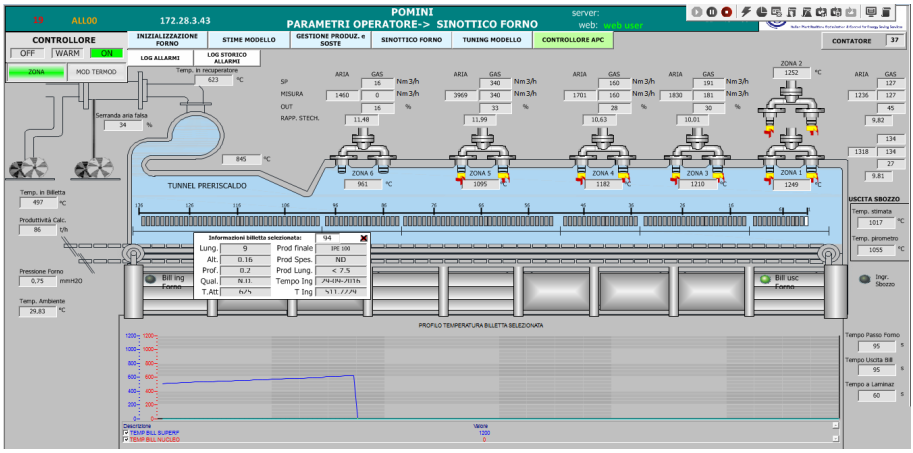

Figure 6.18: *Pusher type* reheating furnace GUI: furnace heating profile of the *43*th billet.

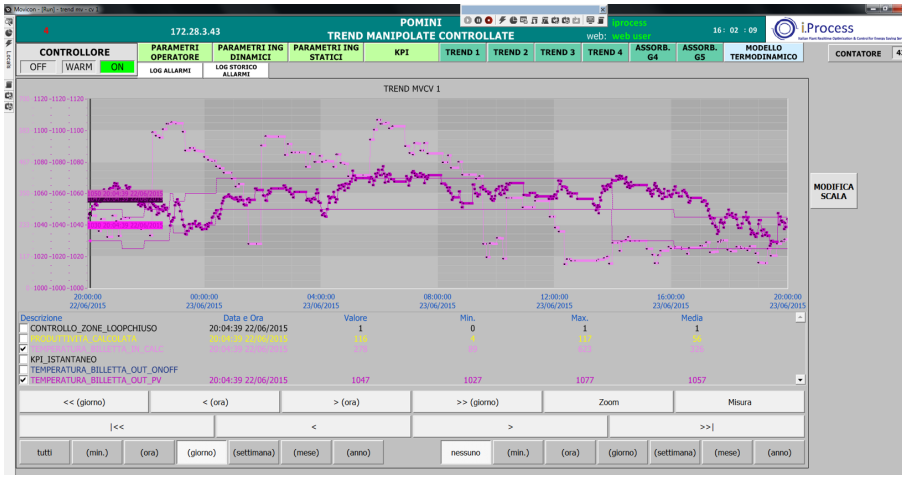

Figure 6.19: *Pusher type* reheating furnace GUI: billets temperature trends.

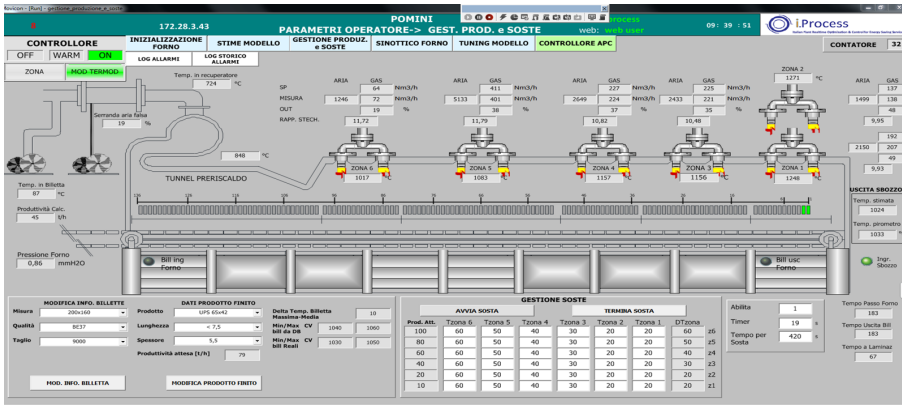

Figure 6.20: *Pusher type* reheating furnace GUI: temporary furnace stop or slowdown page.

Fig. 6.19 shows a page where the process variables and their constraints can be plotted and monitored. For example, in the proposed figure, the billets temperature measurements performed by the optical pyrometer at the exit of the first stage of the rolling mill stands (purple lines), together with the inlet temperature of the just entered billets (pink lines) are shown (note the different scale).

Fig. 6.20 shows a page where the changes on zCVs constraints when *E-FESTO* APC system switches from the *adaptive* control mode to the *zones* control mode can be automatically handled. There is the option for the definition of tables that are applied to the zCVs constraints when, for example, a temporary stop or slowdown of the billets movement along the furnace happens. The tables can take into account different furnace boundary conditions, e.g. the furnace production rate.
When manual conduction of local PID controllers was performed by operators, the simultaneous fulfillment of energy and product quality specifications was difficult to achieve. With the previous control system, operators safely ensured the desired billets exit temperatures and neglected aspects related to fuel minimization, thus achieving a limited energy efficiency. From the first start-up, the designed APC system has reduced the average gap with respect to the billets exit temperature lower bound of about 5 $[°C]$. The registered performances can be straightly related to the average number of billets that have reached the minimum desired exit temperature. With the previous control system, this number was greater than 10; after a year and half from the developed APC system activation, this number has been conducted to the range 6-8.

Figure 6.21: *Pusher type* reheating furnace GUI: KPI page.

For an online monitoring of the fuel specific consumption, which is computed taking into accout the fuel flow rates usage and the furnace production rate, different Key Performance Indicator (KPI) pages have been introduced. Fig. 6.21 shows the daily fuel specific consumption ($[Sm^3/t]$) under the *E-FESTO* APC system control related to September-October 2016 (blue line); the red line indicates the defined project baseline related to the fuel specific consumption. After one year and half from the introduction of *E-FESTO* APC system within the considered *pusher type* billets reheating furnace, an about 1.5 [%] reduction of the fuel specific consumption with respect to the defined project baseline has been achieved. The average specific consumption reduction and, more generally, the energy efficiency achievement (that involves also emissions reduction) allowed obtaining energy efficiency certificates. Furthermore, a service factor greater than 95 [%] has been registered.

6.2 Case study results: *walking beam* reheating furnace

In this section, simulation and field results related to the *walking beam* reheating furnace described in Section 4.4 have been reported. Furthermore, energy efficiency evaluation and computation related to field applications are depicted.

6.2.1 Simulation results

To better understand the following simulation examples, remember that, in the considered case study, each *active* zCV/rCV has been equipped with an own slack variable in *DO* formulation (see Section 4.4). Furthermore, if not differently indicated, no plant-model mismatch on the zCVs-MVs/DVs model and no measurement noise are assumed; the identified zCVs-MVs/DVs model is exploited also as zCVs-MVs/DVs plant model in the proposed simulations.

Walking beam reheating furnace *zones* APC mode: first scenario

The proposed stoichiometric ratios control method (Subsection 4.4.1) within the *zones* APC mode related to the described *walking beam* reheating furnace is shown through a simulation example that emulates a plant operating condition. Tables 6.7-6.8 show the MVs and the zCVs/rCVs that are assumed *active*, i.e. under the APC system handling. The other MVs and zCVs/rCVs are assumed *inactive*. Furthermore, the *inactive* MVs and all DVs are assumed constant, thus not influencing the controlled variables at issue. This choice is motivated only by the fact that, in this way, the performances of the proposed method can be more easily comprehended. Table 6.9 shows the steady-state gain signs

of the considered zCVs-MVs transfer functions. Table 6.10 shows the subpart of the initial *Decoupling Matrix* D_E supplied by *SCADA* system to *DC & DS* block related to the interested zCV. *DC & DS* block and the other modules perform all the operations related to *inactive* process variables, as explained in Chapters 3-4. In particular, all (initial) D_E rows and columns related to *inactive* zCVs and MVs are zeroed by *DC & DS* block.
This simulation example considers having only the furnace zone 4 under control of the proposed APC system. *TOCS* and *DO* modules have to ensure an optimal usage of zone 4 fuel and air flow rates, taking into account zone 4 temperature and zone 4 stoichiometric ratio constraints. In particular, thanks to the decoupling strategy, for zone 4 temperature constraints tightening only the zone 4 fuel flow rate is used.

Table 6.7: *Walking beam* reheating furnace *zones* APC mode simulation results, first scenario: considered set of MVs.

Variable Name	**Acronym [Units]**
Zone 4 Fuel Flow Rate	$Fuel_4$ $[Nm3/h]$
Zone 4 Air Flow Rate	Air_4 $[Nm3/h]$

Table 6.8: *Walking beam* reheating furnace *zones* APC mode simulation results, first scenario: considered set of zCVs/rCVs.

Variable Name	**Acronym [Units]**
Zone 4 Temperature	$Temp_4$ $[°C]$
Zone 4 Stoich. Ratio	R_4 []

Table 6.9: *Walking beam* reheating furnace *zones* APC mode simulation results, first scenario: reduced zCVs-MVs mapping matrix.

Acronym	$Fuel_4$	Air_4
$Temp_4$	$+$	$-$

Table 6.10: *Walking beam* reheating furnace *zones* APC mode simulation results, first scenario: reduced initial *Decoupling Matrix*.

Acronym	$Fuel_4$	Air_4
$Temp_4$	1	0

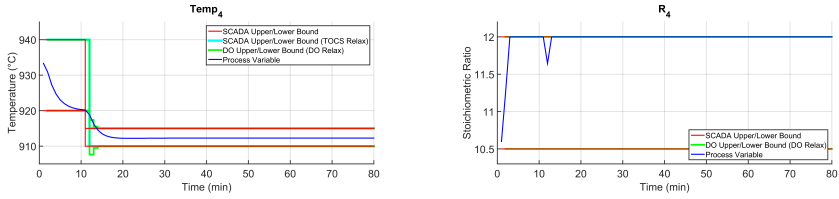

(a) $Temp_4$ (b) R_4

Figure 6.22: *Walking beam* reheating furnace *zones* APC mode simulation results, first scenario: zCVs/rCVs trends.

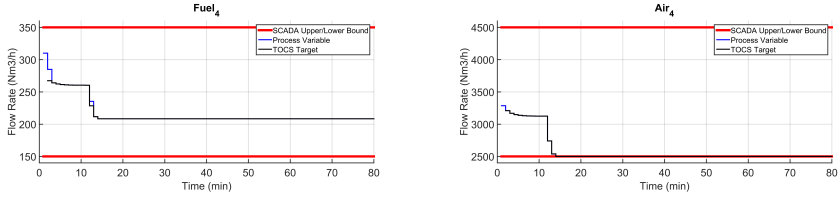

(a) $Fuel_4$ (b) Air_4

Figure 6.23: *Walking beam* reheating furnace *zones* APC mode simulation results, first scenario: MVs trends.

The simulation starting point assumes that $Temp_4$ and R_4 are inside their bounds (Fig. 6.22(a)-6.22(b), blue lines). In the first 10 simulation instants, the cooperation between *TOCS* and *DO* modules conducts the process variables to a more profitable operating condition, defined by $Fuel_4$ and Air_4 steady-state targets (Fig. 6.23(a)-6.23(b), black lines). $Fuel_4$ is minimized (Fig. 6.23(a), blue line), complying with $Temp_4$ constraints (Fig. 6.22(a), red lines) and not requiring *TOCS* and/or *DO* $Temp_4$ constraints relaxation (overlapping of red, cyan and green lines in Fig. 6.22(a)). Air_4 is exploited for R_4 stoichiometric ratio (Fig. 6.22(b), blue line) constraints meeting (Fig. 6.22(b), red lines): *DO* R_4 constraints relaxation is not required (overlapping of red and green lines in Fig. 6.22(b)).

At time instant 11, a constraints change request is simulated: $Temp_4$ lower and upper constraints are lowered of 10 [$^\circ C$] and 25 [$^\circ C$], respectively.
In order to satisfy the request, MVs target is updated by *TOCS* module: *DO* conducts $Fuel_4$ and Air_4 to these lower operating points (Fig. 6.23(a)-6.23(b)). After a brief transient, where a temporary *DO* upper constraints relaxation (6.22(a), green lines) is experienced, $Temp_4$ is restored to its new bounds. As shown in Fig. 6.22(b), no R_4 constraints relaxation is performed by *DO* module.

Walking beam reheating furnace *zones* APC mode: second scenario

The proposed stoichiometric ratios control method (Subsection 4.4.1) within the *zones* APC mode related to the described *walking beam* reheating furnace is shown through a simulation example that emulates a plant operating condition. Tables 6.11-6.12 show the MVs and the zCVs/rCVs that are assumed *active*, i.e. under the APC system handling. The other MVs and zCVs/rCVs are assumed *inactive*. Furthermore, the *inactive* MVs and all DVs are assumed constant, thus not influencing the controlled variables at issue. This choice is motivated only by the fact that, in this way, the performances of the proposed method can be more easily comprehended. Table 6.13 shows the steady-state gain signs of the considered zCVs-MVs transfer functions. Table 6.14 shows the subpart of the initial *Decoupling Matrix* D_E supplied by *SCADA* system to *DC & DS* block related to the interested zCV. *DC & DS* block and the other modules perform all the operations related to *inactive* process variables, as explained in Chapters 3-4. In particular, all (initial) D_E rows and columns related to *inactive* zCVs and MVs are zeroed by *DC & DS* block.
This simulation example considers having only the furnace zone 5 under control of the proposed APC system. *TOCS* and *DO* modules have to ensure an optimal usage of zone 5 fuel and air flow rates, taking into account zone 5 temperature and zone 5 stoichiometric ratio constraints. In particular, thanks to the decoupling strategy, for zone 5 temperature constraints tightening only the zone 5 fuel flow rate is used.

Table 6.11: *Walking beam* reheating furnace *zones* APC mode simulation results, second scenario: considered set of MVs.

Variable Name	**Acronym [Units]**
Zone 5 Fuel Flow Rate	$Fuel_5$ $[Nm3/h]$
Zone 5 Air Flow Rate	Air_5 $[Nm3/h]$

Table 6.12: *Walking beam* reheating furnace *zones* APC mode simulation results, second scenario: considered set of zCVs/rCVs.

Variable Name	**Acronym [Units]**
Zone 5 Temperature	$Temp_5$ $[°C]$
Zone 5 Stoich. Ratio	R_5 []

Table 6.13: *Walking beam* reheating furnace *zones* APC mode simulation results, second scenario: reduced zCVs-MVs mapping matrix.

Acronym	$Fuel_5$	Air_5
$Temp_5$	$+$	$-$

Table 6.14: *Walking beam* reheating furnace *zones* APC mode simulation results, second scenario: reduced initial *Decoupling Matrix*.

Acronym	$Fuel_5$	Air_5
$Temp_5$	1	0

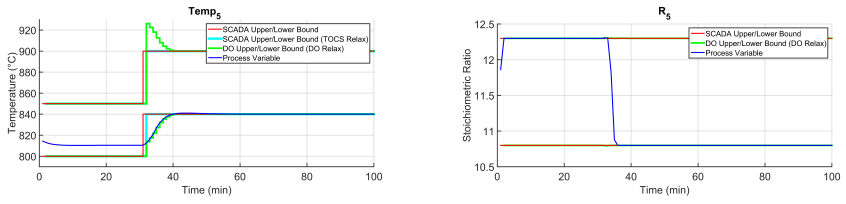

(a) $Temp_5$ (b) R_5

Figure 6.24: *Walking beam* reheating furnace *zones* APC mode simulation results, second scenario: zCVs/rCVs trends.

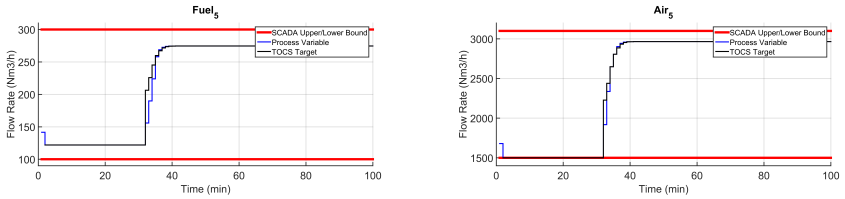

(a) $Fuel_5$ (b) Air_5

Figure 6.25: *Walking beam* reheating furnace *zones* APC mode simulation results, second scenario: MVs trends.

The initial process operating point assumes that the two considered output variables (Fig. 6.24(a)-6.24(b), blue lines) satisfy their constraints. In the first 30 simulation instants, the cooperative action of *TOCS* and *DO* modules ensures zone 5 fuel flow rate minimization (Fig. 6.25(a), blue line), saturating zone 5 stoichiometric ratio upper bound (Fig. 6.24(b), red line) and meeting zone 5 temperature constraints (Fig. 6.24(a), red lines). Furthermore, no *TOCS* and/or *DO* modules constraints softening is required (red, cyan and green lines in Fig. 6.24(a)-6.24(b) overlap). A profitable operating point for zone 5 fuel and air flow rates is guaranteed, saturating the zone 5 air flow rate lower bound (Fig. 6.25(a)-6.25(b), blue lines).
At time instant 31, an operator request is simulated: zone 5 temperature upper and lower constraints are changed of $+50$ $[°C]$ and $+40$ $[°C]$, respectively. Only zone 5 fuel flow rate acts for the satisfaction of the updated temperature constraints, reaching the new *TOCS* target (Fig. 6.25(a), black line).
After a brief transient, requiring a temporary softening of its new lower constraint (Fig. 6.24(a), green lines), zone 5 temperature is restored to its new lower bound. This corrective action on zone 5 fuel flow rate could lead to the violation of zone 5 stoichiometric ratio lower bound: in order to avoid this critical condition, a new target for zone 5 air flow rate is computed by *TOCS* module (Fig. 6.25(b), black line). In this way, zone 5 stoichiometric ratio approaches its lower bound, after a negligible *DO* constraints softening (Fig. 6.24(b), green lines).

Walking beam reheating furnace *zones* APC mode: third scenario

The proposed stoichiometric ratios control method (Subsection 4.4.1) within the *zones* APC mode related to the described *walking beam* reheating furnace is shown through a simulation example that emulates a plant operating condition. Tables 6.15-6.16 show the MVs and the zCVs/rCVs that are assumed *active*, i.e. under the APC system handling. The other MVs and zCVs/rCVs are assumed *inactive*. Furthermore, the *inactive* MVs and all DVs are assumed

constant, thus not influencing the controlled variables at issue. This choice is motivated only by the fact that, in this way, the performances of the proposed method can be more easily comprehended. Table 6.17 shows the steady-state gain signs of the considered zCVs-MVs transfer functions. A nonzero mapping on a MV-zCV pair has been indicated by the gain sign of the correspondent transfer function. Table 6.18 shows the subpart of the initial *Decoupling Matrix* D_E supplied by *SCADA* system to *DC & DS* block related to the interested zCVs. *DC & DS* block and the other modules perform all the operations related to *inactive* process variables, as explained in Chapters 3-4. In particular, all (initial) D_E rows and columns related to *inactive* zCVs and MVs are zeroed by *DC & DS* block.
This simulation example considers having only the furnace zones 4-5 under control of the proposed APC system. *TOCS* and *DO* modules have to ensure an optimal usage of the zones 4-5 fuel and air flow rates, taking into account zone 4-5 temperatures and zone 4-5 stoichiometric ratios constraints. In particular, thanks to the decoupling strategy, for zone 5 temperature constraints tightening only the zone 5 fuel flow rate is used. Similarly, for zone 4 temperature constraints tightening only the zone 4 fuel flow rate is used.

Table 6.15: *Walking beam* reheating furnace *zones* APC mode simulation results, third scenario: considered set of MVs.

Variable Name	**Acronym [Units]**
Zone 5 Fuel Flow Rate	$Fuel_5$ $[Nm3/h]$
Zone 4 Fuel Flow Rate	$Fuel_4$ $[Nm3/h]$
Zone 5 Air Flow Rate	Air_5 $[Nm3/h]$
Zone 4 Air Flow Rate	Air_4 $[Nm3/h]$

Table 6.16: *Walking beam* reheating furnace *zones* APC mode simulation results, third scenario: considered set of zCVs/rCVs.

Variable Name	**Acronym [Units]**
Zone 5 Temperature	$Temp_5$ $[°C]$
Zone 4 Temperature	$Temp_4$ $[°C]$
Zone 5 Stoich. Ratio	R_5 []
Zone 4 Stoich. Ratio	R_4 []

Table 6.17: *Walking beam* reheating furnace *zones* APC mode simulation results, third scenario: reduced zCVs-MVs mapping matrix.

Acronym	$Fuel_5$	$Fuel_4$	Air_5	Air_4
$Temp_5$	+	+	−	
$Temp_4$		+		−

Table 6.18: *Walking beam* reheating furnace *zones* APC mode simulation results, third scenario: reduced initial *Decoupling Matrix*.

Acronym	$Fuel_5$	$Fuel_4$	Air_5	Air_4
$Temp_5$	1	0	0	1
$Temp_4$	1	1	1	0

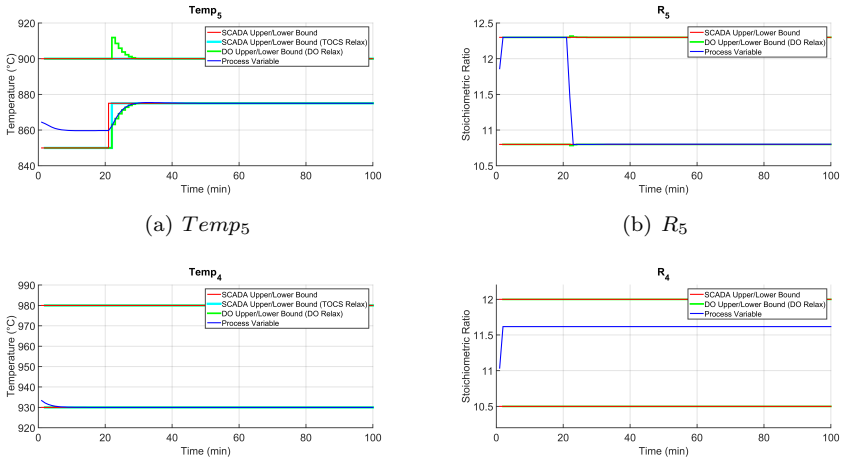

(a) $Temp_5$ (b) R_5

(c) $Temp_4$ (d) R_4

Figure 6.26: *Walking beam* reheating furnace *zones* APC mode simulation results, third scenario: zCVs/rCVs trends.

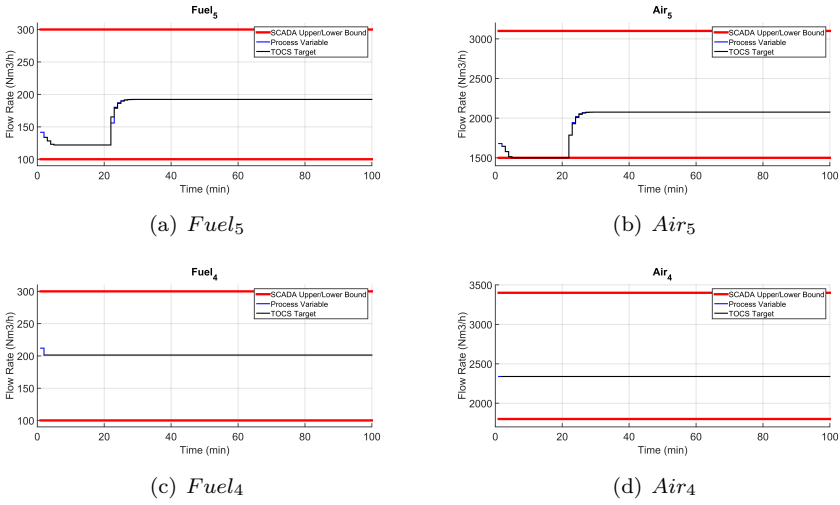

(a) $Fuel_5$ (b) Air_5

(c) $Fuel_4$ (d) Air_4

Figure 6.27: *Walking beam* reheating furnace *zones* APC mode simulation results, third scenario: MVs trends.

The initial process operating point assumes that the four considered output variables (Fig. 6.26(a)-6.26(b)-6.26(c)-6.26(d), blue lines) satisfy their constraints: in the first 20 simulation instants, the cooperative action of *TOCS* and *DO* modules ensures zone 5 and zone 4 fuel flow rate minimization (Fig. 6.27(a)-6.27(c), blue lines), saturating zone 5 stoichiometric ratio upper bound (Fig. 6.26(b), red line) and meeting zone 4 stoichiometric ratio constraints (Fig. 6.26(d), red lines). Furthermore, in this first part of simulation, zones 4-5 temperatures meet the imposed constraints (Fig. 6.26(a)-6.26(c), red lines) and no *TOCS* and *DO* modules constraints softening is required (red, cyan and green lines in Fig. 6.26(a)-6.26(b)-6.26(c)-6.26(d) overlap).
A profitable operating point for zones 4-5 fuel and air flow rates is guaranteed, saturating the zone 5 air flow rate lower bound (Fig. 6.27(a)-6.27(b)-6.27(c)-6.27(d), blue lines).
Subsequently, at time instant 21, an operator request is simulated: zone 5 temperature lower constraint is changed of $+25$ $[°C]$. Thanks to the proposed decoupling strategy, only zone 5 fuel flow rate acts for the satisfaction of the updated temperature constraints, reaching the new *TOCS* target (Fig. 6.27(a), black line). After a brief transient, requiring a temporary softening of its new lower constraint (Fig. 6.26(a), green lines), zone 5 temperature is restored on its new lower bound.
This corrective action on zone 5 fuel flow rate could lead to the violation of the zone 5 stoichiometric ratio lower bound: in order to avoid this critical condition, also zone 5 air flow rate *TOCS* target is changed (Fig. 6.27(b), black

line). In this way, zone 5 stoichiometric ratio approaches its lower bound, after a negligible *DO* constraints softening (Fig. 6.26(b), green lines).
Note that the proposed constraint change does not modify zone 4 variables configuration. Note also that, due to not necessary zone 4 stoichiometric ratio constraints relaxation and to the introduced decoupling strategy, zone 4 air flow rate remains constant at its initial value during the simulation.

Walking beam reheating furnace *zones* APC mode: fourth scenario

The effectiveness of the proposed cooperation policy between *TOCS* and *DO* modules (Subsection 3.1.2) is shown through a simulation example that emulates a plant operating condition. Tables 6.19-6.20 show the MVs and the zCVs/rCVs that are assumed *active*, i.e. under the APC system handling. The other MVs and zCVs/rCVs are assumed *inactive*. Furthermore, the *inactive* MVs and all DVs are assumed constant, thus not influencing the controlled variables at issue. This choice is motivated only by the fact that, in this way, the performances of the proposed method can be more easily comprehended.

Table 6.19: *Walking beam* reheating furnace *zones* APC mode simulation results, fourth scenario: considered set of MVs.

Variable Name	**Acronym [Units]**
Zone 5 Fuel Flow Rate	$Fuel_5$ $[Nm3/h]$
Zone 5 Air Flow Rate	Air_5 $[Nm3/h]$

Table 6.20: *Walking beam* reheating furnace *zones* APC mode simulation results, fourth scenario: considered set of zCVs/rCVs.

Variable Name	**Acronym [Units]**
Zone 5 Temperature	$Temp_5$ $[°C]$
Smoke-Exchanger Temp.	$Temp_{SE}$ $[°C]$
Zone 5 Stoich. Ratio	R_5 []

Table 6.21 shows the steady-state gain signs of the considered zCVs-MVs transfer functions. Table 6.22 shows the subpart of the initial *Decoupling Matrix* D_E supplied by *SCADA* system to *DC & DS* block related to the interested zCVs. *DC & DS* block and the other modules perform all the operations related to *inactive* process variables, as explained in Chapters 3-4. In particular, all (initial) D_E rows and columns related to *inactive* zCVs and MVs are zeroed by

DC & DS block.
This simulation example considers having only the furnace zone 5 under control of the proposed APC system, together with the smoke-exchanger temperature. *TOCS* and *DO* modules have to ensure an optimal usage of zone 5 fuel and air flow rates, taking into account zone 5 temperature, zone 5 stoichiometric ratio and smoke-exchanger temperature constraints. In particular, thanks to the decoupling strategy, for zone 5 temperature constraints tightening only the zone 5 fuel flow rate is used.

Table 6.21: *Walking beam* reheating furnace *zones* APC mode simulation results, fourth scenario: reduced zCVs-MVs mapping matrix.

Acronym	$Fuel_5$	Air_5
$Temp_5$	+	−
$Temp_{SE}$	+	

Table 6.22: *Walking beam* reheating furnace *zones* APC mode simulation results, fourth scenario: reduced initial *Decoupling Matrix*.

Acronym	$Fuel_5$	Air_5
$Temp_5$	1	0
$Temp_{SE}$	1	1

The initial process operating point assumes that the three considered output variables (Fig. 6.28(a)-6.28(b)-6.28(c), blue lines) satisfy their constraints (the lower bound related to the smoke-exchanger temperature, i.e. 0 $[°C]$, is not shown because it is not relevant for the proposed simulation). In the first 30 simulation instants, the initial configuration remains unchanged due to the fact that zone 5 fuel flow rate lies on its lower bound (Fig. 6.29(a)).
At time instant 31, an operator request is simulated: zone 5 temperature lower constraint is changed of +12 $[°C]$. For the satisfaction of the updated constraint, only zone 5 fuel flow rate must act. Regardless of the zone 5 fuel flow rate action, the controller must assign a major priority to zone 5 stoichiometric ratio and to smoke-exhanger constraints (see Subsection 4.4.1).
The full satisfaction of the new request could lead to the violation of the smoke-exchanger upper constraint, so the *TOCS-DO* cooperation must avoid this eventuality. Thanks to the introduced improvement on *TOCS-DO* coopera-

tion, the updated zone 5 temperature lower constraint (Fig. 6.28(a), red line) is *pre-softened* by *TOCS* module (Fig. 6.28(a), cyan line), which changes the steady-state targets of the related air and fuel flow rates (Fig. 6.29(a)-6.29(b), black lines). The updated steady-targets ensure no steady-state violations on zone 5 stoichiometric ratio and smoke-exchanger temperature constraints.
Thanks to the *TOCS pre-softening* action, no conflicting objectives are present in the *DO* formulation, i.e. its steady-state targets and constraints are coherent and consistent.
Through also a correct tuning of $S(H_u)$ matrix in *DO* optimization problem (see Section 3.3), the *DO* module conducts the process to a new configuration that respects the constraints on zone 5 stoichiometric ratio and on smoke-exchanger temperature. In particular, smoke-exchanger temperature upper constraint is saturated (Fig. 6.28(c)).
In order to prove the effectiveness of the improved *TOCS-DO* cooperation policy, the same plant operating condition is simulated but without the additional *TOCS-DO pre-softening* cooperation mode; all parameters are the same as in the previous simulation.
As it can be noted in Fig. 6.30(a)-6.30(b)-6.30(c), the satisfaction of the zone 5 stoichiometric ratio constraints is guaranteed, but the upper constraint related to the smoke-exchanger temperature is violated, together with the updated zone 5 temperature lower constraint.

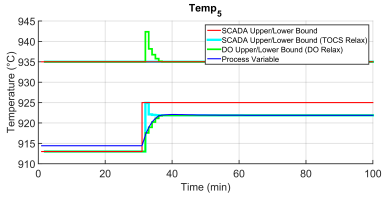

(a) $Temp_5$

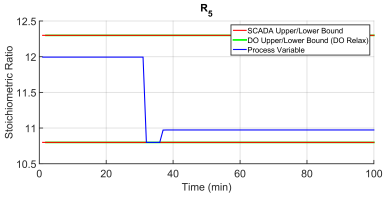

(b) R_5

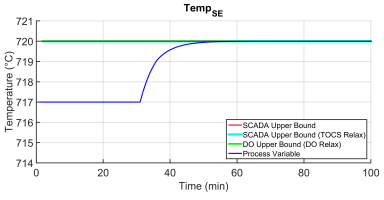

(c) $Temp_{SE}$

Figure 6.28: *Walking beam* reheating furnace *zones* APC mode simulation results, fourth scenario: zCVs/rCVs trends.

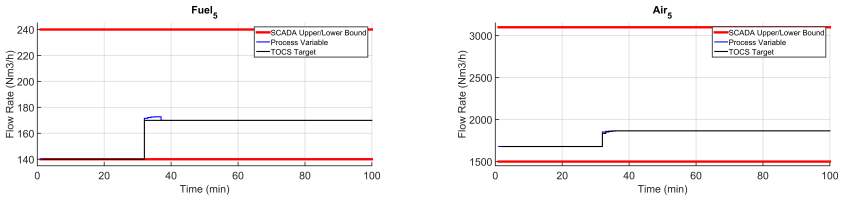

(a) $Fuel_5$ (b) Air_5

Figure 6.29: *Walking beam* reheating furnace *zones* APC mode simulation results, fourth scenario: MVs trends.

This undesired behavior is due to the occurred inconsistency between steady-state targets and steady-state constraints. In particular, the steady-state lower constraint related to the zone 5 temperature that is used by *DO* in its optimization problem is not coherent with respect to the *TOCS*-computed steady-state targets (that are forwarded to *DO* as basic cooperation mode). This inconsistency in *DO* optimization problem leads to the violation of the upper constraint related to the smoke-exchanger temperature in the same tuning conditions of the previous simulation. The previous simulation, on the other hand, exploited the improved *TOCS-DO* cooperation mode.

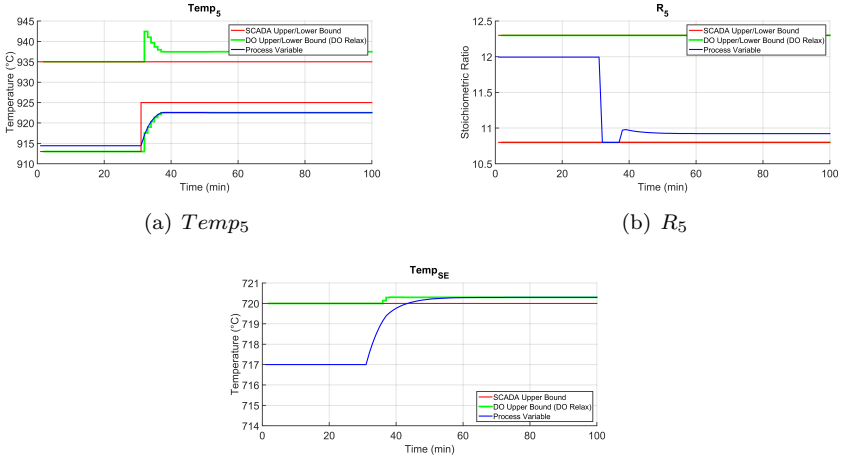

(a) $Temp_5$ (b) R_5

(c) $Temp_{SE}$

Figure 6.30: *Walking beam* reheating furnace *zones* APC mode simulation results, fourth scenario: zCVs/rCVs trends without *TOCS pre-softening* action.

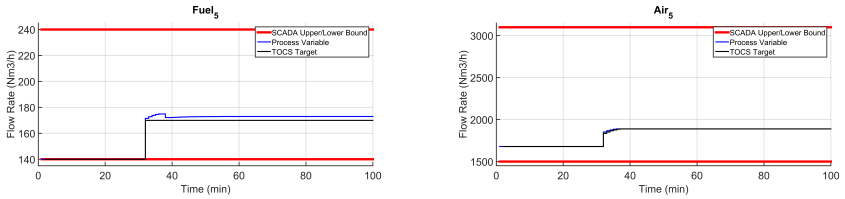

(a) $Fuel_5$ (b) Air_5

Figure 6.31: *Walking beam* reheating furnace *zones* APC mode simulation results, fourth scenario: MVs trends without *TOCS pre-softening* action.

6.2.2 Field results

The study and design phases for the development of the APC system related to the considered *walking beam* billets reheating furnace began in August 2013 and ended in May 2014. In early June 2014, the system has been installed, substituting operators' manual driving of local PID controllers.
In Fig. 6.32, the performances of the proposed control system are compared with those related to the previous one. The billets temperature measurements performed by the optical pyrometer at the exit of the first stage of the rolling mill stands are shown. A 15 hours period is considered: the first 4 hours refer to the previous control system ($APC\ OFF$) while the remaining 11 hours are related to the proposed APC system ($APC\ ON$). The billets temperature constraints (straight lines, 1055 [$^{\circ}C$] – 1080 [$^{\circ}C$]) in the two situations are the same and similar furnace boundary conditions, e.g. billets input temperature and furnace production rate, have been preserved. When the APC system is off, the billets temperature is always very close to its upper bound; in this case, energy saving and environmental impact decreasing aspects are neglected. With the activation of the APC system, billets final temperature decreases, thus approaching its lower bound; this effect is achieved thanks to the optimized usage of fuel and air flow rates.
The developed APC system has been implemented on a SCADA/HMI (Human-Machine Interface) platform that provides an user-friendly GUI (Graphical User Interface). Plant operators can easily handle the APC system: during the commissioning phase, training courses to plant operators have been provided. For this purpose, a training framework has been created, thus allowing plant operators to become proficient in the utilization of the APC system. The implemented GUI is composed by similar pages with respect to what described for the *pusher type* billets reheating furnace considered in Subsection 6.1.2.
As already mentioned, before the introduction of the developed APC system,

plant operators had no information about billets heating profile exhibited inside the furnace. An example on the real performances of the virtual sensor is shown in Fig. 6.33. Analyzing two year and a half process data, a Root Mean Square Error of Prediction (RMSEP) less than 8 [$°C$] has been observed (about 1 [%] of the optical pyrometers measurement range).

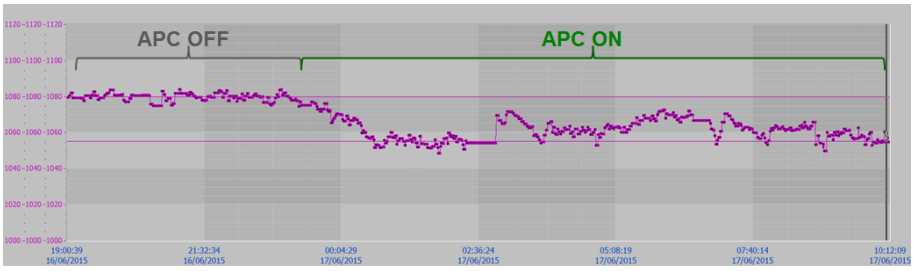

Figure 6.32: *Walking beam* reheating furnace billets final temperature trends and related constraints (straight lines) without ($APC\ OFF$) and with ($APC\ ON$) the designed APC system.

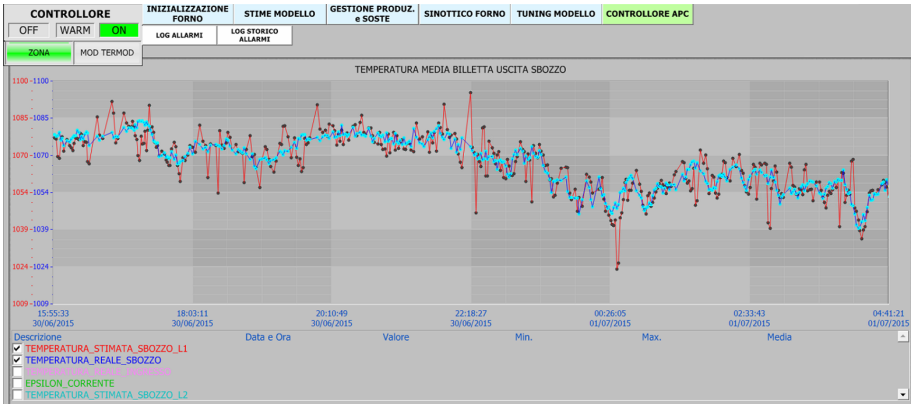

Figure 6.33: *Walking beam* reheating furnace field results: comparison between estimated (red line) and real (blue line) billets temperature at the exit of the first stage of the rolling mill stands.

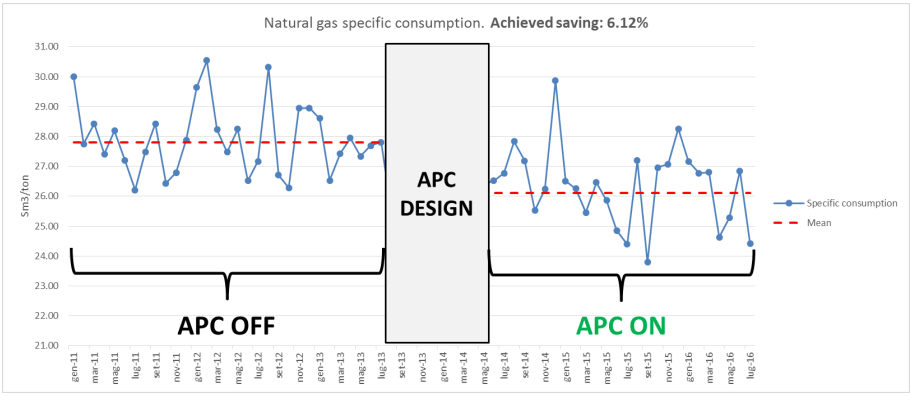

Figure 6.34: *Walking beam* reheating furnace field results: fuel specific consumption before and after the *E-FESTO* APC system activation.

When manual conduction of local PID controllers was performed by operators, the simultaneous fulfillment of energy and product quality specifications was difficult to achieve. With the previous control system, operators safely ensured the desired billets exit temperatures and neglected aspects related to fuel minimization, thus achieving a limited energy efficiency. Fig. 6.34 shows the fuel specific consumption before and after the installation of the APC system. A period of five and half years has been considered. The period January 2011-July 2013 (Fig. 6.34, left side) refers to the industrial process previous control system (project baseline), while the one from June 2014 to July 2016 (Fig. 6.34, right side) is related to the developed control framework. A reduction of approximately 6 [%] of the fuel specific consumption has been observed.
The achieved fuel specific consumption reduction corresponds to a considerable improvement from process performances point of view, i.e. reduction of the statistical properties (expected value and standard deviation) related to the billets furnace exit temperatures and to the combustion smokes temperature. After two years and half from the first start-up, an about 40 [$^{\circ}C$] average reduction (-14 [%]) of the combustion smokes temperature has been registered. This result contributes to the movement of the furnace thermal barycenter toward the *Soaking Area*, thus limiting thermal energy dissipation in the combustion smokes. The average specific consumption reduction and, more generally, the energy efficiency achievement (that involves also emissions reduction) allowed obtaining energy efficiency certificates. Furthermore, a service factor greater than 96 [%] has been registered.
The project related to the considered *walking beam* billets reheating furnace has been awarded in October 2015 during the *Secondo Workshop Annuale CE-*

SEF (organized by "Università Bocconi", Milan) among CESEF (Centro Studi sull'Economia e il Management dell'Efficienza Energetica) Energy Efficiency Awards. In particular, it has been awarded with the "Project Energy Efficiency Award" (http://www.agici.it/eventi/CESEF/2015.html).

Chapter 7

Cement Industry APC system Results

In this chapter, simulation and field results of the developed APC system for the control and the optimization of the *clinker* production phase related to cement industries are reported. The effectiveness of the theoretical and practical considerations detailed in Chapter 5 is proved through the discussion of significant simulation and real examples related to the plants where the developed control system has been installed. The shown results will refer to the two case studies detailed in Sections 5.3-5.4.

7.1 Case study results: dry cement industry *clinker* production phase without precalciner

In this section, simulation and field results related to the dry cement industry *clinker* production phase without precalciner described in Section 5.3 have been reported. Furthermore, energy efficiency evaluation and computation related to field applications are depicted.

7.1.1 Simulation results

In the proposed simulations, if not differently indicated, no plant-model mismatch and no measurement noise are assumed; the identified CVs-MVs/DVs model is exploited also as plant model in the proposed simulations.

Clinker production phase without precalciner: first scenario

In Subsection 5.2.1, a constraints softening decoupling strategy has been introduced: it structurally decouples the formulation of the constraints softening related to each *active* CV.
For the illustration of the proposed decoupling strategy, a subsystem composed

by all MVs and one CV has been selected: NO_x is the considered CV. The interest on this variable is related to the presence of different delays in its modeling with the MVs, i.e. *Fan Speed* and *Kiln Fuel*. These delays are 15 $[min]$ and 6 $[min]$, respectively. Only the cited MVs and CV are assumed *active*, i.e. under the APC system handling. The other CVs are assumed *inactive*. Furthermore, all DVs are assumed constant, thus not influencing the controlled variable at issue. This choice is motivated only by the fact that, in this way, the performances of the proposed method can be more easily comprehended. Table 7.1 shows the steady-state gain signs of the considered CV-MVs transfer functions, together with the related time delays ($[min]$) (in brackets). Both MVs can be used for NO_x constrained control, so the NO_x row of the initial *Decoupling Matrix* D_E supplied by *SCADA* system to *DC & DS* block will be composed by elements all equal to 1. *DC & DS* block and the other modules perform all the operations related to *inactive* process variables as explained in Chapter 3 and in Chapter 5. In particular, all (initial) D_E rows related to *inactive* CVs are zeroed by *DC & DS* block.

Table 7.1: *Clinker* production phase without precalciner CVs-MVs reduced mapping matrix.

Acronym	*Fan Speed*	*Kiln Fuel*
NO_x	+ (15)	+ (6)

Considering NO_x-MVs channels and given the 4th position of the NO_x in the CVs vector (see Table 5.2), the related key scalar parameters for the proposed constraints softening decoupling strategy are $H_{w_4} = 7$ and $h_4 = 2$. Furthermore:

$$f_4 = \begin{bmatrix} f_{4_1} \\ f_{4_2} \end{bmatrix} = \begin{bmatrix} 7 \\ 16 \end{bmatrix} \qquad \varepsilon_{yDO}(k) = \begin{bmatrix} \varepsilon_{yDO_4}(k) \end{bmatrix} \qquad \varepsilon_{yDO_4}(k) = \begin{bmatrix} \varepsilon_{yDO_{4_1}}(k) \\ \varepsilon_{yDO_{4_2}}(k) \end{bmatrix} \tag{7.1}$$

Practically, for the *DO* constraints softening related to NO_x, the task is split between $\varepsilon_{yDO_{4_1}}(k)$ and $\varepsilon_{yDO_{4_2}}(k)$ slack variables. With the selected prediction horizon ($H_p = 120$ $[min]$, see Section 5.3), $\varepsilon_{yDO_{4_1}}(k)$ is related to 7th-15th prediction instants, while $\varepsilon_{yDO_{4_2}}(k)$ is related to 16th-120th prediction instants. In this sense, a decoupling approach has been performed. The elements of $\gamma_{lbyDO}(i)$ and $\gamma_{ubyDO}(i)$ vectors related to NO_x are equally set for the related two slack variables, together with the related weights contained in ρ_{yDO} matrix.

Furthermore, in the simulation, for a better proof of the impact of the pro-

posed constraints softening decoupling strategy, the diagonal elements of $S(i)$ matrices related to *Fan Speed* in *DO* cost function (5.1) have been set to zero. Practically, tracking is not considered as a control objective for *Fan Speed*.
In the example, a variation on NO_x upper constraint is simulated and two different control solutions are compared. The first does not use the proposed constraints softening decoupling strategy and it provides, in the *DO* formulation, a single slack variable for NO_x constraints. The second exploits the decoupling strategy consistently with the design previously depicted. As starting point of the proposed simulation, the following operating condition has been chosen: NO_x lies on its upper constraint, while *Kiln Fuel* is at its lower constraint (6600 $[Kg/h]$); *Fan Speed* is inside its operating limits. *DO* module, with *TOCS* module support, performs economic optimization, leaving unchanged the plant configuration, thus minimizing fuel flow rate. As shown in Fig. 7.1, at time instant 130, as a consequence of an operator request, the NO_x upper constraint is lowered of 50 $[ppm]$. Fig. 7.2(a) shows *Fan Speed*. In Fig. 7.1(a) and in Fig. 7.2(a), the results of the first control solution are reported, while in Fig. 7.1(b)-7.2(a) the results obtained when applying the decoupling control solution are shown. *Kiln Fuel* trends (Fig. 7.2(b)) remain constant at the lower bound for the entire simulation in both control solutions.
When the constraint is changed, in both control solutions no steady-state *pre-softening* is required by *TOCS* module (cyan and red lines in Fig. 7.1 overlap), given the steady-state feasibility of the request. *DO*, because of the presence of time delays in the NO_x–MVs channels, generally can guarantee a reaction of the considered controlled variable from 7th prediction instant onward. In the proposed example, due to the clamping of *Kiln Fuel* to its lower limit, only moves on *Fan Speed* can be exploited to satisfy the operator's request. Therefore *DO*, in this specific case, can guarantee a reaction of the considered controlled variable from 16th prediction instant onward. In the first control solution, the single NO_x slack variable of the *DO* formulation, which is responsible of all NO_x constraints, relaxes the newly set NO_x upper bound (Fig. 7.1(a), green lines): this action is induced on the constraints of 16th-120th predictions by not achievable requirements on the constraints of 7th-15th predictions. In this way, no moves on *Fan Speed* are performed, thus having a failure of the overall control action (Fig. 7.1(a), blue line and Fig. 7.2(a), black line). In the second control solution, constraints related to 7th-15th predictions and the ones related to 16th-120th predictions are structurally independent, thanks to the proposed constraints softening decoupling strategy. Thus, in this case, there is not an induction effect between them: $\varepsilon_{yDO_{4_1}}(k)$ slack variable performs, on the upper constraints of 7th-15th predictions, the same relaxation of the single slack variable in the first control solution (not shown in Fig. 7.1(b)). On the other hand, thanks to the presence of $\varepsilon_{yDO_{4_2}}(k)$

slack variable on the constraints related to 16th-120th predictions, *DO* acts on *Fan Speed* (Fig. 7.2(a), blue line) so as to gradually reduce their softening (Fig. 7.1(b), green lines) and to meet the newly set NO_x upper constraint (Fig. 7.1(b), blue line).

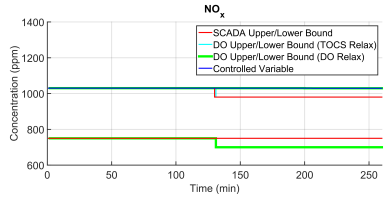

(a) NO_x without constr. soft. dec. strat.

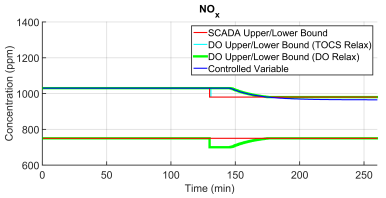

(b) NO_x with constr. soft. dec. strat.

Figure 7.1: *Clinker* production phase without precalciner simulation results, first scenario: NO_x trends without and with the constraints softening decoupling strategy.

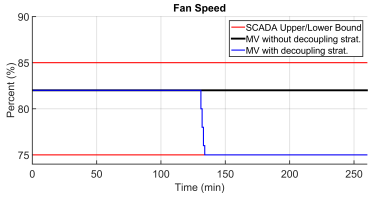

(a) *Fan Speed* without (black) and with (blue) constr. soft. dec. strat.

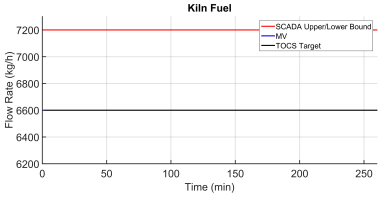

(b) *Kiln Fuel*

Figure 7.2: *Clinker* production phase without precalciner simulation results, first scenario: MVs trends.

7.1.2 Field results

The study and design phases of the project for the development of the *customized* APC system (Section 5.3) began in June 2014 and ended in December 2014. In early January 2015, the system has been installed on the considered Italian cement industry for the optimization of the *clinker* production phase, replacing local PID controllers handled by plant operators. With respect to the previous control solution, the designed controller assured a more profitable trade-off between energy saving, quality monitoring, and pollution impact decreasing. In terms of plant behavior, these improvements are explained by the reduction of some statistical properties related to the main controlled variables: in this way, the controlled variables can approach closer their key operating lim-

its. In this context, economic manipulated variables, such as fuel flow rate, can be minimized. This result contributed to achievement of energy efficiency, reducing the fuel specific consumption. Further benefits are represented by a better kiln conduction in terms of chemical and environmental emissions, given by a reduction of average oxygen and nitrogen oxides concentration.

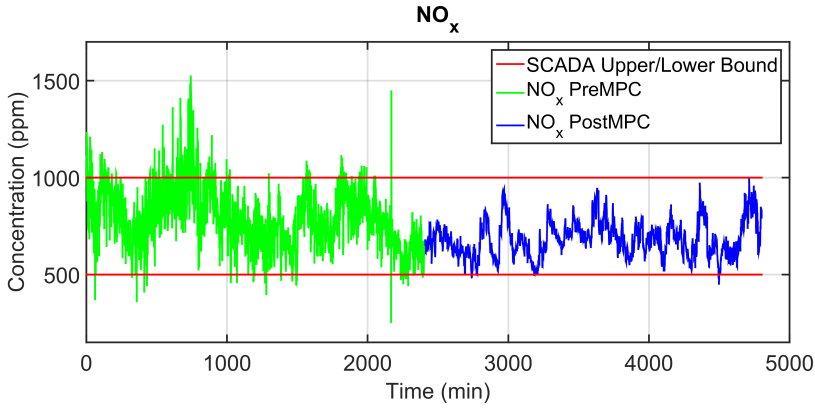

Figure 7.3: *Clinker* production phase without precalciner field results, first scenario: NO_x trends before and after APC activation.

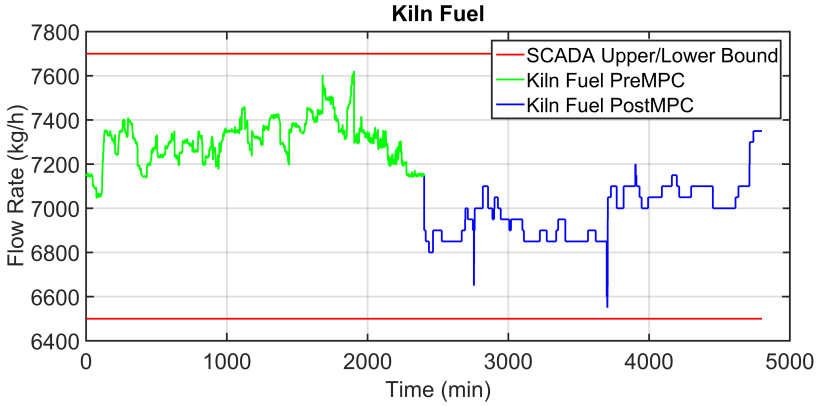

Figure 7.4: *Clinker* production phase without precalciner field results, first scenario: *Kiln Fuel* trends before and after APC activation.

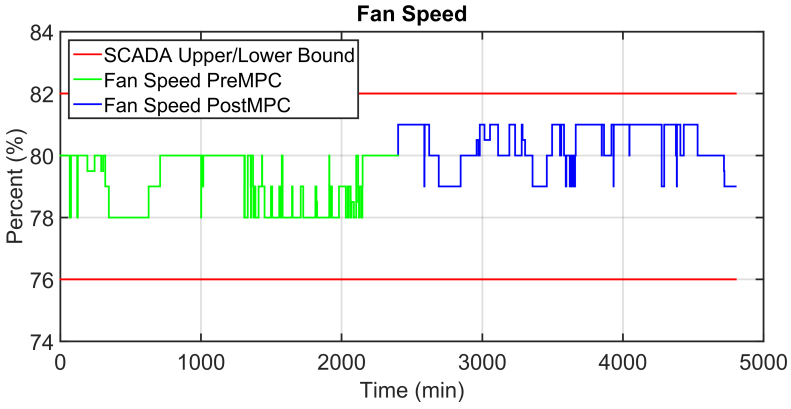

Figure 7.5: *Clinker* production phase without precalciner field results, first scenario: *Fan Speed* trends before and after APC activation.

Fig. 7.3 shows a comparison on NO_x trends related to a real plant condition: green lines refer to system without the APC installation while blue lines refer to the behavior with the APC activation (about a day and a half period has been considered for both situations). Fig. 7.4-7.5 depict the trends of the related MVs. The average boundary conditions, e.g. variables constraints (Fig. 7.3-7.4-7.5, red lines), meal flow rate values, and rotation kiln speed values (that constitute the DVs of the controller design), are similar. In particular, in both situations, average meal flow rate is about 120 $[t/h]$ while average rotation kiln speed is about 2 $[rpm]$.
Fig. 7.6-7.7-7.8 refer to an additional plant operating condition: the specific consumption of the considered process, together with nitrogen oxides concentration and free lime analysis, are reported. The behaviors with manual driving and with APC driving are compared (with similar boundary conditions). The period considered for the comparison refers to about three weeks with and without the APC installation. After APC introduction, a relevant reduction on the nitrogen oxides variance has been observed: the process, optimized by the proposed *TOCS-DO* cooperation, safely operates closer to its constraints (400 $[ppm]$-1500 $[ppm]$ in this situation). In this way, specific kiln consumption (see Fig. 7.6) is reduced, leading to energy efficiency achievement. Furthermore, a better regulation of CVs led to the reduction of chemical and environmental emissions, i.e. to nitrogen oxides concentration lowering. The improvements related to energy efficiency can be also observed through the free lime analysis (carried out once a day in the considered case study) related to the two situations (without and with APC activation): both control solutions meet the "quality constraints" (0.4 [%] - 1 [%]), but with the APC activation the av-

erage free lime value increases. In this way, the process is moved away from possible overburning conditions (free lime analysis less than 0.4 [%]) but, at the same time, it can safely operate preventing possible cooling situations (free lime analysis greater than 1 [%]).

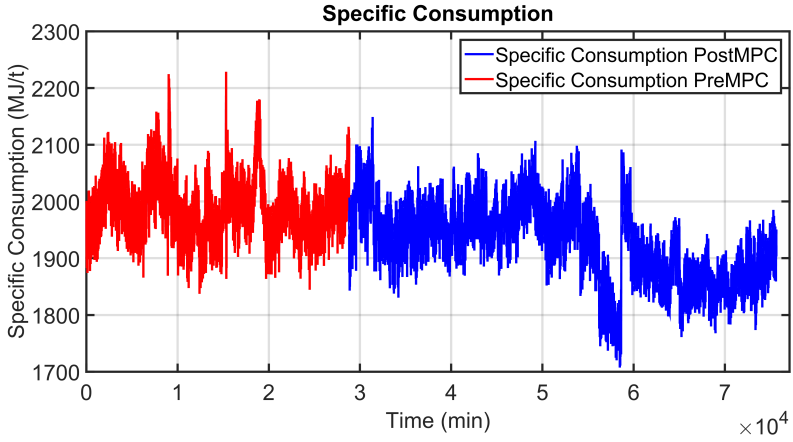

Figure 7.6: *Clinker* production phase without precalciner field results, second scenario: specific consumption trends before and after APC activation.

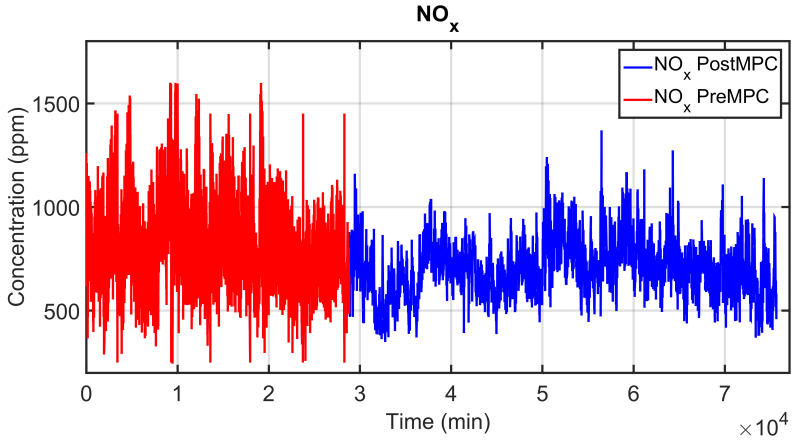

Figure 7.7: *Clinker* production phase without precalciner field results, second scenario: NO_x trends before and after APC activation.

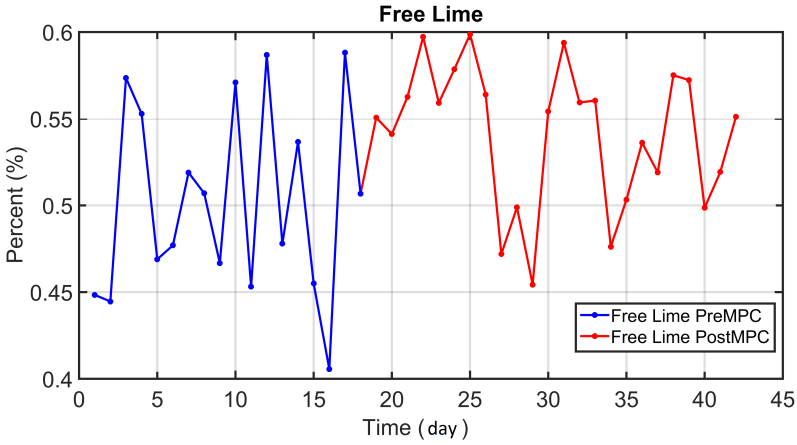

Figure 7.8: *Clinker* production phase without precalciner field results, second scenario: free lime analysis before and after APC activation.

After about two years since the first start-up of the proposed APC system, the following results have been obtained:

- about 7 [%] standard deviation reduction on oxygen concentrations trends, thus achieving an improved control of the combustion;
- about 14 [%] average reduction on nitrogen oxides trends and a 42 [%] reduction of its standard deviation, thus achieving a significant emissions reduction;
- 1.9 [%] reduction on the fuel average specific consumption;
- about 6 [%] average increase of the free lime values;
- about 90 [%] controller service factor.

Average specific consumption has been calculated keeping into account the fuel usage, together with the meal flow rate of the furnace, normalized with respect to nominal free lime and coal heating power. The average specific consumption reduction and, more generally, the energy efficiency achievement (that involves also emissions reduction) allowed to obtain Italian energy efficiency certificates (Italian acronym TEE, also called “white certificates”).

7.2 Case study results: dry cement industry *clinker* production phase with precalciner

The study and design phases of the project for the development of the *customized* APC system (Section 5.4) began in September 2014 and ended in November 2014. In December 2014, the system has been installed on the con-

sidered Italian cement industry for the optimization of the *clinker* production phase, replacing local PID controllers handled by plant operators. With respect to the previous control system, the designed controller assured improved control performances related to oxygen and nitrogen oxides levels, together with an improved management of the cyclones temperatures. In this context, energy saving has been obtained, through the attainment of a profitable trade-off between kiln fuels minimization and meal flow rate maximization. Thanks to the developed constraints softening decoupling strategy (see Subsection 5.2.1), an optimized compensation of the different time delays present on the CVs-MVs channels has been obtained. In terms of plant behavior, these improvements are explained by the reduction of the standard deviation of the main controlled variables, which allows a more safe approach to process operating limits.
Fig. 7.9 shows a comparison between the previous control system and the developed APC system related to the cyclones oxygen control. Thanks to an optimized management of the MVs that have to be used for its control (see Table 5.14), i.e. the fuel flow rates and the ID fan speed, a reduction on its standard deviation is observed. In general, after about two years from the first start-up of the proposed APC system, an average 39 [%] reduction has been registered on cyclones oxygen standard deviation, together with an average 3 [%] increase on its mean value.
Fig. 7.10 shows a comparison between the previous control system and the developed APC system related to the kiln nitrogen oxides control. Thanks to an optimized management of the MVs that have to be used for its control (see Table 5.14), i.e. the kiln fuel flow rate and the meal flow rate, a reduction on its standard deviation is observed. In general, after about two years from the first start-up of the proposed APC system, an average 32 [%] reduction has been registered on kiln nitrogen oxides standard deviation, together with an average 15 [%] decrease on its mean value. This result has been very meaningful, because it implies a strong emissions reduction, thus allowing environmental impact decreasing.
After six months since the first start-up of the proposed APC system, a 2.2 [%] reduction of the kiln average fuel specific consumption has been achieved (see Fig. 7.11), reaching 2.4 [%] after about two years. Average specific consumption has been calculated keeping into account the fuel usage, together with the meal flow rate of the furnace, normalized with respect to nominal free lime and coal heating power. The average specific consumption reduction and, more generally, the energy efficiency achievement (that involves also emissions reduction) allowed to obtain Italian energy efficiency certificates (Italian acronym TEE, also called “white certificates”).

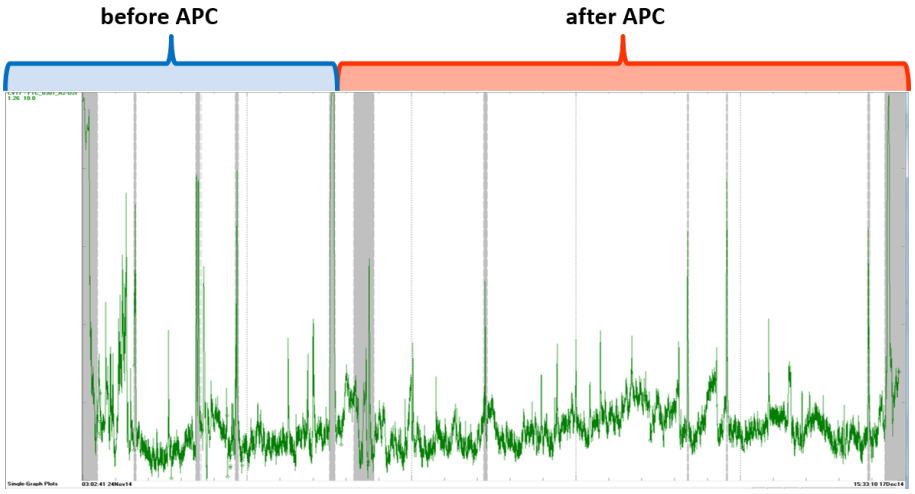

Figure 7.9: *Clinker* production phase with precalciner field results, first scenario: O_{2Cy} trends before and after APC activation.

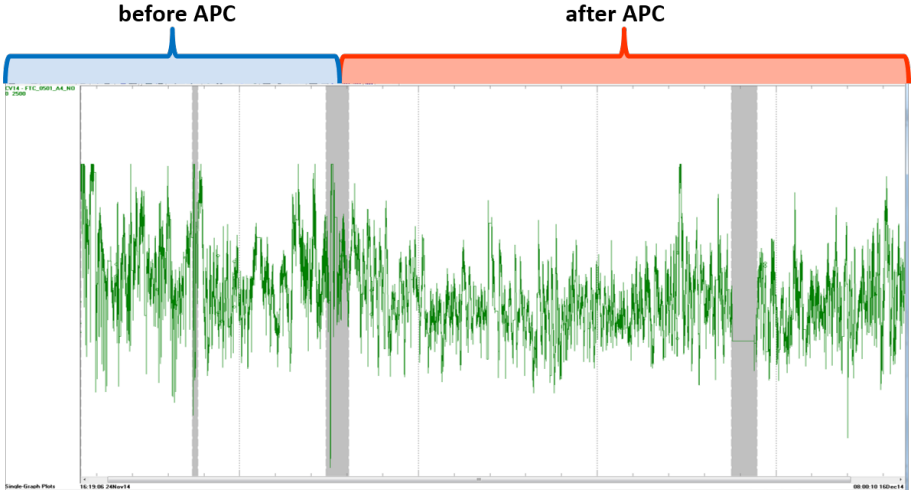

Figure 7.10: *Clinker* production phase with precalciner field results, second scenario: NO_{xKiln} trends before and after APC activation.

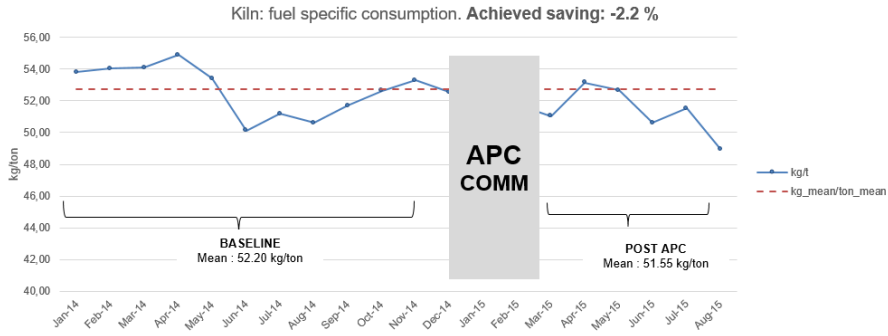

Figure 7.11: *Clinker* production phase with precalciner field results: specific consumption before and after APC activation.

Chapter 8

Conclusion and Future Work

The Ph.D. research activity described in the present dissertation has been co-sponsored by Università Politecnica delle Marche (Dipartimento di Ingegneria dell'Informazione (D.I.I.), Laboratory for Interconnected Systems Supervision and Automation (L.I.S.A.)), the regione Marche, and i.Process (Italian Plant Realtime Optimization & Control for Energy Saving Services) S.r.l., an Italian company that works on the development of control automation solutions for process industries.
The Ph.D. research started with a challenging objective: the development of a proprietary Advanced Process Control (APC) framework aimed at energy efficiency achievement and improvement in energivorous process industries, i.e. steel and cement industries. A control approach based on the Model Predictive Control (MPC) technique has been adopted, which is particularly suited when dealing with control of multivariable constrained processes. The proposed MPC formulation has been based on a linear state space approach that provides an explicit time delays compensation and it has been characterized by a *two-layer* scheme: at the lower layer there is the main MPC module, i.e. a *Dynamic Optimizer* (*DO*), while at the upper layer a steady-state module, named *Targets Optimizing and Constraints Softening* (*TOCS*) module, has been added. At this regard, an innovative contribution is represented by an improved overall *TOCS-DO* cooperation, based on *ad hoc* formulations of consistency relationships; the improved *two-layer* MPC scheme assures a correct management of process variables targets and constraints in all conditions.
In order to perform an efficient handling of critical situations due to the presence of different time delays on the inputs-output channels, an innovative contribution has been provided: the lower layer (*DO* module) has been redesigned with a strategy that performs a structural decoupling on output variables constraints softening.
With the aim to allow more degrees of freedom in the MPC scheme, a strategy that enables a selection on which control inputs to exploit for controlling each single output has been introduced. Two equivalent approaches to the control inputs action inhibition problem have been formulated. The first one is based

on suitable modifications of the initial control problem setup and formalizes a typical industrial practice, while the second one aims to fully exploit the structure of the basic MPC prediction matrices. This second approach represents an innovative contribution and it provides a more intuitive and straight handling of the inhibition specifications, especially in the cases where these specifications may be required to be online changed.
In the developed APC framework, a status value for each process variable involved in the control problem has been introduced and included in the *two-layer* MPC formulation, in order to correctly manage the process variables in all conditions. A tailored online status values definition has been addressed to each process variables group (control inputs, outputs, measured input disturbances). For the introduction of the inhibition specifications and of the status values information related to control inputs and outputs, an innovative unified approach has been provided, that exploits the structure of the basic MPC prediction matrices.
The developed APC framework has been then *customized* for its implementation on real industrial processes, represented by steel industry billets reheating furnaces and cement industry clinker rotary kilns. The studied processes are characterized by high energy consumption, and large energy efficiency margins have been observed. Typically, the considered processes were controlled by local PID control loops manually driven by plant operators, based on their experience and skills. Plant operators usually preferred to conduct the processes in safe operating points, thus neglecting the aspects more strictly related to energy efficiency and environmental impact decreasing.
With regard to the considered steel industry billets reheating furnaces, specific needs for the plants conduction have been taken into account and a *customized* APC framework has been developed. First, considering the lack of information on billets temperature within the furnaces, a virtual sensor has been introduced that has been based on a first principles adaptive nonlinear model. Besides, in order to introduce the billets temperature information within a *customized* linear MPC scheme, a Linear Parameter-Varying (LPV) model has been accordingly derived. An overall furnace model has been obtained by cascading the LPV model and the identified model related to the furnace zones temperature. In order to control the furnaces in all conditions, two main control modes have been introduced: an *adaptive* APC mode and a *zones* APC mode. In some case studies, an additional issue has been addressed, i.e. the need of an *ad hoc* stoichiometric ratios control method. A tailored linear formulation has been included in the *two-layer* MPC scheme, through specific manipulations on stoichiometric ratios exact models. The developed steel industry billets reheating furnaces *customized* APC system has been named as *E-FESTO* and the proposed control method has been awarded with an Italian patent [90].

Five real installations of *E-FESTO* APC system have been commissioned on reheating furnaces located in steel industries of various European countries. A satisfactory reduction of the fuel specific consumption with respect to the defined project baseline has been achieved in all real applications. The average specific consumption reduction and, more generally, the energy efficiency achievement (that involves also emissions reduction) allowed to obtain energy efficiency certificates. Furthermore, the pioneer steel industries APC project has been awarded in October 2015 during the *Secondo Workshop Annuale CESEF* (organized by "Università Bocconi", Milan) among CESEF (Centro Studi sull'Economia e il Management dell'Efficienza Energetica) Energy Efficiency Awards. In particular, it has been awarded with the "Project Energy Efficiency Award" (http://www.agici.it/eventi/CESEF/2015.html).

The application of the developed APC system in the cement field confirmed the validity of the proposed constraints softening decoupling strategy oriented to time delays handling. In fact, very positive control results have been achieved for the analyzed *clinker* production phases that are characterized by different time delays on single inputs-output channels. Furthermore, an additional contribution has been provided with regard to the usage of sporadic feedback information (free lime laboratory analysis) in the MPC scheme, establishing a direct relationship between the sporadic feedback and the constraints of selected control inputs. Different real installations of the APC system have been commissioned on cement industries located in various European countries. Optimal trade-offs between energy saving, environmental impact decreasing and quality and production maximization have been obtained. The resulting fuel specific consumption reduction allowed obtaining energy efficiency certificates. The cement industry APC tool, in one of the different installations, has improved a control system inserted in the 2013 annual report on energy efficiency world best practices provided by International Energy Agency.

The future work of the present research activity will be primarily focused on the improvement of the *customized* APC systems for steel and cement industry. In both contexts, new identification and modellization techniques will be studied and analyzed, in order to obtain more accurate processes models that constitute the core of the MPC strategy.

In steel industry, the future work will be also aimed at extending the steel production phases that are under the APC management. In fact, the actual version of *E-FESTO* APC system is aimed at control and optimize the *Reheating* phase, which is the middle phase of the steel production chain.

In cement industry, the future work will be also aimed at the development of virtual sensors able to guarantee a reliable non-sporadic free lime analysis, in order to ensure an improved clinker quality control and monitoring.

Bibliography

[1] M. Bauer and I. K. Craig, "Economic assessment of advanced process control - a survey and framework," *Journal of Process Control*, vol. 18, no. 1, pp. 2–18, 2008.

[2] P. L. Latour, J. H. Sharpe, and M. C. Delaney, "Estimating Benefits from Advanced Control," *ISA Trans.*, vol. 25, no. 4, pp. 13, 1986.

[3] "ENEA," `http://www.enea.it/it`.

[4] W. M. Canney, "Are you getting the full benefit from your advanced process control system?," *Hydrocarbon Processing*, vol. 84, no. 6, pp. 55–58, 2005.

[5] J. Richalet, A. Rault, J.L. Testud, and J. Papon, "Algorithmic control of industrial processes," in *4th IFAC symposium on identification and system parameter estimation*, 1976, p. 1119–1167.

[6] C. E. Garcia, D. M. Prett, and M. Morari, "Model predictive control: Theory and practice—a survey," *Automatica*, vol. 25, no. 3, pp. 335–348, 1989.

[7] J. B. Rawlings, "Tutorial overview of model predictive control," *IEEE Control Systems Magazine*, vol. 20, pp. 38–52, 2010.

[8] J. M. Maciejowski, *Predictive Control with Constraints*, Prentice Hall, 2002.

[9] E. F. Camacho and C. A. Bordons, *Model Predictive Control*, Springer, 2007.

[10] A. Bemporad, M. Morari, and N. L. Ricker, *Model Predictive Control Toolbox User's Guide 2016a.*

[11] R. Cagienard, P. Grieder, E. C. Kerrigan, and M. Morari, "Move Blocking Strategies in Receding Horizon Control," in *IEEE Conference on Decision and Control*, 2004.

[12] R. Cagienard, P. Grieder, E. C. Kerrigan, and M. Morari, "Move blocking strategies in receding horizon control," *Journal of Process Control*, vol. 17, no. 6, pp. 563–570, 2007.

[13] R. Gondhalekar and J. Imura, "Least restrictive move-blocking model predictive control," in *9th IFAC World Congress*, 2008.

[14] R. R. Fletcher, *Practical Methods of Optimization*, Wiley, 2nd edition, 1987.

[15] J. Richalet, A. Rault, J.L. Testud, and J. Papon, "Model predictive heuristic control: Applications to industrial processes," *Automatica*, vol. 14, pp. 413–428, 1978.

[16] C. R. Cutler and B. L. Ramaker, "Dynamic matrix control—a computer control algorithm," in *Joint American Control Conference*, 1980.

[17] A. I. Propoi, "Use of linear programming methods for synthesising sampled-data automatic systems," *Automation and Remote Control*, vol. 24, pp. 837–844, 1963.

[18] D. Kleinman, "An easy way to stabilise a linear constant system," *IEEE Transactions on Automatic Control*, vol. AC-15, 1970.

[19] W. H. Kwon and A. E. Pearson, "On the stabilization of a discrete constant linear system," *IEEE Transactions on Automatic Control*, vol. AC-20, 1975.

[20] R. Rouhani and R. K. Mehra, "Model algorithmic control (MAC): basic theoretical properties," *Automatica*, vol. 18, pp. 401–414, 1982.

[21] V. Peterka, "Predictor-based self-tuning control," *Automatica*, vol. 20, no. 1, pp. 39–50, 1984.

[22] B. E. Ydstie, "Extended Horizon Adaptive Control," in *9th IFAC World Congress*, 1984.

[23] R. M. C. De Keyser and A. R. Van Cuawenberghe, "Extended Prediction Self-adaptive Control," in *IFAC Symposium on Identification and System Parameter Estimation*, 1985, pp. 1317–1322.

[24] D. W. Clarke, C. Mohtadi, and P. S. Tuffs, "Generalized Predictive Control. Part I. The Basic Algorithm," *Automatica*, vol. 23, no. 2, pp. 137–148, 1987.

[25] D. W. Clarke, C. Mohtadi, and P. S. Tuffs, "Generalized Predictive Control. Part II. Extensions and Interpretations," *Automatica*, vol. 23, no. 2, pp. 149–160, 1987.

[26] J. Richalet, S. Abu el Ata-Doss, C. Arber, H. B. Huntze, A. Jacubash, and W. Schill, "Predictive Functional Control. Application to Fast and Accurate Robots," in *10th IFAC Congress*, 1987.

[27] M. Morari, *Advances in Model-Based Predictive Control*, chapter Model Predictive Control: Multivariable Control Technique of Choice in the 1990s?, Oxford University Press, 1994.

[28] S. J. Qin and T. A. Badgwell, "A survey of industrial model predictive control technology," *Control Engineering Practice*, vol. 11, pp. 733–764, 2003.

[29] J. H. Lee, "Model Predictive Control: Review of the Three Decades of Development," *International Journal of Control, Automation, and Systems*, vol. 9, no. 3, pp. 415–424, 2001.

[30] S. J. Qin and T. A. Badgwell, "Model Predictive Control," in *Innovations That Could Change the Way You Manufacture, SME Annual Conference*, 2012.

[31] "Honeywell," `https://www.honeywellprocess.com`.

[32] M. Brdys and P. Tatjewski, *Iterative Algorithms for Multilayer Optimizing Control*, Imperial College Press, 2005.

[33] W. M. Findeisen, F. N. Bailey, M. Brdys, K. Malinowski, P. Tatjewski, and A. Wozniak, *Control and Coordination in Hierarchical Systems*, J. Wiley & Sons, 1980.

[34] P. Tatjewski, *Advanced Control of Industrial Processes, Structures and Algorithms*, Springer, 2007.

[35] T. L. Blevins, G. K. McMillan, W. K. Wojsznis, and M. W. Brown, *Advanced Control Unleashed*, ISA, 2003.

[36] D. E. Kassmann, T. A. Badgwell, and R. B. Hawkins, "Robust steady-state target calculation for model predictive control," *AIChE Journal*, vol. 46, pp. 1007–1024, 2000.

[37] D. M. Prett and R. D. Gillette, "Optimization and constrained multivariable control of a catalytic cracking unit," in *joint automatic control conference*, 1980.

[38] J. A. Rossiter, *Model-Based Predictive Control*, CRC Press, 2003.

[39] N. M. C. de Oliveira and L. T. Biegler, "Constraint handing and stability properties of model-predictive control," *AIChE Journal*, vol. 40, no. 7, pp. 1138–1155, 1994.

[40] J. B. Rawlings and K. R. Muske, "The stability of constrained receding horizon control," *IEEE Transactions on Automatic Control*, vol. 38, no. 10, 1993.

[41] G. Stephanopoulos M. Morari, Y. Arkun, "Studies in the synthesis of control structures for chemical processes: Part I: Formulation of the problem. Process decomposition and the classification of the control tasks. Analysis of the optimizing control structures," *AIChE Journal*, vol. 26, no. 2, pp. 220–232, 1980.

[42] T. E. Marlin and A. N. Hrymak, "Real-time operations optimization of continuous processes," in *Chemical Process Control-V*, J. C. Kantor, C. E. Garca, and B. Carnahan, Eds., pp. 156–164. CACHE, AIChE, 1997.

[43] I. Miletic and T. E. Marlin, "Results analysis for real-time optimization (RTO): deciding when to change the plant operation," *Computers & Chemical Engineering*, vol. 20, pp. 1077, 1996.

[44] J. Forbes and T. Marlin, "Design Cost: A Systematic Approach to Technology Selection for Model-Based Real-Time Optimization Systems," *Computers & Chemical Engineering*, vol. 20, pp. 717, 1996.

[45] T. Backx, O. Bosgra, and W. Marquardt, "Integration of model predictive control and optimization of processes," in *ADCHEM 2000*, 2000, pp. 249–260.

[46] C. V. Rao and J. B. Rawlings, "Steady States and Constraints in Model Predictive Control," *AIChE Journal*, vol. 45, no. 6, pp. 1266–1278, 1999.

[47] A. M. Morshedi, C. R. Cutler, and T. A. Skrovanek, "Optimal Solution of Dynamic Matrix Control with Linear Programing Techniques (LDMC)," in *American Control Conference*, 1985, p. 208.

[48] C. Brosilow, G. Q. Zhao, and K.C. Rao, "A linear programming approach to constrained multivariable control," in *American Control Conference*, 1984.

[49] C. Yousfi and R. Tournier, "Steady State Optimization Inside Model Predictive Control," in *American Control Conference*, 1991.

[50] P. Marquis and J. P. Broustail, "SMOC, a bridge between state space and model predictive controllers: Application to the automation of a hydrotreating unit," in *IFAC Symposium*, 1988.

[51] K. R. Muske, "Steady State target Optimization in Linear Model Predictive Control," in *American Control Conference*, 1997, pp. 3597–3601.

[52] M. Lawrynczuk, P. M. Marusak, and P. Tatjewski, "MULTILAYER AND INTEGRATED STRUCTURES FOR PREDICTIVE CONTROL AND ECONOMIC OPTIMISATION," in *11th IFAC Symposium on Large*

Scale Complex Systems Theory and Applications, 2007, vol. 40, pp. 198–205.

[53] M. Lawrynczuk, P. M. Marusak, and P. Tatjewski, "Cooperation of model predictive control with steady-state economic optimisation," *Control and Cybernetics*, vol. 37, no. 1, pp. 133–158, 2008.

[54] S. Engell, "Feedback control for optimal process operation," *Journal of Process Control*, vol. 17, pp. 203–219, 2007.

[55] C. M. Ying and B. Joseph, "Performance and stability analysis of LP-MPC and QP-MPC cascade control systems," *AIChE Journal*, vol. 45, no. 7, pp. 1521–1534, 1999.

[56] J. E. Normey-Rico and E. F. Camacho, *Control of Dead-time Processes*, Springer, 2007.

[57] T. L. M. Santos, D. Limon, J. E. Normey-Rico, and T. Alamo, "On the explicit dead-time compensation for robust model predictive control," *Journal of Process Control*, vol. 22, pp. 236–246, 2012.

[58] C. V. Rao, S. J. Wright, and J. B. Rawlings, "Application of interior-point methods to model predictive control," *Journal of Optimization Theory and Applications*, vol. 99, no. 3, pp. 723–757, 1998.

[59] D. Shneiderman and Z. J. Palmor, "Properties and control of the quadruple-tank process with multivariable dead-times," *Journal of Process Control*, vol. 20, no. 1, pp. 18–28, 2010.

[60] S. Olaru and S. I. Niculescu, "Predictive control for linear systems with delayed input subject to constraints," in *17th IFAC World Congress*, 2008, vol. 41, p. 11208–11213.

[61] B. F. Santoro and D. Odloak, "Closed-loop stable model predictive control of integrating systems with dead time," *Journal of Process Control*, vol. 22, pp. 1209–1218, 2012.

[62] T. L. M. Santos, L. Roca, J. L. Guzman, J. E. Normey-Rico, and M. Berenguel, "Practical MPC with robust dead-time compensation applied to a solar desalination plant," in *18th IFAC World Congress*, 2011, vol. 44, p. 4909–4914.

[63] M. A. F. Martins, A. S. Yamashita, B. F. Santoro, and D. Odloak, "Robust model predictive control of integrating time delay processes," *Journal of Process Control*, vol. 23, pp. 917–932, 2013.

[64] *IEEE Standard for SCADA and Automation Systems*, 2007.

[65] E. J. Davison and H. W. Smith, "Pole assignment in linear time-invariant multivariable systems with constant disturbances," *Automatica*, vol. 7, pp. 489–498, 1971.

[66] B. A. Francis and W. M. Wonham, "The internal model principle of control theory," *Automatica*, vol. 12, pp. 457–465, 1976.

[67] H. Kwakernaak and R. Sivan, *Linear Optimal Control Systems*, John Wiley & Sons, 2nd edition, 1972.

[68] H. W. Smith and E. J. Davison, "Design of industrial regulators. Integral feedback and feedforward control," *Proc. IEE*, vol. 119, no. 8, pp. 1210–1216, 1972.

[69] K. R. Muske and T. A. Badgwell, "Disturbance modeling for offset-free linear model predictive control," *Journal of Process Control*, vol. 12, pp. 617–632, 2002.

[70] G. Pannocchia and J. B. Rawlings, "Disturbance models for offset-free model predictive control," *AIChE Journal*, vol. 49, pp. 426–437, 2003.

[71] J. B. Rawlings, E. S. Meadows, and K. R. Muske, "Nonlinear model predictive control: a tutorial and survey," in *ADCHEM Conference*, 1994, pp. 203–214.

[72] S. M. Zanoli, C. Pepe, and M. Rocchi, "Control and Optimization of a Cement Rotary Kiln: a Model Predictive Control approach," in *2nd Indian Control Conference*, 2016, pp. 111–116.

[73] S. M. Zanoli and C. Pepe, "The importance of cooperation and consistency in two-layer Model Predictive Control," in *17th International Carpathian Control Conference*, 2016, pp. 825–830.

[74] S. M. Zanoli and C. Pepe, "Two-Layer Linear MPC Approach Aimed at Walking Beam Billets Reheating Furnace Optimization," *Journal of Control Science and Engineering*, vol. 2017, 2017.

[75] S. M. Zanoli, C. Pepe, and L. Barboni, "Application of Advanced Process Control techniques to a pusher type reheating furnace," *Journal of Physics: Conference Series*, vol. 659, no. 1, 2015.

[76] C. L. Smith, *Advanced Process Control: Beyond Single Loop Control*, Wiley-AIChE, 2010.

[77] F. G. Shinskey, *Process Control Systems*, McGraw-Hill, 4th edition, 1996.

[78] C. Pepe and S. M. Zanoli, "A two-layer Model Predictive Control system with adaptation to variables status values," in *17th International Carpathian Control Conference*, 2016, pp. 573–578.

[79] C. Pepe and S. M. Zanoli, "Input moves selection in Model Predictive Control: a decoupling approach," in *42nd Annual Conference of IEEE Industrial Electronics Society*, 2016, pp. 196–201.

[80] R. Shridhar and D. J. Cooper, "A Tuning Strategy for Unconstrained Multivariable Model Predictive Control," *Industrial & Engineering Chemistry Research*, vol. 37, pp. 4003–4016, 1998.

[81] A. Georgiou, C. Georgakis, and W.L. Luyben, "Nonlinear Dynamic Matrix Control for High-Purity Distillation Columns," *AIChE Journal*, vol. 34, no. 8, pp. 1287–1298, 1988.

[82] P. R. Maurath, A. J. Laub, D. E. Seborg, and D. A. Mellichamp, "Predictive Controller Design by Principal Components Analysis," *Industrial & Engineering Chemistry Research*, vol. 27, pp. 1204–1212, 1998.

[83] J. L. Garriga and M. Soroush, "Model Predictive Control Tuning Methods: A Review," *Industrial & Engineering Chemistry Research*, vol. 49, no. 8, pp. 3505–3515, 2010.

[84] J. H. Lee and Z. H. Yu, "Tuning of Model Predictive Controllers for Robust Performance," *Computers & Chemical Engineering*, vol. 18, no. 1, pp. 15–37, 1994.

[85] D. E. Seborg, T. E. Edgar, and D. A. Mellichamp, *Process Dynamics and Control*, John Wiley & Sons, 2nd edition, 2004.

[86] S. M. Zanoli, C. Pepe, M. Rocchi, and G. Astolfi, "Application of Advanced Process Control techniques for a Cement Rotary Kiln," in *19th International Conference on System Theory, Control and Computing*, 2015, pp. 723–729.

[87] S. M. Zanoli, C. Pepe, and M. Rocchi, "Cement Rotary Kiln: constraints handling and optimization via Model Predictive Control techniques," in *5th Australian Control Conference*, 2015, pp. 288–293.

[88] W. Trinks, M. H. Mawhinney, R. A. Shannon, R. J. Reed, and J. R. Garvey, *Industrial Furnaces*, John Wiley & Sons, 2004.

[89] A. Martensson, "Energy efficiency improvement by measurement and control: a case study of reheating furnaces in the steel industry," in *14th National Industrial Energy Technology Conference*, 1992, pp. 236–243.

[90] G. Astolfi, L. Barboni, F. Cocchioni, and C. Pepe, "METODO PER IL CONTROLLO DI FORNI DI RISCALDO," 2014, Italian Patent n. 0001424136 awarded by Ufficio Italiano Brevetti e Marchi (UIBM) (`http://www.uibm.gov.it/uibm/dati/Avanzata.aspx?load=info_list_uno&id=2253683&table=Invention&`).

[91] A. von Starck, A. Muhlbauer, and C. Kramer, *Handbook of Thermoprocessing Technologies*, Vulkan Verlag, 2005.

[92] W. Walker, "Information technology and the use of energy," *Energy Policy*, pp. 458–476, 1985.

[93] P. Fontana, A. Boggiano, A. Furinghetti, G. Cabaras, and C. A. Simoncini, "An advanced computer control system for reheat furnaces," *Iron and Steel Engineer*, 1983.

[94] F. G. Shinskey, *Energy Conservation through Control*, Academic Press, 1978.

[95] J. H. Jang, D. E. Lee, M. Y. Kim, and H. G. Kim, "Investigation of the slab heating characteristics in a reheating furnace with the formation and growth of scale on the slab surface," *International Journal of Heat and Mass Transfer*, vol. 53, pp. 4326–4332, 2010.

[96] B. Leden, "A Control System for Fuel Optimization of Reheating Furnaces," *Scandinavian Journal of Metallurgy*, vol. 15, pp. 16–24, 1986.

[97] H. Sibarani and Y. Samyudia, "Robust Nonlinear Slab Temperature Control Design for an Industrial Reheating Furnace," *Computer Aided Chemical Engineering*, vol. 18, 2004.

[98] Z. Wang, T. Chai, S. Guan, and C. Shao, "Hybrid Optimization Setpoint Strategy for Slab Reheating Furnace Temperature," in *American Control Conference*, 1999, pp. 4082–4086.

[99] H. S. Ko, J. S. Kim, and T. W. Yoon, "Modeling and Predictive Control of a Reheating Furnace," in *American Control Conference*, 2000, pp. 2725–2729.

[100] J. H. Choi, Y. J. Jang, and S. W. Kim, "Temperature Control of a Reheating Furnace using Feedback Linearization and Predictive Control," in *International Conference on Control, Automation and Systems*, 2001, pp. 103–106.

[101] G. van Ditzhuijzen, D. Staalman, and A. Koorn, "Identification and model predictive control of a slab reheating furnace," in *International Conference on Control Applications*, 2002, pp. 361–366.

[102] L. Balbis, J. Balderud, and M. J. Grimble, "Nonlinear Predictive Control of Steel Slab Reheating Furnace," in *American Control Conference*, 2008, pp. 1679–1684.

[103] Y. X. Liao, J. H. She, and M. Wu, "Integrated Hybrid-PSO and Fuzzy-NN Decoupling Control for Temperature of Reheating Furnace," *IEEE Transactions on Industrial Electronics*, vol. 56, no. 7, pp. 2704–2714, 2009.

[104] A. Steinboeck, D. Wild, and A. Kugi, "Feedback Tracking Control of Continuous Reheating Furnaces," in *18th IFAC World Congress*, 2011, pp. 11744–11749.

[105] A. Steinboeck, D. Wild, and A. Kugi, "Nonlinear model predictive control of a continuous slab reheating furnace," *Control Engineering Practice*, vol. 21, no. 4, pp. 495–508, 2013.

[106] J. Shamma, *Analysis and design of gain scheduled control systems*, Ph.D. thesis, Massachusetts Institute of Technology,Department of Mechanical Engineering, 1988.

[107] J. Mohammadpour and C. W. Scherer, *Control of Linear Parameter Varying Systems with Applications*, Springer, 2012.

[108] Y. A. Cengel, *Introduction to Thermodynamics and Heat Transfer*, McGraw-Hill Companies, 2nd edition, 2008.

[109] L. Ljung, *System Identification: Theory for the User*, Prentice-Hall, 1987.

[110] Y. Zhu, *Multivariable System Identification for Process Control*, Elsevier Science, 2001.

[111] Y. Zhu and T. Backx, *Identification of Multivariable Industrial Processes for Simulation, Diagnosis and Control*, Springer, 1993.

[112] G. Astolfi, L. Barboni, F. Cocchioni, C. Pepe, and S. M. Zanoli, "Optimization of a pusher type reheating furnace: an adaptive Model Predictive Control approach," in *6th International Symposium on Advanced Control of Industrial Processes*, May 28-31, 2017.

[113] G. Astolfi, L. Barboni, F. Cocchioni, C. Pepe, S. M. Zanoli, M. Bianchi Ferri, and M. Capitanio, "E-FESTO: AN ADAPTIVE ALGORITHM AIMED AT ONLINE OPTIMIZATION OF RE-HEATING FURNACES," in *3rd European Steel Technology and Application Days*, June 26-29, 2017.

[114] C. Pepe, S. M. Zanoli, and F. Cocchioni, "Energy saving and environmental impact decreasing in a walking beam reheating furnace," *WIT Transactions on Ecology and The Environment*, vol. 205, pp. 135–146, 2016.

[115] G. Astolfi, L. Barboni, F. Cocchioni, C. Pepe, S. M. Zanoli, M. Bianchi Ferri, and M. Capitanio, "E-FESTO: an Advanced Process Control framework aimed at energy efficiency achieving in steel reheating furnaces," *AIC Magazine*, pp. 19–21, November 2016.

[116] E. Boe, S. J. McGarel, T. Spaits, and T. Guiliani, "Predictive Control and Optimization Applications in a Modern Cement Plant," in *Cement Industry Technical Conference*, 2005, pp. 1–10.

[117] P. A. Alsop, *Cement Plant Operations Handbook*, International Cement Review, 3rd edition, 2001.

[118] "FLSmidth," `http://www.flsmidth.com/`.

[119] S. Arad, V. Arad, and B. Bobora, "Advanced control schemes for cement fabrication processes," *Robotics and Automation in Construction*, vol. 23, pp. 381–404, 2008.

[120] G. Martin, T. Lange, and N. Frewin, "NEXT GENERATION CONTROLLERS FOR KILN/COOLER AND MILL APPLICATIONS BASED ON MODEL PREDICTIVE CONTROL AND NEURAL NETWORKS," in *IEEE/PCA 42nd Cement Industry Technical Conference*, 2000.

[121] Z. Li, "Intelligent Fuzzy Predictive Controller Design for Multivariable Process System," *Journal of Computational Information Systems*, vol. 6, no. 9, pp. 3003–3011, 2010.

[122] J. Ziatabari, A. Fatehi, and M. T. H. Beheshti, "Cement Rotary Kiln Control: A Supervised Adaptive Model Predictive Approach," in *2008 Annual IEEE India Conference*, 2008.

[123] K. S. Stadler, J. Poland, and E. Gallestey, "Model predictive control of a rotary cement kiln," *Control Engineering Practice*, vol. 19, pp. 1–9, 2011.

[124] S. M. Zanoli and C. Pepe, "A constraints softening decoupling strategy oriented to time delays handling with Model Predictive Control," in *American Control Conference*, 2016, pp. 2687–2692.

[125] S. M. Zanoli, C. Pepe, and M. Rocchi, "Improving Performances of a Cement Rotary Kiln: A Model Predictive Control Solution," *Journal of Automation and Control Engineering*, vol. 4, no. 4, pp. 262–267, 2016, `http://www.icecs.org/best.html`.

[126] G. Astolfi, L. Barboni, F. Cocchioni, C. Pepe, S. M. Zanoli, M. Bianchi Ferri, and M. Capitanio, "A TRAINING FRAMEWORK FOR E-FESTO APC SYSTEM," in *3rd European Steel Technology and Application Days*, June 26-29, 2017.